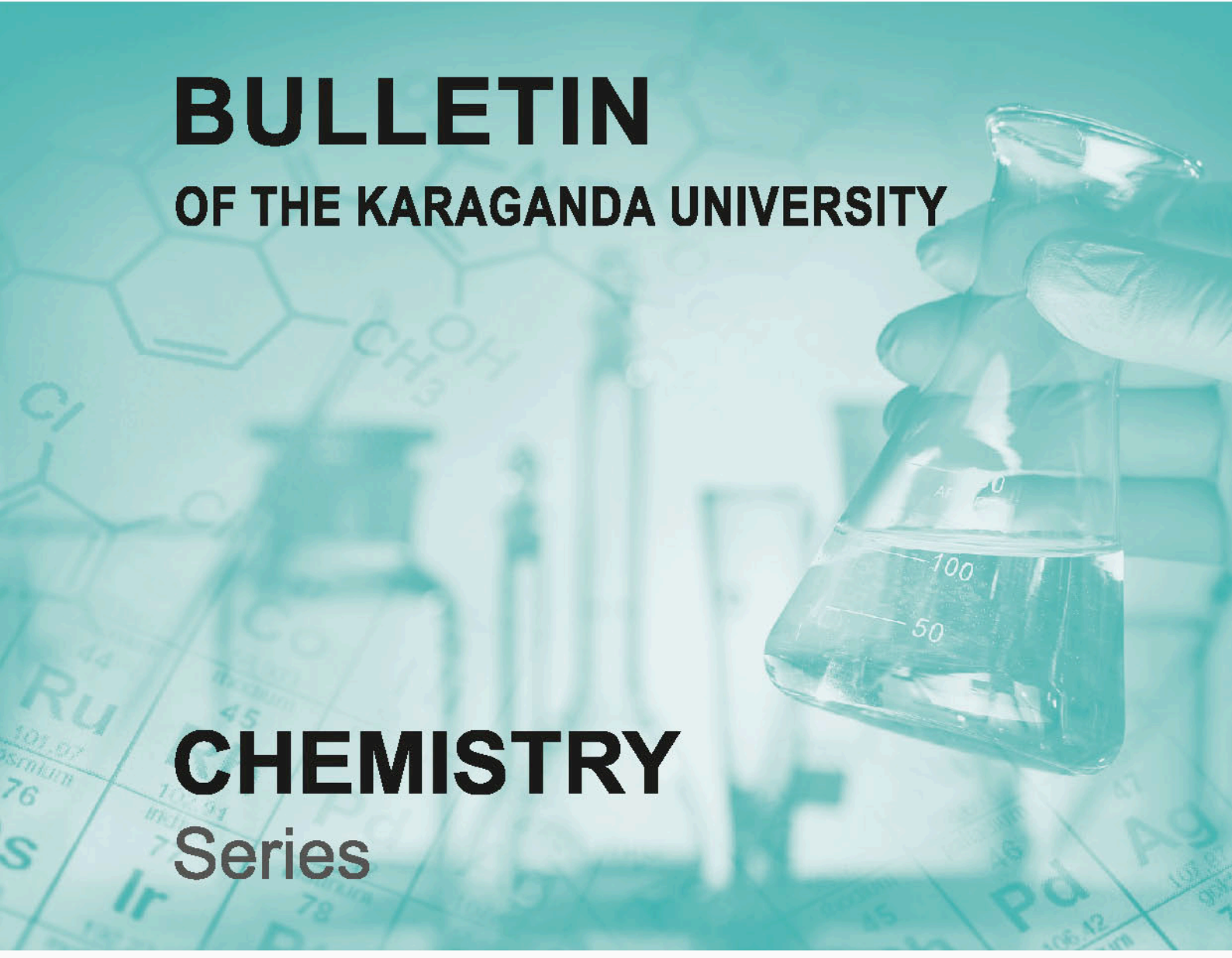




ISSN 2518-718X (Print)
ISSN 2663-4872 (Online)

BULLETIN

OF THE KARAGANDA UNIVERSITY



CHEMISTRY
Series

№ 4(104)/2021

ISSN 2663-4872 (Online)
ISSN-L 2518-718X (Print)
Индексі 74617
Индекс 74617

**ҚАРАҒАНДЫ
УНИВЕРСИТЕТІНІҢ
ХАБАРШЫСЫ**

ВЕСТНИК

**КАРАГАНДИНСКОГО
УНИВЕРСИТЕТА**

BULLETIN

**OF THE KARAGANDA
UNIVERSITY**

ХИМИЯ сериясы

Серия **ХИМИЯ**

CHEMISTRY Series

№ 4(104)/2021

Қазан–қараша–желтоқсан
30 желтоқсан 2021 ж.

Октябрь–ноябрь–декабрь
30 декабря 2021 г.

October–November–December
December, 30th, 2021

1996 жылдан бастап шығады
Издается с 1996 года
Founded in 1996

Жылына 4 рет шығады
Выходит 4 раза в год
Published 4 times a year

Қарағанды, 2021
Караганда, 2021
Karaganda, 2021

Main Editor

Doctor of Chemical sciences
M.Zh. Burkeyev

Responsible secretary

Candidate of chem. sciences
I.A. Pustolaikina

Editorial board

- Z.M. Muldakhmetov**, Academician of NAS RK, Doctor of chem. sciences, Institute of Organic Synthesis and Coal Chemistry of the Republic of Kazakhstan, Karaganda (Kazakhstan);
- S.M. Adekenov**, Academician of NAS RK, Doctor of chem. sciences, International Research and Production Holding “Phytochemistry”, Karaganda (Kazakhstan);
- S.E. Kudaibergenov**, Doctor of chem. sciences, Institute of Polymer Materials and Technologies, Almaty (Kazakhstan);
- V. Khutoryanskiy**, Professor, University of Reading, Reading (United Kingdom);
- Fengyun Ma**, Professor, Xinjiang University, Urumqi (PRC);
- Xintai Su**, Professor, South China University of Technology, Guangzhou (PRC);
- R.R. Rakhimov**, Doctor of chem. sciences, Norfolk State University, Norfolk (USA);
- M.B. Batkibekova**, Academician of the Engineering Academy of the Kyrgyz Republic, Doctor of chem. sciences, Kyrgyz State Technical University named after I. Razzakov, Bishkek (Kyrgyzstan);
- S.A. Beznosyuk**, Doctor of phys.-math. sciences, Altai State University, Barnaul (Russia);
- B.F. Minaev**, Doctor of chem. sciences, Bohdan Khmelnytsky National University of Cherkasy, Cherkasy (Ukraine);
- I.V. Kulakov**, Doctor of chem. sciences, University of Tyumen (Russia);
- R.P. Bhole**, PhD, Associate Professor, Dr. D.Y. Patil Institute of Pharmaceutical Sciences and Research, Sant Tukaram Nagar, Pimpri, Pune (India);
- A.M. Makasheva**, Doctor of techn. sciences, Zh. Abishev Chemical-Metallurgical Institute, Karaganda (Kazakhstan);
- M.I. Baikenov**, Doctor of chem. sciences, Karagandy University of the name of acad. E.A. Buketov (Kazakhstan);
- L.K. Salkeeva**, Doctor of chem. sciences, Karagandy University of the name of acad. E.A. Buketov (Kazakhstan);
- Ye.M. Tazhbaev**, Doctor of chem. sciences, Karagandy University of the name of acad. E.A. Buketov (Kazakhstan);
- O.G. Yaroshenko**, Doctor of Pedagogical Sciences, Academician of the National Academy of Pedagogical Sciences of Ukraine, Institute of Higher Education of the National Academy of Educational Sciences of Ukraine, Kyiv (Ukraine);
- V.N. Fomin**, Cand. of chemical science, Head of the laboratory of engineering profile “Physical and chemical research methods”, Karagandy University of the name of acad. E.A. Buketov (Kazakhstan);

Postal address: 28, University Str., Karaganda, 100024, Kazakhstan

Tel./fax: (7212) 34-19-40.

E-mail: chemistry.vestnik@ksu.kz; meyram.burkeyev@ksu.kz; irina.pustolaikina@ksu.kz

Web-site: <http://chemistry-vestnik.ksu.kz>

Editors Zh.T. Nurmukhanova, S.S. Balkeyeva, Z.E. Ramazanova

Computer layout V.V. Butyaikin

Bulletin of the Karaganda University. Chemistry series.

ISSN 2663-4872 (Online). ISSN-L 2518-718X (Print).

Proprietary: NLC “Karagandy University of the name of academician E.A. Buketov”.

Registered by the Ministry of Information and Social Development of the Republic of Kazakhstan. Rediscount certificate No. KZ27VPY00027382 dated 30.09.2020.

Signed in print 29.12.2021. Format 60×84 1/8. Offset paper. Volume 20,63 p.sh. Circulation 200 copies. Price upon request. Order № 133.

Printed in the Publishing house of NLC “Karagandy University of the name of acad. E.A. Buketov”.

28, University Str., Karaganda, 100024, Kazakhstan. Tel.: (7212) 35-63-16. E-mail: izd_kargu@mail.ru

CONTENTS

MEMORABLE DATES

- Nikolskiy S.N., Pustolaikina I.A., Masalimov A.S.* as the founder and leader of a new direction in ESR spectroscopy and quantum chemistry of free radicals..... 5

ORGANIC CHEMISTRY

- Ayazbayeva A.Ye., Shakhvorostov A.V., Seilkhanov T.M., Aseyev V.O., Kudaibergenov S.E.* Synthesis and characterization of novel thermo- and salt-sensitive amphoteric terpolymers based on acrylamide derivatives 9
- Nurmaganbetov Zh.S., Mukusheva G.K., Ye.V.Minayeva, Turdybekov D.M., Turdybekov K.M., Makhmutova A.S., Zhasymbekova A.R., Nurkenov O.A.* Synthesis, quantum-chemical calculations and virtual screening of the alkaloid cytosine derivatives 21
- Minakova A.A., Chikina M.V., Il'yasov S.G.* Study of uric acid oxidation reaction products in medium of ammonia or primary amines..... 30

PHYSICAL AND ANALYTICAL CHEMISTRY

- Fomin V.N., Aynabaev A.A., Kaykenov D.A., Sadyrbekov D.T., Aldabergenova S.K., Turovets M.A., Kelesbek N.K.* Optimization of coal tar gas chromatography conditions using probabilistic-deterministic design of experiment 39
- Jumadilov T.K., Utesheva A.A., Khimersen Kh., Kondauronov R.G., Grazulevicius J.V.* Abnormal activity of functional groups during uranyl ions sorption by polymethacrylic acid-poly-4-vinylpyridine intergel system..... 47
- Kamani V.G., Sujatha M., Daddala G.B.* Development and validation of a novel stability indicating HPLC method for the separation and determination of darolutamide and its impurities in pharmaceutical formulations..... 57
- Malyshev V.P., Makasheva A.M., Bekbayeva L.A.* Invariants of ratio of crystal-mobile, liquid-mobile, and vaporized chaotized particles in solid, liquid, and gas states of substance 69

INORGANIC CHEMISTRY

- Ismailova A.G., Akanova G.Zh., Kamysbayev D.Kh.* Acid dissolution of neodymium magnet Nd-Fe-B in different conditions..... 79
- Baimuratova Zh.A., Kalmakhanova M.S., Massalimova B.K., Nurlibaeva A.A., Kulazhanova A.S., Diaz de Tuesta J.L., Gomes H.T.* Synthesis and characterization of a new magnetic composite $MnFe_2O_4$ /clay based on a natural clay obtained from Turkestan deposit..... 87

CHEMICAL TECHNOLOGY

- Abdimomyn S., Abduakhytova D., Atchabarova A., Turdean G.L., Tokpayev R., Kishibayev K., Kurbatov A., Nauryzbayev M.* Optimization of the preparation method of a mechanically strong carbon electrode 95
- Abildina A.K., Avchukir K., Jumanova R.Zh., Beiseyeva A.N., Rakhymbay G.S., Argimbayeva A.M.* Preparation and electrochemical characterization of TiO_2 as an anode material for magnesium-ion batteries 104
- Amerkhanova Sh.K., Uali A.S., Shlyapov R.M., Belgibayeva D.S.* Alkali-activated metallurgical slag as a sustainable adsorbent 117
- Mustafin Ye.S., Omarov Kh.B., Borsynbaev A.S., Havlichek D., Pudov A.M., Shuyev N.V.* Production of electrolytic copper from Zhezkazgan Processing Plant tailings leaching solutions using a hydro-impulse discharge 128

<i>Kozhanova A.M., Temirgazyev B.S., Zhanarbek A., Tuleuov B.I., Seilkhanov T.M., Adekenov S.M.</i> Synthesis of a hydrophilic derivative of ecdysterone and development of its water-soluble form	138
<i>Raiymbekov Y.B., Besterekov U., Abdurazova P.A., Nazarbek U.B., Pochitalkina I.A.</i> Recovery of used acetic acid via sulfuric acid	149
Index of articles published in “Bulletin of the Karaganda University. Chemistry Series” in 2021	163

MEMORABLE DATES

UDC 541.515

<https://doi.org/10.31489/2021Ch4/5-8>

S.N. Nikolskiy*, I.A. Pustolaikina

¹*Karagandy University of the name of academician E.A. Buketov, Karaganda, Kazakhstan*
(*Corresponding author`s e-mail: sergeynikolsky@mail.ru)

A.S. Masalimov as the founder and leader of a new direction in ESR spectroscopy and quantum chemistry of free radicals

The article highlights the creative path of A.S. Masalimov, an outstanding Kazakhstan chemist who celebrates his 70th anniversary in 2022. The main stages of his career and significant events of his scientific career are presented here. The contribution of professor A.S. Masalimov in the foundation and development of the school of ESR spectroscopy and quantum chemistry at the Karaganda Buketov University is shown.



The anniversary of the scientist is a good reason to sum up what he has done, to see the significance of his works in the research area. Abay Sabirjanovich Masalimov, Doctor of Chemical Sciences, Professor, the founder and leader of a new direction in ESR spectroscopy and quantum chemistry of free radicals, is a scientist whose works are widely known in Kazakhstan science. His name is associated with the development of a modern model of protolytic processes in acid-base systems with intermolecular hydrogen bonds.

Abay Sabirjanovich was born in the Vvedenka village, Mendykara district, Kostanay region, on January 7, 1952. After school, he entered Kazakh State University named after S.M. Kirov in Almaty, which he successfully graduated in 1974.

After graduation from the university, Masalimov A.S. was sent to the Zhambyl Technological Institute according to the assignment. In 1974–1976 he worked in the ESR-spectroscopy laboratory of the Institute of Organoelement Compounds of the USSR Academy of Sciences in Moscow as a research assistant from the Zhambyl Technological Institute. At this time Masalimov A.S. and his colleagues obtained the kinetic parameters of reversible proton transfer between semiquinone radicals and primary and secondary amines, and also discovered the phenomenon of non-degenerate tautomerism in 3,5-di-tert-butyl-2-chloro-6-hydroxyphenoxy. These were his most significant achievements of that period [1–3].

During the internship, A.S. Masalimov under the leadership of Academician of the USSR Academy of Sciences, M.I. Kabachnik, prepared a candidate dissertation in chemistry entitled: “ESR study of reversible proton transfer reactions” on the 02.00.04 — Physical Chemistry specialty. The defense of the thesis took place at one of the first dissertation councils opened after the reform in Kyiv city in 1978. In 1976–1978 Masalimov A.S. worked as a teacher at the Department of Physical Chemistry of the Zhambyl Technological Institute, then returned to the Institute of Chemical Sciences of the Kazakh SSR Academy of Sciences in Alma-Ata. Here he worked for about three years as a junior researcher at the Laboratory of Physical Methods of Research.

All further job and scientific activities of Masalimov A.S. inseparably linked with the Karaganda State University, where he was invited by the rector Muldakhmetov Z.M. Since 1980 Masalimov A.S. worked at

various positions of the Chemical Faculty of Karaganda State University: as a Senior Lecturer, then as an Associate Professor of the Physical Chemistry Department, as the Head of the Quantum Chemistry Department, and after the faculty reorganization, as the Head of the Physical and Analytical Chemistry Department, as well as the Dean of the Chemical Faculty. In 2001–2005, Masalimov A.S. was the vice-rector of scientific work in the Buketov Karaganda State University. In 2005–2021, he headed the Physical and Analytical Chemistry Department of the Buketov Karaganda State University.

In 1993, Masalimov A.S. successfully defended his doctoral dissertation in chemistry entitled: “Rapid reactions of proton transfer and exchange in semiquinone radicals” on the 02.00.04 — Physical Chemistry specialty. In 1996, he was awarded the title of professor by the Higher Attestation Commission of the Republic of Kazakhstan. In 2002, Masalimov A.S. became an academician of the Kazakhstan Higher Education Academy of Sciences, and in 2005, he became an academician of the International Higher Education Academy of Sciences.

The authority of a scientist in the research community is also can be confirmed by his membership in dissertation councils. For many years, Masalimov Abay Sabirjanovich was a member of doctoral dissertation councils on the Physical Chemistry specialty in the Buketov Karaganda State University and Al-Farabi Kazakh National University. Currently, A.S. Masalimov is the Chairman of the dissertation council on the 6D060600 — Chemistry specialty (8D05301 — Chemistry educational program) in the Buketov Karaganda University.

The scientific interests of Abay Sabirjanovich have always been focused on the key problems of chemical science. His research style is characterized by broad scope and innovation, combined with the precision of an experimental solution. He founded the school of ESR spectroscopy and quantum chemistry at the Karaganda State University. Acid-type spin probes with a wide range of kinetic characteristics were obtained from the different structure stable semiquinone radicals for the study of non-aqueous media [4–6]. Using dynamic ESR spectroscopy and semiquinone spin probes, a technique for determining the rates of rapid protolytic processes in non-aqueous solutions of organic compounds was developed by A.S. Masalimov. The developed technique allows to obtain such paramount characteristics of substances as kinetic basicity and acidity [7–12]. A new theory of proton transfer in intermolecular hydrogen-bonded acid-base systems taking into account the primary elementary act of one-electron transfer was presented by A.S. Masalimov [13].

Our faculty has become one of the leading research centers for chemistry in Central Kazakhstan, a real forge of scientific and pedagogical personnel in the country owing to the high professionalism of Abay Sabirjanovich, his talent as a leader and teacher, dedication and strategic vision of the situation.

A.S. Masalimov, heading a number of significant scientific research, formed a powerful scientific school at the Chemical Faculty. Under his supervision 1 doctor of chemical sciences, 9 candidates of chemical sciences, 1 doctor of PhD and more than 22 masters of science defended their dissertations.

The fruitful scientific activity of Abay Sabirjanovich found its ESR presentation in more than 260 scientific works, including 2 textbooks and numerous publications in the authoritative world scientific databases such as Web of Science and Scopus. At present, the monograph “ESR spectroscopy of protolytic processes” is being prepared for publication, which is the result of many years of scientific research and experiments. His papers are an example of the originality and courage of scientific thought, and his hypotheses are always proven and convincing.

The merits of the celebrant were repeatedly noted at the highest level. In 2005, Masalimov A.S. was awarded the medal “For Merit in the Development of Science” of the Ministry of Education and Science of the Republic of Kazakhstan. In 2006, he became the owner of the grant of the Ministry of Education and Science of the Republic of Kazakhstan “The best teacher of the university”. In 2012, he was awarded the title of Honored Worker of the Buketov Karaganda State University. In 2018, he was awarded the Medal “Excellence in the Chemical Industry of the Republic of Kazakhstan”.

More than 40 years, Masalimov Abay Sabirjanovich has been working at the Buketov Karaganda University. Over the years, he has gone from Senior Lecturer to Dean, Vice-rector for scientific work, Chairman of the dissertation council. Scientific authority, broad erudition, a high degree of professionalism and organizational skills of Abay Sabirjanovich are known and recognized not only in Kazakhstan, but also abroad.

On behalf of the labor collective of the Chemical Faculty of the Buketov Karaganda University, we congratulate Professor A.S. Masalimov on his 70th birthday and express our deep gratitude for his many years of work in our team! We wish Abay Sabirjanovich good health, creative longevity, new scientific achievements, grateful students and followers!

References

- 1 Масалимов А.С. О реакциях протонного обмена и переноса с участием 4,6-ди-трет.бутил-3-хлор-2-оксифеноксиле / А.С. Масалимов, А.И. Прокофьев, С.П. Солодников, Н.Н. Бубнов, М.И. Кабачник // Изв. АН СССР. Сер. хим. — 1978. — Т. 27, № 1. — С. 210–213.
- 2 Масалимов А.С. ESR Исследование методом ЭПР протонного переноса от 3,6-ди-трет.бутил-2-оксифеноксила к первичным и вторичным аминам / А.С. Масалимов, А.И. Прокофьев, Н.Н. Бубнов, С.П. Солодников, М.И. Кабачник // Изв. АН СССР. Сер. хим. — 1977. — Т. 26, № 4. — С. 696–700.
- 3 Масалимов А.С. Невырожденная таутомерия в свободных радикалах. Внутримолекулярная миграция атома водорода в 4,6-ди-трет.бутил-3-хлор-2-оксифеноксиле / А.С. Масалимов, А.И. Прокофьев, Н.Н. Бубнов, С.П. Солодников, М.И. Кабачник // Докл. АН СССР. — 1977. — Т. 236, № 1. — С. 116–119.
- 4 Масалимов А.С. ЭПР-исследование влияния добавок воды на кинетику протонного переноса и обмена в растворах семихинонных радикалов / А.С. Масалимов, К.Т. Бажиков, Л.Э. Мельбардис, А.И. Прокофьев // Изв. РАН. Сер. хим. — 1994. — Т. 43, № 6. — С. 953–956.
- 5 Масалимов А.С. Кинетика протонного переноса между семихинонными и нитроксильными радикалами / А.С. Масалимов, С.Н. Никольский, И.И. Дмитриев, А.И. Прокофьев, З.М. Мулдахметов // Изв. АН СССР. Сер. хим. — Т. 40, № 1. — С. 53–57.
- 6 Масалимов А.С. ЭПР-исследование кинетики протонного переноса в вязких средах / А.С. Масалимов, С.Н. Никольский, А.И. Прокофьев, З.М. Мулдахметов // Изв. РАН. Сер. хим. — 1992. — Т. 41, № 9. — С. 1563–1566.
- 7 Масалимов А.С. ЭПР-исследование протонирования замещенных трехчленных азотистых гетероциклов / А.С. Масалимов, С.Н. Никольский, А.А. Ходак, А.И. Прокофьев, З.М. Мулдахметов, Р.Г. Костяновский // Изв. АН СССР. Сер. хим. — 1991. — Т. 40, № 1. — С. 47–52.
- 8 Масалимов А.С. Таутомерия в ионных парах семихинонных анион-радикалов с аммониевыми катионами / А.С. Масалимов, С.Н. Никольский, О.Д. Кемалов, А.И. Прокофьев, З.М. Мулдахметов // Теоретическая и экспериментальная химия. — 1991. — Т. 27, № 2. — С. 184–188.
- 9 Масалимов А.С. Протолитические реакции 3,6-ди-трет-бутил-2-оксифеноксила с азотистыми основаниями / А.С. Масалимов, А.А. Тур, С.Н. Никольский // Теоретическая и экспериментальная химия. — 2016. — Т. 52, № 1. — С. 57–65.
- 10 Masalimov A.S. Quantum-chemical investigations of the dual protolytic activity of several semiquinone radicals / A.S. Masalimov, A.A. Tur, A.E. Tuktybayeva, S.N. Nikolskiy // Bulletin of the University of Karaganda – Chemistry. — 2015. — № 77. — P. 51–56.
- 11 Nikolskiy S.N. Investigation of intermolecular proton exchange of 3,6-di-tert-butyl-2-oxyphenoxyl with N-phenylanthranilic acid by ESR spectroscopy method / S.N. Nikolskiy, F.Z. Abilkanova, A.S. Golovenko, I.A. Pustolaikina, A.S. Masalimov // Bulletin of the University of Karaganda – Chemistry. — 2020. — № 98. — P. 35–41.
- 12 Nikolskiy S.N. Investigation of intermolecular proton exchange 3,6-di-tert-butyl-2-hydroxyphenoxyl with phenol by ESR spectroscopy method / S.N. Nikolskiy, A.A. Tur, A.A. Yelchibekova, K.Z. Kutzhanova, A.S. Masalimov // Bulletin of the University of Karaganda – Chemistry. — 2015. — № 77. — P. 47–50.
- 13 Масалимов А.С. Кинетические аспекты теории кислот и оснований М.И. Усановича / А.С. Масалимов // Исследование кислотно-основного взаимодействия в двойных и тройных системах: Сб. науч. тр. КазГУ им. С.М. Кирова. — Алма-Ата, 1984. — С. 92–96.

С.Н. Никольский, И.А. Пустолайкина

А.С. Масалимов — бос радикалдардың ЭПР-спектроскопиясы мен кванттық химиясы атты жаңа бағыттың негізін қалаушы, жетекшісі

Мақалада 2022 жылы 70-жылдық мерейтойын атап өтетін көрнекті қазақстандық химик ғалым А.С. Масалимовтың шығармашылық жолы баяндалған. Еңбек қызметінің негізгі кезеңдері мен ғылыми жолындағы елеулі оқиғалары көрсетілді. Профессор А.С. Масалимов академик Е.А. Бөкетов атындағы Қарағанды университетінде ЭПР спектроскопия және кванттық химия мектебін құру және дамытудағы қосқан үлесі атап өтілген.

С.Н. Никольский, И.А. Пустолайкина

А.С. Масалимов — создатель и руководитель нового направления в ЭПР-спектроскопии и квантовой химии свободных радикалов

В статье освещен творческий путь выдающегося казахстанского ученого-химика А.С. Масалимова, который в 2022 г. отметит 70-летний юбилей. Представлены основные этапы его трудовой деятельности и значимые события научной карьеры. Показан вклад профессора А.С. Масалимова в создание и развитие школы ЭПР-спектроскопии и квантовой химии в Карагандинском университете имени академика Е.А. Букетова.

References

- 1 Masalimov, A.S., Prokofev, A.I., Bubnov, N.N., Solodovnikov, S.P., & Kabachnik, M.I. (1978). Proton-exchange and transfer-reactions involving 3,5-di-tert-butyl-6-chloro-2-hydroxyphenoxyl. *Bulletin of the Academy of Sciences of the USSR Division of Chemical Science*, 27(1), 210–213. <https://doi.org/10.1007/bf01153250>
- 2 Masalimov, A.S., Prokofev, A.I., Bubnov, N.N., Solodovnikov, S.P., & Kabachnik, M.I. (1977). ESR investigation of proton-transfer from 3,6-di-tert-butyl-2-hydroxyphenoxyl to primary and secondary-amines. *Bulletin of the Academy of Sciences of the USSR Division of Chemical Science*, 26(4), 696–700. <https://doi.org/10.1007/bf01108183>
- 3 Masalimov, A.S., Prokofiev, A.I., Bubnov, N.N., Solodovnikov, S.P., & Kabachnik, M.I. (1977). Nevyrozhdennaiia tautomeriia v svobodnykh radikalakh. Vnutrimolekuliarnaia migratsiia atoma vodoroda v 4,6-di-tret.butil-3-khlor-2-oksifenoksile [Non-degenerated tautomerism in free-radicals — intramolecular migration of hydrogen-atom in 2-chloro-6-oxy-3,5-di-tret-butylphenoxyl]. *Doklady Akademii Nauk SSSR — Reports of the USSR Academy of Sciences*, 236(1), 116–119 [in Russian].
- 4 Masalimov, A.S., Bazhikov, K.T., Melbardis, L.E., & Prokofev, A.I. (1994). ESR study of the effect of water on the kinetics of proton-transfer and exchange in solutions of semiquinone radicals. *Russian Chemical Bulletin*, 43(6), 953–956. <https://doi.org/10.1007/bf01558055>
- 5 Masalimov, A.S., Nikolskii, S.N., Dmitriev, P.I., Prokofev, A.I., & Muldakhmetov, Z.M. (1991). Kinetics of proton-transfer between semiquinone and nitroxyl radicals. *Bulletin of the Academy of Sciences of the USSR Division of Chemical Science*, 40(1), 53–57. <https://doi.org/10.1007/bf00959629>
- 6 Masalimov, A.S., Nikolskii, S.N., Prokofev, A.I., & Muldakhmetov, Z.M. (1992). ESR analysis of proton-transfer in viscous media. *Bulletin of the Russian Academy of Sciences Division of Chemical Science*, 41(9), 1563–1566. <https://doi.org/10.1007/bf00863573>
- 7 Masalimov, A.S., Nikolskii, S.P., Khodak, A.A., Prokofev, A.I., Muldakhmetov, Z.M., & Kostyanovkii, R.G. (1991). ESR study of protonation of substituted 3-member nitrogen-heterocycles. *Bulletin of the Academy of Sciences of the USSR Division of Chemical Science*, 40(1), 47–52. <https://doi.org/10.1007/bf00959628>
- 8 Masalimov, A.S., Nikolskiy, S.N., Kemalov, O.D., Prokofyev, A.I., & Muldakhmetov, Z.M. (1991). Tautomeriia v ionnykh parakh semikhinonnykh anion-radikalov s ammonievymi kationami [Tautometry in ionic pairs of semiquinone anion-radicals with ammonium cations]. *Teoreticheskaia i eksperimentalnaia khimiia — Theoretical and Experimental Chemistry*, 27(2), 184–188 [in Russian].
- 9 Masalimov, A.S., Tur, A.A., & Nikolskiy, S.N. (2016). Protolytic Reactions of 3,6-Di-tert-Butyl-2-Hydroxyphenoxyl with Nitrogen Bases. *Theoretical and Experimental Chemistry*, 52(1), 57–65. <https://doi.org/10.1007/s11237-016-9451-0>
- 10 Masalimov, A.S., Tur, A.A., Tuktybayeva, A.E., & Nikolskiy, S.N. (2015). Quantum-chemical investigations of the dual protolytic activity of several semiquinone radicals. *Bulletin of the University of Karaganda – Chemistry*, 77, 51–56.
- 11 Nikolskiy, S.N., Abilkanova, F.Z., Golovenko, A.S., Pustolaikina, I.A., & Masalimov, A.S. (2020). Investigation of intermolecular proton exchange of 3,6-di-tert-butyl-2-oxyphenoxyl with N-phenylanthranilic acid by ESR spectroscopy method. *Bulletin of the University of Karaganda – Chemistry*, 98, 35–41. <https://doi.org/10.31489/2020Ch2/35-41>
- 12 Nikolskiy, S.N., Tur, A.A., Yelchibekova, A.A., Kutzhanova, K.Z., & Masalimov, A.S. (2015). Investigation of intermolecular proton exchange 3,6-di-tert-butyl-2-hydroxyphenoxyl with phenol by ESR spectroscopy method. *Bulletin of the University of Karaganda – Chemistry*, 77, 47–50.
- 13 Masalimov, A.S. (1984) Kineticheskie aspekty teorii kislot i osnovanii M.I. Usanovicha [Kinetic aspects of the M.I. Usanovich theory of acids and bases]. *Issledovanie kislotno-osnovnogo vzaimodeistviia v dvoynykh i troinykh sistemakh: Sbornik nauchnykh trudov Kazakhskogo gosudarstvennogo universiteta imeni S.M. Kirova — Study of acid-base interactions in binary and ternary systems: Collection of scientific papers of S.M. Kirov Kazakh State University*, Alma-Ata, pp. 92–96 [in Russian].

Information about addressee and authors

Masalimov, Abay Sabirzhanovich — Full Professor, Doctor of Chemical Sciences, Karagandy University of the name of academician E.A. Buketov, Universitetskaya street, 28, 100024, Karaganda, Kazakhstan; e-mail: masalimov-as@mail.ru; <https://orcid.org/0000-0002-6405-7108>;

Nikolskiy, Sergey Nikolaevich — Full Professor, Doctor of Chemical Sciences, Karagandy University of the name of academician E.A. Buketov, Universitetskaya street, 28, 100024, Karaganda, Kazakhstan; e-mail: sergeynikolsky@mail.ru; <https://orcid.org/0000-0003-3175-6938>;

Pustolaikina Irina Anatolevna — Candidate of chemical sciences, Assoc. Professor, Karagandy University of the name of academician E.A. Buketov, Universitetskaya street, 28, 100024, Karaganda, Kazakhstan; e-mail: ipustolaikina@gmail.com, <https://orcid.org/0000-0001-6319-666X>

ORGANIC CHEMISTRY

UDC 541.64+678.744

<https://doi.org/10.31489/2021Ch4/9-20>

A.Ye. Ayazbayeva^{1*}, A.V. Shakhvorostov², T.M. Seilkhanov³,
V.O. Aseyev⁴, S.E. Kudaibergenov²

¹Satbayev University, Almaty, Kazakhstan;

²Institute of Polymer Materials and Technology, Almaty, Kazakhstan;

³Sh. Ualikhanov University, Kokshetau, Kazakhstan;

⁴University of Helsinki, Helsinki, Finland

(*Corresponding author's e-mail: ayazbayeva.aigerim@gmail.com)

Synthesis and characterization of novel thermo- and salt-sensitive amphoteric terpolymers based on acrylamide derivatives

A novel linear amphoteric terpolymers based on neutral monomer — N-isopropylacrylamide (NIPAM), anionic monomer — 2-acrylamido-2-methyl-1-propanesulfonic acid sodium salt (AMPS), and cationic monomer — (3-acrylamidopropyl) trimethylammonium chloride (APTAC) were synthesized by free-radical polymerization in aqueous solution and characterized by methods of ¹H NMR and FTIR spectroscopy, TGA, GPC, Dynamic light scattering (DLS) and zeta-potential. The thermal and salt sensitivity of amphoteric ternary polymers of various compositions, particularly, [NIPAM]:[AMPS]:[APTAC] = 90:2.5:7.5; 90:5:5; 90:7.5:2.5 mol.% were studied in aqueous and aqueous-salt solutions in the temperature range from 25 to 60 °C and at the NaCl ionic strength μ interval from 10⁻³ to 1M. It was found that due to hydrophobic/hydrophilic balance, the temperature dependent conformational and phase change of macromolecular chains becomes sensitive to salt addition and allows the fine-tuning of the phase transition. In aqueous and aqueous-salt solutions, the average hydrodynamic size of amphoteric terpolymers is varied from 8 to 300 nm exhibiting bimodal distribution at room temperature. The number average (M_n) and weight average (M_w) molecular weights, polydispersity index (PDI), and zeta-potentials of amphoteric terpolymers in aqueous solutions were determined.

Keywords: amphoteric terpolymers, thermal response, salt sensitivity, phase transition temperature, hydrophobic/hydrophilic balance, core-shell structure.

Introduction

Numerous non-ionic thermally responsive homopolymers phase separate from their aqueous solutions upon heating [1]. Such macromolecules are amphiphilic, i.e. they consist of hydrophilic and hydrophobic fragments. Formation of hydrogen bonds between the hydrophilic polar groups of the polymer chain and water molecules contributes favorably to the free energy of mixing in cold water. Strength of the hydrogen bonds decreases upon heating. When the temperature of a solution is raised above the phase separation temperature, the hydrophobic backbone and/or other nonpolar groups of the polymer tend to associate. This causes intra- and intermolecular aggregation leading to a collapse of the individual polymer chains (microphase separation) and precipitation of the polymer (macrophase separation) within narrow temperature range. Poly(N-isopropylacrylamide) (PNIPAM) is the most extensively studied thermally responsive homopolymer [1–3]. PNIPAM exhibits a well-defined lower critical solution temperature (LCST) in water around 32 °C that is a critical temperature, below which all polymer-solvent compositions are miscible [4].

Basic solution properties of thermoresponsive polymers can be chemically altered. Additional highly polar or ionic groups enhance the overall solubility of these polymers in water. Thus, there are numerous examples of the poly(ethylene oxide) (PEO) usage to induce colloidal stability of the aggregates formed above

LCST [5]. This steric stabilization by nonionic hydrophilic polymers results in core-shell architectures and is typically independent of the ionic strength, assuming that the added low-molar-mass salt does not drastically change the thermodynamic quality of the aqueous solvent. Hydrophilization of the thermoresponsive polymers with ionic comonomers typically results to stable spherical particles with charged surface. However, copolymerization of PNIPAM with a weak acid may also disfavor chain expansion: the complexes between methacrylic acid and NIPAM at certain pH are able to undergo an intramolecular conformational transition from a coil state to a more compact folded state without considerable loss of the chain solubility [6].

Copolymerization of PNIPAM with two oppositely charged comonomers (terpolymer) brings up further complexity to the balance of various interactions in solution. On the other hand, a combination of several external stimuli within one macromolecule leads to the formation of multi-responsive NIPAM-based polyampholytes [7-9] that are used as smart sensors [7], drug delivery [8], and metal ion recognition systems [9].

Polyampholytes in general and quenched (strongly charged) polyampholytes in particular are macromolecules, which properties drastically change in response to various stimuli, e.g. temperature, salt, co-solvent, light, etc. [10-12]. Inclusion of thermoresponsive N-isopropylacrylamide (NIPAM) [13, 14] and N-(tert-butyl)methacrylamide [15] monomers into macromolecular chains leads to the targeted modification of conformational and macroscopic phase separation behavior of amphoteric macromolecules upon heating.

Thermally and pH responsive linear and crosslinked polyampholytes based on N-acryloyl-N-ethyl piperazine and maleic acid have recently been prepared by means of the free-radical solution polymerization [16]. The adsorption capacity of the reported hydrogels was investigated using a Congo red as a model dye varied in the range of 8.37-11.45 mg/g that corresponds to an absorption efficiency of 68-93 %. The synthesis of alternating charge-neutral polyampholytes was described via the reversible addition-fragmentation chain transfer (RAFT) statistical copolymerization of cationic styrenic and anionic N-substituted maleimide monomers [17]. The thermoresponsive behavior of the obtained charge-neutral polyampholytes was demonstrated in water and water-alcohol (methanol, ethanol and 2-propanol) mixtures.

In this paper, we report synthesis and characterization of a novel charge-balanced and charge-imbalanced amphoteric terpolymers derived from N-isopropylacrylamide (NIPAM), 2-acrylamido-2-methyl-1-propanesulfonic acid sodium salt (AMPS) and (3-acrylamidopropyl) trimethylammonium chloride (APTAC). The behavior of these ternary polyampholytes has been studied in aqueous and aqueous-salt solutions to evaluate the conformational and phase transitions upon changing of temperature and salt addition. Understanding the physico-chemical properties of the new linear NIPAM-based polyampholytes is an important criterion in the development of targeted drug delivery models.

Experimental

Materials

Monomers — N-isopropylacrylamide (NIPAM, 97 % purity), 2-acrylamido-2-methylpropanesulfonic acid sodium salt (AMPS, 50 wt.%) and (3-acrylamidopropyl) trimethylammonium chloride (APTAC, 75 wt.% in water), ammonium persulfate (APS, 98 % purity), sodium metabisulfite (SMBS, 97 % purity), sodium chloride, dialysis tubing cellulose membrane were purchased from Sigma-Aldrich Chemical Co., and used without further purification.

Methods

FTIR spectra of NIPAM-APTAC-AMPS terpolymers were recorded on a Cary 660 FTIR (Agilent, USA). ^1H NMR spectra in D_2O were registered on an impulse Fourier NMR spectrometer JNN-ECA 400 MHz (Jeol, Japan). Ultraviolet-visible (UV-Vis) spectra were collected using a Specord 210 plus, Germany. Dynamic light scattering (DLS) and zeta-potential measurements were implemented with the help of a Zetasizer Nano ZS 90 (Malvern, UK), equipped with a 633 nm laser source. Thermogravimetric analysis (TGA) was performed applying a LabSys Evo (Setaram, France).

Synthesis of polyampholyte terpolymers based on NIPAM-APTAC-AMPS

Polyampholyte terpolymers were synthesized via conventional redox initiated free radical (co)polymerization at 60 °C for 4 h. Briefly, the desired composition of the monomers was dissolved in de-ionized water at room temperature in a 50 mL beaker under constant stirring. After that the solution of monomers was filtered through a 5-micron syringe filter and purged with argon gas for 15-20 min to remove the dissolved oxygen. The solution then was carefully transferred to a screw cap vial and the dry APS and SMBS powders were added. The vial was immersed in a water bath with periodical shaking of the mixture. Later, the vial was removed from the water bath and cooled at room temperature. Obtained polymer solutions were dialyzed against distilled water for 72 h and then freeze-dried. Synthetic protocol of NIPAM-APTAC-AMPS

terpolymers is given in Table 1. It is seen that the yield of the terpolymers is high and varied from 80 to 93 wt.%.

Table 1

Synthetic protocol of NIPAM-APTAC-AMPS terpolymers

Initial monomer feed, mol. %			NIPAM, g	APTAC, g	AMPS, g	H ₂ O, mL	APS, mg	SMBS, mg	Yield, wt. %
NIPAM	APTAC	AMPS							
90	5	5	2	0.135	0.225	21.8	22	37	89.3
90	7.5	2.5	2	0.406	0.225				80
90	2.5	7.5	2	0.135	0.675				93

Determination of phase transition temperature of NIPAM-APTAC-AMPS terpolymers

The phase transition temperatures of NIPAM-APTAC-AMPS terpolymers in aqueous and aqueous-salt solutions (at the NaCl ionic strength $\mu = 0.001; 0.005; 0.01; 0.05; 0.1; 0.5$ and 1M) were determined by monitoring the change in the solution transmittance upon varying temperature. Aqueous and aqueous-salt solutions of NIPAM-APTAC-AMPS terpolymers are transparent at room temperature, i.e. when temperature is lower than LCST. When the temperature is above LCST, the solution appears as milky white and the transmittance decreases because the NIPAM-APTAC-AMPS terpolymers dehydrate and become more hydrophobic and thus less soluble in water. The phase transition experiments were carried out at $\lambda = 700\text{ nm}$ with the concentration of NIPAM-APTAC-AMPS terpolymers $0.1\text{ wt.}\%$, at the heating rate $0.5\text{ }^\circ\text{C}\cdot\text{min}^{-1}$ and in the temperature range $25\text{--}60\text{ }^\circ\text{C}$.

Results and Discussion

Synthesis and characterization of NIPAM-APTAC-AMPS terpolymers

Linear terpolymers of various compositions [NIPAM]:[APTAC]:[AMPS] = $90:5:5$; $90:7.5:2.5$; $90:2.5:7.5\text{ mol.}\%$, were synthesized via conventional redox initiated free radical polymerization (Fig. 1). The resulted terpolymer samples have randomly distributed charged units along the macromolecular chain [12].

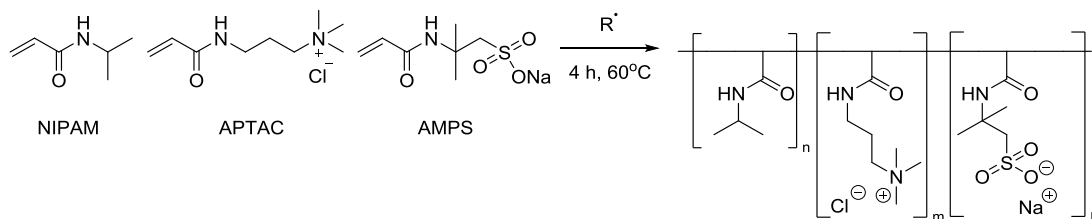


Figure 1. Schematic representation of free-radical polymerization of NIPAM, APTAC and AMPS monomers

The composition of the obtained terpolymers was established by $^1\text{H NMR}$ spectroscopy (Fig. 2).

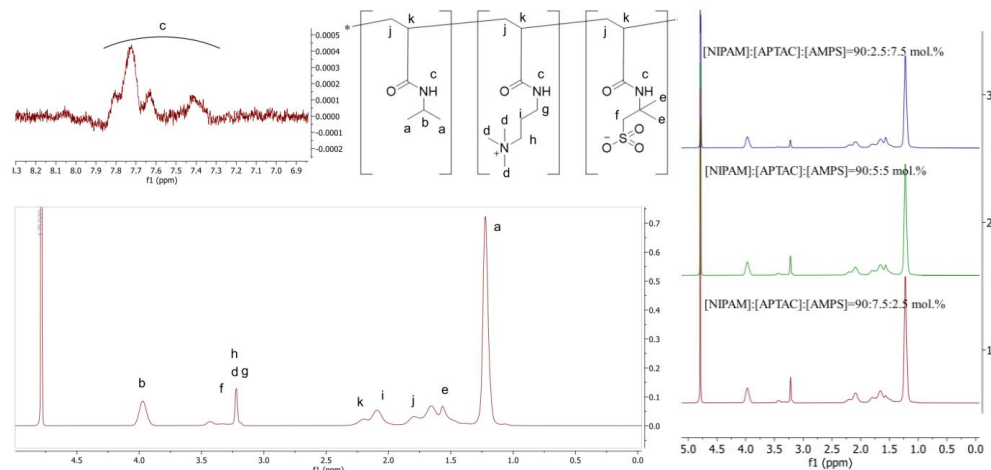


Figure 2. NMR spectra of NIPAM-APTAC-AMPS terpolymers and identification of proton signals

The resonance bands observed at 1.8 and 2.2 ppm were attributed to the protons of methylene and methine groups of the main chain of the terpolymers, respectively. Nevertheless, these peaks overlapped with the peaks of methyl and methylene protons of AMPS and APTAC. The resonance bands at 3.2–3.4 ppm were assigned to suspended protons of methyl and methylene groups in AMPS and APTAC. Since these signals were superimposed each other, the exact compositions of the NIPAM-APTAC-AMPS terpolymers could not be determined from the ^1H NMR spectra. Despite this, it can be assumed that the amount of APTAC and AMPS in terpolymers will be in good agreement with the initial monomer mixture, since the reactivity of all monomers is similar and close to one [12]. Taking into account all above reasons, it can be argued that the final composition of terpolymers possesses charge-balanced and charge-imbalanced structures. For instance, the amphoteric terpolymer $[\text{NIPAM}]:[\text{APTAC}]:[\text{AMPS}] = 90:5:5$ mol.% composed of the equal number of positively (APTAC) and negatively (AMPS) charged monomers refers to a charge-balanced polyampholyte, while the terpolymers $[\text{NIPAM}]:[\text{APTAC}]:[\text{AMPS}] = 90:7.5:2.5$ mol.% and $[\text{NIPAM}]:[\text{APTAC}]:[\text{AMPS}] = 90:2.5:7.5$ mol.% containing an excess of positively (APTAC) or negatively (AMPS) charged monomers belong to charge-imbalanced polyampholytes.

FTIR spectra of NIPAM-APTAC-AMPS terpolymers

Figure 3 illustrates FTIR spectra of the terpolymers. The wide absorption band in the region of $3200\text{--}3500\text{ cm}^{-1}$ corresponds to the secondary and tertiary amine groups, the absorption bands in the region of $2800\text{--}3000\text{ cm}^{-1}$ correspond to the asymmetric and symmetric vibrations of the CH groups. The absorption bands at 1650 and 1530 cm^{-1} belong to the vibrations of the N-substituted groups, i.e. to Amide I and Amide II, respectively. The absorption band at 1450 cm^{-1} is characteristic of bending vibrations of CH groups. The absorption band in the region of 1040 cm^{-1} corresponds to fluctuations of the S=O groups contained in the AMPS fragments.

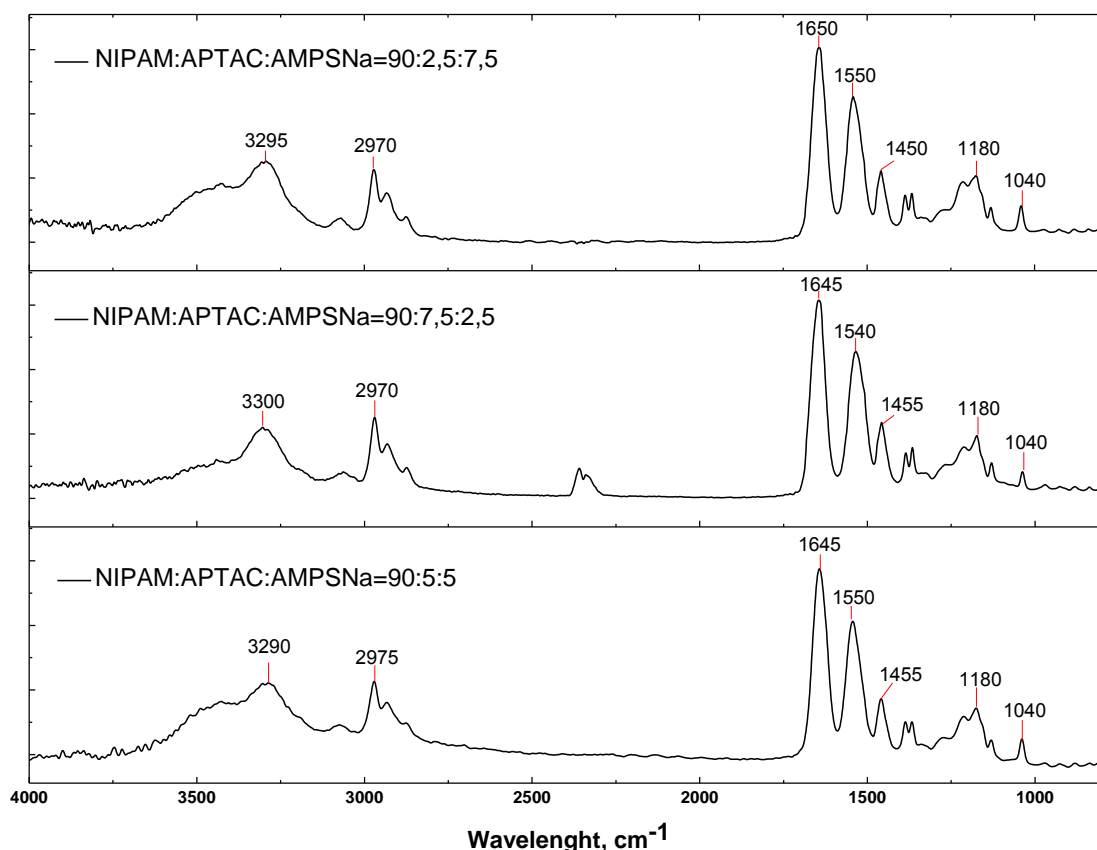
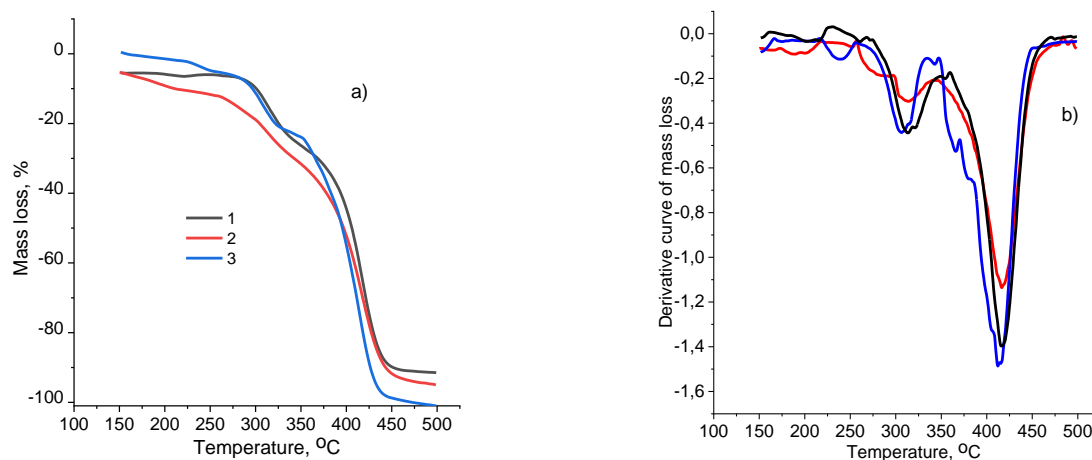


Figure 3. FTIR spectra of NIPAM-APTAC-AMPS terpolymers

TGA and DTA data of NIPAM-APTAC-AMPS terpolymers

Figure 4 shows the results of TGA and DTA. Dry terpolymers demonstrate a weight loss of approximately 5 % between room temperature and $150\text{ }^{\circ}\text{C}$. However, this additional weight loss is hard to assign to water loss alone, as the TGA and DTA data do not indicate a clear jump in this temperature range. In our

opinion, the weight loss up to approximately 200 °C may be a result of evaporation of residual water and beginning of the copolymers decomposition. The complete thermal decomposition of NIPAM-APTAC-AMPS terpolymers takes place in the temperature range from 413 to 417 °C.



Curve 1 — 90:5:5; curve 2 — 90:7.5:2.5; curve 3 — 90:2.5:7.5 mol.%

Figure 4. TGA thermograms (a) and differential curves (b) of copolymers NIPAM-APTAC-AMPS

The weight average molecular weight M_w , the number average molecular weight M_n , and the polydispersity index (PDI) of the NIPAM-APTAC-AMPS terpolymers

Table 2 represents the values of M_w , M_n and PDI for NIPAM-APTAC-AMPS terpolymers measured by gel-permeation chromatography in aqueous solution.

Table 2

The values of M_w , M_n and PDI for NIPAM-APTAC-AMPS terpolymers

Composition, mol. %			$M_w \times 10^{-5}$, Da	$M_n \times 10^{-4}$, Da	PDI = M_w/M_n
NIPAM	APTAC	AMPS			
90	5	5	1.4	4.6	≈ 3.0
90	7.5	2.5	0.5	3.1	≈ 1.6
90	2.5	7.5	2.5	6.4	≈ 4.0

The M_w of terpolymers is in the range of $(0.5-2.5) \cdot 10^5$ Dalton, the M_n is $(3.1-6.4) \cdot 10^4$ Dalton. The PDI of terpolymers is between 1.6 and 4.0. The broad molecular weight distribution of terpolymers is probably due to the use of free-radical polymerization method, which does not allow precise control of the molecular weights of polymers.

Zeta-potentials (ζ) of NIPAM-APTAC-AMPS amphoteric terpolymers in aqueous solutions at 25 °C

Zeta potentials of charge-balanced and charge-imbalanced NIPAM-APTAC-AMPS terpolymers in aqueous solution were measured as a function of polymer concentration (data is not shown). The terpolymer [NIPAM]:[APTAC]:[AMPS] = 90:7.5:2.5 mol.% with the excess of positively charged APTAC monomer independently on the polymer concentration (0.01–0.1 wt.%) has $\zeta = +7 \pm 1$ mV. In contrast, the amphoteric terpolymer [NIPAM]:[APTAC]:[AMPS] = 90:2.5:7.5 mol.% with the excess of negatively charged AMPS monomer slightly depends on concentration (0.01–0.1 wt.%) and has $\zeta = -16 \pm 3$ mV. It can be expected that in the ideal case, when the amount of positive and negative charges in [NIPAM]:[APTAC]:[AMPS] = 90:5:5 mol.% is equal and compensates each other, the total charge of macromolecular chain is electroneutral, the value of ζ should be around zero. However, in our case, the ζ value of the charge-balanced amphoteric terpolymer [NIPAM]:[APTAC]:[AMPS] = 90:5:5 deviates from zero and is slightly positive independently on polymer concentration (0.01–0.1 wt.%). Its value equals $+2 \pm 1$ mV probably due to a tiny excess of the positively charged APTAC monomer. Thus, the fact that we have synthesized the charge-balanced and charge-imbalanced amphoteric terpolymers is obvious.

The average hydrodynamic size and the phase transition temperature of [NIPAM]:[APTAC]:[AMPS] = 90:5:5 mol.% in pure water and salt solutions

The average hydrodynamic size (R_h) and the phase transition temperature ($T_{p.t.t.}$) of charge-balanced amphoteric terpolymer [NIPAM]:[APTAC]:[AMPS] = 90:5:5 mol.% in deionized (DI) water and in NaCl solutions ($\mu = 0.001; 0.005; 0.01; 0.05; 0.1; 0.5; 1\text{ M NaCl}$) are presented in Figures 5 and 6.

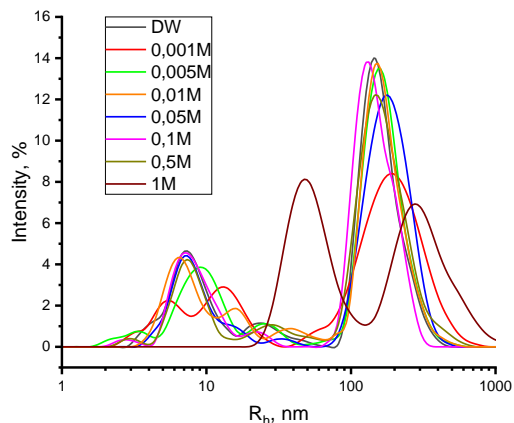


Figure 5. The effect of the μ on the average hydrodynamic size of [NIPAM]:[APTAC]:[AMPS] = 90:5:5 mol.% at 25 °C

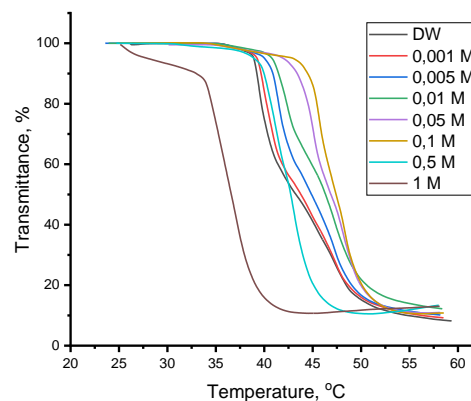


Figure 6. Temperature dependent phase behavior of terpolymer [NIPAM]:[APTAC]:[AMPS] = 90:5:5 mol.% at various μ

Figure 5 illustrates presence of two types of particles in solutions. Average peak value of R_h of [NIPAM]:[APTAC]:[AMPS] = 90:5:5 mol.% equals to 7.4 and 150 nm in pure water. Evidently that 7.4 nm represents individual macromolecules, whereas 150 nm corresponds to multimolecular aggregates. The relative contribution of the aggregates in the intensity distributions is large due to their high mass, though they are minor by their number. The individual chains of amphoteric terpolymer in deionized water may be imagined as well swollen coils since water is a good solvent for PNIPAM at room temperature. However, $R_h=7.4$ nm is not big enough for such a molecule. One should remember that the oppositely charged repeating units of the chain are attracted to each other and can form ion pairs similar to intrapolyelectrolyte complexes in pure water. Their low-molar-mass counterions become free, leave to the bulk water and this way increase the total entropy of the system. Addition of low-molar-mass salt makes this entropic effect less pronounced: added salt breaks the intramolecular ionic pairs and chains become effectively more charged with increasing the ionic strength, though the number of charges along each chain remains constant. Coulomb interactions of ion pairs act on longer distances than H-bonds between PNIPAM and water and create polar regions of bound water within each coil, which enhance total stability of the copolymer against phase separation upon heating.

The model presented above is fully supported by experiments. The phase transition temperature ($T_{p.t.t.}$) of [NIPAM]:[APTAC]:[AMPS] = 90:5:5 mol.% in DI water equals to 38.7 °C (see Table 3) and bigger than $T_{p.t.t.}$ of poly(NIPAM) itself (that is 32 °C) [4]. When the ionic strength (μ) increases, the ion pairs between AMPS and APTAC break apart, copolymer becomes effectively more charged and $T_{p.t.t.}$ shifts to the higher values. At μ above 0.1 M, all ionic pairs are not only broken but added salt screens all the charges of copolymer and original thermal behavior of pure poly(NIPAM) is recovered.

Two phenomena should be discussed separately: 1) Aggregates formed by the copolymer above the phase transition temperature ($T_{p.t.t.}$) are stable against further precipitation; 2) Transmittance vs. temperature curves show a shoulder above $T_{p.t.t.}$ at μ below 0.1 M. Formation of neutral colloiddally stable multimolecular aggregates by poly(NIPAM) has been well-documented and mechanisms responsible for their stability have been suggested [1, 5]. Existence of hydrated ion pairs from AMPS and APTAC within coils additionally contribute to the stability of particles above $T_{p.t.t.}$. Naturally, when aggregates are formed and dehydrate upon further heating, charged units cannot stay inside the organic surrounding, and they migrate to the surface of the aggregates, which is observed as a shoulder in the transmittance curves (Figure 6).

The conformational change of [NIPAM]:[APTAC]:[AMPS] = 90:5:5 mol.% in pure water upon heating is schematically shown in Figure 7. Dehydration of NIPAM fragments and intensification of hydrophobic

interactions with increasing of temperature lead to the formation of a high-density hydrophobic NIPAM “core” surrounded by low-density hydrophilic “shell”. The latter consists of AMPS and APTAC monomers that preserve the whole macromolecules in water and protect them from precipitation.

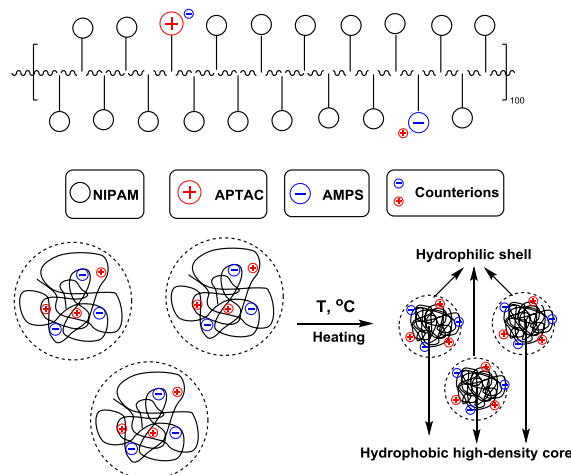


Figure 7. Schematic representation of [NIPAM]:[APTAC]:[AMPS] = 90:5:5 mol.% terpolymer in DI water upon heating

At the interval of the $\mu = 0.001\text{-}0.1\text{M}$ NaCl, the mean R_h values are equal to 7 ± 1 nm and 175 ± 25 nm. However, the value of $T_{p.t.t.}$ gradually increases from 39.88 °C in DI water to 46.08 °C in 0.1M NaCl upon heating (Table 3).

Table 3

The effect of the ionic strength (μ) on the phase transition temperature of [NIPAM]:[APTAC]:[AMPS]=90:5:5 mol.%

μ , mol·L ⁻¹ (NaCl)	DI water	0.001	0.005	0.01	0.05	0.1	0.5	1.0
$T_{p.t.t.}$, °C	39.88	40.29	41.93	41.96	45.5	46.08	42.96	36.84

These results can be explained as follows. Upon heating the swollen in DI water macromolecular chains of amphoteric terpolymer due to strengthening of the hydrophobic interactions are supposed to transform to high-density hydrophobic “core” consisting of mostly NIPAM monomers. At the same time, an increase in the ionic strength adjusted by NaCl that strengthens the compactization of the NIPAM chains, but weakens the electrostatic attraction between positively and negatively charged monomers. As a result, the hydrophilic edge (or a low-density hydrophilic “shell”) consisting of AMPS and APTAC monomers is formed on the surface of compact macromolecules and preserves the polymer particles from precipitation (Fig. 8).

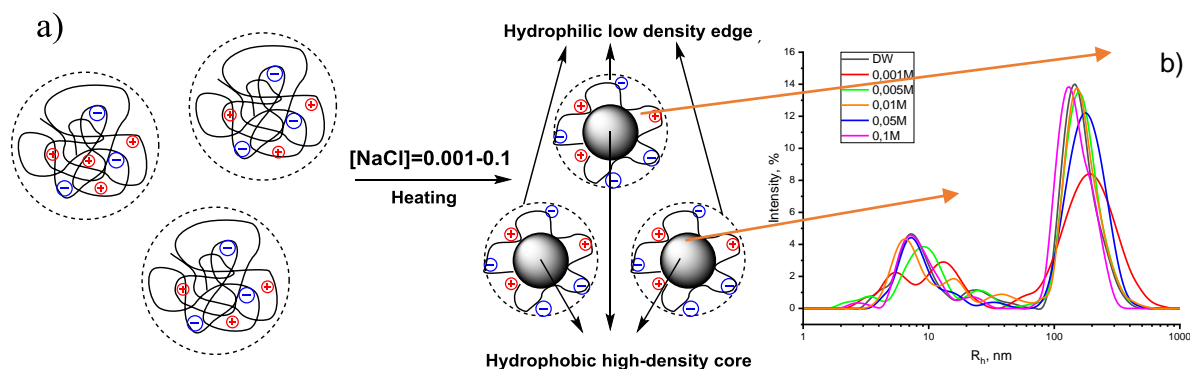


Figure 8. Schematic representation of [NIPAM]:[APTAC]:[AMPS] = 90:5:5 mol.% macromolecules at the interval of $\mu = 0.001\text{-}0.1\text{M}$ NaCl upon heating (a) DLS data at $\mu = 0.001\text{-}0.1\text{M}$ NaCl (b)

However, in 1M NaCl solution the R_h maxima are shifted to 50 and 300 nm, respectively. Apparently, the macromolecular coils are aggregated at high μ . This statement is confirmed by the effect of temperature on the phase behavior of terpolymer [NIPAM]:[APTAC]:[AMPS] = 90:5:5 mol.% in dependence of μ as represented in Figure 9. At the interval of μ between 0.5 and 1M NaCl the $T_{p.t.t.}$ decreases from 39.5 °C to 33.2 °C (see Table 3). The reversal or backward change of the $T_{p.t.t.}$ in 0.5 and 1M NaCl solutions is probably due to aggregation of small particles to bigger one as demonstrated in Figure 9 and confirmed by DLS data. However, in 0.5 and 1M NaCl solutions the precipitation of aggregated macromolecular particles does not occur because the hydrophilic “shell” on the surface of such aggregates preserves them from precipitation.

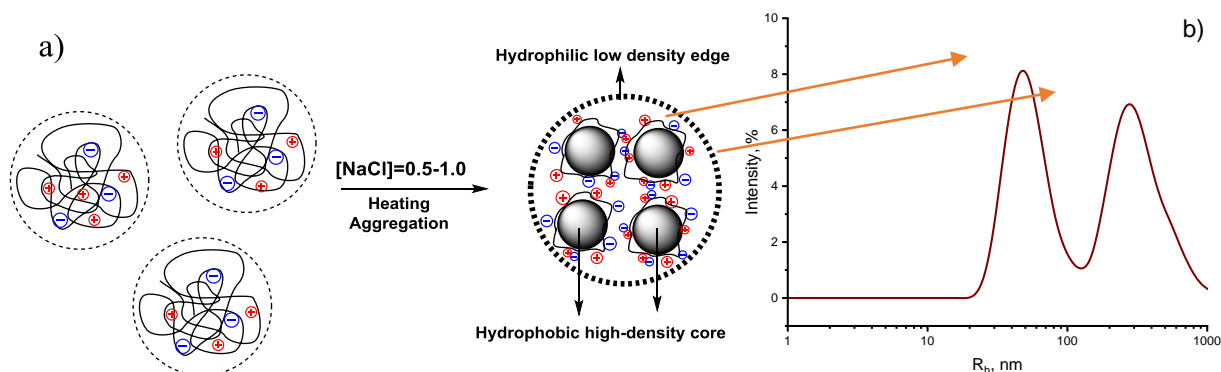


Figure 9. Schematic representation of macromolecular size of [NIPAM]:[APTAC]:[AMPS] = 90:5:5 mol.% at the ionic strength 0.5 and 1M NaCl upon heating (a) and DLS data in 1M NaCl (b)

Thus, as follows from the obtained results, the macromolecular chains of [NIPAM]:[APTAC]:[AMPS] = 90:5:5 mol.% in DI water collapse upon heating due to the dehydration of NIPAM chains and enhancement of hydrophobic interactions. At the interval of $\mu = 0.001-0.1$ M NaCl macromolecular chains gradually shrink upon heating but preserve the solubility in spite of the turbidity. At high ionic strength $\mu = 0.5-1$ M NaCl the formation of bigger aggregates is observed.

The average hydrodynamic size and phase transition temperature of [NIPAM]:[APTAC]:[AMPS] = 90:2.5:7.5 mol.% in aqueous and aqueous-salt solutions

Figure 10 represents the average hydrodynamic size of amphoteric terpolymer [NIPAM]:[APTAC]:[AMPS] = 90:2.5:7.5 mol.% in DI water and in NaCl solutions ($\mu = 0.001; 0.005; 0.01; 0.05; 0.1;$ and 0.5M). In 1M NaCl the terpolymer was insoluble. The average hydrodynamic radius of macromolecules R_h at $\mu = 0.001; 0.005; 0.01; 0.05; 0.1$ M NaCl is about 20-35 nm, but in 0.5M NaCl solution two obvious peaks are observed with R_h equal to 20 and 200 nm.

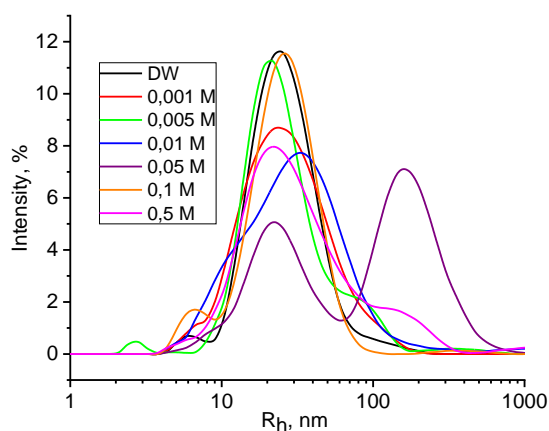


Figure 10. Effect of the μ on the average hydrodynamic size of [NIPAM]:[APTAC]:[AMPS] = 90:2.5:7.5 mol.% at 25 °C

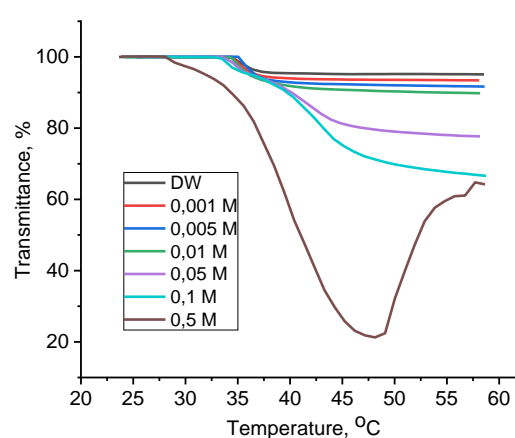


Figure 11. Temperature dependent phase behavior of terpolymer [NIPAM]:[APTAC]:[AMPS] = 90:2.5:7.5 mol.% at different μ

The effect of temperature on the phase behavior of terpolymer [NIPAM]:[APTAC]:[AMPS] = 90:2.5:7.5 mol.% in DI water and at $\mu = 0.001\text{--}0.5\text{M}$ NaCl is demonstrated in Table 4 and Figure 11.

Table 4

The effect of the ionic strength (μ) on the phase transition temperature of [NIPAM]:[APTAC]:[AMPS]=90:2.5:7.5 mol.%

μ , mol·L ⁻¹ (NaCl)	DI water	0.001	0.005	0.01	0.05	0.1	0.5	1.0
$T_{p.t.t.}$, °C	35.45	35.38	35.98	35.33	34.41	34.48	39.42	insoluble

At the interval of μ between 0.001 and 0.05M NaCl the $T_{p.t.t.}$ is slightly shifted to lower or higher temperatures. In this range a gradual increase of the turbidity is observed. Increasing of the μ up to 0.5M NaCl leads to early phase separation of the polymer at 28 °C. At $\mu = 0.5\text{ M}$ NaCl there are fractures on the turbidity curves and the transparency decreases in the range of 40–47.5 °C. Further heating of polymer solution at $T > 47.5\text{ °C}$ causes the precipitation of polymer chains due to the salting-out effect, which leads to a significant increase in transparency.

The average hydrodynamic size and phase transition temperature of [NIPAM]:[APTAC]:[AMPS] = 90:7.5:2.5 mol.% in aqueous and aqueous-salt solutions

In case of [NIPAM]:[APTAC]:[AMPS] = 90:7.5:2.5 mol.% terpolymer, the average hydrodynamic size of macromolecules changes insignificantly as a function of the ionic strength (Fig. 12). The average size of R_h lies in the regions of 6–8 nm and 150–300 nm.

The effect of temperature on the $T_{p.t.t.}$ of the terpolymer [NIPAM]:[APTAC]:[AMPS] = 90:7.5:2.5 mol.% at different ionic strength of the solution is shown in Table 5 and Figure 13.

Table 5

The effect of the ionic strength (μ) on the phase transition temperature of [NIPAM]:[APTAC]:[AMPS]=90:7.5:2.5 mol.%

μ , mol·L ⁻¹ (NaCl)	DI water	0.001	0.005	0.01	0.05	0.1	0.5	1.0
$T_{p.t.t.}$, °C	38.98	37.16	38.35	38.85	42.33	43.2	37.21	37.51

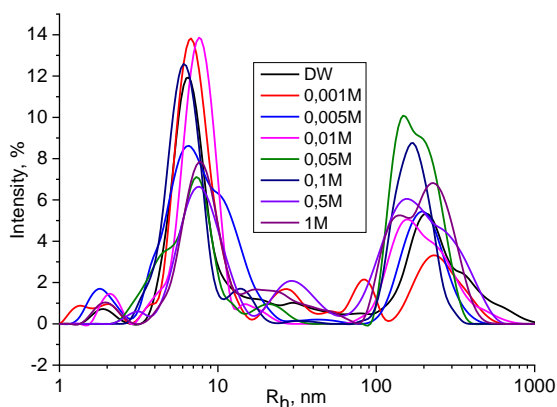


Figure 12. Effect of the ionic strength of the solution on the average hydrodynamic size of [NIPAM]:[APTAC]:[AMPS] = 90:7.5:2.5 mol.% at 25 °C

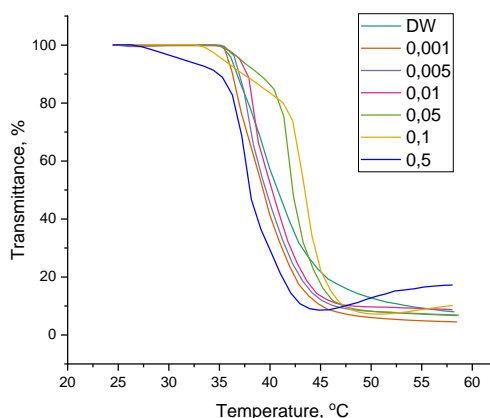


Figure 13. Temperature dependent phase behavior of [NIPAM]:[APTAC]:[AMPS] = 90:7.5:2.5 mol.% at different μ

Increasing of the μ in the range of 0.001–0.1M gradually shifts the $T_{p.t.t.}$ to higher temperatures. This is probably due to the screening of positively charged APTAC fragments by NaCl counterions. However, at a higher ionic strength $\mu = 0.5\text{--}1.0\text{M}$ NaCl the $T_{p.t.t.}$ shifts backward, e.g. to lower temperatures. Apparently, at a high NaCl concentration, the polyelectrolyte effect caused by the excess of positive charges is completely suppressed, and the macromolecular chain becomes close to neutral and more hydrophobic. An increase in temperature enhances the hydrophobic interactions and aggregation of macromolecular chains. Thus, in aqueous-salt solutions the behavior of charge balanced amphoteric terpolymer

([NIPAM]:[APTAC]:[AMPS] = 90:5:5 mol.%) differs from the properties of unbalanced polyampholytes ([NIPAM]:[APTAC]:[AMPS] = 90:7.5:2.5 mol.% and [NIPAM]:[APTAC]:[AMPS] = 90:2.5:7.5 mol.%). A small excess of positive or negative charges in terpolymers leads to the predominance of polyelectrolyte effect. Expanded in pure water polyelectrolyte chains shrink in salt solution due to the screened electrostatic repulsion between uniformly charged monomers (polyelectrolyte effect). Compact structure of charge-balanced quenched polyampholyte unfolds in salt solution due to screening of the electrostatic attraction between oppositely charged monomers (the antipolyelectrolyte effect).

Conclusions

The structure of new amphoteric terpolymers NIPAM-AMPS-APTAC, synthesized by free-radical polymerization of neutral (NIPAM), anionic (AMPS), and cationic (APTAC) monomers was identified by ^1H NMR and FTIR spectroscopy. In aqueous and aqueous-salt solutions, the dynamic light scattering (DLS) data show a bimodal distribution of the average hydrodynamic size of amphoteric macromolecules. Zeta-potential measurements confirm the formation of charge-balanced and charge-imbalanced amphoteric terpolymers. In aqueous and aqueous-salt solutions the amphoteric terpolymers based on NIPAM-AMPS-APTAC demonstrate the temperature-responsive behavior upon heating. The temperature and salt-induced phase transition of amphoteric terpolymers is associated with the hydrophobic-hydrophilic balance and the formation of high-density of hydrophobic “core” surrounded by low-density hydrophilic “shell”. In case of charge-balanced amphoteric terpolymer [NIPAM]:[APTAC]:[AMPS] = 90:5:5 mol.%, the phase transition temperature increases and passes through the maximum at $\mu = 0.1\text{M}$ NaCl. A similar phenomenon is observed for the charge-imbalanced terpolymer [NIPAM]:[APTAC]:[AMPS] = 90:7.5:2.5 mol.% with the excess of cationic monomer (APTAC). The temperature-dependent phase transition of charge-imbalanced terpolymer [NIPAM]:[APTAC]:[AMPS] = 90:2.5:7.5 mol.% with the excess of anionic monomer (AMPS) exhibits complicated behavior at high ionic strength up to phase separation. The phase transition temperature of amphoteric terpolymers can be finely tuned to the desired one by adding the salt. The combination of different stimuli within one macromolecular chain can open up a wide space of sensing applications, in particular as a drug delivery system.

Acknowledgments

This research has been funded by the Science Committee of the Ministry of Education and Science of the Republic of Kazakhstan (Grant No. AP08855552). Vladimir Olegovich Aseyev and Sarkyt Elekenovich Kudaibergenov thank the Horizon 2020 research and innovation program of the European Union Maria Sklodowska-Curie (grant agreement 823883-NanoPol-MSCA-RISE-2018) for financial support.

References

- 1 Aseyev V. Non-ionic thermoresponsive polymers in water / V. Aseyev, H. Tenhu, F. Winnik // *Advances in Polymer Science*. — 2011. — Vol. 242. — P. 29–89. DOI: 10.1007/12_2010_57.
- 2 Heskins M. Solution properties of poly(N-isopropylacrylamide) / M. Heskins, J.E. Guillet // *Journal of Macromolecular Science: Part A — Chemistry*. — 1968. — Vol. 2. — P. 1441-1455. <https://doi.org/10.1080/10601326808051910>
- 3 Schild G.H. Poly(N-isopropylacrylamide): experiment, theory and application / G.H. Schild // *Progress in Polymer Science*. — 1992. — Vol. 17. — P. 163-249. [https://doi.org/10.1016/0079-6700\(92\)90023-R](https://doi.org/10.1016/0079-6700(92)90023-R)
- 4 McNaught A.D. IUPAC Compendium of Chemical Terminology (the "Gold Book") / A.D. McNaught, A. Wilkinson. — Blackwell Scientific Publications, 1997. DOI: 10.1351/goldbook
- 5 Aseyev V. Temperature dependence of the colloidal stability of neutral amphiphilic polymers in water / V. Aseyev, H. Tenhu, F. Winnik // *Advances in Polymer Science*. — 2006. — Vol. 196. — P. 1–85. https://doi.org/10.1007/12_052.
- 6 Burova T.V. Unusual conformational behavior of complexes of poly(N-isopropylacrylamide) with poly(methacrylic acid) / T.V. Burova, N.V. Grinberg, V.Ya. Grinberg, E.V. Kalinina, V.I. Lozinsky, V.O. Aseyev, S. Holappa, H. Tenhu, A.R. Khokhlov // *Macromolecules*. — 2005. — Vol. 38. — P. 1292–1299. <https://doi.org/10.1021/ma0486851>
- 7 Max J.B. Triple-responsive polyampholytic graft copolymers as smart sensors with varying output / J.B. Max, A. Nabiyan, J. Eichhorn, F.H. Schacher // *Macromolecular Rapid Communications*. — 2021. — Vol. 42. — P. 2000671. <https://doi.org/10.1002/marc.202000671>
- 8 Cao Z.F. Preparation and properties of a dually responsive hydrogels based on polyampholyte for oral delivery of drugs / Z.F. Cao, Y. Jin, Q. Miao // *Polymer Bulletin*. — 2013. — Vol. 70. — P. 2675–2689. <https://doi.org/10.1007/s00289-013-0975-3>
- 9 Cheng J. Triple stimuli-responsive N-isopropylacrylamide copolymer toward metal ion recognition and adsorption via a thermally induced sol–gel transition / J. Cheng, G. Shan, P. Pan // *Industrial & Engineering Chemistry Research*. — 2017. — Vol. 56(5). — P. 1223–1232. <https://doi.org/10.1021/acs.iecr.6b03626>
- 10 Kudaibergenov S.E. *Polyampholytes: Synthesis, Characterization and Application* / S.E. Kudaibergenov. — New York, NY: Springer Science+Business Media, 2002.

- 11 Kudaibergenov S.E. Polyampholytes: Past, Present, Perspectives / S.E. Kudaibergenov. — Almaty: Center of Operative Printing, 2021.
- 12 Braun O. Synthesis in microemulsion and characterization of stimuli-responsive polyelectrolytes and polyampholytes based on N-isopropylacrylamide / O. Braun, J. Selb, F. Candau // Polymer. — 2001. — Vol. 42. — P. 8499–8510. [https://doi.org/10.1016/S0032-3861\(01\)00445-1](https://doi.org/10.1016/S0032-3861(01)00445-1)
- 13 Ogawa K. Preparation and characterization of thermosensitive polyampholyte nanogels / K. Ogawa, A. Nakayama, E. Kokufuta // Langmuir. — 2003. — Vol. 19. — P. 3178–3184. <https://doi.org/10.1021/la0267185>
- 14 Li X. Volume phase transition temperature tuning and investigation of the swelling–deswelling oscillation of responsive microgels / X. Li, J. Zuo, Y. Guo, L. Cai, S. Tang, W. Yang // Polymer International. — 2007. — Vol. 56. — P. 968–975. <https://doi.org/10.1002/pi.2221>
- 15 Weaver L.G. Temperature-responsive methacrylamide polyampholytes / L.G. Weaver, R. Stockmann, S.H. Thang, A. Postma // RSC Advances. — 2017. — Vol. 7. — P. 31033–31041. DOI: 10.1039/c7ra04723a
- 16 Deen G.R. New stimuli-responsive polyampholyte: Effect of chemical structure and composition on solution properties and swelling mechanism / G.R. Deen, T.T. Wei, L.K. Fatt // Polymer. — 2016. — Vol. 104. — P. 91–103. <https://doi.org/10.1016/j.polymer.2016.09.094>
- 17 Maji S. Dual pH and thermoresponsive alternating polyampholytes in alcohol/water solvent mixtures / S. Maji, V.V. Jerca, R. Hoogenboom // Polymer Chemistry. — 2020. — Vol. 11. — P. 2205–2211. <https://doi.org/10.1039/D0PY00032A>

А.Е. Аязбаева, А.В. Шахворостов, Т.М. Сейлханов, В.О. Асеев, С.Е. Құдайбергенов

Акриламид туындыларының негізінде алынған жаңа термо- және тұзға сезімтал амфотерлік терполимерлерді синтездеу және зерттеу

Бейтарап мономер N-изопропилакриламид (НИПАМ), аниондық мономер — 2-акриламидо-2-метил-1-пропансульфон қышқылының натрий тұзы (АМПС) және (3-акриламидопропил) триметиламмоний хлориді (АПТАХ) негізіндегі жаңа жоғары зарядталған полиамфолиттер сулы ерітіндіде бос радикалды полимерлену жолымен синтезделді және ¹H ЯМР және ИК-Фурье спектроскопиясымен, ТГА, ГӨХ, ДЛС және дзета-потенциал әдістерімен сипатталды. Өртүрлі құрамдағы үштік амфотерлі полимерлер, атап айтқанда [НИПАМ]:[АМПС]:[АПТАХ] = 90:2.5:7.5; 90:5:5; 90:7.5:2.5 мол.%, температураның 25 пен 60 °C аралығында және ерітіндінің иондық күшінің 10⁻³ пен 1M NaCl аралығында зерттелді. Гидрофобты/гидрофильді тепе-теңдіктің арқасында макромолекулалық тізбектердің температураға байланысты конформациялық және фазалық өзгерісі тұз қосылыстарына сезімтал болып, фазалық ауысулардың жақсы реттелуіне мүмкіндік беретіні анықталды. Су мен тұзды-су ерітінділеріде амфотерлі терполимерлердің орташа гидродинамикалық өлшемдері бөлме температурасында бимодальды таралуды көрсете отырып, 8-ден 300 нм-ге дейін өзгереді. Амфотерлі терполимерлердің сандық орташа (M_n) және салмақтық орташа (M_w) молекулалық салмақтары, полидисперстілік индексі (ПДИ) және дзета потенциалдары су ерітіндісінде анықталды.

Кілт сөздер: күшті зарядталған амфотерлі терполимерлер, термосезімталдық, тұзғасезімталдық, конформациялық және фазалық ауысу, гидрофобты/гидрофильді тепе-теңдік, ядро-қабықша құрылымы.

А.Е. Аязбаева, А.В. Шахворостов, Т.М. Сейлханов, В.О. Асеев, С.Е. Құдайбергенов

Синтез и исследование новых термо- и солечувствительных амфотерных терполимеров на основе производных акриламида

Новые сильнозаряженные линейные полиамфолиты на основе нейтрального мономера — N-изопропилакриламида (НИПАМ), анионного мономера — натриевой соли 2-акриламидо-2-метил-1-пропансульфоновой кислоты (АМПС) и катионного мономера — (3-акриламидопропил) триметиламмоний хлорида (АПТАХ) синтезированы свободнорадикальной полимеризацией в водном растворе и охарактеризованы методами ¹H ЯМР и ИК-Фурье спектроскопии, ТГА, ГПХ, ДЛС и дзета-потенциала. Термо- и солечувствительность амфотерных тройных полимеров различных составов, в частности, [НИПАМ]:[АМПС]:[АПТАХ] = 90:2.5:7.5; 90:5:5; 90:7.5:2.5 мол.%, изучена в диапазоне температур от 25 до 60 °C и в интервале ионной силы раствора от 10⁻³ до 1M NaCl. Найдено, что благодаря гидрофобно-гидрофильному балансу, конформационные и фазовые изменения макромолекулярных цепей в зависимости от температуры становятся чувствительными к добавкам соли и позволяют тонко регулировать фазовые переходы. В воде и водно-солевом растворе среднегидродинамические размеры амфотерных терполимеров изменяются в пределах от 8 до 300 нм, проявляя бимодальное распределение при комнатной температуре. Определены среднечисленные (M_n) и средневесовые (M_w) молекулярные массы, индекс полидисперсности (ИПД) и дзета-потенциалы амфотерных терполимеров в водном растворе.

Ключевые слова: сильнозаряженные амфотерные терполимеры, термочувствительность, солечувствительность, конформационный и фазовый переходы, гидрофобно/гидрофильный баланс, структура «ядро–оболочка».

References

- 1 Aseyev, V., Tenhu, H., Winnik, F. (2011). Non-ionic thermoresponsive polymers in water. *Advances in Polymer Science*, 242, 29–89. DOI: 10.1007/12_2010_57.
- 2 Heskins, M., Guillet, J.E. (1968). Solution properties of poly(N-isopropylacrylamide). *Journal of Macromolecular Science: Part A. Chemistry*, 2, 1441–1455. <https://doi.org/10.1080/10601326808051910>
- 3 Schild, G.H. (1992). Poly(N-isopropylacrylamide): experiment, theory and application. *Progress in Polymer Science*, 17, 163–249. [https://doi.org/10.1016/0079-6700\(92\)90023-R](https://doi.org/10.1016/0079-6700(92)90023-R)
- 4 McNaught, A.D., Wilkinson, A. (1997). *IUPAC Compendium of Chemical Terminology (the "Gold Book")*. Blackwell Scientific Publications. DOI: 10.1351/goldbook
- 5 Aseyev, V., Tenhu, H., Winnik, F. (2006). Temperature dependence of the colloidal stability of neutral amphiphilic polymers in water. *Advances in Polymer Science*, 196, 1–85. DOI: 10.1007/12_052.
- 6 Burova, T.V., Grinberg, N.V., Grinberg, V.Ya., Kalinina, E.V., Lozinsky, V.I., Aseyev, V.O., Holappa, S., Tenhu, H., & Khokhlov, A.R. (2005). Unusual conformational behavior of complexes of poly(N-isopropylacrylamide) with poly(methacrylic acid). *Macromolecules*, 38, 1292–1299. <https://doi.org/10.1021/ma0486851>
- 7 Max, J.B., Nabiyani, A., Eichhorn, J., & Schacher, F.H. (2021). Triple-responsive polyampholytic graft copolymers as smart sensors with varying output. *Macromolecular Rapid Communications*, 42, 2000671. DOI: 10.1002/marc.202000671
- 8 Cao, Z.F., Jin, Y., & Miao, Q. (2013). Preparation and properties of a dually responsive hydrogels based on polyampholyte for oral delivery of drugs. *Polymer Bulletin*, 70, 2675–2689. <https://doi.org/10.1007/s00289-013-0975-3>
- 9 Cheng, J., Shan, G., & Pan, P. (2017). Triple stimuli-responsive N-isopropylacrylamide copolymer toward metal ion recognition and adsorption via a thermally induced sol–gel transition. *Industrial & Engineering Chemistry Research*, 56(5), 1223–1232. <https://doi.org/10.1021/acs.iecr.6b03626>
- 10 Kudaibergenov, S.E. (2002). *Polyampholytes: Synthesis, Characterization and Application*. New York, NY: Springer Science+Business Media.
- 11 Kudaibergenov, S.E. (2021). *Polyampholytes: Past, Present, Perspectives*. Almaty: Center of Operative Printing.
- 12 Braun, O., Selb, J., & Candau, F. (2001). Synthesis in microemulsion and characterization of stimuli-responsive polyelectrolytes and polyampholytes based on N-isopropylacrylamide. *Polymer*, 42, 8499–8510. [https://doi.org/10.1016/S0032-3861\(01\)00445-1](https://doi.org/10.1016/S0032-3861(01)00445-1)
- 13 Ogawa, K., Nakayama, A., & Kokufuta, E. (2003). Preparation and characterization of thermosensitive polyampholyte nanogels. *Langmuir*, 19, 3178–3184. DOI: 10.1021/la0267185
- 14 Li, X., Zuo, J., Guo, Y., Cai, L., Tang, S., & Yang, W. (2007). Volume phase transition temperature tuning and investigation of the swelling–deswelling oscillation of responsive microgels. *Polymer International*, 56, 968–975. <https://doi.org/10.1002/pi.2221>
- 15 Weaver, L.G., Stockmann, R., Thang, S.H., & Postma, A. (2017). Temperature-responsive methacrylamide polyampholytes. *RSC Advances*, 7, 31033–31041. DOI: 10.1039/c7ra04723a
- 16 Deen, G.R., Wei, T.T., & Fatt, L.K. (2016). New stimuli-responsive polyampholyte: Effect of chemical structure and composition on solution properties and swelling mechanism. *Polymer*, 104, 91–103. <https://doi.org/10.1016/j.polymer.2016.09.094>
- 17 Maji, S., Jerca, V.V., & Hoogenboom, R. (2020). Dual pH and thermoresponsive alternating polyampholytes in alcohol/water solvent mixtures. *Polymer Chemistry*, 11, 2205–2211. <https://doi.org/10.1039/D0PY00032A>

Information about the authors

Ayazbayeva Aigerim Yerlanovna (*corresponding author*) — PhD student. Satbayev University, Kazakhstan, Almaty, 050013, Satpayev str., 22. E-mail: ayazbayeva.aigerim@gmail.com; <https://orcid.org/0000-0003-1313-895X>

Shakhvorostov, Alexey Valerievich — PhD. Institute of Polymer Materials and Technology, Kazakhstan, Almaty, 050019, Atyrau-1, 3/1. E-mail: alex.hv91@gmail.com; <https://orcid.org/0000-0003-3502-6123>

Seilkhanov, Tolegen Muratovich — Candidate of Chemical Sciences, Head of the laboratory of engineering profile NMR spectroscopy of Kokshetau State University named after Sh. Ualikhanov MES RK, Kazakhstan, Kokshetau, 020000, Abay str., 76. E-mail: tseilkhanov@mail.ru; <https://orcid.org/0000-0003-0079-4755>

Aseyev, Vladimir Olegovich — Doctor of Chemical Sciences, Professor, Lecturer of University of Helsinki, Finland, Helsinki, 000100, Yliopistonkatu str., 4. e-mail: Vladimir.Aseyev@helsinki.fi; <https://orcid.org/0000-0002-3739-8089>

Kudaibergenov, Sarkyt Elekenovich — Full Professor, Doctor of Chemical Sciences, Director of Institute of Polymer Materials and Technology, Kazakhstan, Almaty, 050019, Atyrau-1, 3/1. E-mail: skudai@mail.ru; <https://orcid.org/0000-0002-1166-7826>

Zh.S. Nurmaganbetov¹, G.K. Mukusheva^{2*}, Ye.V. Minayeva², D.M. Turdybekov³,
K.M. Turdybekov², A.S. Makhmutova¹, A.R. Zhasymbekova², O.A. Nurkenov⁴

¹Karaganda Medical University, Karaganda, Kazakhstan;

²Karagandy University of the name of academician E.A. Buketov, Karaganda, Kazakhstan;

³Karaganda Technical University, Karaganda, Kazakhstan;

⁴Institute of Organic Synthesis and Coal Chemistry, Karaganda, Kazakhstan

(*Corresponding authors e-mail: mukusheva1977@list.ru)

Synthesis, quantum-chemical calculations and virtual screening of the alkaloid cytosine derivatives

The synthesis of some cytosine derivatives was carried out in the work. The article provides the data of quantum-chemical calculation and virtual screening of the alkaloid cytosine derivatives synthesized. At the same time, the reaction centers of the cytosine derivatives molecules were determined. In order to study the reactivity of the derivatives obtained (namely cinnamoylcytosine, lipoylcytosine, and cytosinylisoalantholactone) the quantum-chemical calculations were conducted to determine the energy and charge characteristics of the molecules. The results indicate a sufficient thermodynamic stability of the cinnamoylcytosine and lipoylcytosine molecules. The cytosinylisoalantholactone molecule is not stable according to the results of quantum chemical calculations. The data on the energy values of the frontier molecular orbitals show that, in general, all molecules exhibit electrophilic properties. A bioprediction was implemented using PASS (Prediction of Activity Spectra for Substances) as one of the most efficient and well-known computer program with the aim of detailed study and the probable establishment of the biological activity of the synthesized cytosine derivatives. Based on the results of virtual screening, promising types of alkaloid cytosine derivatives were identified, which are potential sources of original drugs.

Keywords: alkaloids, cytosine, synthesis, physicochemical properties, derivatives, quantum-chemical calculation, virtual screening, prediction of activity spectra for substances.

Introduction

Carrying out directed synthetic transformations of available substances of plant origin in order to create new biologically active compounds is an actively developing area of fine organic synthesis and medicinal chemistry [1–4]. Taking into account the valuable biological properties of alkaloids and their derivatives, the search for new ways of chemical modification of alkaloids is undoubtedly relevant, and the attention of researchers is attracted by the obtaining of more complexly constructed heterocyclic systems. Interest in research on the chemical transformation of the alkaloid cytosine is due to the wide spectrum of biological activity of its derivatives. To date, a large number of derivatives of the cytosine alkaloid with various groups at the nitrogen atom have been synthesized [5–6]. Research on the transformation of available alkaloids, the use of which in medicine is not possible due to significant side effects, is being successfully developed.

It should be noted that compounds with other types of biological activity, not typical for cytosine itself, namely antispasmodic, antiarrhythmic, hepatoprotective, analgesic, cholinergic, insecticidal, fungicidal etc., are constantly found among the various cytosine derivatives, which attracts attention and encourages the implementation of syntheses and its new derivatives investigation [7–12]. Recently, a new class of heterocyclic compounds with a fundamental 1,4-dihydropyridine base, possessing high antihypertensive and nootropic activity, has begun to be widely used in medical practice [13–14]. The aim of this work is to synthesize and develop derivatives of the cytosine alkaloid with various functionally substituted fragments in terms of further obtaining new modified structures applying quantum-chemical calculations and pharmacological activity evaluation.

Experimental

¹H and ¹³C NMR spectra of compounds (2-4) were recorded on a JNN-ECA Jeol 400 spectrometer (frequencies 399.78 and 100.53 MHz, respectively) using a DMSO-d₆ solvent. Chemical shifts were measured relative to the signals of residual protons or carbon atoms of DMSO-d₆. The reaction progress and the ob-

tained purity of compounds were monitored by thin layer chromatography on Silufol UV-254 plates in isopropyl alcohol-ammonia-water 7:2:1, ethanol-chloroform 1:4 systems. The plates were developed with iodine vapors. The reaction products were isolated by recrystallization or by column chromatography on alumina. All solvents used in this work were purified and absolutized according to standard methods.

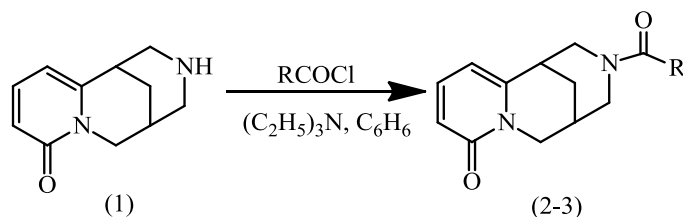
N-Cinnamoylcytisine (2). 9 g (6.0 mmol) of triethylamine and a solution of 15 g (6.0 mmol) of cinnamoyl chloride in 200 ml of benzene were added with stirring to a solution of 17.1 g (6.0 mmol) of cytosine in 500 ml of benzene. The reaction mixture was stirred for 3.3 hours at room temperature until a precipitate formed. The formed precipitate of triethylamine hydrochloride was filtered off, the mother liquor was evaporated, and the residue was treated with diethyl ether. There was obtained 14.25 g (95 %) of *N*-cinnamoylcytisine (2) in the form of a white powder with a yellowish tint, m.p. 130-134°C. ¹H NMR spectrum, δ , ppm (J, Hz): 1.86-1.97 m (2H, H8.8), 2.44 br.s. (1H, H9), 2.90-3.40 m (3H, H7.11ax, 13ax), 3.63-3.97 m (2H, H10ax, 10eq), 4.24-4.65 m (2H, H11eq, 13eq), 6.14 d (2H, H3, 5. 3J 6.1), 6.49-6.75 m (1H, H15), 7.16-7.64 m (7H, H4, 15, 18-22). ¹³C NMR spectrum, δ C, ppm: 25.95 (C8), 27.86 (C9), 35.13 (C7), 49.05 (C10), 51.31 (C11), 53.04 (C13), 105.29 (C5), 116.40 (C3), 128.85 (C15), 129.24 (C18, 19, 21, 22), 129.99 (C20), 135.55 (C4), 139.09 (C16), 141.32 (C17), 150.47 (C6), 162.66 (C2), 165.65 (C14) ppm HMQC (¹H-¹³C) NMR cross peaks, ppm: H8-C8 (1.96, 26.60), H9-C9 (2.44, 28.48), H7-C7 (3.13, 35.65), H10ax-C10ax (3.59, 49.56), H10ax-C10ax (3.98, 49.58), H5-C5 (6.14, 105.76), H3-C3 (6.12, 116.82) and H18,19,21,22-C18,19,21,22 (7.37, 129.52).

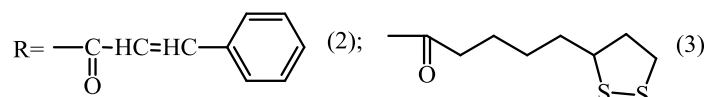
N-Lipoylcytisine (3). A solution of 29.61 g (8.78 mmol) of lipoyl chloride [obtained from 67.5 g (21.95 mmol) of lipoic acid and 48.96 g (27.43 mmol) of thionyl chloride], dissolved in 250 ml of benzene was added with stirring to a solution of 25.05 g (8.78 mmol) of cytosine and 18.3 ml (8.78 mmol) of triethylamine in 500 ml of benzene. The reaction mixture was stirred for 3 hours at room temperature until a precipitate formed. The precipitate was filtered off, the mother liquor was evaporated, and the residue was chromatographed on silica gel (eluent: benzene-chloroform). 13.8 g (64.56%) lipoylcytisine (3) was isolated as yellowish thick oil.

In order to study the reactivity of the derivatives obtained, quantum-chemical calculations were conducted to determine the energy and charge characteristics of molecules, namely cinnamoylcytisine (2), lipoylcytisine (3), and cytisinylisoalantholactone (4). The semiempirical methods AM1 and PM6 were applied quantum-chemical calculations. In addition, we can note the following: in *ab initio* methods, all integrals included in the system of Hartree-Fock equations are calculated explicitly and no experimentally determined parameters are used, except for fundamental physical constants, while the PM6 method combines experimental data as well as *ab initio* data. The AM1 method was applied to compare hydrogen bonds. The calculations were carried out with the help of MOPAC2009 [15]. The ChemOffice software made it possible to construct the geometry of the studied molecules.

Results and Discussion

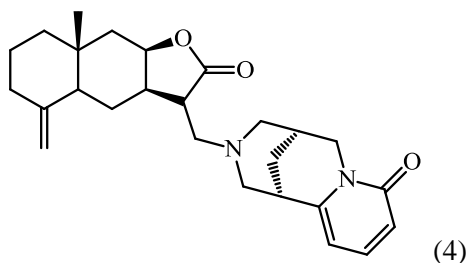
The cytosine source availability and the analysis of its structure designate a significance of carrying out its synthetic transformations with the compounds, which are structurally similar to a number of natural metabolites and other practically significant compounds. Thus, the acylation of cytosine with acid chlorides and anhydrides is the simplest and most convenient method for the preparation of its acyl derivatives [16]. Continuing studies of the transformation of cytosine (1) and in order to search for pharmacologically active compounds in this series, we have synthesized acyl derivatives by the interaction of cytosine with carboxylic acid chlorides, where cinnamoyl chloride and lipoyl chloride were used as acylating agents [17–18]. The acylation of cytosine with carboxylic acid chlorides was implemented in benzene in the presence of triethylamine at room temperature. The reactions proceeded smoothly and led to the production of *N*-acyl derivatives of cytosine (2-3) with a yield of 64-95 %. The synthesized compounds (2, 3) are white crystalline substances, readily soluble in organic solvents.





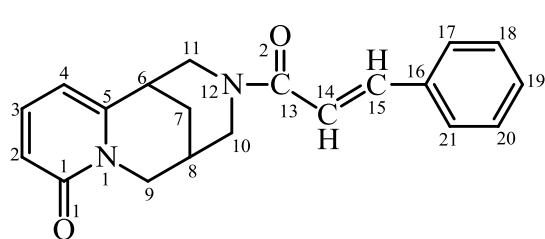
The ^1H NMR spectrum of compound (2) is characterized by the presence of multiplet in the upfield region at 1.86-1.97 ppm with the 2H intensity of two H8 protons of the heterocyclic nucleus. The H9 proton resonates as a broadened singlet at 2.44 by the integral 1H. Then, a multiplet appeared in the region of 2.90-3.40 ppm with an integrated intensity of 3H, corresponding to the H7 proton and the axial protons $\text{H}^{11\text{ax}}$ and $\text{H}^{13\text{ax}}$. Equatorial protons $\text{H}^{11\text{eq}}$ and $\text{H}^{13\text{eq}}$ appeared as a multiplet signal at 4.24-4.65 ppm with an integral intensity of 2H. Two protons $\text{H}^{10\text{ax}}$, $\text{H}^{10\text{eq}}$ as a result of spin-spin coupling, as well as spin-spin splitting through three bonds with the proton H9 appeared as a multiplet in the region of 3.63-3.97 ppm with integral 2H. Doublet at 6.14 ppm with integral 2H and 3J, 6.1 Hz corresponds to protons H3 and H5. An unsaturated proton H15 (1H) appeared in the region of olefinic protons resonance with a multiplet at 6.49-6.75 ppm, while the adjacent unsaturated proton H16 was detected together with aromatic protons H18-22 and a proton H4 multiplet in the lowest-field part of the spectrum with an integrated intensity of 7H at 7.16-7.64 ppm.

On the basis of the alkaloid cytosine and isoalantholactone, cytisinylisoalantholactone (4) was synthesized with m.p. 196–198 °C, formula $\text{C}_{26}\text{H}_{34}\text{N}_2\text{O}_3$, $M=422.256$ g/mol.

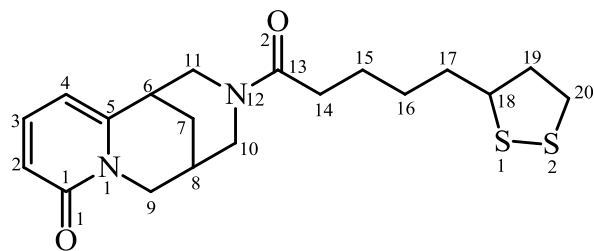


The structure was established and confirmed using spectral methods and comparison of the literature data [19].

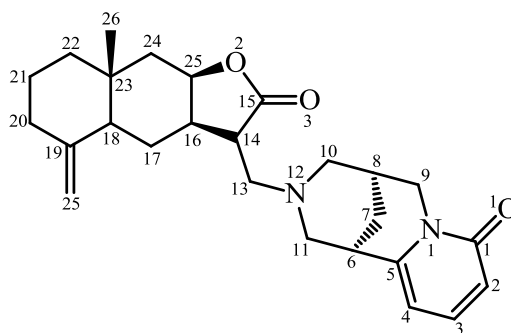
In order to study the reactivity of the molecules of cinnamoylcytosine (2), lipoylcytosine (3), and cytisinylisoalantholactone (4), determine their energy and charge characteristics quantum-chemical calculations were carried out. The calculations were conducted by semiempirical quantum-chemical methods in the AM1 and PM6 parametrization.



(2)



(3)



(4)

A quantum-chemical calculations of molecules main energy characteristics were performed to study the thermodynamic stability. The obtained results are illustrated in Table 1.

Energy characteristics of molecules (2-4)

Energy characteristics	Method	Molecules		
		(2)	(3)	(4)
Heat of formation, kJ / mol	AM1	32.922	-243.137	623.483
	PM6	-114.86	-379.245	412.703
Total energy, eV	AM1	-3889.28	-4235.07	-5094
	PM6	-3662.65	-3973.06	-4804.12
Ionization potential, eV	AM1	8.774	8.163	8.597
	PM6	8.996	8.414	8.704
HOMO, eV	AM1	-8.775	-8.163	-8.597
	PM6	-8.996	-8.414	-8.704
LUMO, eV	AM1	-0.550	-1.454	-0.812
	PM6	-0.547	-1.094	-0.330

The results presented in the Table 1 indicate a sufficient thermodynamic stability of molecules (2-3). Molecule (4) is not stable according to the results of quantum-chemical calculations. The data on the energy values of the frontier orbitals demonstrate that the molecules (2-4) exhibit electrophilic properties. The Mulliken charge distribution on non-hydrogen atoms was calculated to determine the position of the reaction centers in molecules (2-4). The results are shown in Figure 1.

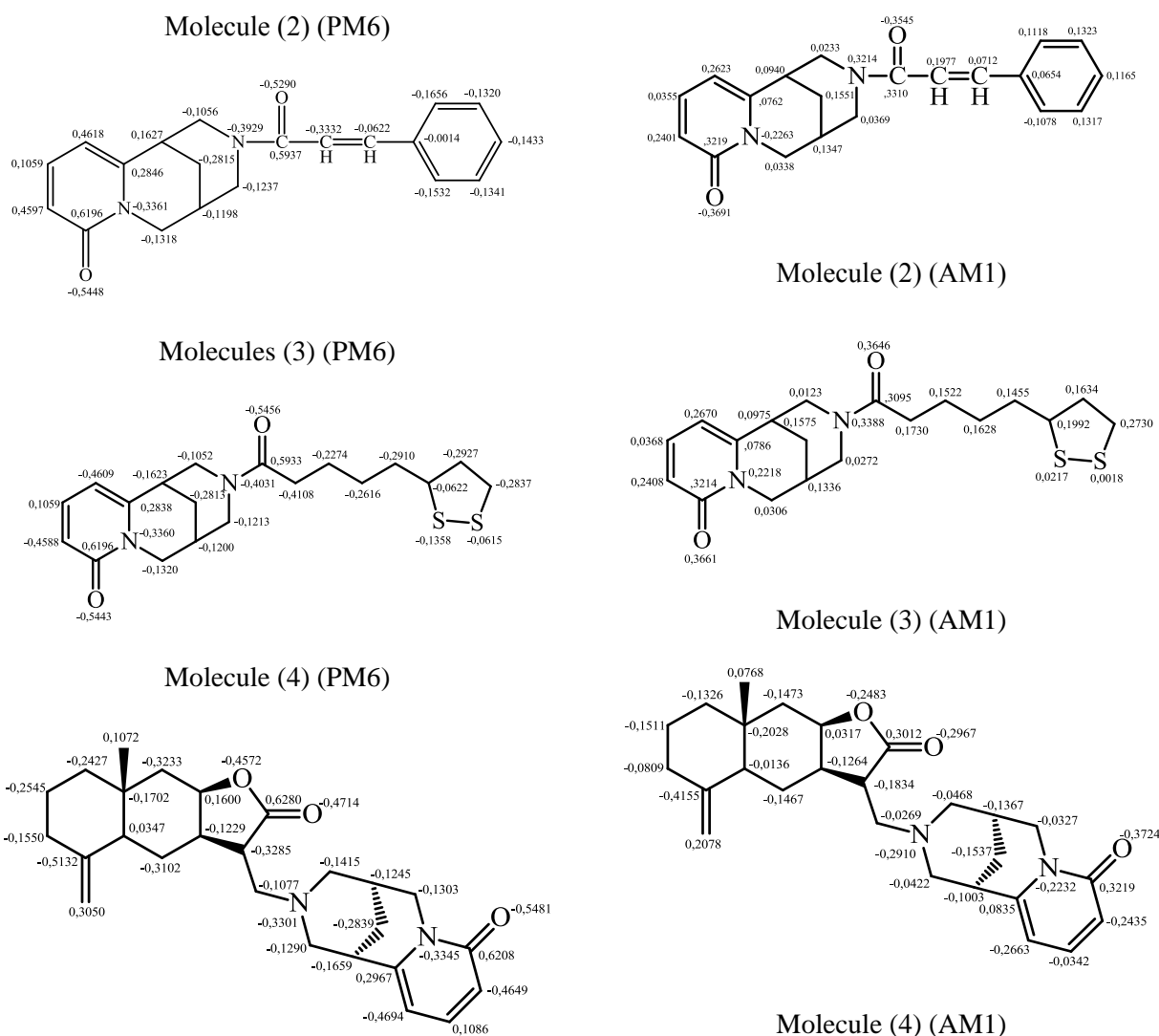


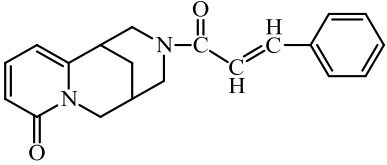
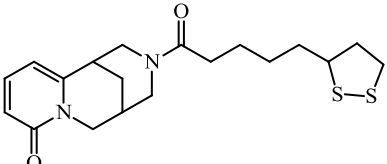
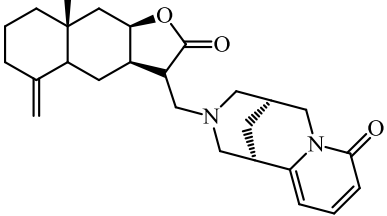
Figure 1. Mulliken charge distribution on non-hydrogen atoms in molecules (2-4)

Based on the data presented above, it can be concluded that the preferred centers for attack by nucleophilic reagents in molecule (2) are C1, C2, C4, and C13 atoms, in molecule (3) — C1, C5, and C13, and in molecule (4) — C1, C5, C15 and C25, which is explained by the presence of an aromatic ring and the adjacent position of keto groups in the structures of the molecules studied.

In terms of a detailed study and establishment of the probable biological activity of synthesized cytisine derivatives, we performed a bioprediction using PASS (Prediction of Activity Spectra for Substances) as one of the most effective and well-known computer programs to date [20]. The results of the bioprediction of the compounds synthesized are presented in the Table 2, in the form of the proposed activity name and the coefficients of the probability of the presence (P_a) and absence (P_i), of each type of activity, which have values from 0 to 1. In this analysis of the predicted list of activities, the conditions were selected, where $P_a > 70\%$.

Table 2

Results of computer screening of compounds synthesized (2-4)

No.	Structural formula	P_a (Pharmacological Active)	P_i (Pharmacological Inactive)	Intended type of activity
1		0.927	0.002	Nicotinic alpha-2-beta-2 receptor antagonist
		0.844	0.001	Alpha-4-beta-2 nicotinic receptor antagonist
		0.766	0.010	Respiratory analeptic
		0.653	0.014	Analeptic
		0.559	0.025	Anticonvulsant
		0.532	0.003	Alpha-6 nicotinic receptor agonist
		0.545	0.039	Phosphatidylcholine retinol-O-acyltransferase inhibitor
		0.476	0.019	Cognitive disorders treatment
		0.503	0.060	Neurotransmitter uptake inhibitor
		0.472	0.035	All-trans retinyl palmitate hydrolase inhibitor
2		0.783	0.002	Alpha-4-beta-2 nicotinic receptor antagonist
		0.753	0.017	Nicotinic alpha-2-beta-2 receptor antagonist
		0.718	0.025	Antiischemic, cerebral
		0.659	0.010	Treatment of neurodegenerative diseases
		0.648	0.004	Growth stimulant
		0.633	0.004	Chemoprotective
		0.612	0.006	Treatment of liver diseases
		0.573	0.010	Cognitive disorders treatment
		0.525	0.010	Antiparkinsonian
		0.530	0.029	Anticonvulsant
0.462	0.005	Growth hormone agonist		
0.454	0.025	Muscular dystrophy treatment		
0.447	0.019	Alzheimer's disease treatment		
3		0.830	0.004	Analeptic
		0.829	0.007	Respiratory analeptic
		0.796	0.019	Anti-eczematic
		0.738	0.002	Alpha-4-beta-2 nicotinic receptor antagonist
		0.733	0.021	Antineoplastic
		0.678	0.018	Phosphatase inhibitor
		0.583	0.004	Antineoplastic drugs (pancreatic cancer)
		0.591	0.013	Polarization stimulator
		0.579	0.016	Cardiovascular analeptic
		0.556	0.010	Antimetastatic
0.575	0.036	Neurotransmitter uptake inhibitor		
0.514	0.029	Dermatological		
0.532	0.048	Anti-inflammatory agent		

Computer prognosis demonstrated that cinnamoylcytisine probably ($P_a > 0.5$) has antidepressant and nootropic properties, and also revealed the possibility of its using in the treatment of nicotine addiction in the future.

As a result of predicting the spectrum of biological activity in the PASS online system, the presence of hepatoprotective, antiparkinsonian, neurotropic, nootropic, anabolic actions for lipoylcytisine with a proba-

bility of $P_a > 0.5$ were revealed; and for cytosinylisoantholactone antitumor, anti-inflammatory, neurotropic effects with a probability of $P_a > 0.5$, as well as the possibility of its use as an analeptic agent in chronic heart failure were predicted.

Thus, the bioscreening of synthesized cytosine derivatives showed the promising use of such compounds in medicine as inhibitors of neurotransmitters uptake, an inhibitor of phosphatidylcholine-retinol-O-acyltransferase, an inhibitor of all-trans-retinyl palmitate hydrolase, etc. This circumstance is significant, since medicines can be obtained on the basis of these compounds.

Conclusions

On the basis of the cytosine molecule, samples of cinnamoylcytisine (2), lipoylcytisine (3), and cytosinylisoantholactone were synthesized. According to the results of quantum-chemical calculations of these molecules, it was established that the preferred centers for attack by nucleophilic reagents in molecule (2) are C1, C2, C4, and C13 atoms, in molecule (3) — C1, C5, and C13, and in molecule (4) — C1, C5, C15 and C25, which can be explained by the presence of an aromatic ring and the adjacent position of keto groups in the structures of the molecules studied. In addition to it, data of virtual bioscreening of cytosine alkaloid derivatives are provided.

Acknowledgments

The work was carried out within the framework of the project No. AP08855433 on grant financing of the Science Committee of the Ministry of Education and Science of the Republic of Kazakhstan.

References

- 1 Юнусов С.Ю. Алкалоиды: моногр. / С.Ю. Юнусов. — Ташкент: ФАН, 1972. — 270 с.
- 2 Нуркенов О.А. Синтетические трансформации алкалоида цитизина: моногр. / О.А. Нуркенов, И.В. Кулаков, С.Д. Фазылов. — Караганда: Гласир, 2012. — 210 с.
- 3 Тлегенов Р. Синтез, строение и свойства производных лупинина, анабазина, цитизина и ряда азотсодержащих гетероциклов: автореф. дис. ... д-ра хим. наук / Р. Тлегенов. — 2008. — 54 с.
- 4 Takagi K. Synthesis of new 3(5)-(2-hydroxyphenyl)pyrazoles as potential analgesic agents and platelet aggregation inhibitors / K. Takagi, M. Tanaka, Y. Murakami, H. Morita, T. Aotsuka // Eur. J. Med. Chem. Chim. Ther. — 1986. — Vol. 21. — P. 65–68. <https://doi.org/10.1002/chin.198627339>
- 5 Садыков А.С. Алкалоиды хинолизидинового ряда: моногр. / А.С. Садыков, Х.А. Асланов, Ю.К. Кушмурадов. — М.: Наука, 1975. — 292 с.
- 6 Нуркенов О.А. Алкалоид анабазин и его производные: моногр. / О.А. Нуркенов, С.Д. Фазылов, И.В. Кулаков, Л.А. Мусина. — Караганда: Гласир, 2010. — 224 с.
- 7 Kulakov I.V. Synthesis of N-aminoglycosides derived from alkaloid cytosine, their biological activity and crystal structure of N-(β -D-galactopyranosyl)cytosine / I.V. Kulakov, O.A. Nurkenov, D.M. Turdybekov, R.B. Sejdahmetova, K.M. Turdybekov // Chemistry of Heterocyclic Compounds. — 2010. — Vol. 46, No. 2. — P. 240–244. <https://doi.org/10.1002/chin.201049202>
- 8 Gazaliev A.M. Synthesis and fungicidal activity of alkaloid-containing carbohydrates / A.M. Gazaliev, O.A. Nurkenov, I.V. Kulakov, A.A. Ainabaev, D.V. Bessonov // Russian Journal of Applied Chemistry. — 2006. — Vol. 79, No. 3. — P. 508–510. <https://doi.org/10.1134/S1070427206030402>
- 9 Kulakov I.V. Synthesis and biological activity of 3,4-dihydropyrimidin-2-thione aminomethylene derivatives based on the alkaloid cytosine / I.V. Kulakov // Chemistry of Natural Compounds. — 2011. — Vol. 47, No. 4. — P. 597–599.
- 10 Kulakov I.V. Synthesis and biological activity of aminoacyl phenothiazine derivatives based on the alkaloids cytosine, anabasine, and d-pseudoephedrine / I.V. Kulakov // Chemistry of Natural Compounds. — 2010. — Vol. 46, No. 1. — P. 68–71.
- 11 Yazlovitskii A.V. Synthesis of N-Acylamino-Acid Derivatives of Cytisine / A.V. Yazlovitskii, M.M. Garazd, V.G. Kartsev // Chemistry of Natural Compounds. — 2016. — Vol. 52. — P. 272–275.
- 12 Rouden J. (–)-Cytisine and derivatives: synthesis, reactivity, and applications / J. Rouden, M.C. Lasne, J. Blanchet, J. Baudoux // Chem. Rev. — 2014. — Vol. 114, No. 1. — P. 712–778. <https://doi.org/10.1021/cr400307e>
- 13 Tsypysheva I.P. Synthesis and Nootropic Activity of new 3-Amino-12-N-Methylcytosine Derivatives / I.P. Tsypysheva, A.V. Koval'skaya, A.N. Lobov, N.S. Makara, P.R. Petrova, E.I. Farafontova, L.F. Zainullina, Yu.V. Vakhitova, F.S. Zarudii // Chem. Nat. Compd. — 2015. — Vol. 51. — P. 910–915. <https://doi.org/10.1007/s10600-015-1446-x>
- 14 Tsypysheva I.P. Synthesis and specific nootropic activity of (–)-cytosine derivatives with carbamide and thiocarbamide moieties in their structure / I.P. Tsypysheva, A.V. Koval'skaya, N.S. Makara, A.N. Lobov, I.A. Petrenko, E.G. Galkin, T.A. Sapozhnikova, F.S. Zarudii, M.S. Yunusov // Chem. Nat. Compd. — 2012. Vol. 48. — P. 629–634. <https://doi.org/10.1007/s10600-012-0329-7>

- 15 James J.P. Stewart, MOPAC 2009, Stewart Computational Chemistry / J.P. James. — Colorado Springs, CO, USA, 2008. <http://OpenMOPAC.net>.
- 16 Тлегенов Р. Синтез N-ацильных производных алкалоида цитизина / Р. Тлегенов // Химия раст. сырья. — 2007. — №1. — С. 49–52.
- 17 Нуркенов О.А. Синтез, строение и биологическая активность циннамоилсодержащих производных алкалоидов цитизина и анабазина / О.А. Нуркенов, Ж.С. Нурмаганбетов, Т.М. Сейлханов, С.Д. Фазылов, Ж.Б. Сатпаева, К.М. Турдыбеков, С.А. Талипов, Р.Б. Сейдахметова // Журн. общ. хим. — 2019. — Т. 89, № 10. — С. 1550–1559. <https://doi.org/10.1134/S0044460X19100093>
- 18 Nurkenov O.A. Synthesis and structured N-acyl and thiourea derivatives citizine and anabazine / O.A. Nurkenov, Zh.S. Nurmaganbetov, T.M. Seilkhanov, S.D. Fazylov, V.M. Manasheva, A.R. Zhasymbekova, A.S. Serikbolov // News of the academy of sciences of the Republic of Kazakhstan. — 2020. — No. 1(439). — P. 37–46. <https://doi.org/10.32014/2020.2518-1491.5>
- 19 Klochkov S.G. Modification of alantolactones by natural alkaloids / S.G. Klochkov, S.V. Afanas'eva, A.B. Ermatova, A.V. Chudinov // Chemistry of natural compounds. — 2011. — Vol. 47, No. 5. — P. 716–725. <https://doi.org/10.1007/s10600-011-0043-x>
- 20 Садым А.В. Интернет-система прогноза спектра биологической активности химических соединений / А.В. Садым, А.А. Лагунин, Д.А. Филимонов, В.В. Поройков // Хим. фарм. журн. — 2002. — Т. 36, № 10. — С. 21–26. <https://doi.org/10.30906/0023-1134-2002-36-10-21-26>

Ж.С. Нурмаганбетов, Г.К. Мұқышева, Е.В. Минаева, Д.М. Тұрдыбеков,
Қ.М. Тұрдыбеков, А.С. Махмұтова, А.Р. Жасымбекова, О.А. Нуркенов

Цитизин алкалоиды туындыларының синтезі, кванттық-химиялық есептеулері және олардың виртуалды скринингі

Мақалада цитизиннің кейбір туындыларына синтез жүргізілген. Цитизин алкалоидының синтезделген туындыларын кванттық-химиялық есептеу және виртуалды скринингтің деректері алынды. Бұл ретте цитизин туындыларының молекулаларындағы реакция орталықтары анықталды. Алынған туындылардың реакцияға қабілеттілігін зерттеу мақсатында молекулалардың энергиялық және зарядтық сипаттамаларын анықтау үшін циннамоилцитизин, липпоилцитизин, цитизинилизоалантолактон молекулаларына кванттық-химиялық есептеулер жүргізілді. Ұсынылған нәтижелер циннамоилцитизин, липпоилцитизин молекулаларының жеткілікті термодинамикалық тұрақтылығын көрсетеді. Кванттық химиялық есептеулердің нәтижелері бойынша цитизинилизоалантолактон молекуласы онша тұрақты емес екендігі байқалды. Шектік молекулалық орбитальдардың мәндері туралы мәліметтер, жалпы алғанда, барлық молекулалардың электрофильді қасиетке ие екендігін растайды. Синтезделген цитизин туындыларының биологиялық белсенділігін анықтау мақсатымен ең тиімді және танымал компьютерлік бағдарламалардың бірі — PASS (Prediction of Activity Spectra for Substances) көмегімен биоболжамдау жүргізілді. Виртуалды скрининг нәтижелері бойынша бастапқы препараттардың әлеуетті көздері болып табылатын цитизин алкалоидының туындыларының перспективалы түрлері анықталды.

Кілт сөздер: алкалоидтар, цитизин, синтез, физикалық-химиялық қасиеттері, туындылар, кванттық-химиялық есептеулер, виртуалды скрининг, заттардың биологиялық белсенділігін болжамдау.

Ж.С. Нурмаганбетов, Г.К. Мукушева, Е.В. Минаева, Д.М. Турдыбеков,
К.М. Турдыбеков, А.С. Махмұтова, А.Р. Жасымбекова, О.А. Нуркенов

Синтез, квантово-химические расчеты производных алкалоида цитизина и их виртуальный скрининг

В статье проведен синтез некоторых производных цитизина. Получены данные квантово-химического расчета и виртуального скрининга синтезированных производных алкалоида цитизина. Определены реакционные центры в молекулах производных цитизина. С целью изучения реакционной способности полученных производных авторами проведены квантово-химические расчеты определения энергетических и зарядовых характеристик молекул: циннамоилцитизина, липпоилцитизина, цитизинилизоалантолактона. Представленные результаты свидетельствуют о достаточной термодинамической стабильности молекул циннамоилцитизина и липпоилцитизина. Молекула цитизинилизоалантолактона, по результатам квантово-химических расчетов, малостабильна. Данные значений граничных молекулярных орбиталей показывают, что, в целом, все молекулы проявляют электрофильные свойства. В плане детального изучения и вероятного установления биологической активности синтезированных производных цитизина был сделан биопрогноз с использованием одной из наиболее эффективных и

известных на сегодняшний день компьютерных программ – PASS (Prediction of Activity Spectra for Substances). По результатам виртуального скрининга выявлены перспективные типы производных алкалоида цитизина, являющиеся потенциальными источниками оригинальных препаратов.

Ключевые слова: алкалоиды, цитизин, синтез, физико-химические свойства, производные, квантово-химический расчет, виртуальный скрининг, прогнозирование спектров активности веществ.

References

- 1 Yunussov, S.Yu. (1972). *Alkaloidy [Alkaloids]*. Tashkent: FAN [in Russian].
- 2 Nurkenov, O.A., Kulakov, I.V., & Fazylov, S.D. (2012). *Sinteticheskiye transformatsii alkaloida tsitizina [Synthetic transformations of cytisine alkaloid]*. Karaganda: Glasir [in Russian].
- 3 Tlegenov, R. (2008). Sintez, stroieniie, i svoistva proizvodnykh lupinina, anabazina, tsitizina i riada azotsoderzhashchikh heterotsiklov [Synthesis, structure and properties of derivatives of lupinine, anabasine, cytisine and a number of nitrogen-containing heterocycles]. *Extended abstract of Doctor's thesis* [in Russian].
- 4 Takagi, K., Tanaka, M., Murakami, Y., Morita, H., & Aotsuka T. (1986). Synthesis of new 3(5)-(2-hydroxyphenyl)pyrazoles as potential analgesic agents and platelet aggregation inhibitors. *Eur. J. Med. Chem. Chim. Ther.* 21, 65-68. <https://doi.org/10.1002/chin.198627339>
- 5 Sadykov, A.S., Aslanov, Kh.A., & Kushmuradov, Yu.K. (1975). *Alkaloidy khinolizidinovoho riada [Quinolizidine alkaloids]*. Moscow: Nauka [in Russian].
- 6 Nurkenov, O.A., Fazylov, S.D., Kulakov, I.V., & Musina, L.A. (2010). *Alkaloid anabazin i eho proizvodnyie [The alkaloid anabazine and its derivatives]*. Karaganda: Glasir [in Russian].
- 7 Kulakov, I.V., Nurkenov, O.A., Turdybekov, D.M., Sejdahmetova, R.B., & Turdybekov, K.M. (2010). Synthesis of N-aminoglycosides derived from alkaloid cytisine, their biological activity and crystal structure of N-(β-D-galactopyranosyl)cytisine. *Chemistry of Heterocyclic Compounds*, 46(2), 240–244. <https://doi.org/10.1002/chin.201049202>
- 8 Gazaliev, A.M., Nurkenov, O.A., Kulakov, I.V., Ainabaev, A.A., & Bessonov, D.V. (2006). Synthesis and fungicidal activity of alkaloid-containing carbohydrates. *Russian Journal of Applied Chemistry*, 9(3), 508–510. <https://doi.org/10.1134/S1070427206030402>
- 9 Kulakov, I.V. (2011). Synthesis and biological activity of 3,4-dihydropyrimidin-2-thione aminomethylene derivatives based on the alkaloid cytisine. *Chemistry of Natural Compounds*, 47(4), 597–599.
- 10 Kulakov, I.V. (2010). Synthesis and biological activity of aminoacyl phenothiazine derivatives based on the alkaloids cytisine, anabasine, and d-pseudoephedrine. *Chemistry of Natural Compounds*, 46(1), 68–71.
- 11 Yazlovitskii, A.V., Garazd, M.M., & Kartsev, V.G. (2016). Synthesis of N-Acylamino-Acid Derivatives of Cytisine. *Chemistry of Natural Compounds*, 52, 272–275.
- 12 Rouden, J., Lasne, M.C., Blanchet, J. & Baudoux, J. (2014). (–)-Cytisine and derivatives: synthesis, reactivity, and applications. *Chem. Rev.*, 114, 712. <https://doi.org/10.1021/cr400307e>
- 13 Tsypysheva, I.P., Koval'skaya, A.V., Lobov, A.N., Makara, N.S., Petrova, P.R., & Farafontova, E.I., et al. (2015). Synthesis and Nootropic Activity of new 3-Amino-12-N-Methylcytisine Derivatives. *Chem. Nat. Compd.*, 51, 910-915. <https://doi.org/10.1007/s10600-015-1446-x>
- 14 Tsypysheva, I.P., Koval'skaya, A.V., Makara, N.S., Lobov, A.N., Petrenko, I.A., & Galkin, E.G., et al. (2012). Synthesis and specific nootropic activity of (–)-cytisine derivatives with carbamide and thiocarbamide moieties in their structure. *Chem. Nat. Compd.*, 48, 629-634. <https://doi.org/10.1007/s10600-012-0329-7>
- 15 James J.P. (2008). *Stewart, MOPAC 2009, Stewart Computational Chemistry*. Colorado Springs, CO, USA, <http://OpenMOPAC.net>.
- 16 Tlegenov, R. (2007). Sintez N-atsilnykh proizvodnykh alkaloida tsitizina [Synthesis of N-acyl derivatives of the alkaloid cytisine]. *Khimiia rastitelnogo syria — Chemistry of plant raw materials*, 1, 49–52 [in Russian].
- 17 Nurkenov, O.A., Nurmaganbetov, Zh.S., Seilkhanov, T.M., Fazylov, S.D., Satpayeva, Zh.B., & Turdybekov, K.M., et al. (2019). Sintez, stroenie i biologicheskaya aktivnost tsinnamoylsoderzhashchikh proizvodnykh alkaloidov tsitizina i anabazina [Synthesis, structure and biological activity of cinnamoyl-containing derivatives of cytisine and anabasine alkaloids]. *Zhurnal obshchei khimii — Journal of General Chemistry*, 89(10), 1550–1559 [in Russian]. <https://doi.org/10.1134/S0044460X19100093>
- 18 Nurkenov, O.A., Nurmaganbetov, Zh.S., Seilkhanov, T.M., Fazylov, S.D., Manasheva, V.M., & Zhasymbekova, A.R., et al. (2020). Synthesis and structured N-acyl and thiourea derivatives citizine and anabazine *News of the academy of sciences of the Republic of Kazakhstan*, 1(439), 37–46. <https://doi.org/10.32014/2020.2518-1491.5>
- 19 Klochkov, S.G., Afanas'eva, S.V., Ermatova, A.B., & Chudinov, A.V. (2011). Modification of alantolactones by natural alkaloids *Chemistry of natural compounds*, 47(5), 716-725. <https://doi.org/10.1007/s10600-011-0043-x>
- 20 Sady, A.V., Lagunin, A.A., Filimonov, D.A., & Poroikov, V.V. (2002). Internet-sistema prognoza spectra biologicheskoi aktivnosti khimicheskikh soedinenii [Internet-system for prediction of the spectrum of biological activity of chemical compounds]. *Khimiko-farmatsevticheskii zhurnal — Chem. pharm. journal*, 36(10), 21–26 [in Russian]. <https://doi.org/10.30906/0023-1134-2002-36-10-21-26>

Information about authors

Nurmaganbetov Zhangeldy Seitovich — Candidate of chemical sciences, Associated Professor, Karaganda Medical University, Gogol str., 40, 100000, Karaganda, Kazakhstan; e-mail: nzhangeldy@yandex.ru; <https://orcid.org/0000-0002-0978-5663>;

Mukusheva Gulim Kenesbekovna (*corresponding author*) — Candidate of chemical sciences, Associated Professor, Karaganda University of the name of academician E.A. Buketov, Universitetskaya str., 28, 100024, Karaganda, Kazakhstan; e-mail: mukusheva1977@list.ru; <https://orcid.org/0000-0001-6706-4816>;

Minayeva Yelena Viktorovna — Candidate of chemical sciences, Karaganda University of the name of academician E.A. Buketov, Universitetskaya str., 28, 100024, Karaganda, Kazakhstan; e-mail: yelenaminayeva@yandex.ru; <https://orcid.org/0000-0001-9382-5965>;

Zhasymbekova Aigerym Rysbekovna — PhD student, Karaganda University of the name of academician E.A. Buketov, Universitetskaya str., 28, 100024, Karaganda, Kazakhstan; e-mail: aigera-93-93@mail.ru; <https://orcid.org/0000-0003-1272-9096>;

Turdybekov Dastan Mukhtarovich — Candidate of chemical sciences, Karaganda Technical University, N. Nazarbayev str., 56, 100010, Karaganda, Kazakhstan; e-mail: turdas@mail.ru; <https://orcid.org/0000-0002-0245-0224>;

Turdybekov Koblandy Muboryakovich — Doctor of chemical sciences, Professor, Karaganda University of the name of academician E.A. Buketov, Universitetskaya str., 28, 100028, Karaganda, Kazakhstan; e-mail: xray-phyto@yandex.kz; <https://orcid.org/0000-0001-9625-0060>;

Makhmutova Almagul Satybaldievna — Candidate of chemical sciences, Associate Professor, Karaganda Medical University, Gogol str., 40, 100000, Karaganda, Kazakhstan; e-mail: almagul_312@mail.ru; <https://orcid.org/0000-0002-0194-8739>;

Nurkenov Oralgazy Aktayevich — Doctor of chemical sciences, Professor, LLP “Institute of Organic Synthesis and Coal Chemistry”, Alikhanov str. 1, 100000, Karaganda, Kazakhstan; e-mail: nurkenov_oral@mail.ru; <https://orcid.org/0000-0003-1878-2787>.

A.A. Minakova*, M.V. Chikina, S.G. Il'yasov

*Institute for Problems of Chemical and Energetic Technologies,
Siberian Branch of the Russian Academy of Sciences (IPCET SB RAS), Biysk, Russia*

(* Corresponding author's e-mail: nastya.sinitsyna.1994@mail.ru)

Study of uric acid oxidation reaction products in medium of ammonia or primary amines

This work is considered in more detail the most important stage of obtaining one of the promising heteroatomic polycyclic compounds 3,7,10-trioxo-2,4,6,8,9,11-hexaaza[3.3.3]propellane (THAP). THAP is a potential compound for creating high-energy substances due to the presence of six nitrogen atoms in the structure and tight packing. Uric acid is the starting compound in the THAP synthesis chain. When it is oxidized by sodium persulfate or potassium ferrocyanide, 1,5-diaminoglycoluril is formed, from which the propellane structure is formed by the tricyclization reaction. This work expanded the range of oxidants for the conversion of uric acid to 1,5-diaminoglycoluril. It was found that 1,5-diaminoglycoluril was formed with a yield of 29 % when using equimolar proportions of uric acid and KMnO_4 . When using MnO_2 in a ten times more excess, the yield of 1,5-diaminoglycoluril was 38 %. The article also presents the results of a study of the interaction of uric acid with some amines. The reaction of interaction of uric acid with benzylamine was studied in more detail, the reaction products of which were 4-benzylimino-5-benzylaminoallantoin, 4-benzylimino-1-benzylamino-allantoin and 4-benzyliminoallantoin. Based on the synthesis of 4-benzyliminoallantoin, a number of promising derivatives of 4-iminoallantoin were obtained, namely 4-ethyliminoallantoin, 4-propyliminoallantoin, 4-*i*-propyliminoallantoin, 4-*n*-butyliminoallantoin, 4-*i*-butyliminoallantoin, 4-*tert*-butyliminoallantoin.

Keywords: uric acid, 1,5-diaminoglycoluril, 3,7,10-trioxo-2,4,6,8,9,11-hexaaza[3.3.3]propellane (THAP), oxidative amination, 4-alkyliminoallantoins.

Introduction

An important task of modern organic chemistry is the discovery of new substances previously unknown to science, which could expand the area of our knowledge and replenish the range of high-energy substances or biologically active products. 3,7,10-Trioxo-2,4,6,8,9,11-hexaaza [3.3.3]propellane (THAP) and its derivatives are the latest products of the heterocycles class, their nitrogen-containing polycyclic structure suggests interesting and useful properties, which determines the undoubted relevance of the topic of this work [1-7]. The synthesis of 3,7,10-trioxo-2,4,6,8,9,11-hexaaza[3.3.3]propellane **7** was proposed by Lee [7] (Figure 1). It can be seen from the reaction scheme that it is necessary to carry out three stages of synthesis to obtain compound **7**.

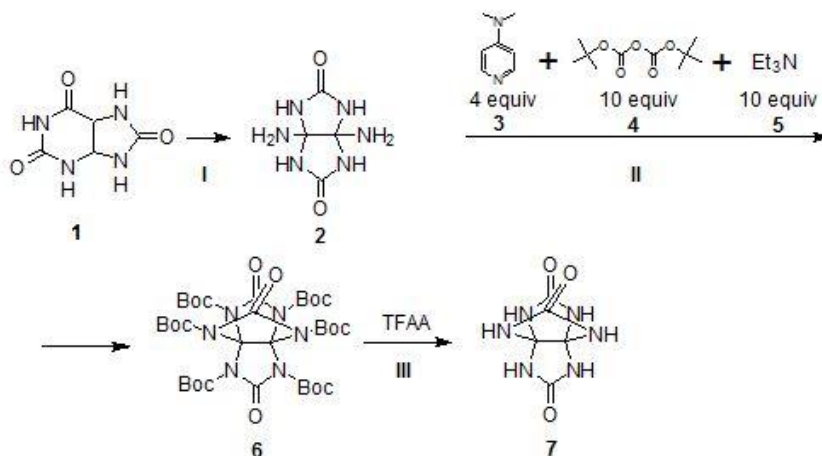


Figure 1. A synthetic protocol for 3,7,10-trioxo-2,4,6,8,9,11-hexaaza[3.3.3]propellane **7**

The first stage involves the oxidation of uric acid **1** by sodium persulfate or potassium ferrocyanide for 1,5-diaminoglycoluril **2** [8, 9]. The formation of tricyclic compound **6** with six protective groups (Boc) at nitrogen atoms occurs in 69 % yield in the second stage (II). Compound **7** was obtained from compound **6** by treating it with trifluoroacetic acid (stage III) in 91 % yield.

The production of 1,5-diaminoglycoluril (DiAGU) by oxidation of uric acid in ammonia is an important stage in the synthesis of THAP. However, in the literature, the number of oxidants capable of converting uric acid to 1,5-diaminoglycoluril is relatively low. The oxidation products of uric acid can also be 4-iminoallantoin and 5-amino-4-iminoallantoin, the latter compound being an intermediate in the preparation of 1,5-diaminoglycoluril.

The aim of this work is to search for new oxidants of uric acid at the first stage of the process of obtaining 3,7,10-trioxo-2,4,6,8,9,11-hexaaza[3.3.3]propellane, and in the preparation of derivatives of 1,5-diaminoglycoluril.

Experimental

Synthesis of 1,5-diaminoglycoluril: 0.01 mol (1.68 g) of uric acid and 4 g of sodium chloride are added to 7 ml of water and 15 ml of 25 % aqueous ammonia solution, and the reaction mixture is cooled to $-10\text{ }^{\circ}\text{C}$. Then 0.04 mol (9.52 g) of $\text{Na}_2\text{S}_2\text{O}_8$ or 0.015 mol (2.37 g) of KMnO_4 or 0.1 mol (8.7 g) of MnO_2 are gradually added and the mixture is kept for 2 h at this temperature, and then 10 ml of 25 % aqueous ammonia solution are added and stirring is raised at room temperature for 1 h. The mother liquor is left at a temperature of $5\text{ }^{\circ}\text{C}$ for 48 h; the precipitate formed is filtered, washed with water, ethyl alcohol, and diethyl alcohol. The product yield is 69 % (20 % and 38 %, respectively). IR, cm^{-1} : 3350, 3300, 1734, 1682, 1621. M.p. $> 300\text{ }^{\circ}\text{C}$. NMR ^1H (δ , ppm): 7.08 (NH, 4H, s), 2.36 (NH_2 , 4H, s). ^{13}C (δ , ppm): 87.72 (C), 158.41 (C=O). Calculated (%): C 27.90; H 4.48; N 48.92 $\text{C}_4\text{H}_8\text{N}_6\text{O}_2$ Found (%): C 27.91; H 4.68; N 48.82 %.

4-benzylimino-5-benzylaminoallantoin (10): 4.76 g (0.02 mol) of sodium persulfate was gradually added to a mixture cooled to $-5\text{ }^{\circ}\text{C}$, consisting of 30 ml of water, 1.68 g (0.01 mol), 2.14 g (0.02 mol) of benzylamine and 4 g of sodium chloride. The mixture was stirred at a temperature of -8 to $-5\text{ }^{\circ}\text{C}$ for 2 h, after which the reaction mixture was filtered. Product **10** was collected, washed with water, ethyl alcohol and diethyl ether. The yield was 77 % (2.71 g). M.p. $> 300\text{ }^{\circ}\text{C}$. IR, cm^{-1} : 3500, 3241, 3015, 2945, 1750, 1720, 1651, 1588, 1453. NMR ^1H (400 MHz, DMSO-*d*6) δ 3.59 (t, 2H, NH_2), 4.14, 4.18, 4.27, 4.35 (4H, 2 CH_2), 7.19-7.31 (m, 10CH), 7.84 (s, 3H, 3NH). ^{13}C NMR (100 MHz, DMSO-*d*6) 43.21, 46.43, 80.08 (C_{tert}), 127.32-128.54, 137.01, 139.65, 156.12 (C=N), 168.71 (C=O), 169.68 (C=O).

Synthesis of 4-alkyliminoallantoins. General methodology: 0.01 mol of uric acid, 7 ml of 25 % aqueous ammonia, 0.02 mol of primary amine and 4.76 g (0.02 mol) of $\text{Na}_2\text{S}_2\text{O}_8$ were added to 30 ml of distilled water at a temperature of $25\text{ }^{\circ}\text{C}$, after keeping the reaction mass for 3 h at this temperature, the product was isolated. When obtaining **13-15**, the reaction mass was evaporated 2 times, the precipitate was filtered off. When obtaining **12, 16-18**, the resulting precipitate was filtered off immediately after the end of exposure. The resulting precipitates were dried in air to constant weight.

4-benzyliminoallantoin (12). Yield was 78 %. ^1H NMR (400 MHz, DMSO-*d*6) 8.63 (1H, t, NH), 7.61 (1H, s, NH), 7.26-7.32 (5CH, m), 6.81-6.83 (1H, d, NH), 5.79 (2H, s, NH_2), 5.67-5.74 (1H, d, NH), 4.46 (2H, t, 2 CH_2). ^{13}C NMR (100 MHz, DMSO-*d*6) 169.42, 158.32 (C=N), 138.81, 127.41-128.79, 62.80 (CH), 45.78.

4-ethyliminoallantoin (13). Yield 67 %. ^1H NMR (400 MHz, DMSO-*d*6) 7.24 (1H, s, CH), 5.43 (3H, s, 3NH), 3.61 (2H, t, NH_2), 2.70-2.74 (2H, m, CH_2), 1.10 (3H, t, CH_3). ^{13}C NMR (100 MHz, DMSO-*d*6) 177.31 (C=O), 160.12, 158.35 (C=N), 62.67 (CH), 35.03 (CH_2), 14.38 (CH_3).

4-propyliminoallantoin (14). Yield was 69 %. ^1H NMR (400 MHz, DMSO-*d*6) 7.39 (1H, s, CH), 5.41 (3H, s, 3NH), 3.64 (2H, t, NH_2), 2.63-2.67 (4H, m, 2 CH_2), 1.16 (3H, t, CH_3). ^{13}C NMR (100 MHz, DMSO-*d*6) 15.12 (CH_3), 38.37 (CH_2), 64.19 (CH), 158.13 (C=N), 164.48, 176.07 (C=O).

4-*i*-propyliminoallantoin (15). Yield was 74 %. ^1H NMR (400 MHz, DMSO-*d*6) 7.40 (1H, s, CH), 5.36 (3H, s, 3NH), 3.51 (2H, t, NH_2), 1.44-1.50 (3H, m, CH_3), 1.22 (1H, s, CH), 0.86-0.90 (3H, m, CH_3). ^{13}C NMR (100 MHz, DMSO-*d*6) 177.02 (C=O), 162.61, 157.88 (C=N), 62.48 (CH), 42.06 (CH), 14.09 (CH_3).

4-butyliminoallantoin (16). Yield was 73 %. ^1H NMR (400 MHz, DMSO-*d*6) 7.53 (1H, s, CH), 5.41 (3H, s, 3NH), 3.22 (2H, t, NH_2), 2.67-2.74 (6H, m, 3 CH_2), 0.87 (3H, t, CH_3). ^{13}C NMR (100 MHz, DMSO-*d*6) 160.12 (C=O), 158.29, 147.42 (C=N), 62.67 (CH), 42.17 (CH_2), 30.87 (CH_2), 19.89 (CH_2), 14.11 (CH_3).

4-*i*-butyliminoallantoin (17). Yield was 71 %. ^1H NMR (400 MHz, DMSO-*d*6) 7.56 (1H, s, CH), 5.43 (3H, s, 3NH), 3.10 (2H, t, NH_2), 2.53 (2H, t, CH_2), 1.86-1.90 (1H, m, CH), 0.88 (6H, t, 2 CH_3). ^{13}C NMR

(100 MHz, DMSO-*d*₆) 167.78 (C=O), 167.51, 147.70 (C=N), 58.42 (CH), 49.82, 29.61 (CH₂), 20.89 (CH₃), 20.47.

4-*tert*-butyliminoallantoin (18). Yield was 79 %. ¹H NMR (400 MHz, DMSO-*d*₆) 7.10 (1H, s, CH), 5.41 (3H, s, 3NH), 3.21 (2H, t, NH₂), 1.23 (9H, s, 3CH₃). ¹³C NMR (100 MHz, DMSO-*d*₆) 158.32 (C=O), 158.31, 147.32 (C=N), 62.81 (CH), 43.29 (C_{tert}), 27.61 (CH₃).

Results and Discussion

All reactions were carried out at a temperature of -5 °C and a reaction time of 2 h, which is sufficient for complete conversion of uric acid. It was found that not only the yield of **2** depended on the molar ratio of the reactants, but the formation of the by-product 4-iminoallantoin **8a** was also observed.

Oxidation of uric acid by sodium persulfate

It was identified that the oxidation of **1** by Na₂S₂O₈ at a molar ratio of 1:1 led to the formation of **8a** only (Fig. 2).

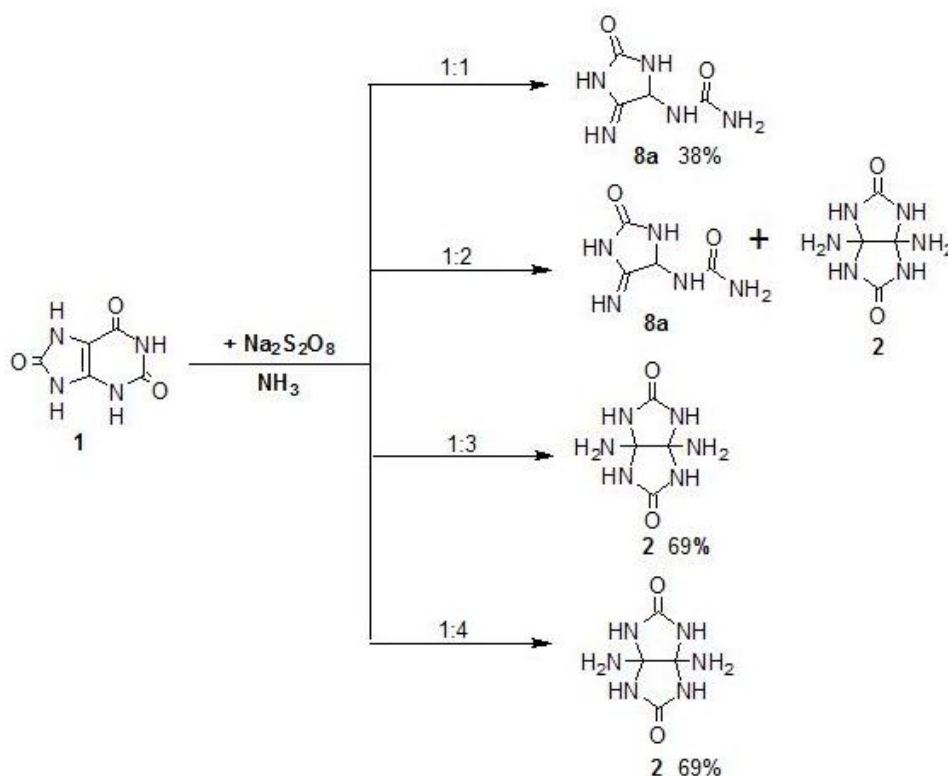


Figure 2. Oxidation of uric acid **1** by sodium persulfate

In the [8], the oxidation process of **1** by potassium ferrocyanide was studied, where two compounds **8a** and **8b** were found as intermediate reaction products, using a labeled carbon atom (Fig. 3).

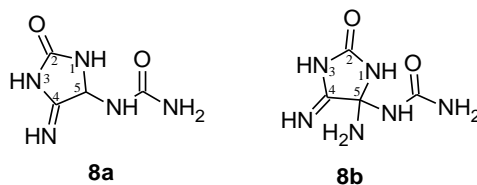


Figure 3. 4-iminoallantoin **8a** and 4-imino-5-aminoallantoin **8b**

Only the structure of intermediate **8a** was found in our studies, using heteronuclear NMR spectroscopy. The presence of a proton at position 5 is characterized by two doublets in the proton spectrum in the range of 6.76-6.78 ppm and 5.56-5.58 ppm, as well as a peak at 62.85 ppm characteristic of the CH bond in the ¹³C spectrum (Fig. 4).

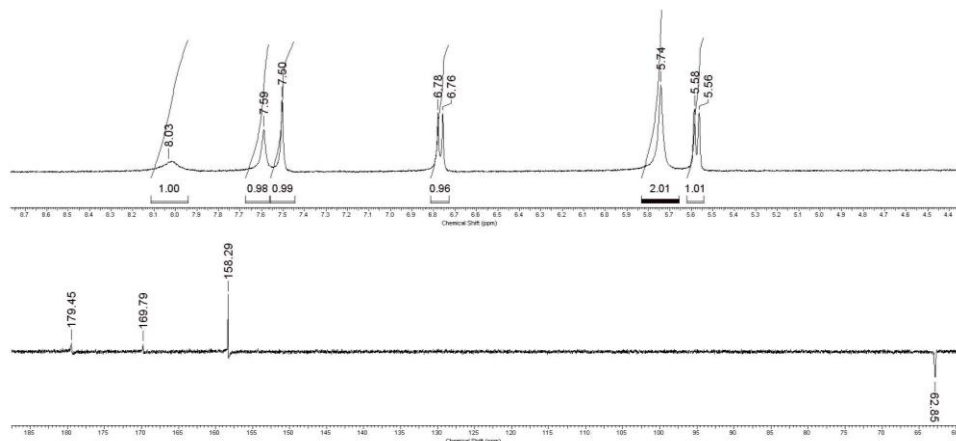


Figure 4. ^1H NMR spectrum and ^{13}C NMR spectrum of compound **8a**

A two times more increase in the amount of the oxidizing agent led to the formation of an intractable mixture, **2** and **8a**. At molar ratios of 1:3 and 1:4, 1,5-diaminoglycoluril is selectively formed, with almost the same yield of 69 % (Fig. 2). The reaction of **1** with ammonia does not proceed without an oxidizing agent.

Oxidation of uric acid by potassium permanganate

The amount of KMnO_4 was varied in order to find the optimal conditions for obtaining **2**, and, as a result, the pattern presented in Figure 5 was revealed.

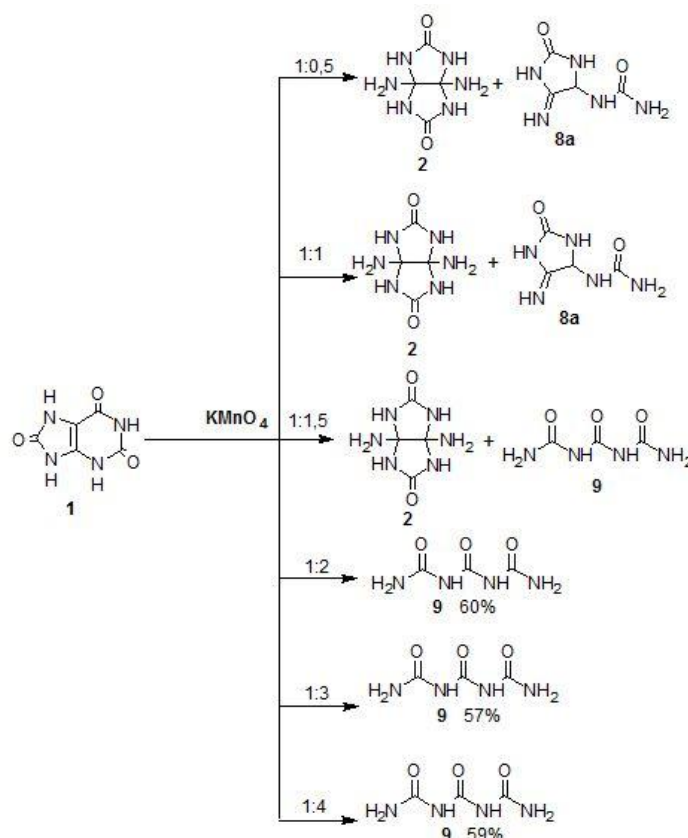


Figure 5. Oxidation of uric acid **1** by potassium permanganate

At molar ratios of 1:0.5 and 1:1 of uric acid **1** with KMnO_4 , products **2** and **8a** are formed. An increase in the amount of the oxidizing agent leads to the formation of compound **9** — triuret, which is described in the literature [10]. In all cases, 1,5-diaminoglycoluril **2** is present in the product mixture.

Potassium permanganate KMnO_4 is converted to MnO_2 (II), which must be converted into a water-soluble MnCl_2 salt to isolate reaction products **2** and **8a**.

With an increase in the reaction time to 4 h at a temperature of -5°C and with a molar ratio of $1:\text{KMnO}_4$ 1:1, the reaction product is only **2** with a yield of 20 % (Fig. 6).

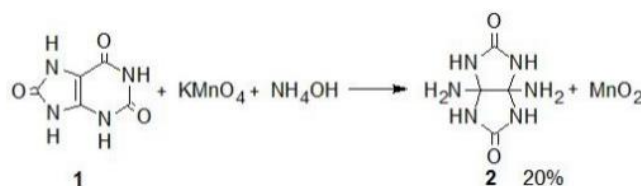


Figure 6. Selective synthesis of 1,5-diaminoglycoluril **2** through the oxidation of uric acid by potassium permanganate

Oxidation of uric acid by manganese (IV) oxide

The using of small amounts of MnO_2 does not allow to complete conversion; the only reaction product is **8a** (Fig. 7). It is necessary to use a 10-fold excess of MnO_2 for the conversion of uric acid to DiAGU with a yield of 34 %. An increase in the reaction time to 4 hours slightly increases the yield of the target product to 38 %.

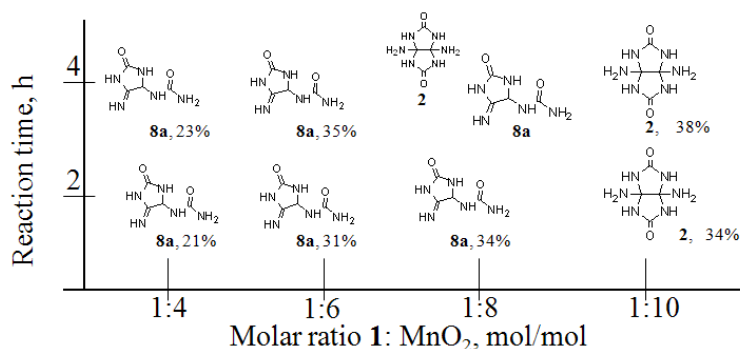


Figure 7. Products of the oxidation reaction of uric acid by MnO_2 , depending on the molar ratio and duration of the reaction

Thus, it was determined that 1,5-diaminoglycoluril could be obtained by oxidation of uric acid by sodium persulfate, potassium permanganate, and manganese (IV) oxide in 69 %, 20 % and 38 % yields, respectively.

Some compounds were investigated, namely BaO , V_2O_5 , CuO , Cr_2O_3 , KClO_3 in the ratio of uric acid : oxidant 1:4 and 1:10 to expand the range of oxidants for the conversion of uric acid into 1,5-diaminoglycoluril. It was found that the listed oxidants did not undergo conversion of uric acid; therefore, the mixture of the starting compound and the oxidizing agent was quantitatively recovered.

We put forward a hypothesis that replacing ammonia with primary amines will result in the formation of a glycoluril structure with various substituents, which would make it possible to expand the range of derivatives of 3,7,10-trioxo-2,4,6,8,9,11-hexaaza[3.3.3]propellane. Figure 8 illustrates a possible synthesis of substituted hexaazapropellanes.

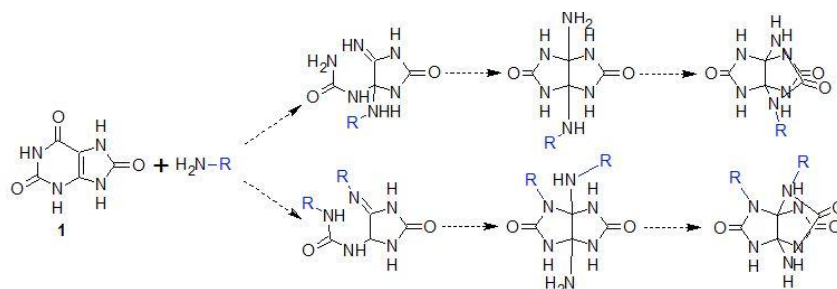


Figure 8. Presumptive scheme for obtaining derivatives of 3,7,10-trioxo-2,4,6,8,9,11-hexaaza[3.3.3]propellane with both the same and different types of substituents

At the first stage, the effect of the molar ratio of reactants on the oxidation of uric acid by sodium persulfate in the presence of benzylamine was investigated. It was found that the interaction of uric acid **1** with benzylamine in a molar ratio of 1: 4 in an aqueous medium in the presence of the oxidizing agent $\text{Na}_2\text{S}_2\text{O}_8$ led to the formation of a mixture of products, namely 4-benzylimino-5-benzylaminoallantoin **10** and 4-benzylimino-1-benzylaminoallantoin **11**. With a decrease in the amount of benzylamine to 1:3 and 1:2, 4-benzylimino-5-benzylaminoallantoin **10** was isolated as a reaction product; at a molar ratio of 1:2, the yield of **10** was higher. Compound **11** without impurity of **10** cannot be isolated (Fig. 9).

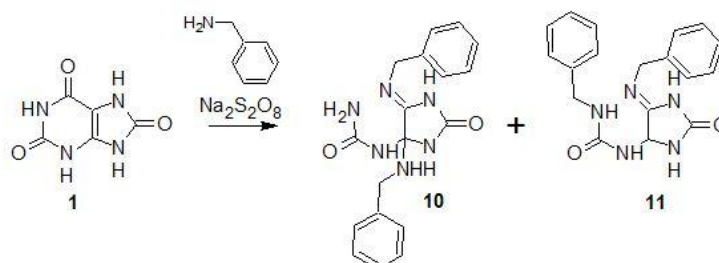


Figure 9. Interaction of uric acid with benzylamine in the presence of sodium persulfate

4-Benzylimino-5-benzylaminoallantoin **10** does not cyclize to the glycoluril structure, which is probably due to steric effects. It was shown that when **10** was treated with an aqueous ammonia solution in the presence of NaCl and at a temperature of 0°C , the reaction product was 4-benzyliminoallantoin **12** (Fig. 10).

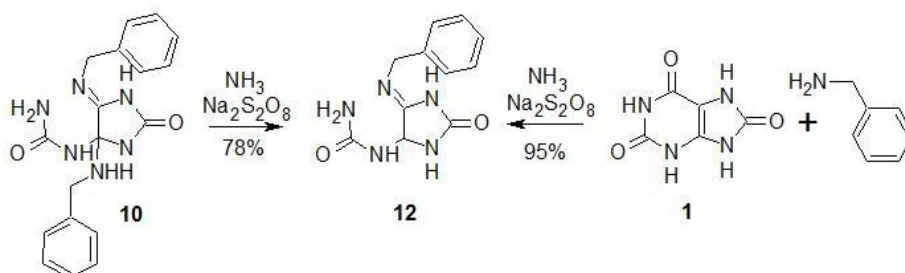


Figure 10. Synthesis of 4-benzyliminoallantoin

As can be seen from Figure 10, during the oxidation of **10**, one benzyl group was cleaved off instead of substitution by the amino group. At the same time, the simultaneous interaction of uric acid with benzylamine and ammonia also led to the formation of compound **12**.

Under conditions similar to synthesis of **12**, a number of new heterocyclic compounds **13-18** were obtained (Fig. 11).

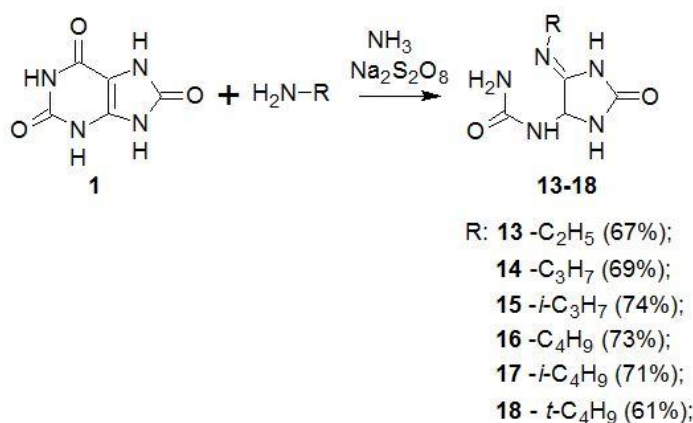


Figure 11. Synthesis of various 4-alkylallantoins

The structure of all obtained compounds **13-18** was proved using IR and heteronuclear NMR spectroscopy. It was found that the signals of iminoallantoin in all compounds were practically identical; the spectra differ only in the signals of the alkyl fragment.

Conclusions

Some stages of the synthesis of 3,7,10-trioxo-2,4,6,8,9,11-hexaaza[3.3.3]propellane are considered in more detail. It was illustrated that not only potassium ferrocyanide and sodium persulfate, but also potassium permanganate and manganese (IV) oxide could be used for the synthesis of one of the key starting compounds of 1,5-diaminoglycoluril with a yield of 20 % and 38 %, respectively.

A study of the interaction of uric acid with benzylamine in the presence of the oxidizing agent sodium persulfate in an aqueous medium was carried out. It was shown that 4-benzylimino-5-benzylaminoallantoin was formed at a molar ratio of 1:2 and 1:3, while an increase in the molar ratio to a 4-fold excess gave a mixture of 4-benzylimino-5-benzylaminoallantoin and 1-benzylamino-4-benzyliminoallantoin, the latter was formed only in a mixture under the conditions studied by us. 4-Benzyliminoallantoin is formed in two ways:

- One-stage: interaction of uric acid with benzylamine and ammonia;
- Two-stage: at the first stage, the interaction of uric acid with benzylamine occurs with the formation of 4-benzylimino-5-benzylaminoallantoin; in the second stage, the oxidation of 4-benzylimino-5-benzylaminoallantoin by sodium persulfate in the presence of ammonia is conducted.

A number of new derivatives of iminoallantoin (4-ethyliminoallantoin, 4-propyliminoallantoin, 4-isopropyliminoallantoin, 4-*n*-butyliminoallantoin, 4-isobutyliminoallantoin, 4-*tert*-butyliminoallantoin, 4-propargyliminoallantoin, 4-phenyliminoallantoin) were obtained by the interaction of uric acid with various amines in the presence of the oxidizing agent sodium persulfate in an aqueous medium at a temperature of 25 °C.

Acknowledgments

The work was carried out on the basic topic № 0308-2021-0003 and using the instrument base of the Biysk Regional Center for Collective Use of the SB RAS (IPCET SB RAS, Biysk).

References

- 1 Aizawa N. Instant low-temperature cross-linking of poly(N-vinylcarbazole) for solution-processed multilayer blue phosphorescent organic light-emitting devices / N. Aizawa, Y.-J. Pu, T. Chiba // *J. Adv. Mater.* — 2014. — Vol. 26. — P. 7543–7546. <https://doi.org/10.1364/SOLED.2014.DW5C.3>
- 2 Oxley J.C. Synthesis and Characterization of Urea Nitrate and Nitrourea / J.C. Oxley, J.L. Smith // *J. Propellants, Explos. Pyrotech.* — 2013. — Vol. 38. — P. 335–344. <https://doi.org/10.1002/prop.201200178>
- 3 Pagoria P.F. 1,1,1-Trimethylhydrazinium iodide: a novel, highly reactive reagent for aromatic amination via vicarious nucleophilic substitution of hydrogen / A.R. Mitchell, E.S. Jessop // *J Prop Explos Pyrotech.* — 1996. — Vol. 21. — P. 14–18. <https://doi.org/10.1021/jo952257z>
- 4 Altman E. Propellanes—I: Tricyclic compounds conjoined in a carbon-carbon single bond / E. Altman, J. Babad, D. Ginsburg // *J. Tetrahedron.* — 1966. — Vol. 22, S. 8. — P. 279–304.
- 5 Boileau, J. ChemInform Abstract: Methods for the preparation of nitro and nitroacetylated derivatives of glycoluril / J. Boileau, E. Wimmer, M. Carail, R. Gallo // *Chemischer Informationsdienst.* — 1986. — Vol. 17, No. 44. <https://doi.org/10.1002/chin.198644179>
- 6 Zhang J. Synthesis, structure characterizations, and theoretical studies of novel tricyclic multiple(urea) molecules / J. Zhang, Y. Liu, F. Bi, J. Zhou, B. Wang // *Journal of Molecular Structure.* — 2017. — Vol. 1141. — P. 268–275. <https://doi.org/10.1016/j.molstruc.2017.03.092>
- 7 Lee B. Synthesis of 2,4,6,8,9,11-hexaaza[3.3.3]propellanes as a new molecular skeleton for explosives / B. Lee, M. Shin, Y. Seo, M.H. Kim, H.R. Lee, J.S. Kim, K.-H. Chung, D. Yoo, Y.G. Kim // *Tetrahedron.* — 2018. — Vol. 74, No. 1 — P. 130–134. <https://doi.org/10.1016/j.tet.2017.11.046>
- 8 Qiu H. Preparation, Crystal Structure, thermal Decomposition, and DFT Calculation of a novel 3D Infinite Structure Coordination Polymer [Na₂(H₂O)₄(ITDO)₂]_n (ITDO = 2H-imidazo[4,5-*e*]-as-1,2,4-triazine-2,7-dihydro-3,6-dione) / H. Qiu, J. Rong, Sh. Li // *Z. Anorg. Allg. Chem.* — 2015. — Vol. 641, No. 2. — P. 424–429. <https://doi.org/10.1002/zaac.201400413>
- 9 Popovic T. Synthesis and structure of dehydro-4-iminoallantoin and its covalent adducts / T. Popovic, L. Sokolic, N. Modric, A. Palkovic, M. Poje // *Tetrahedron.* — 1991. — Vol. 47, No. 2. — P. 317–322. <https://doi.org/10.1002/chin.199112197>
- 10 Kulasegaram S. Zinc monoglycerolate as a catalyst for the conversion of 1,3- and higher diols to diurethanes / S. Kulasegaram, U. Shaheen, T.W. Turney, W.P. Gatesc, A.F. Patti // *RAC Advances.* — 2015. — Iss. 59. — P. 47809–47812. <https://doi.org/10.1039/C5RA05032D>

А.А. Минакова, М.В. Чикина, С.Г. Ильясов

Аммиак немесе біріншілік аминдер ортасында несеп қышқылының тотығу реакциясы өнімдерін зерттеу

Мақалада перспективалы гетероатомды полициклді қосылыстардың бірі 3,7,10-триоксо-2,4,6,8,9,11-гексаза[3.3.3]пропелланды (ТНАР) алудың маңызды кезеңі жан-жақты қарастырылған. Құрылымындағы алты азот атомының болуы себебінен және тығыз орналасуы нәтижесінде ТНАР жоғары энергиялы заттарды жасау үшін қажетті қосылыс болып саналады. Зәр қышқылы ТНАР синтез тізбегіндегі бастапқы қосылыс болып табылады. Оны натрий персульфатымен немесе калий ферроцианидмен тотықтырғанда 1,5-диаминогликолурил және одан трициклдену реакциясы арқылы пропелландық құрылым түзіледі. Осы мақалада несеп қышқылын 1,5-диаминогликолурилге айналдыру үшін тотықтырғыштардың ауқымы кеңейтілген. Несеп қышқылы мен KMnO_4 эквимолярлық қатынасын қолданғанда 1,5-диаминогликолурилдың шығымы 20 % болатыны, ал MnO_2 мөлшерін он есе артық қолданғанда 1,5-диаминогликолурил шығымы 38 % құрайтыны анықталды. Авторлар мақалада сонымен қатар несеп қышқылының кейбір аминдермен әрекеттесуін зерттеу нәтижелерін келтірген. Реакция өнімдері 4-бензилимин-5-бензиламиналлантоин, 4-бензилимин-1-бензиламиналлантоин және 4-бензилиминаллантоин болып табылатын несеп қышқылының бензиламинмен әрекеттесу реакциясы толығырақ зерттелген. 4-бензилиминаллантоин синтезі негізінде 4-иминоаллантоиннің 4-этилиминаллантоин, 4-пропилиминаллантоин, 4-изопропилиминоаллантоин, 4-*n*-бутилиминаллантоин, 4-*изо*-бутилиминаллантоин, 4-трет.-бутилиминаллантоин сияқты бірқатар перспективалы туындылары алынды.

Кілт сөздер: несеп қышқылы, 1,5-диаминогликолурил, 3,7,10-триоксо-2,4,6,8,9,11-гексаза[3.3.3]-пропеллан (ТНАР), тотығу аминденуі, 4-алкилиминаллантоиндер.

А.А. Минакова, М.В. Чикина, С.Г. Ильясов

Исследование продуктов реакции окисления мочевой кислоты в среде аммиака или первичных аминов

В статье подробно рассмотрен важный этап получения одного из перспективных гетероатомных полициклических соединений — 3,7,10-триоксо-2,4,6,8,9,11-гексаза[3.3.3]пропеллана (ТНАР). Благодаря наличию шести атомов азота в структуре и плотной упаковке ТНАР является потенциальным соединением для создания высокоэнергетических веществ. Мочевая кислота является исходным соединением в цепочке превращения синтеза ТНАР. При ее окислении персульфатом натрия или ферроцианидом калия получается 1,5-диаминогликолурил, из которого реакцией трициклизации образуется структура пропеллана. Авторами расширен ряд окислителей для превращения мочевой кислоты в 1,5-диаминогликолурил. Было обнаружено, что 1,5-диаминогликолурил образуется с выходом 20 % при использовании эквимолярных соотношений мочевой кислоты и KMnO_4 , а при применении десятикратного избытка MnO_2 выход 1,5-диаминогликолурила составил 38 %. Кроме того, представлены результаты исследования взаимодействия мочевой кислоты с некоторыми аминами. Подробно изучена реакция взаимодействия мочевой кислоты с бензиламином, продуктами реакции которой являются 4-бензилимино-5-бензиламиноаллантоин, 4-бензилимино-1-бензиламиноаллантоин и 4-бензилиминоаллантоин. На основе синтеза 4-бензилиминоаллантоина был получен ряд перспективных производных 4-иминоаллантоина: 4-этилиминоаллантоин, 4-пропилиминоаллантоин, 4-изопропилиминоаллантоин, 4-*n*-бутилиминоаллантоин, 4-*изо*-бутилиминоаллантоин, 4-трет.-бутилиминоаллантоин.

Ключевые слова: мочевая кислота, 1,5-диаминогликолурил, 3,7,10-триоксо-2,4,6,8,9,11-гексаза[3.3.3]пропеллан (ТНАР), окислительное аминирование, 4-алкилиминоаллантоины.

References

- 1 Aizawa, N., Pu, Y., Chiba, T., Kawata, S., Sasabe, H., & Kido, J. (2014). Organic Light-Emitting Devices: Instant Low-Temperature Cross-Linking of Poly(N-vinylcarbazole) for Solution-Processed Multilayer Blue Phosphorescent Organic Light-Emitting Devices (Adv. Mater. 45/2014). *Advanced Materials*, 26(45), 7675–7675. doi: 10.1002/adma.201470311
- 2 Oxley, J.C., Smith, J.L., Vadlamannati, S., Brown, A.C., Zhang, G., Swanson, D.S., & Canino, J. (2013). Synthesis and Characterization of Urea Nitrate and Nitrourea. *Propellants, Explosives, Pyrotechnics*, 38(3), 335–344. doi: 10.1002/prop.201200178
- 3 Pagoria, P.F., Mitchell, A.R., & Schmidt, R.D. (1996). 1,1,1-Trimethylhydrazinium Iodide: A Novel, Highly Reactive Reagent for Aromatic Amination via Vicarious Nucleophilic Substitution of Hydrogen. *The Journal of Organic Chemistry*, 61(9), 2934–2935. doi:10.1021/jo952257z

- 4 Altman E., Babad, J. & Ginsburg, D. (1966). Propellanes–I: Tricyclic Compounds Conjoined in a Carbon–carbon Single Bond. *J. Tetrahedron*, 22(8), 279–304.
- 5 Boileau, J., Wimmer, E., Carail, M., & Gallo, R. (1986). ChemInform Abstract: Methods for the Preparation of Nitro and Nitroacetylated Derivatives of Glycoluril. *Chemischer Informationsdienst*, 17(44). doi: 10.1002/chin.198644179
- 6 Zhang, J., Liu, Y., Bi, F., Zhou, J., & Wang, B. (2017). Synthesis, structure characterizations, and theoretical studies of novel tricyclic multiple(urea) molecules. *Journal of Molecular Structure*, 1141, 268–275. doi: 10.1016/j.molstruc.2017.03.092
- 7 Lee, B., Shin, M., Seo, Y., Kim, M.H., Lee, H.R., Kim, J.S., & Kim, Y.G. (2018). Synthesis of 2,4,6,8,9,11-hexaaza[3.3.3]propellanes as a new molecular skeleton for explosives. *Tetrahedron*, 74(1), 130–134. doi: 10.1016/j.tet.2017.11.046
- 8 Qiu, H., Rong, J., Li, S., Tong, W., Zhang, T., & Yang, L. (2014). Preparation, Crystal Structure, Thermal Decomposition, and DFT Calculation of a Novel 3D Infinite Structure Coordination Polymer $[\text{Na}_2(\text{H}_2\text{O})_4(\text{ITDO})_2]_n$ (ITDO = 2H-imidazo-[4,5-e]-as-1,2,4-triazine-2,7-dihydro-3,6-dione). *Zeitschrift Für Anorganische Und Allgemeine Chemie*, 641(2), 424–429. doi: 10.1002/zaac.201400413
- 9 Popović, T., Sokolić, L., Modrić, N., Palković, A., & Poje, M. (1991). Synthesis and structure of dehydro-4-iminoallantoin and its covalent adducts. *Tetrahedron*, 47(2), 317–322. doi:10.1016/s0040-4020(01)80927-3
- 10 Kulasegaram, S., Shaheen, U., Turney, T.W., Gatesc, W.P., & Patti, A.F. (2015). Zinc monoglycerolate as a catalyst for the conversion of 1,3- and higher diols to diurethanes. *RAC Advances*, 59, 47809-47812. doi: 10.1039/C5RA05032D

Information about authors:

Minakova Anastasia Aleksandrovna (*corresponding author*) — Junior Research Scientist at the Laboratory of High-Energy Compounds Synthesis, Institute for Problems of Chemical and Energetic Technologies, Siberian Branch of the Russian Academy of Sciences (IPCET SB RAS), Russia; e-mail: nastya.sinitsyna.1994@mail.ru. ORCID: <https://orcid.org/0000-0003-3850-3132>

Chikina Maya Victorovna — Candidate of chemical sciences, Research Scientist at the Laboratory of High-Energy Compounds Synthesis, Institute for Problems of Chemical and Energetic Technologies, Siberian Branch of the Russian Academy of Sciences (IPCET SB RAS), e-mail: chikina_maya@mail.ru. ORCID: <https://orcid.org/0000-0002-1783-7718>

Sergey Gavrilovich Il'yasov — Doctor of Chemical Sciences, Deputy Director for Research, Head of Laboratory, Laboratory of High-Energy Compounds Synthesis, Institute for Problems of Chemical and Energetic Technologies, Siberian Branch of the Russian Academy of Sciences (IPCET SB RAS), Russia; e-mail: ilysov@ipcet.ru. ORCID: <https://orcid.org/0000-0002-7853-6118>

PHYSICAL AND ANALYTICAL CHEMISTRY

UDC 543.544.3+519.242.7

<https://doi.org/10.31489/2021Ch4/39-46>

V.N. Fomin, A.A. Aynabaev, D.A. Kaykenov, D.T. Sadyrbekov,
S.K. Aldabergenova*, M.A. Turovets, N.K. Kelesbek

*Karagandy University of the name of academician E.A. Buketov, Karaganda, Kazakhstan
(Corresponding author's e-mail: aldsau@mail.ru)*

Optimization of coal tar gas chromatography conditions using probabilistic-deterministic design of experiment

The development of physicochemical methods for the analysis of objects of complex composition requires the application of methods of mathematical experiment design. This article investigates the possibility of using probabilistic-deterministic design of experiment (PDDoE) for obtaining a mathematical model of the chromatographic separation process of coal tar hydrogenation products on an Agilent 7890A device with an Rxi-5ms column. It is shown that the relationship between the column heating rate and the carrier gas pressure with the values averaged for the entire chromatogram can be established with a high accuracy. It is noted that the accuracy of modeling the individual characteristics of the mixture components' peaks is less, but remains sufficient for many practical needs. Nonlinear multiple correlation coefficients (NMC) for the dependence of the average retention time and average intensity on the considered factors are more than 0.99; they are more than 0.98 for the average peak width. NMC for the dependence of the resolution with the relation to the peaks of naphthalene and 2-ethylphenol is more than 0.8 at a significant level that sufficient for practice. The quality of the mathematical model was checked by triple registration of the chromatogram at the values of the column heating rate and carrier gas pressure that were not used in the training experiment. The measurement results are excellent squared with those calculated using the obtained generalized equations. The PDDoE method can be recommended as a method for mathematical design of an optimization experiment in gas chromatography.

Keywords: gas chromatography, design of experiment, coal tar, GC-MS, PDDoE, optimization, retention time, peak width and height.

Introduction

Gas chromatography (GC) is one of the most effective methods being used to separate complex mixtures of substances. The separation quality depends on a number of the experiment parameters, including device settings [1]. Most gas chromatography devices allow one to set two parameters of the chromatographic separation process, namely the flow rate (pressure) of the carrier gas and the column heating rate. The influence of each of these two factors on the retention time of substances is qualitatively predictable based on general laws, specifically the relative retention time decreases with increasing gas pressure and temperature. Column efficiency is not linearly dependent on gas flow rate and temperature, and is unique to each column. Thus, controlling the temperature and gas flow rate allows to control the chromatogram quality and the analysis rate. Considering the unique characteristics of chromatography devices and analytes, it seems impossible to predict the retention time of a particular component and the resolution capability of the method in the case of a given object by using the fundamental laws. On the other hand, empirical formulas, that link instrument settings to chromatogram characteristics, can be obtained relatively easily. These parameters have a combined effect on the results; therefore, it is considered effective to use mathematical experiment design to optimize them [2].

The authors of a number of works achieved a significant improvement in the characteristics of the developed methods by applying traditional methods of experiment design to the chromatography process or to sample preparation. In [3], the authors optimize the sample preparation of biological fluids for the determination of formaldehyde using mathematical design of the experiment. In most works, conditions optimization of a gas chromatography is carried out by the empirical selection of parameters until satisfactory results are achieved. The low efficiency of this method compared to design of experiment has been repeatedly discussed in various sources. Publications [4–5] show that the optimization of GC parameters can significantly improve the components separation, and, as a consequence, reduce the limit of detection and determination limit, as well as simplify their identification.

Analysis of the literature indicates that probabilistic-deterministic design of experiment [6], that is being used successfully in the study of chemical-technological processes [7, 8], can be also used in the development of methods of physical and chemical analyses [9, 10]. It seems interesting to investigate the possibility of using PDDoE to optimize the conditions of a gas chromatography.

Coal tar is a valuable source of a number of organic compounds. An international group of researchers, including professor M.I. Baikenov and his employees who conducted the research on the production of liquid fuels from light oil and other fractions of coal tar [8, 11, 12]. These studies require systematic control of the qualitative and quantitative composition of the reaction mixtures by gas chromatography – mass spectrometry (GC-MS).

The aims of the study are as follows:

- 1) Obtaining mathematical models linking the carrier gas pressure and the column heating rate with the average values of the retention time, height, and width of the main peaks in the chromatogram.
- 2) Verification of the mathematical model in a control experiment.
- 3) Obtaining a mathematical model for the resolution of closely spaced peaks, for example, naphthalene and 4-ethylphenol.

Experimental

A solution of a light fraction of coal tar in chloroform was used as a test mixture. An Agilent 7890A gas chromatography device with an Agilent 5975C mass selective detector has applied. 0.01 g of the sample was dissolved in the solvent, so the volume of the solution was 10 ml. The solution was filtered and injected into the column using an autosampler. The analysis was carried out under the following conditions: column type was Rxi-5ms, column length was 30 m; column diameter was 0.25 mm; column adsorbent thickness was 0.25 μm , evaporator temperature was 250 $^{\circ}\text{C}$; thermostat temperature was 60–250 $^{\circ}\text{C}$; carrier gas was helium; sample volume was 0.2 μl with a 1:1 sample separation. The heating rate of the thermostat and the pressure of the carrier gas were set according to the design of a four-factor experiment with three levels of variation, and then chromatograms were recorded. The positions of two factors in the design of experiment were left vacant. The structure of the PDDoE design and the mathematical processing of the results of its application, as well as calculations based on the obtained empirical equations, were carried out using the previously developed program “PDDoE” (Auth. Sert. RK No. 26 dated 01.10.2018).

As a matter of convenience, peaks with high intensity corresponding to the highest content of the substance in the mixture were selected for the study. The primary processing of the results was carried out automatically using the standard program “GC-MS Data Analysis”, containing a database of mass spectra of nearly 1,000,000 compounds.

Considering the high reproducibility of the GC method and the unique features of the PDDoE method, it is possible to avoid the errors of a singular measurement [9], so the optimization experiment was carried out in one repetition. The chromatogram obtained under the conditions determined by the PDDoE method was recorded three times to assess the performance and quality of the model.

Results and Discussion

Table 1 illustrates the design of a four-factor experiment for the optimization of the GC conditions with three levels of factors variation, as well as some results of its application. The rate of column temperature rise and the pressure of the carrier gas were selected as variable factors. The positions of two factors were left vacant.

Table 1

Design and results of the optimization experiment

No.	$\Delta T, ^\circ\text{C}/\text{min}$	P, psi	Vac. 1	Vac. 2	\bar{t}_R, min	$\bar{\omega}, \text{min}$	$\bar{I} * 10^{-4}$
1	1	2	1	1	84.93	0.389	300.9
2	1	5	2	2	81.71	0.334	272.7
3	1	10	3	3	77.44	0.338	190.45
4	6	2	2	3	21.51	0.0945	1390.9
5	6	5	3	1	20.71	0.0936	1236.4
6	6	10	1	2	19.83	0.0845	884.54
7	12	2	3	2	12.8	0.06	1754.5
8	12	5	1	3	12.27	0.06	1777.3
9	12	10	2	1	11.6	0.06	1413.6

Here, $\Delta T, ^\circ\text{C}/\text{min}$ is column heating rate; P, psi is a carrier gas pressure; Vac. 1, Vac. 2 are values of vacant factors, \bar{t}_R, min is an average retention time, $\bar{\omega}, \text{min}$ is an average peak width, $\bar{I} * 10^{-4}$ is an average intensity over 11 peaks.

The main goal of the optimization experiment was to achieve a balance between the resolution and the duration of the chromatogram registration process. In Figure 1 it can be seen that changing the conditions process significantly affects the chromatogram.

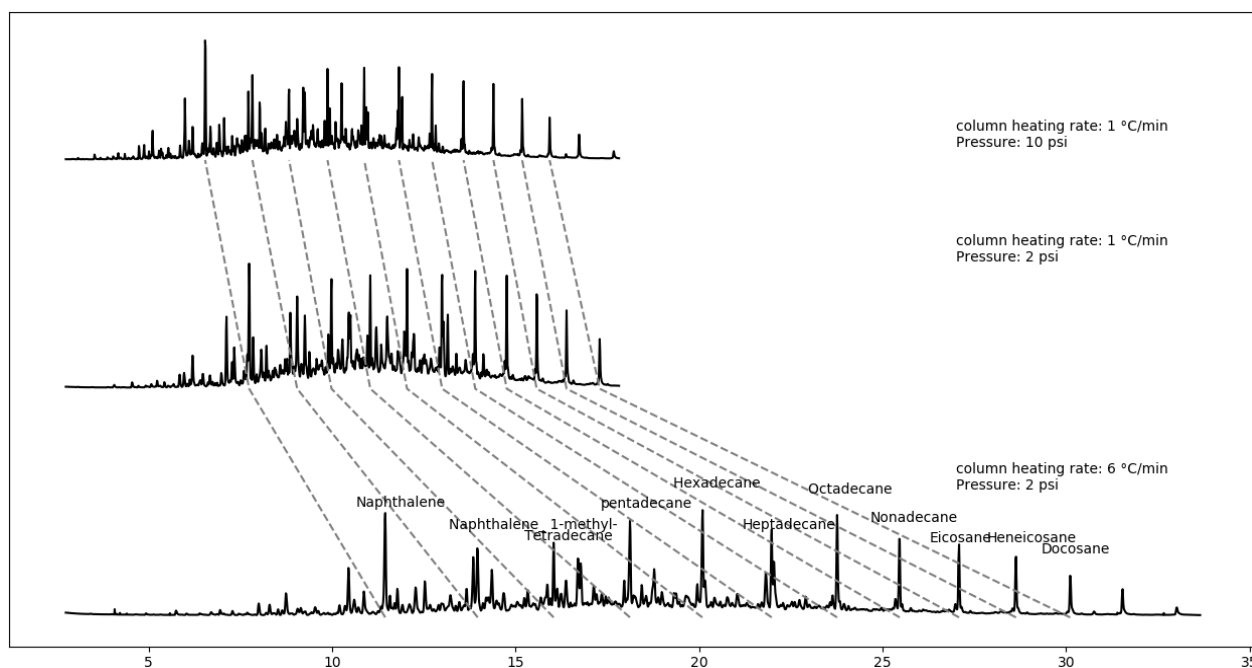


Figure 1. Influence of helium pressure and column heating rate on chromatogram quality

The figure perfectly illustrates that there is the general tendency of the process acceleration with increasing pressure and, more specifically, increasing heating rate, and an increase in resolution with decreasing carrier gas pressure. The data in Table 1 were processed using PDDoE to establish a quantitative relationship between gas pressure, heating rate, and some parameters of the chromatogram. Since three levels of factors variation create only three points for approximating the partial dependence, the list of used approximating functions was limited to linear and intrinsically linear ones. Figure 2 shows the dependence of the average retention time on significant parameters. Analysis of the curves clearly demonstrates that the average distance between the peaks decreases rapidly with an increase of the heating rate and slightly decreases with an increase of the carrier consumption. The dependences on the vacant factors are expressed by straight lines that practically coincide with the line of average values, which indicates the minimal influence of unaccounted and random factors on the experiment result.

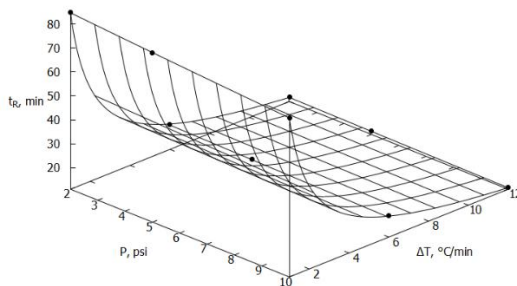


Figure 2. Dependence of the average retention time on heating rate and helium pressure

Generalized equation (1) describes the dependence of the average retention time on the considered factors:

$$\bar{t}_R = 81.26 \times \Delta T^{-0.7631} \times \frac{1}{0.03421 + 0.0004116 \times P} / 27.3804, R = 0.9917, t_R = 146.9447. \quad (1)$$

The dependences of the average width of the peaks in the chromatogram on the considered parameters (Fig. 3) also turned out to be decreasing. The heating rate plays a dominant role, as in the case of the average retention time.

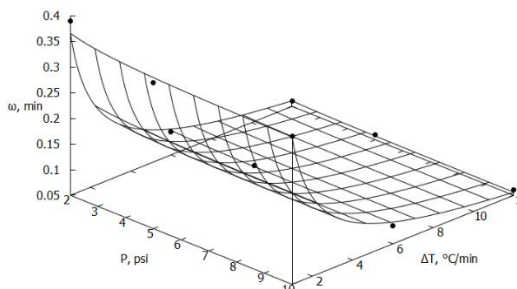


Figure 3. Dependence of the average width of the peak on heating rate and helium pressure

Generalized equation (2) describes the dependence of the average retention time on the considered factors:

$$\bar{\omega} = 0.3478 \times \Delta T^{-0.7219} \times (0.117 + \frac{0.0255}{P}) / 0.1234, R = 0.9857, t_R = 85.0297. \quad (2)$$

The partial dependences of the average peak height on the conditions of chromatographic separation, presented in Fig. 4, allow us to conclude that the relationship between the width and height of the peaks is ambiguous. The average height logically increases with an increase of the heating rate, but decreases with an increase of the carrier gas pressure, more than the average width.

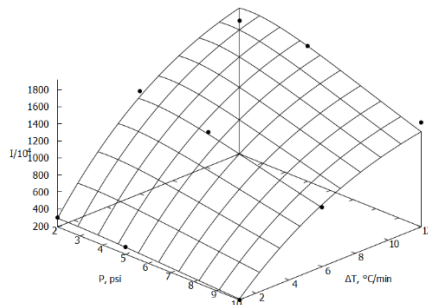


Figure 4. Dependence of the average height of the peak on heating rate and helium pressure

Generalized equation (3) describes the dependence of the average retention time on the considered factors:

$$\bar{I} \times 10^{-4} = 264.9e^{-0.05799\Delta T} \times \Delta T^{1.014} \times 925.8e^{-0.09389P} \times P^{0.2335} / 778.2956, R = 0.9928, t_R = 169.4889. \quad (3)$$

For multicomponent systems, as a rule, it is not possible to select the conditions for a chromatogram registration that are equally suitable for a clear separation of all components. At the same time, the obtained mathematical model (equations 1–3) is applicable for an optimization of the general qualitative and semi-quantitative analysis.

Based on the recorded chromatograms, a model can be built for any other measurement result (for example, for the resolution with a relation to certain signals) without repeated measurements. This point is the undoubted advantage of the PDDoE in comparison to other methods of mathematical experiment design.

For mathematical models of the resolution with a relation to a particular pair of peaks, a slight decrease in accuracy is observed, which is most likely associated with the variance in determining the width of the peaks. For example, the dependence of the resolution (R_s) of the peaks of naphthalene and 4-ethylphenol on the considered parameters is described with the help of the equation (4):

$$R_s = (0.083 + 0.2346/P) \times (0.1364 + 0.08223/\Delta T) / 0.1577, R = 0.8003, t_R = 5.4526. \quad (4)$$

The experimental value of the resolution for these peaks was obtained according to the generally accepted formula $R_s = \frac{2d}{\omega_1 + \omega_2}$, in which d is a distance between the tops of the peaks, ω is a width of the peak.

Figure 5 allows to see that individual experimental points are located at a relatively large distance from the approximated surface.

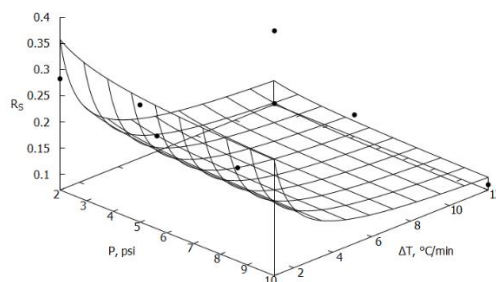


Figure 5. Dependence of the resolution (R_s) of the peaks of naphthalene and 4-ethylphenol on heating rate and helium pressure

The calculation of the maximum achievable value of the resolution of the indicated peaks leads to a value of 0.3575 at $P = 2$ psi $\Delta T = 1$ °C/min.

Experimental verification of the obtained dependencies was carried out by triple registration of the chromatogram at a pressure of 3 psi and a heating rate of 2 °C/min. Considering the Student's coefficient for three measurements and a probability of 0.95, equal to 4.3, the results are represented in Table 2.

Table 2

Results of the experimental verification of the model

Y	Y _{calc}	Y _{exper}
\bar{t}_R	49.5026	49.55±1.89
$\bar{\omega}$	0.2145	0.2164±0.0085
\bar{I}	549.75	549.01±19.11
R_s	0.2082	0.2185±0.0833

The result of the control experiment shows that the mathematical model is adequate and the assessment of its accuracy is correct. The accuracy of the generalized equations generally correlates with the reproducibility of the quantities.

Conclusions

Summarizing all of the results, we can conclude that probabilistic-deterministic design of experiment can be successfully used to optimize the conditions for gas chromatography of complex mixtures. When using the method, it should be considered that the averaged parameters of the chromatogram are explained by

generalized equations with an accuracy higher than 0.98, while for individual characteristics (the height of one peak, the resolution of 2 peaks, the retention time of the component, etc.), the accuracy of the models turns out to be noticeably lower due to the worse experimental reproducibility of these values. In general, PDDoE can be recommended for carrying out an optimization of the experiment in gas chromatography.

References

- 1 Вяхирев Д.А. Руководство по газовой хроматографии: учеб. пособие для хим. и хим.-технол. спец. вузов. — 2-е изд., перераб. и доп. / Д.А. Вяхирев, А.Ф. Шушунова. — М.: Высш. шк., 1987. — 335 с.
- 2 Смагунова А.Н. Математическое планирование эксперимента в методических исследованиях аналитической химии: учеб. пос. — 2-е изд., испр. / А.Н. Смагунова, Г.В. Пашкова, Л.И. Белых. — СПб.: Лань, 2017. — 120 с.
- 3 Алексеенко А.Н. Применение математического планирования эксперимента при выборе оптимальных условий парофазного газохроматографического определения формальдегида в моче / А.Н. Алексеенко, О.М. Журба // Гигиена и санитария. — 2018. — Т. 97, № 10. — С. 985–989. DOI: <http://dx.doi.org/10.18821/0016-9900-2018-97-10-985-989>
- 4 Alladio E. Optimization and validation of a GC–MS quantitative method for the determination of an extended estrogenic profile in human urine: Variability intervals in a population of healthy women / E. Alladio, E. Amante, C. Bozzolino et al. // Biomedical Chromatography. — 2021. — Vol. 35. — e4967. <https://doi.org/10.1002/bmc.4967>.
- 5 Hibbert D. Experimental design in chromatography: A tutorial review // Journal of chromatography. B, Analytical technologies in the biomedical and life sciences. — 2012. — P. 910. <https://doi.org/10.1016/j.jchromb.2012.01.020>.
- 6 Беляев С.В. Пути развития вероятностно-детерминированного планирования эксперимента // Комплексная переработка минерального сырья Казахстана. Состояние, проблемы, решения: [В 10 т.]. Т. 9. Информационные технологии в минерально-сырьевом комплексе. Гл. 8 / С.В. Беляев, В.П. Малышев. — Алматы, 2008. — С. 599–633.
- 7 Ibishev K.S. Preparation of nanosized nickel powder by direct-current electrolysis combined with high-voltage spark discharge / K.S. Ibishev, V.P. Malyshev, S.V. Kim, B.Sh. Sarsembaev, N.B. Egorov // High Energy Chemistry. — 2017. — Vol. 51. — № 3. — P. 219–223.
- 8 Akhmetkarimova, Z.S. Mathematical simulation of the hydrogenation of Borodino coal / Z.S. Akhmetkarimova, M.I. Baikenov, A.M. Dyusekenov // Solid Fuel Chem. — 2017. — Vol. 51, No. 2. — P. 111–114. <https://doi.org/10.3103/S0361521917020021>
- 9 Fomin V.N. Method for increasing the accuracy of quantitative determination of iron by LIBS / V.N. Fomin, S.K. Aldabergenova, K.T. Rustembekov, A.V. Dik, Yu.Yu. Kim, I.E. Rozhkovoy // Bulletin of the Karaganda University. Chemistry series. — 2018. — No. 3(91). — P. 74–83
- 10 Фомин В.Н. Оптимизация параметров лазерно-искрового эмиссионного спектрометра с применением вероятностно-детерминированного планирования эксперимента / В.Н. Фомин, С.К. Алдабергенова, К.Т. Рустембеков, Х.Б. Омаров, И.Е. Рожковой, А.В. Дик, Д.М. Саулебеков // Заводская лаборатория. Диагностика материалов. — 2021. — No. 87(5). — С. 14–19. <https://doi.org/10.26896/1028-6861-2021-87-5-14-19>
- 11 Balpanova N. Kinetics of cavitation of an intermediate fraction of coal tar / N. Balpanova, A. Tusipkhan, A. Gyl'maliev, F. Ma, A. Kyzkenova, D. Aitbekova, Z. Khalikova, G. Baikenova, M. Baikenov // Solid Fuel Chemistry. — 2020. — Vol. 54. — P. 208–213. [10.3103/S0361521920040023](https://doi.org/10.3103/S0361521920040023).
- 12 Baikenov M. Thermal decomposition of a mixture of tar with primary coal tar with the additives of iron compounds / M. Baikenov, E. Kochegina, Z. Khalikova, Z. Absat, A. Karimova, N. Rakhimzhanova, A. Tusipkhan, G. Baikenova // Solid Fuel Chemistry. — 2019. — Vol. 53. — P. 96–104. <https://doi.org/10.3103/S0361521919020034>

В.Н. Фомин, А.А. Айнабаев, Д.А. Кайкенов, Д.Т. Садырбеков,
С.К. Алдабергенова, М.А. Туровец, Н.К. Келесбек

Эксперименттің ықтималды детерминистік жоспарлауын қолданумен көмір шайырының газ хроматографиясы жағдайларын оңтайландыру

Құрамы күрделі объектілерді талдаудың физика-химиялық әдістерін әзірлеу үшін экспериментті математикалық жоспарлау әдістерін қолдануды талап етеді. Мақалада Rxi-5ms бағаны бар Agilent 7890A аспабында таскөмір шайырын гидрогенизациялау өнімдерін хроматографиялық бөлу үдерісінің математикалық моделін алу үшін эксперименттің ықтималды-детерминистік жоспарлауды (ЭЫДЖ) қолдану мүмкіндігі зерттелген. Бағанның қыздыру жылдамдығы мен тасымалдаушы газ қысымының барлық хроматограмма үшін орташа мәндерімен байланысын жоғары дәлдікпен орнатуға болатындығы көрсетілген. Қоспаның құрамдас бөліктерінің шыңдарының жеке сипаттамаларын модельдеудің дәлдігі аз, бірақ көптеген практикалық қажеттіліктер үшін жеткілікті болып табылады. Орташа ұстау уақыты мен орташа қарқындылықтың қарастырылатын факторларға тәуелділігі үшін сызықтық емес көпше корреляция коэффициенттері (СККК) 0,99-дан асты, шыңның орташа ені үшін

ол 0,98-ді құрады. Нафталин мен 2-этилфенол шыңдарына қатысты айыру қабілетінің тәуелділігі үшін СККК практика үшін маңыздылық деңгейі жеткілікті жағдайында 0.8-ден асты. Математикалық модельдің сапасы оқыту экспериментінде қолданылмаған бағанның қыздыру жылдамдығы мен тасымалдаушы газдың қысымы мәндерінде хроматограмманы үш рет тіркеу жолымен тексерілді. Алынған жалпыланған теңдеулермен есептелген нәтижелер өлшеу нәтижелерімен жақсы үйлеседі. Газ хроматографиясында оңтайландырылған экспериментті математикалық жоспарлаудың әдісі ретінде ЭЫДЖ әдісін ұсынуға болады.

Кілт сөздер: газ хроматографиясы, экспериментті жоспарлау, көмір шайыры, МС-ГХ, экспериментті ықтималды-детерминистік жоспарлау, оңтайландыру, айыру уақыты, шыңның биіктігі мен ені.

В.Н. Фомин, А.А. Айнабаев, Д.А. Кайкенов, Д.Т. Садырбеков,
С.К. Алдабергенова, М.А. Туровец, Н.К. Келесбек

Оптимизация условий газовой хроматографии каменноугольной смолы с применением вероятностно-детерминированного планирования эксперимента

Разработка физико-химических методов анализа объектов сложного состава требует применения методов математического планирования эксперимента. В статье исследована возможность использования вероятностно-детерминированного планирования эксперимента (ВДПЭ) для получения математической модели процесса хроматографического разделения продуктов гидрирования каменноугольной смолы на приборе Agilent 7890A с колонкой Rxi-5ms. Показано, что взаимосвязь скорости нагревания колонки и давления газа-носителя с величинами, усредненными для всей хроматограммы, может быть установлена с высокой точностью. Отмечено, что точность моделирования индивидуальных характеристик пиков компонентов смеси меньше, однако остается достаточной для многих практических нужд. Коэффициенты нелинейной множественной корреляции (КНМК) для зависимости среднего времени удерживания и средней интенсивности от рассматриваемых факторов превысили 0,99, для средней ширины пика составили более 0,98. КНМК для зависимости разрешающей способности по отношению к пикам нафталина и 2-этилфенола превысили 0,8 при достаточном для практики уровне значимости. Качество математической модели проверено трёхкратной регистрацией хроматограммы при значениях скорости нагревания колонки и давления газа-носителя, не использовавшихся в обучающем эксперименте. Результаты измерений отлично согласуются с вычисленными по полученным обобщённым уравнениям. Метод ВДПЭ может быть рекомендован в математическом планировании оптимизационного эксперимента в газовой хроматографии.

Ключевые слова: газовая хроматография, планирование эксперимента, каменноугольная смола, ГХ-МС, ВДПЭ, оптимизация, время удерживания, высота и ширина пика.

References

- 1 Viakhirev, D.A., & Shushunova, A.F. (1987). *Rukovodstvo po gazovoi khromatografii [Gas Chromatography Guide]*. Moscow: Vysshaya shkola [in Russian].
- 2 Smagunova, A.N., Pashkova, G.V., & Belykh, L.I. (2017) *Matematicheskoe planirovanie eksperimenta v metodicheskikh issledovaniyakh analiticheskoi khimii [Mathematical planning of an experiment in methodological research in analytical chemistry]*. Saint Petersburg: Lan [in Russian].
- 3 Alekseenko, A.N., & Zhurba, O.M. (2018). Primenenie matematicheskogo planirovaniia eksperimenta pri vybore optimalnykh uslovii parofaznogo gazokhromatograficheskogo opredeleniia formaldegida v moche [The use of mathematical planning of the experiment when choosing the optimal conditions for the headspace gas chromatographic determination of formaldehyde in urine]. *Gigiena i sanitariia — Hygiene and sanitation*, 97(10), 985–989. <http://dx.doi.org/10.18821/0016-9900-2018-97-10-985-989> [in Russian].
- 4 Alladio, E., Amante, E., & Bozzolino, C., et al. (2021). Optimization and validation of a GC–MS quantitative method for the determination of an extended estrogenic profile in human urine: Variability intervals in a population of healthy women. *Biomedical Chromatography*, 35, e4967. <https://doi.org/10.1002/bmc.4967>.
- 5 Hibbert, D. (2012). Experimental design in chromatography: A tutorial review. *Journal of chromatography. B, Analytical technologies in the biomedical and life sciences*. <https://doi.org/10.1016/j.jchromb.2012.01.020>.
- 6 Beliaev, S.V., & Malyshev, V.P. (2008). Puti razvitiia veroiatnostno-determinirovannogo planirovaniia eksperimenta [Ways of stochastic-determined design of experiments development]. (Vols. 1-10; Vol. 9): *Informatsionnye tehnologii v mineralno-syryevom komplekse — Information technologies in the mineral-raw complex*, 8, Almaty [in Russian].
- 7 Ibishev, K.S., Malyshev, V.P., Kim, S.V., Sarsembaev, B.Sh., & Egorov, N.B. (2017). Preparation of nanosized nickel powder by direct-current electrolysis combined with high-voltage spark discharge. *High Energy Chemistry*, 51(3), 219–223.

- 8 Akhmetkarimova, Z.S., Baikenov, M.I., & Dyusekenov, A.M. (2017). Mathematical simulation of the hydrogenation of Borodino coal. *Solid Fuel Chem.*, 51(2), 111–114. <https://doi.org/10.3103/S0361521917020021>
- 9 Fomin, V.N., Aldabergenova, S.K., Rustembekov, K.T., Dik, A.V., Kim, Yu.Yu., & Rozhkovoy, I.E. (2018). Method for increasing the accuracy of quantitative determination of iron by LIBS. *Bulletin of the Karaganda University. Chemistry series*, 3(91), 74–83.
- 10 Fomin, V.N., Aldabergenova, S.K., Rustembekov, K.T., Omarov, Kh.B., Rozhkovoy, I.E., Dik, A.V., & Saulebekov, D.M. (2021). Optimizatsiia parametrov lazerno-iskrovogo emissionnogo spektrometra s primeneniem veroiatnostno-determinirovannogo planirovaniia eksperimenta [Optimization of the parameters of a laser induced breakdown spectrometer (LIBS) using probabilistic-deterministic design of experiment]. *Zavodskaiia laboratorii. Diagnostika materialov — Industrial laboratory. Diagnostics of materials*, 87(5), 14–19. <https://doi.org/10.26896/1028-6861-2021-87-5-14-19> [in Russian].
- 11 Balpanova, N., Tusipkhan, A., Gyulmaliev, A., Ma, F., Kyzkenova, A., & Aitbekova, D., et al. (2020). Kinetics of cavitation of an intermediate fraction of coal tar. *Solid Fuel Chemistry*, 54, 208–213. <https://doi.org/10.3103/S0361521920040023>.
- 12 Baikenov, M., Kochegina, E., Khalikova, Z., Absat, Z., Karimova, A., & Rakhimzhanova, N., et al. (2019). Thermal decomposition of a mixture of tar with primary coal tar with the additives of iron compounds. *Solid Fuel Chemistry*, 53, 96–104. <https://doi.org/10.3103/S0361521919020034>.

Information about authors

Fomin Vitaly Nikolaevich — Candidate of chemical sciences, Head of LEP “PCMA” of Karagandy University of the name of academician E.A. Buketov, Mukanov street, 41, 100000, Karaganda, Kazakhstan; e-mail: vitaliynikolaevich.fomin@mail.ru; <https://orcid.org/0000-0002-2182-2885>

Ainabaev Assanali Anuarovich — Candidate of chemical sciences, Leading Researcher of LEP “PCMA”, Karagandy University of the name of academician E.A. Buketov, Mukanov street, 41, 100000, Karaganda, Kazakhstan; e-mail: aliopel_82t@mail.ru; <http://orcid.org/0000-0002-3443-446X>

Kaykenov Daulethan Asanovich — Candidate of chemical sciences, Leading Researcher of LEP “PCMA”, Karagandy University of the name of academician E.A. Buketov, Mukanov street, 41, 100000, Karaganda, Kazakhstan; e-mail: krq.daykai@mail.ru; <http://orcid.org/0000-0003-4621-7603>

Sadyrbekov Daniyar Tleuzhanovich — Candidate of chemical sciences, Leading Researcher of LEP “PCMA”, Karagandy University of the name of academician E.A. Buketov, Mukanov street, 41, 100000, Karaganda, Kazakhstan; e-mail: acidbear@mail.ru; <http://orcid.org/0000-0002-3047-9142>

Aldabergenova Saule Kidirbaevna (*corresponding author*) — Candidate of chemical sciences, Associate Professor of Karagandy University of the name of academician E.A. Buketov, Mukanov street, 41, 100000, Karaganda, Kazakhstan; e-mail: aldsau@mail.ru; <https://orcid.org/0000-0002-4262-911X>;

Turovets Milana Alexandrovna — 3rd year student, Department of Physical and Analytical Chemistry, Karagandy University of the name of academician E.A. Buketov, Mukanov street 41, 100000, Karaganda, Kazakhstan; e-mail: turovec26.07@mail.ru; <https://orcid.org/0000-0002-0493-6426>;

Kelesbek Nabira Kydyrbekkyzy — 2nd year PhD student, Department of Inorganic and Technical Chemistry, Karagandy University of the name of academician E.A. Buketov, Mukanov street, 41, 100000, Karaganda, Kazakhstan; e-mail: knk_93@bk.ru; <https://orcid.org/0000-0002-8578-8081>.

T.K. Jumadilov¹, A.A. Utesheva^{2,3*}, Kh. Khimersen^{1,4},
R.G. Kondaurov¹, J.V. Grazulevicius⁵

¹*Institute of Chemical Sciences named after A.B. Bekturov, Almaty, Kazakhstan;*

²*Kazakh-British Technical University, Almaty, Kazakhstan;*

³*Institute of High Technologies, Almaty, Kazakhstan;*

⁴*Abai Kazakh National Pedagogical University, Almaty, Kazakhstan;*

⁵*Kaunas University of Technology, Kaunas, Lithuania*

(*Corresponding author's e-mail: utesheva_93@bk.ru)

Abnormal activity of functional groups during uranyl ions sorption by polymethacrylic acid-poly-4-vinylpyridine intergel system

Uranyl ions sorption by intergel system consisting of polymethacrylic acid hydrogel (hPMAA) and poly-4-vinylpyridine hydrogel (hP4VP) has been studied. First, reciprocal activation of PMAA and P4VP polymeric hydrogels in water environment was examined in order to predict intergel system sorption activity. Based on the obtained results, it was found that area of maximum hydrogel activation was within the ratios of 100 % hPMAA and 67 % hPMAA:33 % hP4VP. The maximum rate of uranyl ions extraction was also observed within these ratios. The highest uranyl ions sorption by intergel system occurred at 83 %hPMAA:17 % hP4VP ratio. Maximum uranyl ions extraction rate after 56 hours of hydrogels remote interaction was 82.5 %, when polymeric chain binding rate was 9.94 % and effective dynamic exchange capacity was 1.12 mmol/g. Significant increase of intergel system sorption activity within the ratios of 100 % hPMAA and 67 % hPMAA:33 % hP4VP in comparison with initial inactivated hydrogels 100 % hPMAA and 100 % hP4VP was confirmed by combined calculation data of extraction rates of inactivated PMAA and P4VP polymeric hydrogels. The obtained results illustrated changes of initial polymeric hydrogels' electrochemical sorption properties in intergel system leading to functional groups obtaining higher reactive ability, which made it possible to use them for further development of highly efficient uranyl ions extraction sorption technology.

Keywords: hydrogels, intergel systems, reciprocal activation, sorption, extraction rate, polymethacrylic acid, poly-4-vinylpyridine, uranyl ion.

Introduction

Rare-earth element containing ores extraction is often complicated in terms of their radioactivity, which is caused by containing uranium, thorium, and their half-life products in their composition. Due to this fact, the issue of rare-earth elements separation from radioactive elements, particularly uranium, is of high importance nowadays [1-3]. Uranium can be removed from solutions by sorption, extraction, and other methods. At present, sorption methods are more preferred than extraction ones. Sorption methods are more eco-friendly and have fewer technological cycles than extraction technologies [4, 5]. Ion-exchange uranium extraction process is based on ion-exchange resins ability to absorb uranium selectively and quantitatively from solutions and pulps after lixiviation. In sulfurous solutions, hexavalent uranium can be present as uranyl cation (UO_2^{2+}) and as anion sulphatic complexes ($[\text{UO}_2(\text{SO}_4)_2]^{2-}$, $[\text{UO}_2(\text{SO}_4)_3]^{4-}$) [6].

The objective of our research is to study functional hydrogels initial state and remote interaction (activation) time influence on polymers ratio in intergel systems, depth of uranyl ions sorption during their interaction with intergel systems and prospects of using these intergel systems for uranium extraction from product solutions.

Experimental

Equipment. A MARK 603 conductometer (Russia) and Metrohm 827 pH-Lab pH-meter (Switzerland) were used for measuring specific electrical conductivity and solutions pH. Sorbent mass was determined by weighing at electronic analytical scales MSE125P-100-DU Sartorius Cubis (Germany).

Materials. The research was performed in water environment and in solution of hexaqua uranyl nitrate (UO_2^{2+} concentration = 100 mg/l). Cross-linked by divinylbenzene hydrogel poly-4-vinylpyridine (hP4VP) of Sigma-Aldrich was used. Polymethacrylic acid hydrogels were synthesized applying cross-linking agent N,N-methylene-bis-acrylamide and red-ox system $\text{K}_2\text{S}_2\text{O}_8 - \text{Na}_2\text{S}_2\text{O}_3$ in water environment. Synthesized

PMAA hydrogel was reduced to smaller dispersions and separated by size. Fractions of $250 < d < 425 \mu\text{m}$ were used in the process. Hydrogel swelling ratios were $\alpha_{(\text{hPMAA})} = 21.00 \text{ g/g}$, $\alpha_{(\text{hP4VP})} = 3.20 \text{ g/g}$.

For the research objective, synthesized hPMAA and hP4VP hydrogels were combined into polymethacrylic acid gel — poly-4-vinylpyridine gel (hPMAA-hP4VP) intergel couple.

Experiment. Experiments were carried out at room temperature. hPMAA and hP4VP hydrogels were taken in swollen state. Study of the intergel systems was done as follows: each hydrogel in dry state was placed in separate polypropylene cages. hPMAA and hP4VP hydrogels were previously left in distilled water for 24 hours for swelling. Then polypropylene cages with swollen hydrogels were placed in glasses with water and hexaqua uranyl nitrate solutions. Electroconductivity and overgel liquid pH were determined with hydrogels present in the solution.

Research of individual polymeric hydrogels sorption properties was done as follows:

1) Estimated amount of each hydrogel (polymethylacrylic acid, poly-4-vinylpyridine) in dry state was placed into polypropylene cages.

2) Uranyl ions sorption by individual hydrogels of PMAA and P4VP was done for 56 hours. During this period aliquots were taken for further determination of uranyl ions concentration.

Research of intergel systems sorption properties was done as follows:

1) Intergel system hPMAA-hP4VP was combined from synthesized PMAA and P4VP hydrogels;

2) Estimated amount of each hydrogel in dry state was placed into polypropylene cages;

3) Uranyl ions sorption by these intergel systems was done for 56 hours. During this period aliquots were taken for further determination of uranyl ions concentration.

Uranyl ions determination procedure. Measurement of uranium mass concentration was carried out by volumetric titanium-phosphate-vanadate method based on red-ox properties of uranium (IV) and uranium (VI) and its reduction and oxidation reactions.

Uranyl ions extraction (sorption) rate was calculated according to the formula:

$$\eta = \frac{C_{in} - C_{res}}{C_{in}} * 100 \%,$$

where C_{in} is uranyl ions initial concentration in solution, mg/l; C_{res} is uranyl ions residual concentration in solution, mg/l.

Total polymer chain binding rate was calculated according to the formula:

$$\theta = \frac{v_{sor}}{v} * 100 \%,$$

where v_{sor} is an amount of sorbed uranyl ions, mole; v is hydrogel weighed portion (if two hydrogels are present in the solution, this is calculated as summed amount of each of them), mole.

Effective dynamic exchange capacity of individual hydrogels and intergel system was calculated according to the formula:

$$Q = \frac{v_{sor}}{m_{sorbent}},$$

where v_{sor} is an amount of sorbed uranyl ions, mole; m is polymer weighed portion (if two hydrogels are present in the solution, this is calculated as summed weight of each of them), g.

Calculation of total inactivated hydrogels PMAA and P4VP sorption rate was done according to the formula:

$$\Sigma \eta = \left(\frac{\eta_1 * 83 \%}{100 \%} + \frac{\eta_2 * 17 \%}{100 \%} \right),$$

where η_1 is 83 % hPMAA uranyl ions extraction rate, %; η_2 is 17 % hP4VP uranyl ions extraction rate, %.

Results and Discussion

Previously performed studies [7, 8] have shown that almost all intergel systems based on acidic (polyacrylic and polymethacrylic acids) and basic (poly-4-vinylpyridine and poly-2-methyl-5-pyridine) lightly cross-linked polymeric hydrogels display higher activity than their initial components. It has also been found that polymer ratios, which provide higher ions sorption, differ significantly depending on nature of acidic and basic hydrogels and nature of rare-earth metals.

These results were obtained after studying sorption of lanthanum, cerium, dysprosium, neodymium, samarium, and erbium by intergel systems. Influence of initial hydrogel state on sorption process was also

identified. Depending on what gel is used for intergel couple formation (dry, swollen or partially swollen) there can be different hydrogel ratios in intergel systems with high sorption capacity and rare-earth metal ions sorption rate. However, no work was done to determine optimal conditions for maximum sorption and ions selectivity in case of using intergel systems for uranyl ions extraction.

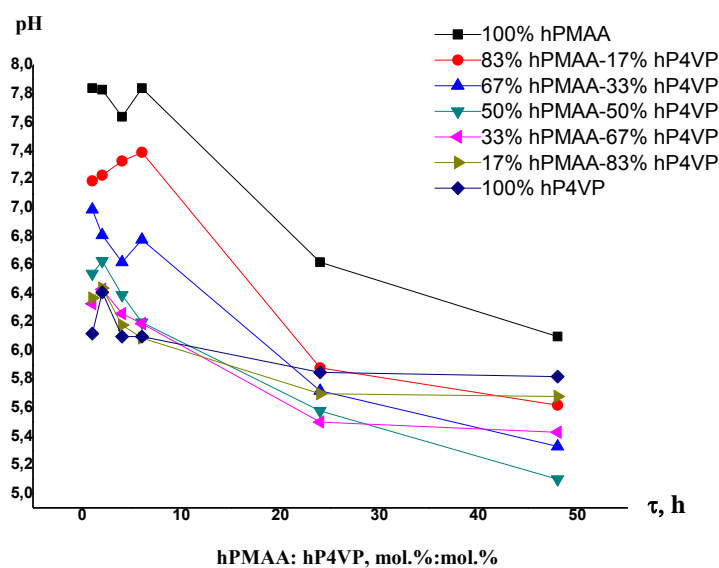


Figure 1. Water solutions pH dependency on time in the presence of hPMAA-hP4VP intergel system

Figure 1 illustrates water solutions pH dependency on time in the presence of hPMAA-hP4VP intergel system. It can be seen that initial PMAA hydrogel and intergel systems within ratios of 83 % hPMAA:17 % hP4VP and 50 % hPMAA:50 % hP4VP have significantly lower pH, which is caused by H^+ ions emission into solution as a result of functional carboxylic groups dissociation process. Twenty four hours later dissociation continues less intensive, which indicates approaching electrochemical equilibrium in the solution. Initial P4VP hydrogel and intergel systems within ratios of 33 % hPMAA:67 % hP4VP and 17 % hPMAA:83 % hP4VP have minor pH decrease in initial area, which is most likely caused by solution protons binding by nitrogen atom in vinylpyridine. Forty eight hours later the systems did not show pH changes.

As a result of remote interaction, hydrogels form functional groups without counter-ions, which leads to significant increase of intergel system sorption capacity.

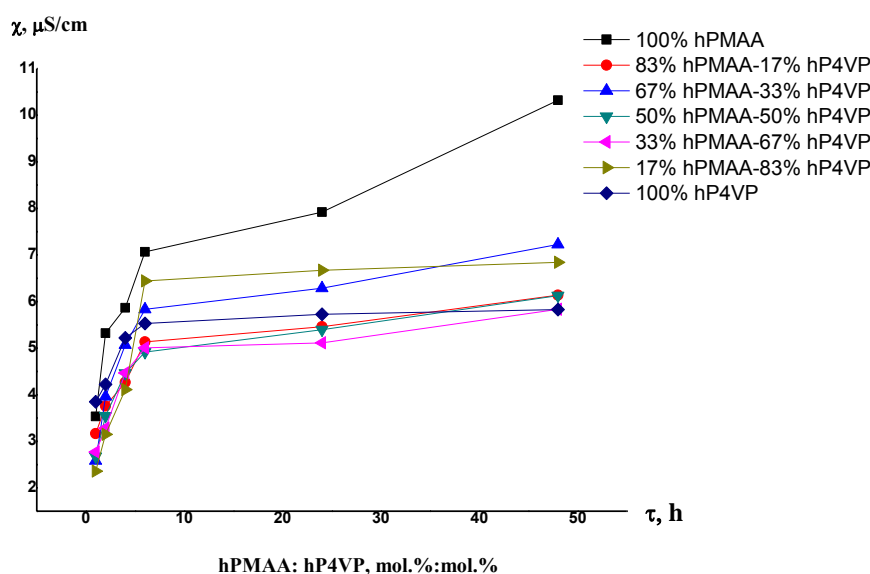


Figure 2. Water solutions' specific electrical conductivity time dependence in the presence of hPMAA-hP4VP intergel system

Figure 2 shows hPMAA-hP4VP water solutions' specific electrical conductivity time dependence. When environment pH decreases, concentration of H^+ ions or H_3O^+ hydroxonium increases, which leads to specific electrical conductivity rise. It can be noticed from Figure 2 that, water electrical conductivity increases over time in the presence of initial PMAA hydrogel. This is facilitated by functional group dissociation at macromolecule interstitial units. As a result, hydrogen ions are emitted into the solution and carboxylate anions are formed. Initial P4VP hydrogel and intergel systems display specific electrical conductivity increase only at an early stage. Further rise during 24-hour period is not intense. Then during 48-hour period specific electrical conductivity increase is almost not seen, which suggests that electrochemical equilibrium is reached.

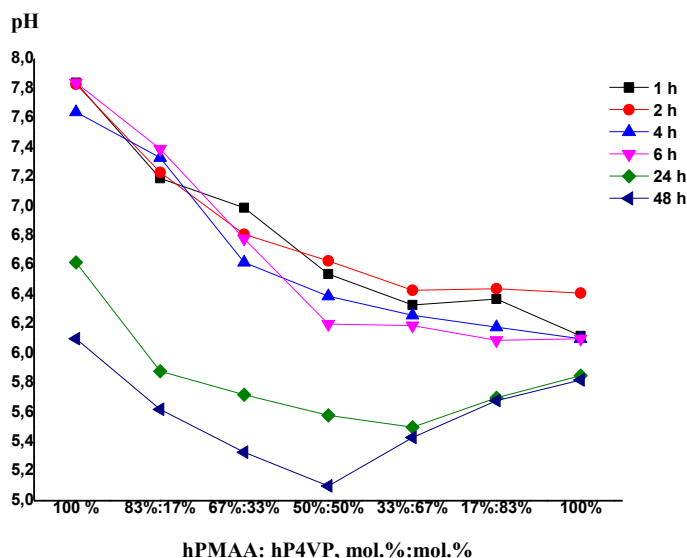


Figure 3 (a). Water solutions pH dependence on hPMAA-hP4VP mole ratio over time

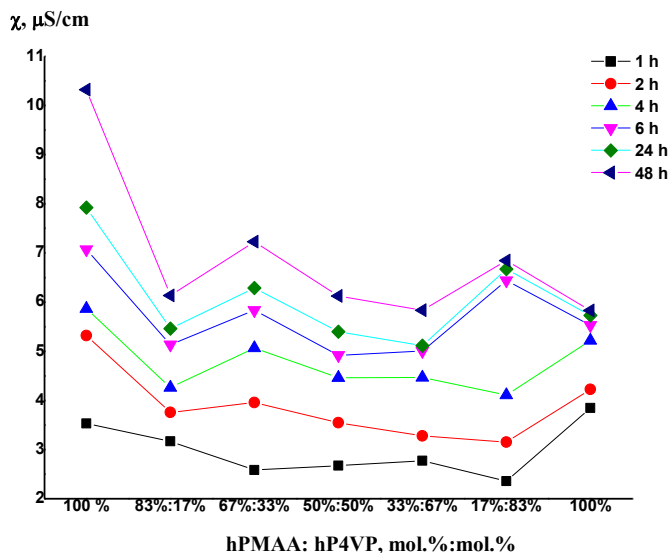


Figure 3 (b). Water solutions specific electrical conductivity dependence on hPMAA-hP4VP mole ratio over time

Figure 3 *a, b* represents hydrogen ions concentration and solutions' specific electrical conductivity change dependence on hydrogels mole ratio over time. Initial PMAA hydrogel and intergel systems within ratios of 83 % hPMAA:17 % hP4VP and 50 % hPMAA:50 % hP4VP display reduction of solutions pH. When environment pH decreases, concentration of H^+ ions, H_3O^+ hydroxonium or other ions increases, which leads to specific electrical conductivity rise. Besides, new negatively charged ions may appear in the system. Increase of H^+ ions concentration happens due to PMAA hydrogel functional carboxylic groups'

dissociation. Initial PMAA hydrogel and intergel systems within ratios of 33 % hPMAA:67 % hP4VP and 17 % hPMAA:81 % hP4VP display no significant changes in H^+ ions content. Water solution's specific electrical conductivity rise during hydrogels remote interaction when H^+ ions concentration does not change may be caused by OH^- ions presence in the solution as a result of interaction between P4VP hydrogel polybase and water molecules.

By virtue of the processes mentioned above, hydrogels mutual activation happens. This implies hydrogels switching to highly ionized state, which leads to significant increase of intergel system sorption capacity.

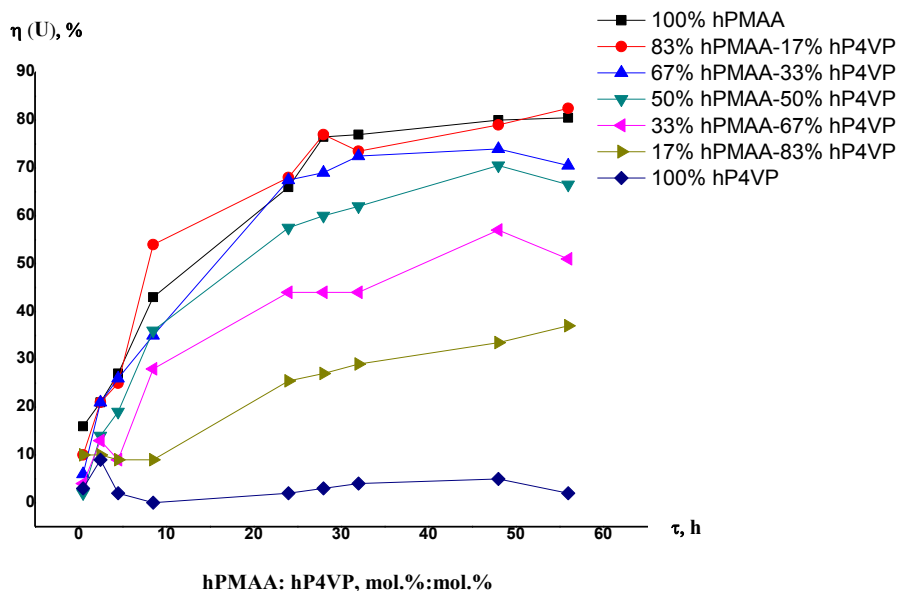


Figure 4. Dependence of uranyl ions extraction rate by hPMAA-hP4VP intergel systems over time

Figure 4 demonstrates dependence of uranyl ions extraction rate by initial hydrogels and hPMAA-hP4VP intergel systems over time. It should be noted that polymeric macromolecules switching to highly ionized state due to hydrogels mutual activation during their remote interaction leads to significantly increased uranyl ions extraction rate with polymeric hydrogels in intergel couples in comparison with initial hydrogels.

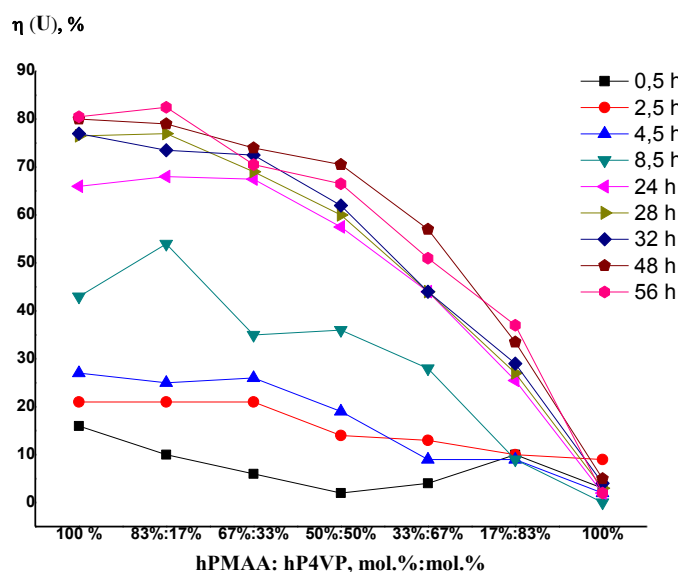


Figure 5. Dependence of uranyl ions extraction rate by hPMAA-hP4VP intergel systems on hydrogels mole ratio over time

Major amount of uranyl ions is sorbed by initial PMAA hydrogel and intergel systems over 56 hours of their interaction with salt solutions. Maximum uranyl ions extraction rate, namely 82.5 % is observed in intergel system within the ratios of 100 % hPMAA and 67 % hPMAA:33 % hP4VP 56 hours later. Uranyl ions extraction rate by initial polymeric hydrogels 100 % hPMAA and 100 % hP4VP is 80.5 % and 2.0 %, respectively. Initial P4VP hydrogel shows minor sorption rate only at an early stage, it remains unchanged over time. However, P4VP hydrogel, not having significant uranyl ions sorption rate, participates in initial PMAA hydrogel activation, which can be seen prominently within the ratios of 100 % hPMAA and 67 % hPMAA:33 % hP4VP.

Figure 5 indicates dependence of uranyl ions extraction rate by hPMAA-hP4VP intergel systems on hydrogels mole ratio over time. It can be seen from the graph that the highest uranyl ions sorption happens within ratio of 83 %hPMAA:17 %hP4VP. Especially high-sorption rate increase is observed after 8.5 hours; uranyl ions extraction rate at this point is 54.0 %. Uranyl ions extraction rate by individual polymeric hydrogels 100 %hPMAA and 100 %hP4VP is 43.0 % and 0.0 %, respectively. The main reason for such a high extraction rate is high ionization of polymeric structures as a result of their mutual activation.

For the purpose of estimating intergel systems' sorption activity within the ratios of 100 % hPMAA and 67 % hPMAA:33 % hP4VP in comparison with initial PMAA and P4VP hydrogels, 83 % hPMAA:17 % hP4VP intergel systems were selected and summary calculations of extraction rates were done individually for inactivated 83 % hPMAA and 17 % hP4VP hydrogels. Based on the results, difference of total extraction rates between initial hydrogels and intergel systems was calculated. The outcomes show that intergel system due to mutual activation has a higher uranyl ions sorption capacity than initial hydrogels. For calculation of hydrogels activity through initial inactivated 100 % hPMAA and 100 % hP4VP hydrogels, an assumption was made of initial hydrogels sorption capacity persistency in case of their concentration decrease in water environment. The obtained data are shown in Table 1 and it is seen that intergel system sorption capacity increase in relation to initial inactivated hydrogels over time occurs differently. 0.5 hour later, there is no sorption rate increase; 2.5 hours later sorption rate increase is 10.53 %. Then 4.5 hours later, there is minor decrease of sorption rate; the rate at this moment is 9.65 %. 8.5 hours later, there is a rapid increase of intergel system's sorption capacity, namely 50.84 %. Then, during 32-hour period, there is another decrease of sorption activity; subsequently, after reaching 48-hour time, there is an increase. Intergel system's sorption rate increase in relation to initial inactivated hydrogels according to calculation data was 19.39 %. This dynamics of intergel system's sorption activity change in relation to initial inactivated hydrogels that is most likely related to a group of factors, one of which is conformational transformations significantly influencing reaction mechanism. This way, intergel system's sorption capacity increase calculations point out a significant increase of intergel system's sorption capacity in relation to initial inactivated hydrogels.

Table 1

Experimental results with 83 %hPMAA:17 %hP4VP ratio of intergel system extraction rates and total calculation data of inactivated hydrogels

Sorption parameters	Sampling period, hours								
	0.5	2.5	4.5	8.5	24	28	32	48	56
100 % hPMAA initial hydrogel extraction rate	16.0	21.0	27.0	43.0	66.0	76.5	77.0	80.0	80.5
100 % hP4VP initial hydrogel extraction rate	3.0	9.0	2.0	0.0	2.0	3.0	4.0	5.0	2.0
83 % hPMAA inactivated hydrogel extraction rate calculation data	13.3	17.5	22.5	35.8	55.0	63.8	64.2	66.7	68.8
17 % hP4VP inactivated hydrogel extraction rate calculation data	0.5	1.5	0.3	0.0	0.3	0.5	0.7	0.8	0.3
83 % hPMAA and 17 % hP4VP inactivated hydrogels extraction rate summary calculation data	13.8	19.0	22.8	35.8	55.3	64.3	64.9	67.5	69.1
83 % hPMAA:17 % hP4VP intergel system extraction rate	10.0	21.0	25.0	54.0	68.0	77.0	73.5	79.0	82.5
intergel system sorption capacity in relation to initial inactivated hydrogels, %	0.00	10.53	9.65	50.84	22.97	19.75	13.25	17.04	19.39

Table 2 shows polymeric chain binding rates (in relation to uranyl ions) by initial polymers and hPMAA-hP4VP intergel systems over time. The most intense uranyl ions' binding by initial polymers and intergel systems occurs during the period of 48-56 hours. High values of polymeric chain binding rates in relation to uranyl ions are observed within the ratios of 100 % hPMAA and 67 % hPMAA:33 % hP4VP and equal to 9.94 %. This suggests a high rate of molecules ionization as a result of hPMAA and hP4VP polymers mutual activation. hPMAA and hP4VP individual polymers chain binding rates in relation to uranyl ions after 56 hours are 9.70 % and 0.24 %, respectively.

Table 2

**Polymeric chain binding rates (in relation to uranyl ions)
by initial hydrogels and hPMAA-hP4VP intergel systems over time, %**

Polymer chain binding rate (in relation to uranyl ions), %									
τ , h	0.5	2.5	4.5	8.5	24	28	32	48	56
100 % hPMAA	1.93	2.53	3.25	5.18	7.95	9.21	9.27	9.64	9.70
83 % hPMAA:17 % hP4VP	1.20	2.53	3.01	6.50	8.19	9.27	8.85	9.52	9.94
67 % hPMAA:33 % hP4VP	0.72	2.53	3.13	4.22	8.13	8.31	8.73	8.91	8.49
50 % hPMAA:50 % hP4VP	0.24	1.69	2.29	4.34	6.93	7.23	7.47	8.49	8.01
33 % hPMAA:67 % hP4VP	0.48	1.57	1.08	3.37	5.30	5.30	5.30	6.87	6.14
17 % hPMAA:83 % hP4VP	1.20	1.20	1.08	1.08	3.07	3.25	3.49	4.04	4.46
100 % hP4VP	0.07	1.08	0.24	0.00	0.24	0.36	0.48	0.60	0.24

Table 3 illustrates effective dynamic exchange capacity (in relation to uranyl ions) by initial hydrogels and hPMAA-hP4VP intergel systems over time. The obtained data suggests that polymeric hydrogels' mutual activation in intergel couples leads to significant increase of exchange capacity values in comparison with initial P4VP hydrogel. This is the most distinctive value after 56 hours of remote interaction. Intergel system reaches maximum values of effective dynamic exchange capacity within the ratios of 100 % hPMAA and 67 % hPMAA:33 % hP4VP after 56 hours of remote interaction and is 1.12 mmol/g.

Table 3

**Effective dynamic exchange capacity (in relation to uranyl ions)
by initial hydrogels and hPMAA-hP4VP intergel systems over time, %**

Effective dynamic exchange capacity (in relation to uranyl ion), mmol/g									
τ , h	0.5	2.5	4.5	8.5	24	28	32	48	56
100 % hPMAA	0.22	0.29	0.38	0.60	0.92	1.07	1.08	1.12	1.11
83 % hPMAA:17 % hP4VP	0.14	0.28	0.34	0.73	0.92	1.04	0.99	1.07	1.12
67 % hPMAA:33 % hP4VP	0.08	0.27	0.34	0.46	0.88	0.90	0.95	0.97	0.92
50 % hPMAA:50 % hP4VP	0.03	0.18	0.24	0.45	0.73	0.76	0.78	0.89	0.84
33 % hPMAA:67 % hP4VP	0.05	0.16	0.11	0.34	0.54	0.54	0.54	0.70	0.62
17 % hPMAA:83 % hP4VP	0.12	0.12	0.11	0.11	0.30	0.32	0.34	0.40	0.44
100 % hP4VP	0.03	0.10	0.02	0.00	0.02	0.03	0.05	0.06	0.02

Conclusions

During the research, it was identified that hydrogels maximum activity was within the ratios of 100 % hPMAA and 67 % hPMAA:33 % hP4VP. Due to hydrogels mutual activation during their remote interaction, polymeric macromolecules switch to a highly ionized state, which leads to a significant increase of polymeric hydrogels uranyl ions extraction rate in intergel couples in comparison with initial polymers. The highest uranyl ions sorption by intergel system occurs at 83 % hPMAA:17 % hP4VP ratio. Maximum uranyl ions extraction rate after 56 hours of hydrogels remote interaction was 82.5 %, when polymeric chain binding rate was 9.94 %, and effective dynamic exchange capacity was 1.12 mmol/g. Significant increase of uranyl ions sorption rate by intergel system in comparison with initial hydrogels is related to high rate of hydrogels ionization in intergel couple. Considerable increase of intergel system sorption activity within the ratios of 100 % hPMAA and 67 % hPMAA:33 % hP4VP in comparison with initial inactivated 100 % hPMAA and 100 % hP4VP hydrogels was confirmed by combined calculation data of extraction rates of

inactivated PMAA and P4VP polymeric hydrogels. Intergel system's sorption activity in comparison with initial inactivated hydrogels grows differently over time. Especially high increase of intergel system's sorption activity, namely 50.84 % can be seen after 8.5 hours. Intergel system's sorption rate in comparison with initial inactivated hydrogels after 56 hours was 19.39 %, according to calculation data. The obtained results suggest that intergel systems can be used for highly efficient sorption technology of extracting uranyl ions and other elements from commercial solutions as well as for concentration, separation of different ions from water solutions for performing technological, environmental, and other objectives.

References

- 1 Lapidus G.T. Selective thorium and uranium extraction from monazite: II. Approaches to enhance the removal of radioactive contaminants/ G.T. Lapidus, F.M. Doyle // *Hydrometallurgy*. — 2015. — Vol. 155. — P. 161–167. <https://doi.org/10.1016/j.hydromet.2015.03.015>
- 2 Garcia A.C. Separation of Radioactive Elements from Rare Earth Element-Bearing Minerals/ A.C. Garcia, M. Latifi, A. Amini, J. Chaouki // *Metals*. — 2020. — Vol. 10, No. 11. — P. 1524. <https://doi.org/10.3390/met10111524>
- 3 Yanliang Wang. Process for the separation of thorium and rare earth elements from radioactive waste residues using Cyanex® 572 as a new extractant / Yanliang Wang, Chao Huang, Fujian Li, Yamin Dong, Xiaoqi Sun // *Hydrometallurgy*. — 2017. — Vol. 169. — P. 158–164. <https://doi.org/10.1016/j.hydromet.2017.01.005>
- 4 Самойлов В.И. Анализ состояния технологии сорбционного извлечения урана в гидрометаллургических урановых производствах / В.И. Самойлов, А.Т. Садуақасова, Н.А. Куленова // *Международный журнал экспериментального образования*. — 2015. — № 5-1. — С. 80–87.
- 5 Abdikerim B.E. Uranium extraction with modified sorbents/ B.E. Abdikerim, B.K. Kenzhaliyev, T.Yu. Surkova, N. Didik, A.N. Berkinbayeva, Z.D. Dosymbayeva, N.S. Umirbekova // *Kompleksnoe ispolzovanie mineralnogo syria = Complex Use of Mineral Resources = Mineraldik Shikisattardy Keshendi Paidalanu*. — 2020. — № 3 (314). — P. 84–90. <https://doi.org/10.31643/2020/6445.30>
- 6 Тураев Н.С. Химия и технология урана: учеб. пос. для вузов / Н.С. Тураев, И.И. Жерин. — М.: ЦНИИАТОМ-ИНФОРМ, 2005. — 407 с.
- 7 Alimbekova B.T. Features of polymethacrylic acid and poly-2-methyl-5-vinylpyridine hydrogels remote interaction in an aqueous medium / B.T. Alimbekova, Zh.K. Korganbayeva, H. Himersen, R.G. Kondaurov, T.K. Jumadilov // *Journal of chemistry and chemical engineering*. — 2014. — Vol. 3, № 8. — P. 265–269. <https://doi.org/10.17265/1934-7375/2014.03.008>
- 8 Jumadilov T.K. Influence of polyacrylic acid and poly-4-vinylpyridine hydrogels mutual activation in intergel system on their sorption properties in relation to lanthanum (III) ions / T.K. Jumadilov, R.G. Kondaurov, Zh.A. Abilov, J.V. Grazulevicius, A.A. Akimov // *Polymer Bulletin*. — 2017. — Vol. 74. — P. 4701–4713. <https://doi.org/10.1007/s00289-017-1985-3>

Т.Қ. Жұмаділов, А.А. Утешева, Х. Химэрсэн,
Р.Г. Кондауров, Ю.В. Гражулявичюс

Полиметакрил қышқылы-поли-4-винилпиридин интергелді жүйелерімен уранил иондарын сорбциялау барысындағы функционалды топтардың аномальды активтілігі

Полиметакрил қышқылы (ПМАҚг) және поли-4-винилпиридин (П4ВПг) гидрогелдерінен тұратын интергелді жүйелердің уранил иондарына сорбциясы қарастырылған. Интергелді жүйелердің сорбциясын болжау үшін алдымен полимерлік гидрогелдердің (ПМАҚг, П4ВПг) су ортасындағы өзара активтену процесі зерттелді. Алынған нәтижелер негізінде гидрогелдердің максималды активтенуі 100 % ПМАҚг, 67 % ПМАҚг : 33 % П4ВПг қатынастарында болатыны анықталды. Уранил иондарын максималды шығару дәрежесі осы қатынастарда байқалады. Интергелді жүйелердің уранил иондарына максималды сорбциясы 83 % ПМАҚг : 17 % П4ВПг қатынастарында болатыны табылды. Гидрогелдердің қашықтан өзара әрекеттесуінің 56 сағатынан кейін уранил иондарын максималды шығару дәрежесі 82,5 %, полимерлік тізбектің байланысу дәрежесі 9,94 % және тиімді динамикалық алмасу сыймдылығы — 1,12 ммоль/г болды. Бастапқы активтенбеген 100 % ПМАҚг және 100 % П4ВПг гидрогелдерімен салыстырғанда интергелді жүйелердің сорбциялық белсенділігінің 100 % ПМАҚг, 67 % ПМАҚг:33 % П4ВПг қатынастарында анағұрлым жоғары болатынын активтенбеген гидрогелдердің жалпы есептік мәндері дәлелдеді. Алынған нәтижелер интергелді жүйелерде бастапқы полимерлік гидрогелдердің электрохимиялық және сорбциялық қасиеттерінің өзгеретінін, яғни функционалды топтардың реакцияға түсу қабілеті артатынын көрсетті. Бұл оларды уранил иондарын шығарудың жоғары тиімді сорбциялық технологиясын жасау үшін қолдануға мүмкіндік береді.

Кілт сөздер: гидрогелдер, интергелді жүйелер, өзара активтену, сорбция, шығару дәрежесі, полиметакрил қышқылы, поли-4-винилпиридин, уранил ионы.

Т.К. Джумадилов, А.А. Утешева, Х. Химэрсэн,
Р.Г. Кондауров, Ю.В. Гражулявичюс

Аномальная активность функциональных групп при сорбции ионов уранила интергелевой системой «полиметакриловая кислота – поли-4-винилпиридин»

Изучена сорбция ионов уранила интергелевой системой, состоящей из гидрогеля полиметакриловой кислоты (гПМАК) и гидрогеля поли-4-винилпиридина (гП4ВП). Для прогнозирования сорбционной активности интергелевой системы первоначально была изучена взаимная активация полимерного гидрогеля ПМАК с П4ВП в водной среде. На основе полученных результатов было установлено, что область максимальной активации гидрогелей находится в пределах соотношений между 100 % гПМАК и 67 % гПМАК : 33 % гП4ВП. В этой же области наблюдается максимальная степень извлечения ионов уранила. Установлено, что наибольшая сорбция ионов уранила интергелевой системой происходит при соотношении 83 % гПМАК : 17 % гП4ВП. Максимальная степень извлечения ионов уранила по истечении 56 ч дистанционного взаимодействия гидрогелей составила 82,5 %, при этом степень связывания полимерной цепи равнялась 9,94 %, а эффективная динамическая обменная емкость — 1,12 ммоль/г. Значительный рост сорбционной активности интергелевых систем в пределах соотношений между 100 % гПМАК и 67 % гПМАК : 33 % гП4ВП, по сравнению с исходными неактивированными гидрогелями 100 % гПМАК и 100 % гП4ВП, подтвердил суммарные расчётные данные степеней извлечения неактивированных гидрогелей ПМАК и П4ВП. Полученные результаты свидетельствуют об изменении электрохимических, сорбционных свойств исходных полимерных гидрогелей в интергелевой системе, приводящем к тому, что функциональные группы приобретают более высокую реакционную способность, и предоставляют возможность их применения в последующей разработке высокоэффективной сорбционной технологии извлечения ионов уранила.

Ключевые слова: гидрогели, интергелевые системы, взаимная активация, сорбция, степень извлечения, полиметакриловая кислота, поли-4-винилпиридин, ион уранила.

References

- 1 Lapidus, G.T., & Doyle, F.M. (2015). Selective thorium and uranium extraction from monazite: II. Approaches to enhance the removal of radioactive contaminants. *Hydrometallurgy*, 155, 161–167. <https://doi.org/10.1016/j.hydromet.2015.03.015>
- 2 Garcia, A.C., Latifi, M., Amini, A., & Chaouki, J. (2020). Separation of Radioactive Elements from Rare Earth Element-Bearing Minerals. *Metals*, 10(11), 1524. <https://doi.org/10.3390/met10111524>
- 3 Yanliang, Wang, Chao, Huang, Fujian, Li, Yamin, Dong, & Xiaoqi, Sun. (2017). Process for the separation of thorium and rare earth elements from radioactive waste residues using Cyanex® 572 as a new extractant. *Hydrometallurgy*, 169, 158–164. <https://doi.org/10.1016/j.hydromet.2017.01.005>
- 4 Samoilov, V.I., Saduakasova, A.T., & Kulenova, N.A. (2015). Analiz sostoiianii tekhnologii sorbtionnogo izvlecheniia urana v gidrometallurgicheskikh uranovykh proizvodstvakh [Analysis of the state of the technology of sorption extraction of uranium in hydrometallurgical uranium production]. *Mezhdunarodnyi zhurnal eksperimentalnogo obrazovaniia — International Journal of Experimental Education*, 5-1, 80–87 [in Russian].
- 5 Abdikerim, B.E., Kenzhaliyev, B.K., Surkova, T.Yu., Didik, N., Berkinbayeva, A.N., Dosymbayeva, Z.D., & Umirbekova, N.S. (2020). Uranium extraction with modified sorbents. *Kompleksnoe ispolzovanie mineralnogo syria = Complex Use of Mineral Resources = Mineraldik Shikisattardy Keshendi Paidalanu*, 3(314), 84–90. <https://doi.org/10.31643/2020/6445.30>
- 6 Turaev, N.S., & Zherin, I.I. (2005). *Khimiia i tekhnologiia urana [Uranium chemistry and technology]*. Moscow: TsNIIATOMINFORM [in Russian].
- 7 Alimbekova, B.T., Korganbayeva, Zh.K., Himersen, H., Kondaurov, R.G., & Jumadilov, T.K. (2014). Features of polymethacrylic acid and poly-2-methyl-5-vinylpyridine hydrogels remote interaction in an aqueous medium. *Journal of chemistry and chemical engineering*, 3, 8, 265–269. <https://doi.org/10.17265/1934-7375/2014.03.008>
- 8 Jumadilov, T.K., Kondaurov, R.G., Abilov, Zh.A., Grazulevicius, J.V., & Akimov, A.A. (2017). Influence of polyacrylic acid and poly-4-vinylpyridine hydrogels mutual activation in intergel system on their sorption properties in relation to lanthanum (III) ions. *Polymer Bulletin*, 74, 4701–4713. <https://doi.org/10.1007/s00289-017-1985-3>

Information about authors

Jumadilov Talkybek Kozhataevich — Doctor of Chemical Sciences, Professor, Chief Researcher at JSC “Institute of Chemical Sciences named after A.B. Bekturov”, Academician of the Russian Academy of Natural History, 106 Valikhanov street, 050013, Almaty, Kazakhstan, e-mail: jumadilov@mail.ru, <https://orcid.org/0000-0001-9505-3719>;

Utesheva Ainamgul Altaevna (*corresponding author*) — Master of Science, PhD student at JSC “Kazakh-British Technical University”, School of Chemical Engineering, 59 Tole bi street, 050000, Almaty, Kazakhstan, e-mail: utesheva_93@bk.ru, <https://orcid.org/0000-0002-6243-1610>;

Khimersen Khuangul — Master of Science, PhD student at Abai Kazakh National Pedagogical University, 13 Dostyk avenue, 050013, Almaty, Kazakhstan, e-mail: huana88@mail.ru; <https://orcid.org/0000-0002-5138-5997>;

Kondaurov Ruslan Gennadievich — PhD, Head of the Laboratory of Synthesis and Physicochemistry of Polymers at JSC “Institute of Chemical Sciences named after A.B. Bekturov”, 106 Valikhanov street, 050013, Almaty, Kazakhstan, e-mail: r-kondaurov@mail.ru, <https://orcid.org/0000-0001-5998-8453>;

Juozas Vidas Grazulevicius — Doctor of Chemical Sciences, Professor at Kaunas University of Technology, Department of Polymer Chemistry and Technology, K. Donelaičio St. 73,44249, Kaunas, Lithuania, e-mail: juozas.grazulevicius@ktu.lt, <https://orcid.org/0000-0002-4408-9727>.

V.G. Kamani^{1*}, M. Sujatha¹, G.B. Daddala²

¹Koneru Lakshmaiah Education Foundation, Vaddeswaram, Guntur, India;

²Piramal Pharma Ltd, Ennore, Chennai, Tamil Nadu, India

(*Corresponding author's e-mail: venukamani@gmail.com)

Development and validation of a novel stability indicating HPLC method for the separation and determination of darolutamide and its impurities in pharmaceutical formulations

This study reports for the first time about a stability indicating RP-HPLC method for analysis of darolutamide and its impurities 1, 2, and 3 in bulk and formulations. The separation was achieved on Phenomenex column with Luna C18 (250 mm × 4.6 mm, 5 μm) as stationary phase, and 50 mM ammonium acetate: methanol solution 15:80 (v/v) at pH 5.2 as mobile phase at 1.0 mL/min flow rate. UV detection was carried at wavelength of 239 nm. In these conditions the retention time of darolutamide and its impurities 1, 2, and 3 was 7.05, 8.90, 4.63 and 5.95 min, respectively. The method was validated for system suitability, range of analysis, precision, specificity, stability, and robustness. Forced degradation study was done through exposure of the analyte to five different stress conditions and the % degradation was small in all degradation condition. The proposed method can separate and estimate the drug and its impurities in pharmaceutical formulations. Hence, the developed method was suitable for the quantification of darolutamide and can separate and analyse impurities 1, 2, and 3.

Keywords: darolutamide, impurity analysis, HPLC method development, method validation, ruggedness, forced degradation study, formulation assay, impurity analysis in Nubeqa®.

Introduction

Darolutamide (Fig. 1a) is an androgen antagonist (antiandrogen) drug approved for the treatment of non-metastatic castration-resistant prostate cancer (nmCRPC) in combination with medical or surgical castration [1]. It is prescribed for the treatment of nmCRPC in men [2, 3]. Darolutamide acts on androgen receptors (AR) potentiating the growth and survival of prostate cancer cells. It is competitively inhibiting the androgens from binding to their receptors, inhibiting the AR-mediated transcription as well as AR nuclear translocation. Hence, decreases the tumor cell size as well as prostate cancer cell proliferation [4].

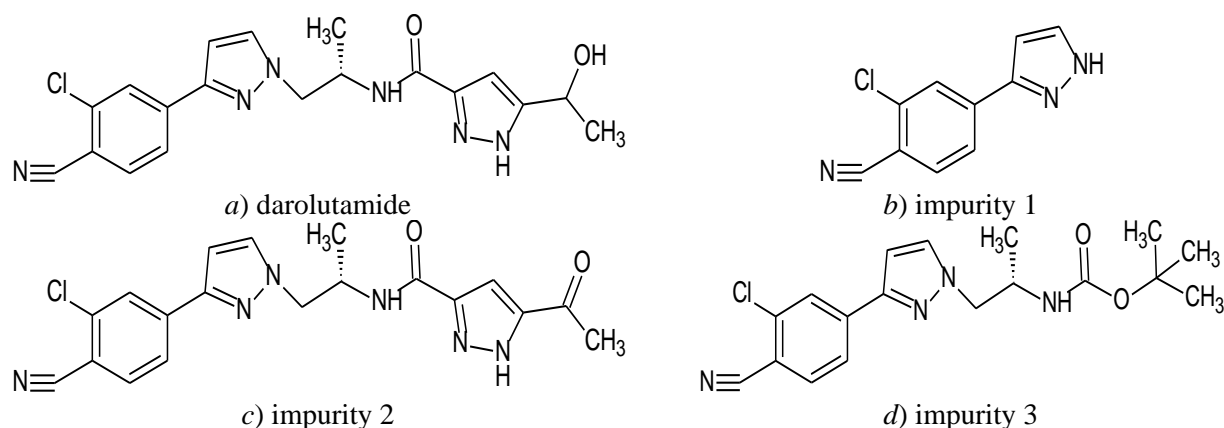


Figure 1. Chemical structure of darolutamide and its impurities in the study

Pain in extremities, fatigue, rashes, and asthenia are the common side effects of darolutamide. Increased aspartate aminotransferase, decreased neutrophil count and increased bilirubin are the abnormalities associated with darolutamide in terms of laboratory test [5].

Strict control of impurities is necessary for the manufacturing of drug products. These impurities may be present in the materials, formed as by-products during the process of production or appear as degradation

products during storage. Both actual and potential impurities should be studied and detected by a reliable and convenient method. Though a method was referred to in a patent of Takeda, the practicability of this method has not been verified [6].

A literature review of the available analytical methods for darolutamide analysis confirms that there are few analytical methods available for the assessment of darolutamide along with its active metabolites in biological samples using HPLC [7] and LC-MS / MS [8-11] methods. The main disadvantages of the previously developed methods are the reported methods that were insufficient to separate the potential impurities of darolutamide. The applicability of the reported methods were summarised in Table 1.

Table 1

Comparison of the literature methods and reason for proposal of new method for analysis of darolutamide

S No	Reference method	Reported method applicability	Reason for proposal of new method
1	Ashok et al., 2018 [7]	HPLC method reported for the simultaneous estimation of darolutamide along with other drugs such as apalutamide, enzalutamide, N-desmethylenzalutamide in mice plasma and in pharmacokinetic studies	The method is not suitable for the separation of darolutamide impurities
2	Neraj et al., 2018 [8]	LC-MS method reported for the estimation of enzalutamide, N-desmethylenzalutamide, darolutamide in mice plasma.	LC-MS is expensive than the HPLC and the reported method not suitable for the separation of darolutamide impurities.
3	Sreekanth et al., 2017 [9]	LC-MS/MS-ESI method reported for simultaneous quantification of darolutamide and its active metabolite, ORM-15341 in mice plasma and its application to a pharmacokinetic study	Reported method only suitable for separation of darolutamide and its active metabolite only and can not separate the impurities
4	Suresh et al., 2018 [10]	LC-MS/MS method reported for simultaneous quantitation of enzalutamide, N-desmethylenzalutamide, apalutamide, darolutamide and ORM-15341 in mice plasma as well as pharmacokinetic study.	LC-MS is expensive than the HPLC and the reported method not suitable for the separation of darolutamide impurities
5	Narayanan et al., 2018 [11]	LC-MS/MS-ESI method for the simultaneous quantification of darolutamide and its optical isomer 1 and 2 in mice plasma as well as pharmacokinetic study.	The reported method only suitable for the separation of optical isomers of darolutamide and is not applicable for the separation of impurities of darolutamide

Thus, the present work aimed to develop a simple and precise analytical HPLC method for the estimation of darolutamide and its impurities 1, 2 and 3. The molecular structure of darolutamide impurities 1, 2 and 3 in the study were given in Figure 1b, 1c and 1d respectively. The method has been validated for Nubeqa[®] a newly introduced tablet dosage form of darolutamide.

Experimental

Reagents:

The pure standard of drug darolutamide (98.85 % purity), impurity 1, 2 and 3 in the study along with the formulation dosage form (Nubeqa[®] – 300 mg) were obtained from Bayer Pharmaceuticals Private Limited, Thane West, Maharashtra. The HPLC grade methanol, acetonitrile, and ultra-pure (Milli-Q[®]) water were obtained from Merck chemicals, Mumbai.

Instrumentation:

HPLC analysis of darolutamide and its impurities was performed on Agilent 1100 (USA) HPLC equipped with Quaternary pump (G 1311A) for solvent delivery, autosampler with thermostatic (G 1329A) having 0.1–1500 µL of sample injection capacity and UV detector (G 1314A). Agilent chemical station LC software was used for integrating the chromatogram.

Preparation of solutions:

Darolutamide and impurity solutions:

A standard stock solution of darolutamide and its studied impurities 1, 2 and 3 were prepared separately by accurately weighing of 50 mg of the compound and dissolving in 50 mL of methanol solvent. From this solution, selected and required concentration of darolutamide and its impurities were prepared separately.

Then the mixed standard solution was prepared by mixing equal volumes of concentrations of standard and impurities.

Formulation solution:

Tablets of Nubeqa[®] brand containing 300 mg of darolutamide was powdered using a sterile mortar and pestle. Then, an amount of tablet powder equivalent to 50 mg of darolutamide was accurately weighed and dissolved in 50 mL solvent applying sonicator and filtered through 0.45 μ membrane filter. Afterwards it was diluted while doing the formulation analysis.

Method Development:

Based on a literature review, it has identified that there is no analytical method reported for assay of darolutamide and its impurities. The method specified in the regulatory document by the manufactures of the standard, as well as formulation were not available easily. Thus, the present work was aimed to develop a simple and accurate HPLC method for simultaneous assay of darolutamide and its impurities.

In the initial stage of method development, the suitable detector wavelength for the simultaneous detection of darolutamide and its impurities was determined using UV — visible spectrophotometer. The iso-absorption wavelength of darolutamide and its impurities was selected as suitable wavelength in the study. Then by keeping the detector wavelength as constant, different configurations of stationary phases for the separation of darolutamide and its impurities were examined. After that, the composition, pH and flow rate of the mobile phase was optimised. In each cases, the resolution between the compounds, the shape of the individual peak, base line throughout the run time and the system suitability conditions for each peak corresponds to all the analytes in the study was summarised. The conditions that provide the best chromatographic results were selected as appropriate for the validation study [12–14].

Method Validation:

Standard solution containing darolutamide and its impurities at recovery ranges was analysed for the evaluation of the system suitability of the method. The acceptance developed method should have the system suitability parameters such as asymmetric factor (< 2), plate count (> 2000), and resolution factor (> 2).

A series of darolutamide standard stock solutions containing 1 % of each studied impurity was prepared separately and analysed in the developed method. The calibration plot was constructed using peak area of the resultant chromatograms vs concentration of the analyte prepared. The range of the method was determined using least square analysis and the correlation coefficient and regression equation was calculated.

The accuracy/recovery of the method was determined by spiked recovery at 50 %, 100 % and 150 % spiked levels in the calibration range. The % recovery in each spiked level for darolutamide and its impurities were calculated separately by comparing with standard calibration results and a % recovery of less than 2 was considered as accurate.

The standard solution of darolutamide with its impurities in the calibration was analysed six times in the same day for intraday precision, six times in three different days for interday precision and six times in the day with change in three different analysts for ruggedness study. The % relative standard deviation (% RSD) of the peak areas observed in each study was calculated for darolutamide and its impurities separately and the % RSD of less than 2 was considered as acceptable.

The influence of small change in the analytical conditions on the separation and quantification of darolutamide and its impurities was determined in robustness study. The ± 5 mL change in organic modifier, ± 0.1 factor change in mobile phase pH and ± 5 nm change in detector wavelength was study and the % change in the peak area of darolutamide and its impurities was calculated in each changed condition and a % change of less than 2 was considered as the method is robust.

Forced degradation study was conducted for determining the efficiency of the developed method for the separation and detection of unknown impurities/stress degradation compounds formed during the degradation study. 50 mg of standard drug darolutamide was mixed with 50 mL of 0.1 N HCl, 0.1 N NaOH and 3 % hydrogen peroxide solution separately for 24 h in acidic, basic and oxidative degradation study. Then the solution was neutralized and diluted to standard concentration. 50 mg of standard drug darolutamide was kept in an air oven at 60 ^oC for 24 h in thermal degradation study and kept under UV light at 254 nm for 24 h for photolytic degradation study. Then it was diluted to standard concentration and the degradation solutions were analysed in the developed method. The number of degradation compounds formed and the % of degradation was calculated by comparing with unstressed results of darolutamide.

The sensitivity of the method for the detection of impurities in the darolutamide was confirmed by determining limit of detection (LOD) and limit of quantification (LOQ). The applicability of the developed

method for the detection and quantification of impurities in formulation was confirmed by analysing the formulation solution prepared from cream formulation of darolutamide (Nubeqa[®] — 300 mg) [15–18].

Results and Discussions

The summary of the method developed for the separation and quantification of darolutamide and its impurities was given in Table 2.

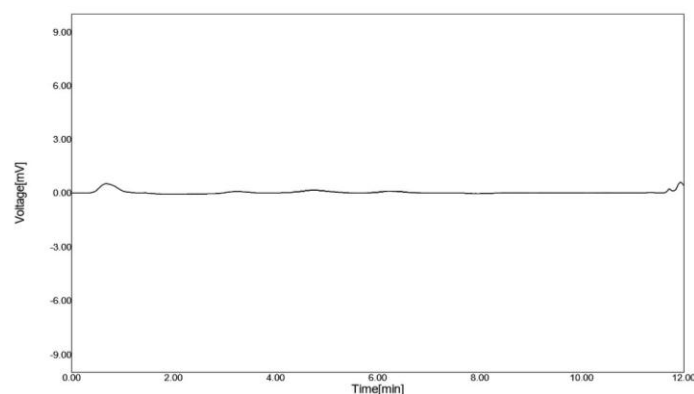
Table 2

Method development conditions studied in the optimization process

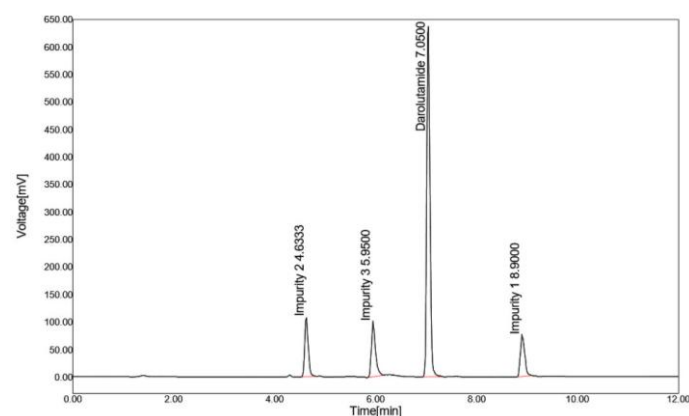
S.No	Method conditions	Chromatographic result observed	Conclusion
1	MP: Methanol and sodium acetate buffer pH 5.6 in 50:50 (v/v); SP: Kromasil C18 (250 mm × 4.6 mm, 5 μm) column; WL: 239 nm; FR: 1.0 mL/min	There is no separation of compounds identified in the chromatogram	Method rejected
2	MP: Acetonitrile and sodium acetate buffer pH 5.6 in 50:50 (v/v); SP: Kromasil C18 (250 mm × 4.6 mm, 5 μm) column; WL: 239 nm; FR: 1.0 mL/min	There is no separation of compounds identified in the chromatogram	Method Rejected
3	MP: triethyl amine: methanol 75:25 (v/v); SP: ProntoSIL ODS C18 (250×4.6 mm; 5 μ id; WL: 239 nm; FR: 1.0 mL/min	Peaks were identified for standard, and impurities studied but the separation of compounds, symmetry of the identified peaks and the peak responses was very poor and not acceptable	Method Rejected
4	MP: 50 mM ammonium acetate, acetonitrile in 25:75 (v/v) at pH 5.9; SP: Inertsil ODS 3V (250 mm × 4.6 mm, 5 μm); WL: 239 nm; FR: 1.0 mL/min	Peaks were identified for standard, and impurities studied but the separation of compounds, symmetry of the identified peaks and the peak responses was very poor and not acceptable.	Method Rejected
5	MP: 50 mM ammonium acetate, methanol in 25:75 (v/v) at pH 5.9; SP: Phenomenex Luna C18 (250 mm × 4.6 mm, 5 μm) column; WL: 239 nm; FR: 1.0 mL/min	The separation of compound and peak symmetry of the identified peaks was not acceptable	Method Rejected
6	MP: 50 mM ammonium acetate, methanol in 05:95 (v/v) at pH 5.2; SP: Phenomenex Luna C18 (250 mm × 4.6 mm, 5 μm) column; WL: 239 nm; FR: 1.0 mL/min	Individual peaks were observed for darolutamide and its impurities. The separation of compounds is not satisfactory and peaks doesn't satisfy the system suitable conditions	Method Rejected
7	MP: 50 mM ammonium acetate, methanol in 15:80 (v/v) at pH 5.2; SP: Phenomenex Luna C18 (250 mm × 4.6 mm, 5 μm) column; WL: 239 nm; FR: 1.0 mL/min	Peaks with acceptable symmetry and separation with acceptable system suitability was identified for darolutamide and its impurities	Method Accepted

Note: MP = Mobile phase; WL = detector wavelength; FR = mobile phase flow rate.

The separation of darolutamide, impurity 1, 2 and 3 was achieved on Phenomenex column with Luna C18 (250 mm × 4.6 mm, 5 μm) as stationary phase, and 50 mM ammonium acetate : methanol solution in the ratio of 15:80 (v/v) at pH 5.2 as mobile phase. The mobile phase was pumped in isocratic mode at a flow rate of 1.0 mL/min. The separated compounds were detected applying UV detector at a wavelength of 239 nm. In the optimised condition, the chromatogram observed for blank and standard was given in Figure 2a and 2b, respectively.



a) blank chromatogram



b) standard chromatogram

Figure 2. System suitability chromatograms of darolutamide, impurity 1 and 2 in the developed method

The LOD (limit of detection) was identified as 0.045 $\mu\text{g/mL}$ for impurity 1 and 0.020 $\mu\text{g/mL}$ for impurities 2 and 3. The limit of quantification (LOQ) was calculated as 0.15 $\mu\text{g/mL}$ for impurity 1, 0.07 $\mu\text{g/mL}$ for impurities 2 and 3. The calibration curve was constructed from LOQ concentration i.e 0.15 $\mu\text{g/mL}$ and the dilutions were made such that 1 % of each impurity was present in the standard solution. The linear calibration curve was observed within the concentration range of 15 — 90 $\mu\text{g/mL}$ for darolutamide and 0.15 — 0.90 $\mu\text{g/mL}$ for impurities. The regression equation was found to be

$$y = 15527x + 33019 \quad (R^2 = 0.9999),$$

$$y = 106785x + 1519.1 \quad (R^2 = 0.9997),$$

$$y = 161678x + 1574.3 \quad (R^2 = 0.9994) \text{ and}$$

$$y = 123963x + 1931.9 \quad (R^2 = 0.9997)$$

for darolutamide, impurity 1, 2 and 3 respectively. Table 3 gives the results of linearity in the developed method.

Table 3

Linearity results

S. No	Darolutamide		Impurity 1		Impurity 2		Impurity 3	
	Con*	Peak Area	Con*	Peak Area	Con*	Peak Area	Con*	Peak Area
1	15	263950	0.15	17450	0.15	26887	0.15	19959
2	30	502422	0.30	33026	0.30	48959	0.30	39157
3	45	725137	0.45	49827	0.45	73485	0.45	58254
4	60	969627	0.60	66513	0.60	98626	0.60	76459
5	75	1202760	0.75	81546	0.75	124451	0.75	95683
6	90	1425163	0.90	97126	0.90	146325	0.90	112563

Note: *Con = concentration studied in $\mu\text{g/mL}$.

The system suitability parameters such as the number of theoretical plates, asymmetric factor, resolution factor, retention time and relative retention time was calculated in the developed method and the results were found to be within the acceptable limit (Table 4) for darolutamide, impurity 1, 2 and 3 confirms that the method is suitable for the analysis.

Table 4

System suitability results

Compound	Concentration in $\mu\text{g/mL}$	Retention Time (min) [#]	RRT [#]	Theo plate	Tail Factor	Resolution
Darolutamide	45	7.017 \pm 0.017	-	7626	1.08	5.29
	60	7.028 \pm 0.025	-	7591	1.08	5.21
	75	7.033 \pm 0.017	-	7685	1.06	5.25
Impurity 1	0.45	8.887 \pm 0.012	1.267 \pm 0.001	6758	1.12	4.91
	0.60	8.903 \pm 0.012	1.267 \pm 0.004	6713	1.11	4.89
	0.75	8.913 \pm 0.012	1.267 \pm 0.004	6807	1.13	4.92
Impurity 2	0.45	4.606 \pm 0.010	0.656 \pm 0.001	4953	1.09	-
	0.60	4.624 \pm 0.008	0.658 \pm 0.001	5095	1.08	-
	0.75	4.626 \pm 0.009	0.658 \pm 0.002	4976	1.09	-
Impurity 3	0.45	6.022 \pm 0.067	0.858 \pm 0.009	9158	0.89	7.98
	0.60	5.978 \pm 0.035	0.851 \pm 0.008	9036	0.91	7.91
	0.75	6.022 \pm 0.067	0.856 \pm 0.011	9173	0.89	7.95

Note: # n=3.

The darolutamide standard solution containing 60 $\mu\text{g/mL}$ of darolutamide and 1 % levels of each impurity was analyzed in the developed method for the evaluation of precision (repeatability) and ruggedness (reputability). The % RSD in the peak area response was 0.12, 0.25, 0.20 and 0.23 in intraday precision, 0.38, 0.29, 0.35 and 0.24 in interday precision and 0.67, 0.46, 0.53 and 0.36 in ruggedness respectively for darolutamide, impurity 1, 2 and 3 respectively. This confirms that the method is rugged and precise.

The robustness of the method was evaluated by analysing a standard solution containing impurities at the 1 % level with small variations. The % RSD of the peak area response was within the acceptable limit of less than 2 for darolutamide and its impurities. The system suitability conditions were also evaluated for standard, and its impurities under various conditions and results found that there was no significant change in the results observed (Table 5), which confirms the robustness of the method.

Table 5

Robustness results

S No	Compound	Change*	Peak Area	% Change	Plate Count	Tail factor	Resolution
1	Darolutamide	MP 1	962213	0.76	7595	1.09	5.21
2		MP 2	961102	0.88	7563	1.07	5.24
3		pH 1	955093	1.50	7518	1.08	5.20
4		pH 2	963618	0.62	7527	1.09	5.19
5		WL 1	956924	1.31	7533	1.08	5.22
6		WL 2	962219	0.76	7539	1.09	5.23
7	Impurity 1	MP 1	66011	0.76	6711	1.12	4.92
8		MP 2	65594	1.38	6693	1.11	4.90
9		pH 1	66213	0.45	6685	1.13	4.91
10		pH 2	65867	0.97	6692	1.11	4.89
11		WL 1	65736	1.17	6688	1.12	4.88
12		WL 2	66273	0.36	6676	1.10	4.95
13	Impurity 2	MP 1	98577	0.05	4868	1.09	-
14		MP 2	97211	1.43	4891	1.08	-
15		pH 1	98016	0.62	4873	1.09	-
16		pH 2	98258	0.37	4809	1.07	-
17		WL 1	97732	0.91	4833	1.09	-
18		WL 2	98558	0.07	4932	1.07	-

Continuation of Table 5

S No	Compound	Change*	Peak Area	% Change	Plate Count	Tail factor	Resolution
19	Impurity 3	MP 1	75860	0.78	9027	0.88	7.91
20		MP 2	75955	0.66	9063	0.89	7.95
21		pH 1	75564	1.17	9012	0.88	7.93
22		pH 2	75722	0.96	9106	0.90	7.92
23		WL 1	75290	1.53	9089	0.91	7.95
24		WL 2	76155	0.40	9099	0.89	7.93

Note: * MP (mobile phase) 1: 50 mM ammonium acetate : methanol in 10:90 (v/v); MP 2: 50 mM ammonium acetate : methanol in 25:75 (v/v); WL (wavelength) 1: 244 nm; WL 2: 234 nm; pH 1: 5.3; pH 2: 5.1.

Accuracy of the method was performed by spiked recovery at 50 %, 100 % and 150 % spiked levels of target 30 µg/mL of darolutamide and 0.30 µg/mL of each impurity studied. An acceptable % recovery in each analysis, % RSD in each spiked level was observed (Table 5) for darolutamide, impurities 1, 2 and 3. This confirmed the accuracy of the method.

Table 5

Recovery results

S. No	Compound	Recovery Level	Concentration in µg/mL			Amount found* Mean ± SD	% recovered* Mean ± SD	% RSD of Recovery
			Target	Spiked	Final			
1	Darolutamide	50 %	30	15	45	44.679±0.237	99.29±0.526	0.53
2		100 %	30	30	60	59.604±0.177	99.34±0.295	0.30
3		150 %	30	45	75	74.105±0.416	98.81±0.555	0.56
4	Impurity 1	50 %	0.30	0.15	0.45	0.446±0.003	99.08±0.600	0.61
5		100 %	0.30	0.30	0.60	0.597±0.002	99.42±0.303	0.30
6		150 %	0.30	0.45	0.75	0.739±0.002	98.52±0.330	0.34
7	Impurity 2	50 %	0.30	0.15	0.45	0.446±0.002	99.14±0.499	0.50
8		100 %	0.30	0.30	0.60	0.594±0.003	98.98±0.555	0.56
9		150 %	0.30	0.45	0.75	0.740±0.001	98.61±0.147	0.15
10	Impurity 3	50 %	0.30	0.15	0.45	0.447±0.002	99.32±0.398	0.40
11		100 %	0.30	0.30	0.60	0.591±0.001	98.51±0.208	0.21
12		150 %	0.30	0.45	0.75	0.744±0.003	99.26±0.397	0.40

Note: *n = 3.

The stress degradation study confirms that in UV light degradation illustrates high percentage degradation followed by base degradation. In acid degradation, the % degradation of darolutamide was 8.59 % and six degradation compounds were identified and retained at a retention time of 2.0, 5.4, 6.6, 7.5, 9.5, and 10.0 min. In this degradation study the impurity 2 was identified at a retention time of 4.6 min and the other impurities studied were not detected (Fig. 3). In base degradation study, 9.03 % degradation was observed for darolutamide. Also 5 degradation compounds were identified at a retention time of 3.5, 4.3, 5.6, 7.6 and 9.6 min. In this study, the impurity 2 was identified and retained at a retention time of 4.6 min (Fig. 4). The % degradation of 7.85 % was observed in peroxide degradation study. Here five degradation compounds were separated along with impurities 2 and 3 (Fig. 5). Among all the degradation conditions studied, a very less % degradation of 6.91 % was observed in thermal degradation. In this condition, four degradation compounds were identified and impurities 2 and 3 were also detected (Fig. 6). A very high % degradation of 9.57 % was observed in UV light degradation study. In this study impurity 3 was identified along with six degradation compounds (Fig. 7). In all the stress degradations studied, the degradation compounds were well resolved and retained in the developed method. There is no interference of the unknown degradation compounds with the known impurities in the study as well as the standard darolutamide. This confirms that the method is effectively separates the known impurities and unknown degradation compounds formed during the stress study confirms the stability indicating nature of the method.

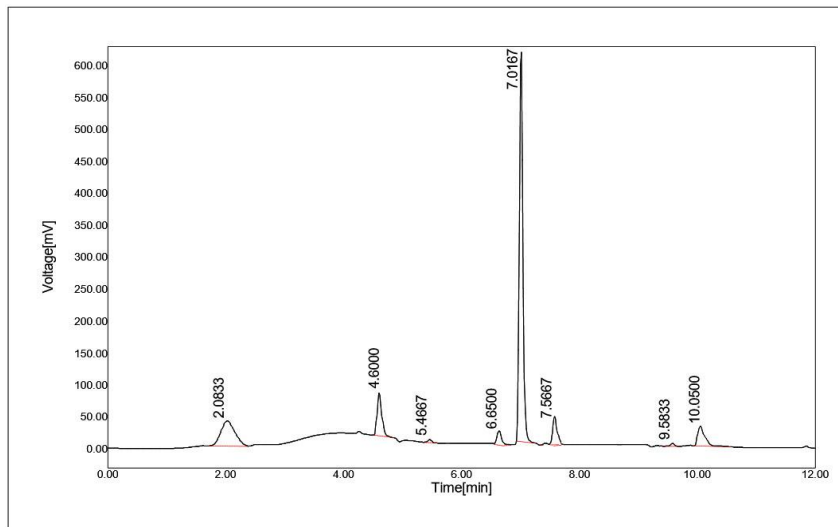


Figure 3. Acid degradation chromatogram of darolutamide

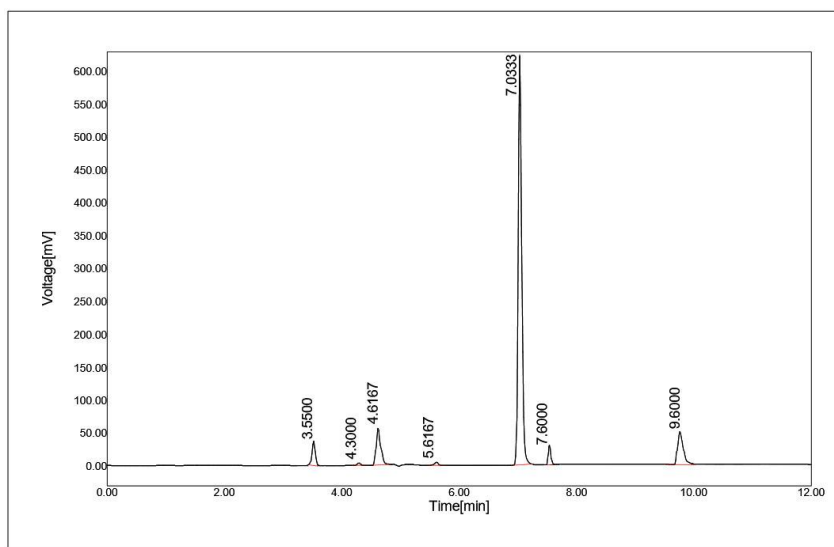


Figure 4. Base degradation chromatogram of darolutamide

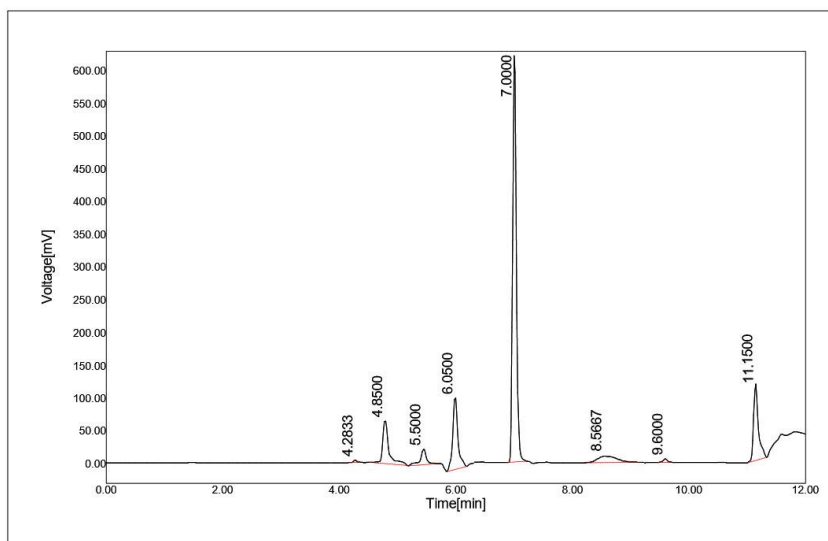


Figure 5. Peroxide degradation chromatogram of darolutamide

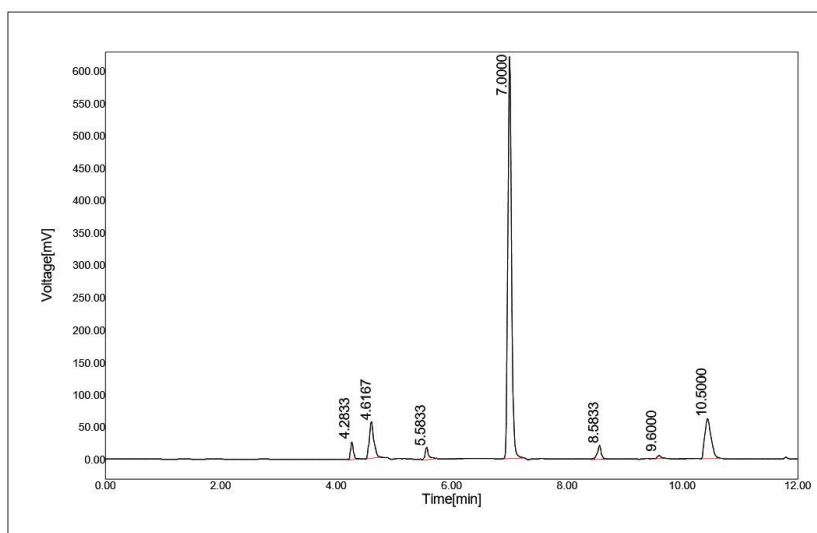


Figure 6: Thermal degradation chromatogram of darolutamide

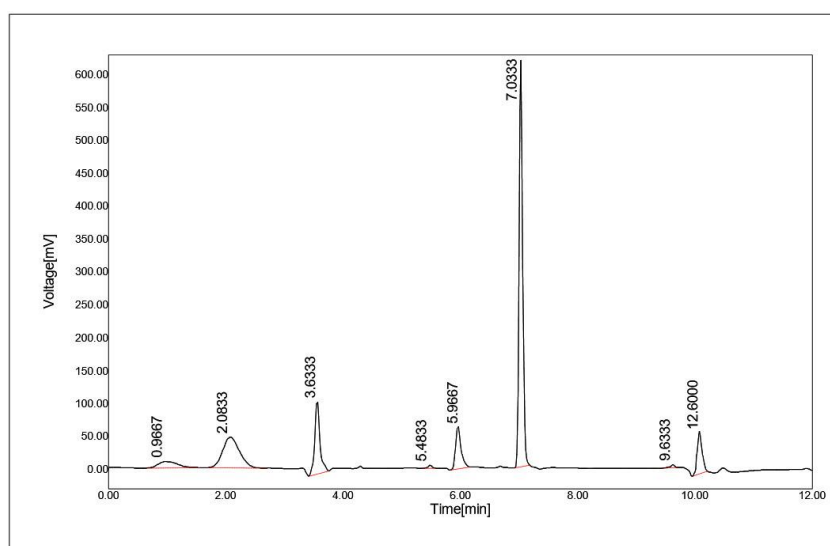


Figure 7: UV light degradation chromatogram of darolutamide

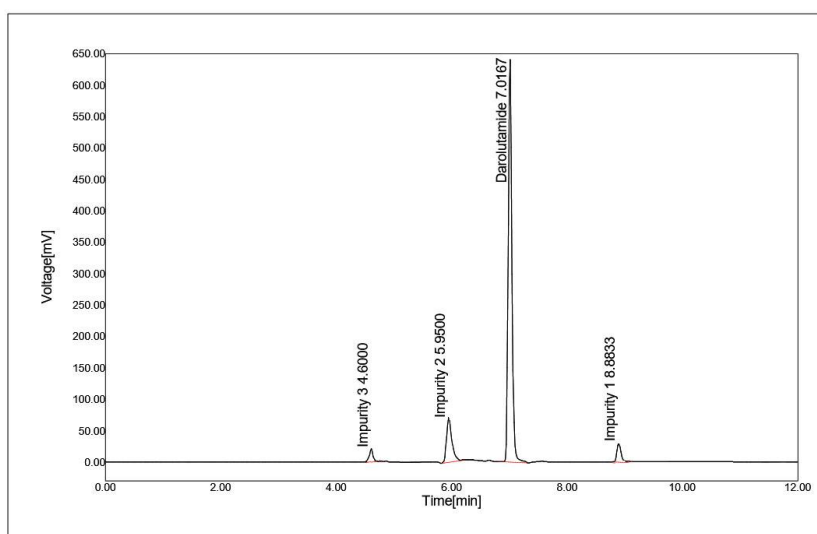


Figure 8: Formulation chromatogram of darolutamide

The method developed in the present study is applied for the estimation of darolutamide, impurities 1, 2 and 3 in pharmaceutical formulation. The % assay in formulation sample was observed to be 98.58 %, 0.08, 0.24 and 0.12 % for darolutamide, impurities 1, 2 and 3 respectively. In the formulation chromatogram (Fig. 8), the formulation excipients were not detected and the retention time of darolutamide and its impurities. The impurities were observed to be within the acceptable limit and prove that the method is applicable for the routine analysis of darolutamide and its impurities.

Conclusion

A simple, novel, and robust analytical RP-HPLC method developed and satisfactorily validated the validation parameters such as accuracy, ruggedness, robustness, and system suitability for the separation and simultaneous quantification of darolutamide and its known impurities 1, 2, and 3. The method having a sensitive linearity range of 0.15-0.90 µg/mL for impurities, as well as 15–90 µg/mL for darolutamide. Meanwhile, the method successfully separates the unknown degradation compounds formed during forced degradation study along with known impurities. Hence, it can be concluded that the method is stable and suitable for the separation and simultaneous quantification of darolutamide and its impurities in bulk drug, as well as formulations.

References

- 1 Mowszowicz (1989). Antiandrogens. Mechanisms and paradoxical effects, *Ann. Endocrinol. Paris.*, 50(3), 189–199.
- 2 Lieberman, R. (2001). Androgen deprivation therapy for prostate cancer chemoprevention: current status and future directions for agent development, *Urology*, 58(2), 83–90 [https://doi.org/10.1016/S0090-4295\(01\)01247-X](https://doi.org/10.1016/S0090-4295(01)01247-X)
- 3 Sciarra F., Toscano, V., Concolino, G., & Di Silverio, F. (1990). Antiandrogens: clinical applications, *J. Steroid Biochem. Mol. Biol.*, 37(3), 349–362 [https://doi.org/10.1016/0960-0760\(90\)90484-3](https://doi.org/10.1016/0960-0760(90)90484-3)
- 4 Fizazi, K., Smith, M.R., & Tombal, B., (2018). Clinical Development of Darolutamide: A Novel Androgen Receptor Antagonist for the Treatment of Prostate Cancer, *Clin Genitourin Cancer.*, 16(5), 332–340 <https://doi.org/10.1016/j.clgc.2018.07.017>
- 5 Liang, D., Richard, C.Z., Wei, X., Theo, M.R., & Kenneth, J.P. (2019). Metastatic prostate cancer remains incurable, why?, *Asian J Urol.*, 6(1), 26–41 <https://doi.org/10.1016/j.ajur.2018.11.005>
- 6 Samia Rocha de Oliveira Melo, Mauricio Homem-de-Mello, Damaris Silveira & Luiz Alberto Simeoni, (2014). Advice on Degradation Products in Pharmaceuticals: A Toxicological Evaluation, *PDA J Pharm Sci Technol.*, 68(3), 221–238 <https://doi.org/10.5731/pdajpst.2014.00974>
- 7 Ashok, Z., Vinay, K., Umesh, T., Suresh, P.S., & Ramesh, M., (2018). RP-HPLC-UV Method for Simultaneous Quantification of Second Generation Non-Steroidal Antiandrogens Along with their Active Metabolites in Mice Plasma: Application to a Pharmacokinetic Study, *Drug Res.*, 69(10), 537–544 <https://doi.org/10.1055/a-0790-8309>
- 8 Neraj, K.S., Suresh, P.S., Mohd, Z., & Ramesh, M. (2018). Development and validation of a novel method for simultaneous quantification of enzalutamide, darolutamide and their active metabolites in mice dried blood spots using LCMS/MS: application to pharmacokinetic study in mice, *ADMET & DMPK*, 6(3), 242–257 <https://doi.org/10.5599/admet.557>
- 9 Sreekanth, D, Pavan, K.V.S.P.N., Suresh, P.S., Syed, M. S., Sadanand, R. M., & Mohd, Z., et al. (2017) LC-MS/MS-ESI method for simultaneous quantification of darolutamide and its active metabolite, ORM-15341 in mice plasma and its application to a pharmacokinetic study, *J. Pharm. Biomed. Anal.*, 145, 454–461. <https://doi.org/10.1016/j.jpba.2017.06.074>
- 10 Suresh, P.S., Neeraj, K.S., Prasanthi, D., Sai, B.P., & Ramesh, M. (2018). Validation of an LC-MS/MS method for simultaneous quantitation of enzalutamide, N-desmethylenzalutamide, apalutamide, darolutamide and ORM-15341 in mice plasma and its application to a mice pharmacokinetic study, *J. Pharm. Biomed. Anal.*, 156, 170–180. <https://doi.org/10.1016/j.jpba.2018.04.038>
- 11 Narayanan, B., Suresh, P.S., Neeraj, K.S., Siva, K.A., & Ramesh, M. (2018). Validation of a chiral LC-MS/MS-ESI method for the simultaneous quantification of darolutamide diastereomers in mouse plasma and its application to a stereoselective pharmacokinetic study in mice, *Biomed. Chromatogr.*, 1–8. <https://doi.org/10.1002/bmc.4173>
- 12 Bikshal, B.K., Useni, R.M., Venkateswara, R.A., & Maheshwara, R.L., (2018). Intended high-performance liquid chromatography procedure for the quantification of norfloxacin and its potential impurities in active pharmaceutical ingredient and tablet dosage forms, *Thai J. Pharm. Sci.*, 42(1), 27–36.
- 13 Mallu, U.R., Anna, V.R., & Kasimala, B.B. (2019). Rapid Stability Indicating HPLC Method for the Analysis of Leflunomide and Its Related Impurities in Bulk Drug and Formulations, *Turk J Pharm Sci.*, 16, 457–465 <https://doi.org/10.4274/tjps.galenos.2018.34635>
- 14 Prasad, S.S., Krishna Mohan, G.V., & Naga Babu, A., (2019). Development of simple and robust RP-HPLC method for determination of everolimus and its impurities in oral solid dosage form, *Asian J. Chem.*, 31(5), 1002–1008 <https://doi.org/10.14233/ajchem.2019.21723>
- 15 Palacharla, S.K., & Krishna Mohan, G.V. (2019). HPLC method for determination of aspirin, rosuvastatin, ezetimibe and clopidogrel in combination drug products, *Asian J. Chem.*, 31(10), 2275–2283 <https://doi.org/10.14233/ajchem.2019.22050>

16 Palacharla, S.K., Krishna Mohan, G.V., & Naga Babu, A. (2019). RP-HPLC estimation of bumetanide and its impurities in oral solid dosage form, *Asian J. Chem.*, 31(10), 2275–2283 <https://doi.org/10.14233/ajchem.2019.22069>

17 Bikshal, B.K., Venkateswara, R.A., & Useni, R.M. (2018). Stability-Indicating Reversed-Phase HPLC Method for the Separation and Estimation of Related Impurities of Cilnidipine in Pharmaceutical Formulations, *Indian Drugs*, 55(12), 41–49.

18 Sri Girija, K., Bikshal, B.K., & Venkateswara, R.A. (2021). A new high-performance liquid chromatography method for the separation and simultaneous quantification of eptifibatide and its impurities in pharmaceutical injection formulation, *Int J App Pharm.*, 13(2), 165–172 <https://doi.org/10.22159/ijap.2021v13i2.39895>

В.Г. Камани, М. Суджата, Г. Даддала

Даролутамид пен оның фармацевтикалық препараттардағы қоспаларын бөлу және анықтау үшін жаңа сенімді ЖТСХ әдісін жасау және валидациялау

Мақалада даролутамид пен оның 1, 2, 3 қоспаларын жеке күйінде және қосылыстарда талдаудың жаңа сенімді ҚФ-ЖТСХ әдісі алғаш рет ұсынылған. Бөліну тұрақты фаза ретінде Luna C18 (250 мм × 4,6 мм, 5 мкм) және жылжымалы фаза ретінде 50 мМ аммоний ацетаты ерітіндісі мен метанолдың 15:80 қатынасында (көлем/көлем) Phenomenex мұнарасында іске асырылды (рН = 5,2 және ағын жылдамдығы 1,0 мл/мин). УК анықтау 239 нм толқын ұзындығында орындалды. Осы жағдайларда даролутамид пен оның 1, 2 және 3-ші қоспаларының ұсталу уақыты сәйкесінше 7,05, 8,90, 4,63 және 5,95 мин болды. Әдіс жүйелік жарамдылыққа, талдау ауқымына, дәлдігіне, ерекшелігіне, тұрақтылығына және сенімділігіне тексерілді. Мәжбүрлі деградацияны зерттеу талданатын затты бес түрлі стресс жағдайына ұшырату арқылы жүргізілді және деградацияның барлық жағдайларында ыдырау %-ы өте төмен болды. Ұсынылған әдіс дәрілік затты және оның фармацевтикалық құрамдағы қоспаларын бөлуге және бағалауға мүмкіндік береді. Жалпы, әзірленген әдіс даролутамидті сандық анықтауға жарамды екені және 1, 2 және 3 қоспаларды бөлуге, сондай-ақ талдауға мүмкіндік беретіні көрсетілді.

Кілт сөздер: даролутамид, қоспаларды талдау, ЖТСХ әдісі, әдісті валидациялау, валидация, мәжбүрлі ыдырауды зерттеу, құрамды талдау, Nubeqa® ішіндегі қоспаларды талдау.

В.Г. Камани, М. Суджата, Г. Даддала

Разработка и валидация нового надежного метода ВЭЖХ для разделения и определения даролутамида и его примесей в фармацевтических препаратах

В статье впервые представлен новый надежный ОФ-ВЭЖХ метод анализа даролутамида и его примесей 1, 2, 3 в индивидуальном виде и в композициях. Разделение было достигнуто на колонке Phenomenex с Luna C18 (250 мм × 4,6 мм, 5 мкм) в качестве стационарной фазы и раствора 50 мМ ацетата аммония : метанола, соотношением 15:80 (объем/объем) в качестве подвижной фазы (рН=5,2, скорость потока 1,0 мл/мин). УФ-детектирование осуществлялось при длине волны 239 нм. В этих условиях время удерживания даролутамида и его примесей 1, 2 и 3 составило 7,05, 8,90, 4,63 и 5,95 мин соответственно. Метод был проверен на системную пригодность, диапазон анализа, точность, специфичность, стабильность и надежность. Исследование принудительной деградации проводилось путем воздействия на аналит пяти различных стрессовых условий, и во всех условиях деградации процент разложения был очень низким. Предложенный метод позволяет разделять и оценивать лекарственное средство и его примеси в фармацевтических составах. В целом, было показано, что разработанный метод подходит для количественного определения даролутамида и разделения и анализа примесей 1, 2 и 3.

Ключевые слова: даролутамид, анализ примесей, разработка метода ВЭЖХ, проверка метода, валидация, исследование принудительного разложения, анализ состава, анализ примесей в Nubeqa®.

Information about authors

Venu Gopal Kamani — PhD student, Department of Chemistry, Koneru Lakshmaiah Education Foundation, Vaddeswaram, Guntur — 522502, A.P., India; e-mail: venukamani@gmail.com; <https://orcid.org/0000-0002-1834-7227>;

Dr. M. Sujatha — Associate Professor, Department of Chemistry, Koneru Lakshmaiah Education Foundation, Vaddeswaram, Guntur — 522502, A.P., India; e-mail: sujathaenviero@kluniversity.in; <https://orcid.org/0000-0001-9645-3298>;

Guna Bhushana Daddala — Chief Scientist, Department of Analytical and Research, Piramal Pharma Ltd, Ennore, Chennai — 600057, Tamil Nadu, India; e-mail: gunabhushana.daddala@piramal.com; <https://orcid.org/0000-0001-5878-1653>.

V.P. Malyshev¹, A.M. Makasheva^{2*}, L.A. Bekbayeva²

¹Abishev Chemical-Metallurgical Institute, Karaganda, Kazakhstan;

²Karaganda Technical University, Karaganda, Kazakhstan

(*Corresponding author's e-mail: astra_mun@mail.ru)

Invariants of ratio of crystal-mobile, liquid-mobile, and vaporized chaotized particles in solid, liquid, and gas states of substance

The authors of the article have developed the concept of chaotic particles based on the Boltzmann distribution over the kinetic energy of the particles' chaotic motion. This distribution allows to combine the solid, liquid, and gaseous states of matter with the help of energetic particles called crystal-mobile, liquid-mobile, and vapor-mobile. The ratio of the proportions of such randomized particles determines a certain state of matter aggregation. The sum of the shares of these particles in all combinations at any temperature is equal to unity. During the study it has identified that qualitative and quantitative analysis of states with a priority basic effect of a randomized component of a substance can be conducted. Certain regularities of states were discovered, independent of the specific type of substance and consistent with the physicochemical properties. The entropy of mixing of all three energy classes of chaotic particles was calculated for simple substances. It was characterized by a maximum in the interval of the boiling point of substances. This feature testifies to the unique variety of possibilities for the implementation of the most complex heterogeneous processes in terrestrial conditions at atmospheric pressure, which ultimately ensured the self-organization of life.

Keywords: Boltzmann distribution, kinetic energy, chaotic particles, entropy, zero approximation, barium, melting point, boiling point.

Introduction

Until now, there is no sufficiently complete theory of the liquid state of matter, if only because, in contrast to the gaseous and solid states, there is no “zero approximation” for the intermediate state [1]. So, there is no attraction or electronic repulsion of particles in an ideal gas, that is, the potential energy of their interaction is neglected. In an ideal crystal, there are no violations in the correctness of the crystal lattice due to neglect of the kinetic (thermal) energy of the chaotic motion of particles. If we understand the ideal liquid state of matter as an intermediate one in terms of these neglects, then we get an absurd paradox: in an ideal liquid, both potential and kinetic energy should be neglected.

Such a result is a consequence of a logical error, which is known in philosophy in the form of a statement: any definition through negation is flawed. One should focus on *the preservation* of any feature or property, and not on its absence. In this case, thermal energy turns out to be a single primordial property of matter in all its states of aggregation, which should be taken as a zero approximation for the state of matter as a whole, avoiding opposing one state of aggregation to another, which leads more to paradoxes than to understanding the essence of the matter.

The proposed zero approximation turns out to be constructive because there is a universal tool for its use — the fundamental distribution, or energy spectrum of Boltzmann, which is also applicable to separately taking into account the effect of kinetic energy on a given distribution not only for gaseous, but also for concentrated states [2]. In this case, it is sufficient to know the melting points T_m and boiling points T_b of the substance in order to distinguish the energy classes of random particles located above or below these barriers from the thermal barriers of melting RT_m and boiling RT_b , and to judge their character of influence on the solid, liquid, and gaseous states in the corresponding temperature intervals; $0 - T_m, T_m - T_b, T_b - \infty$.

The concept of chaotic particles put forward by the authors is based on this idea [3], which allows using the Boltzmann distribution (E_i is the kinetic energy):

$$P_i = e^{-\frac{E_i}{RT}} / \sum_{i=1}^{\infty} e^{-\frac{E_i}{RT}} \quad (1)$$

to determine the share of low-energy particles called crystal-mobile:

$$P_{crm} = 1 - \exp\left(-\frac{RT_m}{RT}\right) = 1 - \exp\left(-\frac{T_m}{T}\right), \quad (2)$$

the share of medium-energy particles called liquid-mobile:

$$P_{lqm} = \exp\left(-\frac{T_m}{T}\right) - \exp\left(-\frac{T_b}{T}\right), \quad (3)$$

and the share of high-energy particles called vapor-mobile:

$$P_{vm} = \exp\left(-\frac{T_b}{T}\right), \quad (4)$$

subject to the condition

$$P_{crm} + P_{lqm} + P_{vm} = 1. \quad (5)$$

This mathematical model is the “zero approximation” of all three aggregate states individually and as a whole, since their shares are compatible at any temperature.

The purpose of this work is to qualitatively and quantitatively estimate the entropy invariants of mixing of randomized particles using the Boltzmann distribution for simple substances.

Experimental

In this model, invariants of the P_{crm} , P_{lqm} , P_{vm} ratios are immediately revealed under boundary temperature conditions. So, at $T = 0$, the share of crystal-mobile particles is equal to unity and, accordingly, the shares of liquid and vapor-mobile particles are zero. This characterizes the solid state of matter in the form of an ideal crystal. At $T = \infty$, only vapor-mobile particles exist and the state of matter corresponds to the concept of an ideal gas. At the melting point, $P_{crm} = 0.632$, and the sum $P_{lqm} + P_{vm} = 0.368$. If we assume that crystal-mobile particles provide the stability of the solid state of matter, and liquid and vapor-mobile ones violate this stability, then the ratio 0.632:0.368 should be understood as the limiting invariant of the preservation of the solid state, related to the system-wide characteristics of stability. The golden ratio of 0.618:0.382 is the closest to this ratio, which serves as a universal measure of the structural harmony of the system, their structural and chaotic sides in the widest class of objects [4, 5].

The same applies to the boiling point, with the difference that there is a transition from a condensed state to a vapor state and the sum of the crystal-mobile and liquid-mobile particles is the binding component, and the content of the vapor-mobile particles is chaotic. This follows from the fact that at $T = T_b$ $P_{vm} = 0.368$, and $P_{crm} + P_{lqm} = 0.632$.

Knowledge of the specific values of T_m and T_b is required for a more detailed analysis of the $P_{crm}:P_{lqm}:P_{vm}$ ratio at any temperature, although in the most general form, it is possible to establish its own invariants for each state.

So, in the interval $0 \rightarrow T_m$, the share of crystal-mobile particles changes from unity to $P_{crm} = 0.632$, and function (2) undergoes an inflection, further tending to zero at $T \rightarrow \infty$. This inflection is detected by double differentiation (2)

$$\frac{\partial^2 P_{crm}}{\partial T^2} = \frac{T_m}{T^3} \left(2 - \frac{T_m}{T}\right) \exp\left(-\frac{T_m}{T}\right), \quad (6)$$

from which, when equating to zero, in addition to the asymptotic approximation of function (2) to unity at $T \rightarrow 0$ and to zero $T \rightarrow \infty$, the position of the inflection point of this function is established at $T = 0.5T_m$. At this point, there is a maximum decrease in crystal-mobile particles and, accordingly, an increase in the sum of liquid- and vapor-mobile particles. In this case, the crystal retains high connectivity $P_{crm} = 0.865$, but turns out to be noticeably loosened $P_{lqm} + P_{vm} = 0.135$ and thus prone to plastic deformation and melting.

This is consistent with the well-known Bochvar-Tamman temperature, which refers to the optimal temperature of plastic deformation $T_{opt} \approx 0.5T_m$ and is either experimentally recorded or generalized on the basis of a large number of experimental data [6]. At this temperature, diffusion in the lattice of the solid becomes noticeable and its reactivity begins to manifest itself.

There are also more subtle features of the temperature dependence of the properties of a solid. According to Tamman, the mobility of particles on the crystal surface is found to be about $0.3T_m$. It has been also found that at temperatures above $0.5T_m$ deformation is not accompanied by hardening and the metal flows at a constant rate under a constant load, which is characterized as its creep. This is explained by the increased role of vacancies, and the number of atoms in the inter-aisles, and indeed the entire set of defects in the crys-

tal. The movement of defects occurs due to thermal fluctuations, the frequency of which always decreases with decreasing temperature. It is noted that the region $(0.4 \div 0.8)T_m$ is the most typical for creep [6, 7].

Thus, in addition to the optimal plasticity temperature $0.5T_m$, the zone of manifestation of plasticity effects $(0.3 \div 0.8)T_m$ is also the empirical invariants of plasticity. In this case, the beginning of this zone can be interpreted as an area of acceleration of these effects manifestation, and the end of the zone — as an area of slowing down of this process. However, as applied to the temperature dependence of the share of crystal-mobile particles (2), Eq. (6) takes on the meaning of the rate of decrease in the content of these particles. This will allow it to be used to express acceleration by taking the third derivative

$$\frac{\partial^3 P_{crm}}{\partial T^3} = T_m T^{-4} \left(-6 + 6T_m T^{-1} T_m^2 T^{-2} \right) \exp\left(-\frac{T_m}{T}\right), \quad (7)$$

in which, the asymptotic tendency of acceleration to zero at $T = 0$ and $T = \infty$, equating the trinomial to zero leads to the quadratic equation

$$6T^2 - 6T_m T + T_m^2 = 0, \quad (8)$$

having two real roots

$$T_{1,2} = \frac{T_m(3 \pm \sqrt{3})}{6}. \quad (9)$$

From this, within the framework of the chaotic particles concept, two extreme invariant points are found, namely the maximum acceleration of the decrease in the share of crystal-mobile particles,

$$T_1 = \left(0.5 - \frac{\sqrt{3}}{6}\right) T_m \approx 0.21T_m, \quad (10)$$

and the minimum acceleration of the loss of these particles,

$$T_2 = \left(0.5 + \frac{\sqrt{3}}{6}\right) T_m \approx 0.79T_m, \quad (11)$$

which correlate with the experimentally found plasticity zone $(0.3 \div 0.8) T_m$.

The obtained results allowed the authors to express for the first time the useful energy costs for plastic deformation at any temperature in the form of an addition to the thermal energy at the melting point

$$\Delta E = RT_m - RT = R(T_m - T) \quad (12)$$

and determine the energy efficiency of rolling mills [7].

The temperature dependence of the share of vapor-mobile particles (4) mathematically corresponds to the inverse mapping of dependence (2) for crystal-mobile particles, with the difference that the temperature is normalized according to T_b . Nevertheless during differentiation, the form of the derivatives differs only in sign (the function increases instead of decreasing) while maintaining the same form of the invariants: inflection points at $0.5T_b$, $T_1 = \left(0.5 - \sqrt{3}/6\right)T_b \approx 0.21T_b$, $T_2 = \left(0.5 + \sqrt{3}/6\right) \approx 0.79T_b$. However, if the range of invariants of crystal-mobile particles refers to the solid state, then a similar range for the gaseous state as a whole enters the condensed state with a possible strike even in a solid in dependence on the specific ratio of T_b and T_m for each substance.

It can be expected that the revealed features for the behavior of vapor-mobile particles directly relate to the temperature dependences of vapor in equilibrium with a solid and a liquid, as well as to some subtle effects of the presence of vapor-mobile particles in the condensed bodies themselves, since the invariant at T_1 , $0.5T_b$ and T_2 correspond small fractional values P_{vm} equal to: 0.086; 0.135 and 0.282, against those set for crystal-mobile particles: 0.992; 0.865 and 0.718.

The mathematical model for liquid-mobile particles (3) is determined by the influence of both the melting and boiling points, and therefore, taking into account the opposite nature of the corresponding temperature dependences for crystal-mobile and vapor-mobile particles, it should contain a maximum. It can be found analytically by differentiating function (3) and equating the derivative to zero:

$$\frac{dP_{lqm}}{dT} = \frac{1}{T^2} \left[T_m \exp(-T_m/T) - T_b \exp(-T_b/T) \right] = 0, \quad (13)$$

whence we found, in addition to the horizontal asymptotes at $T = 0$ and $T = \infty$, also the maximum point P_{lqm}

$$T_{max,lqm} = \frac{T_b - T_m}{\ln(T_b/T_m)}, \quad (14)$$

Substituting (14) into (3), we determine the maximum share of liquid-mobile particles

$$P_{lqm,max} = \exp \left[-\frac{T_m \ln \left(\frac{T_b}{T_m} \right)}{T_b - T_m} \right] - \exp \left[-\frac{T_b \ln \left(\frac{T_b}{T_m} \right)}{T_b - T_m} \right].$$

For any ratio of T_m and T_b , this invariant of liquid-mobile particles is entirely in a liquid state, and this can be proved by limiting oneself to the natural conditions $T_b > T_m$ and, accordingly, $\frac{T_b}{T_m} > 1$.

To this end, we first prove the inequality $T_{max,lqm} > T_m$:

$$\frac{T_b - T_m}{\ln(T_b / T_m)} > T_m. \quad (15)$$

By means of identical transformations (15), we arrive at the expression

$$\frac{T_b}{T_m} > 1 + \ln \frac{T_b}{T_m}, \quad (16)$$

from which it follows that since $\ln \frac{T_b}{T_m} > 0$, then $\left(1 + \ln \frac{T_b}{T_m} \right) > 1$ and then $T_b > T_m$ in accordance with the initial conditions.

To prove that $T_{max,lqm} < T_b$,

$$\frac{T_b - T_m}{\ln(T_b / T_m)} < T_b, \quad (17)$$

by similar identical transformations (17) is reduced to the inequality

$$\frac{T_m}{T_b} - \ln \frac{T_m}{T_b} > 1. \quad (18)$$

Taking into account that for the region $0 < \frac{T_m}{T_b} < 1$ the inequalities $\frac{T_m}{T_b} > \ln \frac{T_m}{T_b}$ and $\frac{T_m}{T_b} < \left| \ln \frac{T_m}{T_b} \right|$, the validity of inequality (18) follows, which is confirmed by its numerical analysis.

Belonging to the extreme content of liquid-mobile particles indicates its particular complexity, which, together with the present crystal-mobile and vapor-mobile particles in the same area, gives rise to widespread ideas about its mechanical mixture of solid and gaseous states [1]. However, the discussed extremality (14) does not at all refer to the equality of the shares of crystal-mobile and vapor-mobile particles, but to the algebraic equality of their increments.

Results and Discussion

All the noted features can be illustrated more clearly by the example of the relationship of aggregate states for barium — a typical metal of the second group of the Periodic Table of Chemical Elements (Fig. 1).

Figure 1 illustrates that the equality of the shares of *crm*- and *vm*- particles falls almost strictly at the boiling point. If we set it into the equation of equality of the shares of crystal-mobile (2) and vapor-mobile particles (4),

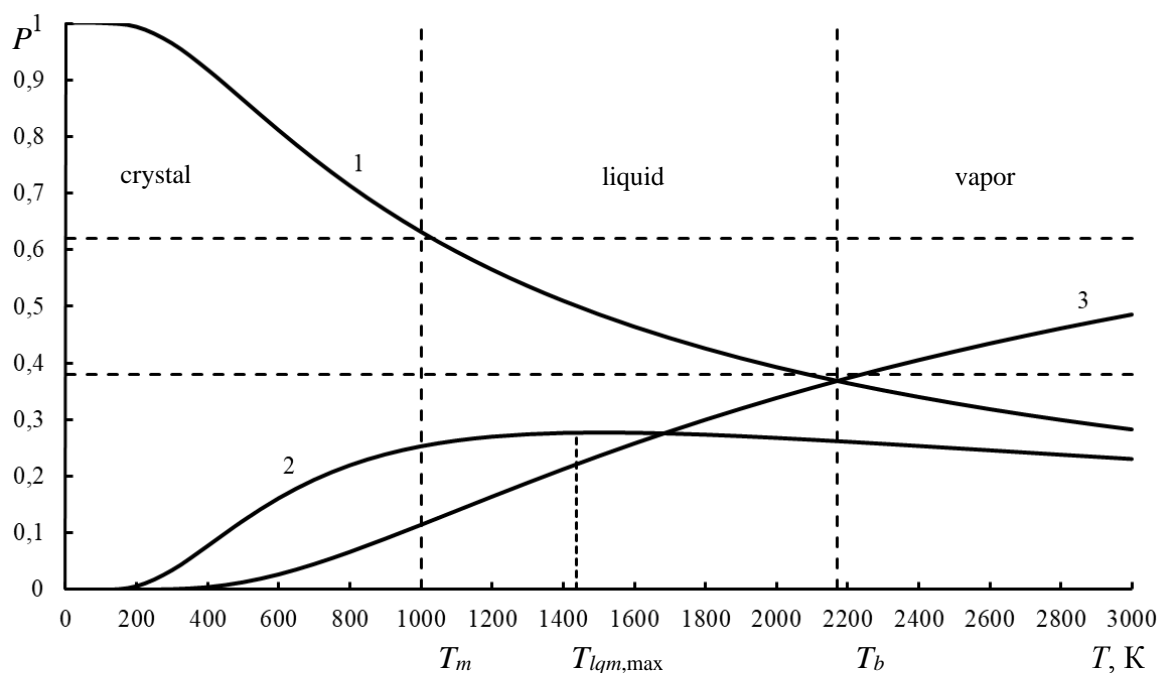
$$1 - \exp \left(-\frac{T_m}{T_b} \right) = \exp \left(-\frac{T_b}{T_b} \right), \quad (19)$$

then we get the solution

$$\frac{T_m}{T_b} = -\ln(1 - e^{-1}) \cong 0.46, \quad (20)$$

whence follows

$$T_m \cong 0.46T_b. \quad (21)$$



Vertical lines — by melting point T_m and boiling point T_b ,
 horizontal lines — according to the proportion of the golden ratio (~ 0.62 and ~ 0.38).
 Highlighted the temperature of the maximum of the share of liquid-mobile particles

Figure 1. Dependence of the shares of crystal-mobile (1), liquid-mobile (2), and vapor-mobile (3) particles on temperature for barium

This value is consistent with the average value of the T_b/T_m ratio, established for 55 metals and equal to 2.2 [7], from which $T_m \cong 0,44T_b$ has been found. This indicates a certain regularity in referring the equality of the shares of *crm*- and *vm*- particles to the boiling point.

The equality of shares, and hence the probability of detecting any signs of distinguishability of any objects, has a deeper meaning, which is associated with the achievement of the maximum uncertainty, or the system entropy [8-10, 5]. From this point of view, attention is drawn to the proximity of the shares of *crm*, *lqm*- and *vm*- particles referred to the boiling point. In this case, according to (2)-(5) at $T = T_b$, the ratio $P_{crm}:P_{lqm}:P_{vm} = 0.37:0.37:0.26$ is obtained. Full equality of the shares of these particles can be achieved by the condition $P_{crm} = P_{lqm} = P_{vm} = 1/3$, which allows us to find the necessary invariant relation by (4)

$$\frac{1}{3} = \exp(-T_b / T). \quad (22)$$

In this ideal case, the temperature of the substance should be equal to $T = (T_b / \ln 3) \cong 0.91T_b$, which confirms its proximity to the boiling point.

The required T_b/T_m ratio (22) under real conditions can be observed only under suitable conditions, since the boiling point strongly depends on the external pressure, which is 101325 Pa on the Earth's surface and taken as normal conditions. The melting point depends on the external pressure to a much lesser extent, and therefore, the T_b/T_m ratio can vary over a wide range, both natural and artificial.

The ratio of the shares of crystal-mobile, liquid-mobile, and vapor-mobile particles at any temperature can be expressed generally in the form of the entropy of mixing of these particles in accordance with their virtual existence and interconversion

$$S_{mix} = -R \sum_1^n p_i \ln p_i, \quad (23)$$

where p_i is the proportion of different elements of the system to be mixed, n is their number, R is the universal gas constant equal to 8.314472 J/mol, when the process is expressed in terms of physical entropy. It can be presented in the form of

$$S_{mix} = -R(P_{crm} \ln P_{crm} + P_{lqm} \ln P_{lqm} + P_{vm} \ln P_{vm}), \quad (24)$$

or in more detail, taking into account (2)–(5) as

$$S_{mix} = -R \left\{ \left[1 - \exp\left(-\frac{T_m}{T}\right) \right] \ln \left[1 - \exp\left(-\frac{T_m}{T}\right) \right] + \left[\exp\left(-\frac{T_m}{T}\right) - \exp\left(-\frac{T_b}{T}\right) \right] \times \right. \\ \left. \times \ln \left[\exp\left(-\frac{T_m}{T}\right) - \exp\left(-\frac{T_b}{T}\right) \right] - \left(\frac{T_b}{T}\right) \exp\left(-\frac{T_b}{T}\right) \right\}. \quad (25)$$

It is enough to differentiate (25) and equate the derivative to zero to find the temperature, at which the maximum entropy is realized. It seems impossible to analytically determine the position of this maximum due to the difficulty of freeing the temperature from the resulting transcendental equations; therefore, this temperature $T_{S_{mix,max}}$ was determined numerically for all metals, for which reference data are available [11].

In general, the formation of the function maximum (24) is necessary, since these functions take zero values both at $T = 0$ and at $T \rightarrow \infty$ due to the presence of only one kind of particles at this value, respectively $P_{crm} = 1$ and $P_{vm} = 1$, due to which all fragments of equation (24) are zeroed both by the condition $1 \ln 1 = 0$ and by the condition $0 \ln 0 = 0 \cdot (-\infty) \cdot 0$.

The results of calculating the entropy of mixing of three energy classes of chaotic particles are shown by the example of barium in Table 1 and Figure 2.

Table 1

Entropy of mixing of *crm*-, *lqm*- and *vm*-particles depending on temperature for barium

T, K	$S_{mix}, J/mol$	T, K	$S_{mix}, J/mol$	T, K	$S_{mix}, J/mol$	T, K	$S_{mix}, J/mol$
0	0	800	6.270	1600	8.824	2300	9.016
100	$4.2 \cdot 10^{-3}$	900	6.871	1700	8.912	2400	8.989
200	0.387	$T_m=1000$	7.364	1800	8.974	2500	8.954
300	1.309	1100	7.764	1900	9.014	2600	8.914
400	2.503	1200	8.086	2000	9.036	2700	8.867
500	3.650	1300	8.344	2100	9.041	2800	8.816
600	4.672	1400	8.547	$T_b=2170$	9.038	2900	8.762
700	5.542	1500	8.704	2200	9.034	3000	8.705

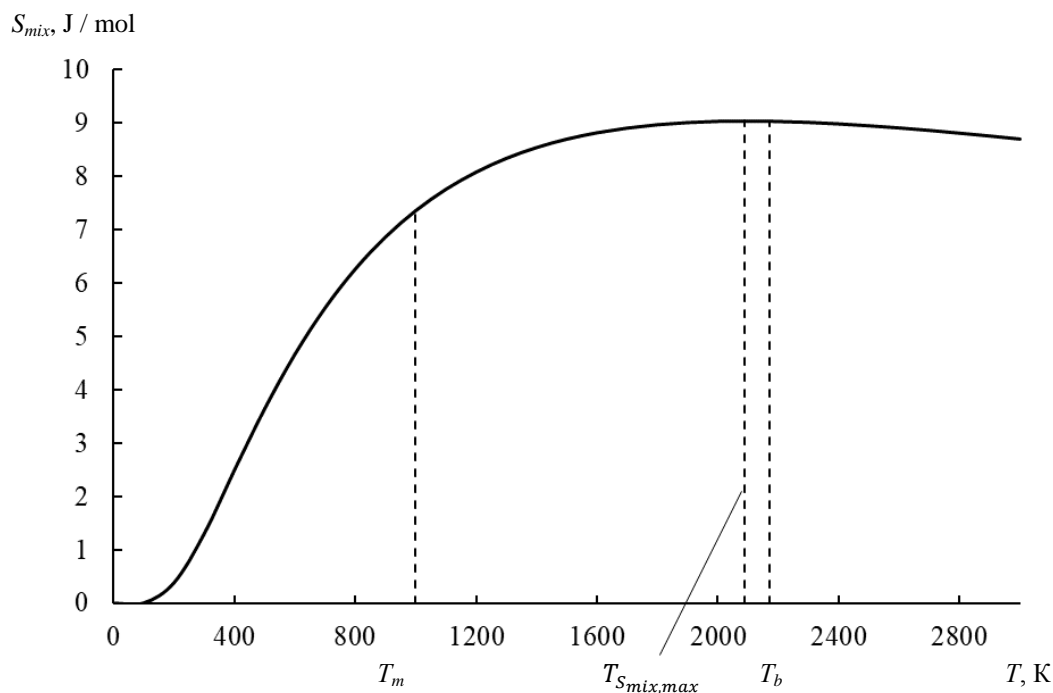
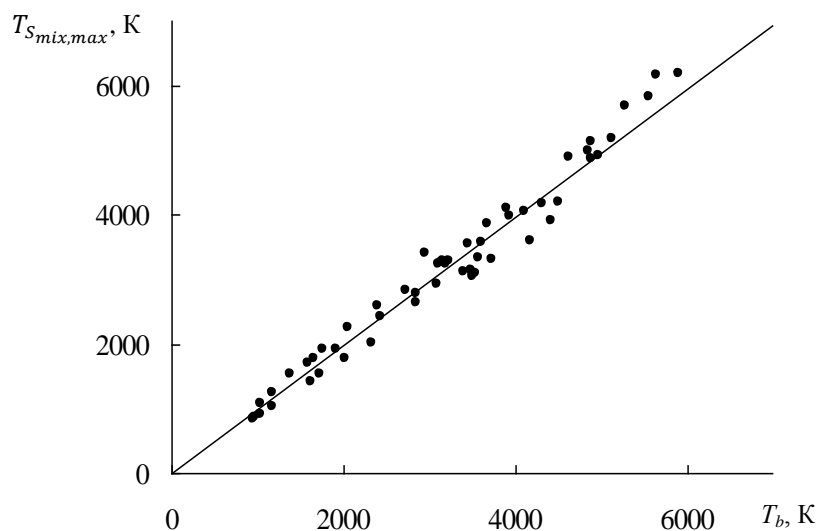


Figure 2. Dependence of the entropy of mixing of three energy classes of randomized particles on the barium temperature. Melting points, boiling points, and maximum entropy of mixing are indicated

As can be seen from these data, the region of the maximum entropy of mixing is expressed rather smoothly, adjacent directly to the boiling point of barium with a value of 9.041 J/mol at a temperature of 2090 K, which is $0.963T_b$. In this case, the difference between the values of the entropy of mixing themselves is even smaller: at T_b $S_{mix} = 9.038$ J/mol, which ensures the ratio $\frac{S_{mix,T_b}}{S_{mix,max}} = 0.99967$.

Similar results were obtained for 54 metals according to reference data for T_m and T_b [12], which made it possible to plot the dependence of the temperature, at which the maximum entropy of mixing was reached on the boiling point (Fig. 3).



$T_{S_{mix,max}}$ is temperature of the maximum entropy of mixing, T_b is boiling temperature.
Points — calculation according to reference data [12] through T_m and T_b according to (24),
straight line — according to the dependence

Figure 3. Dependence of the temperature of the maximum entropy of randomized particles mixing on the metals boiling point

In this case, a straight-line dependence was obtained, starting from the origin of coordinates:

$$T_{S_{mix,max}} = 0.9947T_b, \quad (26)$$

indicative of the functional nature of this dependence. It is retained when supplemented with reference data for other simple substances. However, considering the dependence of the boiling point on atmospheric pressure, the resulting invariant applies only to terrestrial conditions, although this limitation is of extremely great evolutionary significance.

Indeed, in this case, the maximum entropy for the joint presence and mixing of crystal-mobile, liquid, and vapor-mobile particles creates unique conditions for the realization likelihood of the widest variety of heterogeneous processes occurring on the Earth's surface, primarily with the participation of volcanic processes with the eruption of liquid lava, geysers, dust and gas clouds both on the land surface and into the atmosphere as well as into the oceans depths. Isn't it this ideal chaotization of solid, liquid, and gaseous states of matter and their mutual penetration into each other in the form of three energy classes of chaotic particles due to the extremely small probability of self-organization of life on Earth?

Conclusions

As a "zero approximation" for the solid, liquid, and gaseous states of matter as a whole, it is proposed to use a unified Boltzmann distribution over the kinetic energy of chaotic (thermal) particle motion with the allocation of three energy classes, specifically crystal-mobile with thermal energy no higher than RT_m ; liquid-mobile with energies above RT_m , but below RT_b ; vapor-mobile with an energy of at least RT_b . The sum of the shares of these particles in all combinations at any temperature is equal to unity.

The ratio of the shares of *crm*-, *lqm* and *vm*-particles determines the originality of each state of matter and their relationship as a whole, which can be regarded as a generalization of the previously known scat-

tered “zero approximations”. At the same time, it is possible to carry out not only a qualitative, but also a quantitative analysis of states with a priority basic effect of a randomized component of a substance.

Such an analysis revealed certain invariants of states, independent of the specific type of substance and consistent with the physicochemical properties. So, at $T = 0$, the substance is provided only by crystal-mobile particles, which corresponds to the concept of an ideal crystal, and at $T \rightarrow \infty$, only vapor-mobile particles remain, and this is consistent with the concept of an ideal gas. At melting points T_m and boiling points T_b , the shares of particles responsible for the structural stability of the states, respectively, solid and condensed, are close to the golden ratio. Differential analysis of the temperature dependence of the share of crystal-mobile particles established an inflection point equal to $0.5T_m$ and corresponding to the optimal temperature of plastic deformation of Bochvar-Tamman, as well as the range of plasticity effects manifestation $(0.3-0.8)T_m$, analytically determined on the basis of the same dependence. The temperature dependence of the share of liquid-mobile particles analytically reveals a maximum in the range of the liquid state, which indicates the complexity of this state under the influence of the opposite effect of the dependence for crystal-mobile and vapor-mobile particles [13].

The entropy of mixing of all three energy classes of chaotic particles is characterized by a maximum in the area of the substances boiling point, which indicates a unique variety of possibilities for the implementation of the most complex heterogeneous processes under terrestrial conditions at atmospheric pressure, which ultimately ensured the self-organization of life.

This invariant is illustrated, like all of the above, using barium as an example. The relationship between the maximum entropy of mixing of *crm*-, *lqm*- and *vm*-particles with the boiling point is established for simple substances and is highly adequate.

References

- 1 Еланский Г.Н. Структура и свойства металлических расплавов: учеб. пос. для вузов / Г.Н. Еланский, Д.Г. Еланский. — М.: Юрайт, 2020. — 212 с.
- 2 Леонтович М.А. Введение в термодинамику. Статистическая физика / М.А. Леонтович. — М.: Высш. шк., 1983. — 416 с.
- 3 Малышев В.П. Концепция хаотизированных частиц как основа единого отображения твердого, жидкого и газообразного состояний вещества / В.П. Малышев, А.М. Нурмагамбетова (Макашева) // Вестн. Казах. нац ун-та. Сер. хим. — 2004. — № 3(35). — С. 53–67.
- 4 Сороко Э.М. Структурная гармония систем / Э.М. Сороко. — Минск: Наука и техника, 1984. — 246 с.
- 5 Малышев В.П. Вероятностно-детерминированное отображение / В.П. Малышев. — Алматы: Ғылым, 1994. — 376 с.
- 6 Хоникомб Р. Пластическая деформация металлов; пер. с англ. / Р. Хоникомб. — М.: Мир, 1972. — 389 с.
- 7 Малышев В.П. Плавкость и пластичность металлов / В.П. Малышев, Б.Т. Абдрахманов, А.М. Нурмагамбетова. — М.: Научный мир, 2004. — 148 с.
- 8 Хартли Р. Передача информации. Теория информации и ее приложения / Р. Хартли. — М.: ИЛ, 1959. — С. 5-35.
- 9 Maslov V.P., Maslova T.V. Unbounded Probability Theory and Its Applications // Theory of Probability and Its Applications. — 2013. — Vol. 57, No. 3. — P. 444–467. <https://doi.org/10.1137/S0040585X97986084>.
- 10 Mahdy M. Weighted Entropy Measure: A New Measure of Information with its Properties in Reliability Theory and Stochastic Orders // Journal of Statistical Theory and Applications. — 2018. — Vol. 17, No. 4. — P. 703–718. <https://doi.org/10.2991/jsta.2018.17.4.11>.
- 11 Волков А.И. Большой химический справочник / А.И. Волков, И.М. Жарский. — Минск: Современная школа, 2005. — 608 с.
- 12 Malyshev V.P. Viscosity, fluidity and density of substances. Aspect of Chaotization / V.P. Malyshev, A.M. Makasheva, N.S. Bekturganov. — Lambert Academic Publishing (Germany), 2013. — 340 p.
- 13 Malyshev V.P. Relationship between the cluster theory of liquids and the Frenkel-Andrade viscosity model / V.P. Malyshev, A.M. Makasheva // Russian Chemical Bulletin. — 2020. — № 69. — P. 1296–1305. <https://doi.org/10.1007/s11172-020-2901-9>.

В.П. Малышев, А.М. Мақашева, Л.А. Бекбаева

Заттың қатты, сұйық және газ тәрізді күйіндегі кристалл қозғалатын, сұйық қозғалатын және бу қозғалатын ретсіз бөлшектердің арақатынасының инварианттары

Мақала авторлары Больцман бөлшектерінің хаотикалық қозғалысының кинетикалық энергиясы бойынша таралуына негізделген ретсіз бөлшектер тұжырымдамасын жасаған. Бұл бөлу заттың қатты, сұйық және газ тәрізді күйлерін кристалл қозғалатын, сұйық және бу қозғалатын деп аталатын энергия бөлшектерімен біріктіруге мүмкіндік береді. Мұндай ретсіз бөлшектердің үлестерінің қатынасы заттың белгілі бір агрегаттық күйін анықтайды. Кез келген температурада барлық комбинациялардағы осы бөлшектердің үлестерінің қосындысы бірге тең. Зерттеулер заттың хаотикалық құрамының басым негізгі әсерімен күйлерге сапалы және сандық талдау жүргізуге болатындығын көрсетті. Заттың белгілі бір түріне тәуелсіз және физика-химиялық қасиеттеріне сәйкес келетін күйлердің белгілі бір заңдылықтары табылды. Қарапайым заттар үшін хаотикалық бөлшектердің барлық үш энергетикалық класының жылжу энтропиясы есептелді. Ол заттардың қайнау температурасы аймағында максимуммен сипатталады. Бұл мүмкіндік атмосфералық қысым кезінде жер жағдайындағы ең күрделі гетерогенді процестерді жүзеге асыру үшін мүмкіндіктердің ерекше әртүрлілігін көрсеткен, нәтижесінде осы мүмкіндіктермен өздігінен ұйымдастырылатын өмірді қамтамасыз етеді.

Кілт сөздер: Больцманның таралуы, кинетикалық энергия, ретсіз бөлшектер, энтропия, нөлдік жақындау, барий, балку температурасы, қайнау температурасы.

В.П. Малышев, А.М. Мақашева, Л.А. Бекбаева

Инварианты соотношений кристаллоподвижных, жидкоподвижных и пароподвижных хаотизированных частиц в твердом, жидком и газообразном состояниях вещества

Авторами статьи разработана концепция хаотизированных частиц, основанная на распределении Больцмана по кинетической энергии хаотического движения частиц. Данное распределение позволяет объединить твердое, жидкое и газообразное состояния вещества с помощью энергетических частиц, названных кристаллоподвижными, жидкоподвижными и пароподвижными. Соотношение долей таких хаотизированных частиц определяет агрегатное состояние вещества. Сумма долей этих частиц во всех сочетаниях при любой температуре равна единице. Исследования показали, что можно проводить качественный и количественный анализ состояний с приоритетным базовым влиянием хаотизированной составляющей вещества. Были обнаружены определенные закономерности состояний, независимые от конкретного вида вещества и согласующиеся с физико-химическими свойствами. Кроме того, авторами рассчитана энтропия смешения всех трех энергетических классов хаотизированных частиц для простых веществ. Она характеризуется максимумом в области точки кипения веществ. Эта особенность свидетельствует об уникальном разнообразии возможностей для реализации сложнейших гетерогенных процессов в земных условиях при атмосферном давлении, которыми, в конечном итоге, обеспечилась самоорганизация жизни.

Ключевые слова: распределение Больцмана, кинетическая энергия, хаотизированные частицы, энтропия, нулевое приближение, барий, температура плавления, температура кипения.

References

- 1 Elansky, G.N., & Elansky, D.G. (2020). *Stroenie i svoystva metallicheskih rasplavov [The Structure and Properties of Metal Melts]*. Moscow: Yurait [in Russian].
- 2 Leontovich, M.A. (1983). *Vvedenie v termodinamiku. Statisticheskaya fizika [Introduction to Thermodynamics. Statistical Physics]*. Moscow: Vysshaya shkola [in Russian].
- 3 Malyshev, V.P., & Nurmagambetova (Makasheva), A.M. (2004). Kontseptsii khaotizirovannykh chastits kak osnova edinogo otobrazheniya tverdogo, zhidkogo i gazoobraznogo sostoiiani veshchestva [The concept of chaotic particles as the basis for a single representation of the solid, liquid and gaseous states of matter]. *Vestnik Kazakhskogo natsionalnogo universiteta — Bulletin of the KazNU*, 3(35), 53–67 [in Russian].
- 4 Soroko, E.M. (1984). *Strukturalnaya garmoniia sistem [Structural harmony of systems]*. Minsk: Nauka i tekhnika [in Russian].
- 5 Malyshev, V.P. (1994). *Veroiatnostno-determinirovannoe otobrazhenie [Probabilistic-deterministic mapping]*. Almaty: Gylym [in Russian].

- 6 Honicomb, R. (1972). *Plasticheskaia deformatsiia metallov [Plastic deformation of metals]*. Moscow: Mir [in Russian].
- 7 Malyshev, V.P., Abdrakhmanov, B.T., & Nurmagambetova, A.M. (2004). *Plavkost i plastichnost metallov [Fusibility and ductility of metals]*. Moscow: Nauchnyi mir [in Russian].
- 8 Hartley, R. (1959). *Peredacha informatsii. Teoriia informatsii i ee prilozheniia [Transfer of information. Information theory and its applications]*. Moscow: Inostrannaia literatura [in Russian].
- 9 Maslov, V.P., & Maslova, T.V. (2013). Unbounded Probability Theory and Its Applications. *Theory of Probability and Its Applications*, 57, 3, 444–467. <https://doi.org/10.1137/S0040585X97986084>.
- 10 Mahdy, M. (2018). Weighted Entropy Measure: A New Measure of Information with its Properties in Reliability Theory and Stochastic Orders. *Journal of Statistical Theory and Applications*, 17, 4, 703–718. <https://doi.org/10.2991/jsta.2018.17.4.11>.
- 11 Volkov, A.I., & Zharsky, I.M. (2005). *Bolshoi khimicheskii spravochnik [Big chemical reference book]*. Minsk: Sovremennaia shkola [in Russian].
- 12 Malyshev, V.P., Makasheva, A.M., & Bekturganov, N.S. (2013). *Viscosity, fluidity and density of substances. Aspect of Chaotization*. Lambert Academic Publishing (Germany).
- 13 Malyshev, V.P., & Makasheva, A.M. (2020). Relationship between the cluster theory of liquids and the Frenkel-Andrade viscosity model. *Russian Chemical Bulletin*, 69, 7, 1296–1305. <https://doi.org/10.1007/s11172-020-2901-9>.

Information about authors

Malyshev Vitalyi Pavlovich — Doctor of Technical Sciences, Professor, Chief Researcher, Abishev Chemical-Metallurgical Institute, Ermekov street, 63, 100009, Karaganda, Kazakhstan; e-mail: eia_hmi@mail.ru; <https://orcid.org/0000-0002-3996-1533>;

Makasheva Astra Mundukovna (corresponding author) — Doctor of Technical Sciences, Professor, Karaganda Technical University, Karaganda, Nazarbaev av., 56, 100027, Kazakhstan; e-mail: astra_mun@mail.ru; <https://orcid.org/0000-0003-2249-3435>;

Bekbayeva Lazzat Akyldaikyzy — Doctoral student, Karaganda Technical University, Karaganda, Nazarbaev av., 56, 100027, Kazakhstan; e-mail: lyazzat.bekbaeva@mail.ru; <https://orcid.org/0000-0003-2543-6380>.

INORGANIC CHEMISTRY

UDC 543.054

<https://doi.org/10.31489/2021Ch4/79-86>

A.G. Ismailova, G.Zh. Akanova*, D.Kh. Kamysbayev

Al-Farabi Kazakh National University, Almaty, Kazakhstan
(*Correspondence author's e-mail: gulsara_48@mail.ru)

Acid dissolution of neodymium magnet Nd-Fe-B in different conditions

The separation of rare-earth elements (REE) from a neodymium magnet has been widely studied last year. During the research it was identified that the waste of computer hard disk contains 25.41 % neodymium, 64.09 % iron, and <<1 % boron. To further isolate rare-earth metals, the magnet was acidically dissolved in open and closed systems. In both methods of dissolution, concentrated nitric acid was used. The difference between these methods is the conditions of dissolution of magnet. The magnet was dissolved in a microwave sample preparation system at different temperatures and pressures in a closed system. In the open system, the acid dissolution of the magnet is conducted at room temperature. 0.2 g of the neodymium magnet sample was taken under two conditions, and the dissolution process in the closed system lasted 1 hour, and in the open system 30-40 minutes. The open system is a non-laborious, simple, and cheap method of dissolving the magnet by comparing both systems. Therefore, an open sample preparation system is used for further work. To remove the iron in the magnet, oxalic acid was used and REEs are precipitated as oxalates under both conditions. According to the result of the Inductively coupled plasma mass spectrometry (ICP-MS) method, it was identified that the neodymium and iron contents in the precipitate are 24.66 % and 0.06 %, respectively. This shows that the iron has almost completely passed to the filtrate.

Keywords: acid dissolution, neodymium magnet, rare-earth metals, neodymium, praseodymium, dysprosium, open system, microwave sample preparation system, ICP-MS analysis.

Introduction

Currently, rare-earth metals are widely used in electronic devices and equipment and their production is constantly growing. For example, neodymium magnet NdFeB from computer hard disk HDD, LiH lithium hydride batteries, fluorescent lamps, etc. At this rate of growth of electronic equipment with REE, the amount of electronic waste will increase. As a result, every year a large amount of waste from REE is released into the environment. According to the United Nations Global Monitoring Organization, in 2019, the global volume of electronic wastes reached 53.6 million tons [1]. This creates serious environmental and economic problems. The separation of metals and REE from electronic wastes reduces environmental problems and helps the development of waste-free production. At the same time, it is important to effectively separate REE. The dissolution of neodymium magnets and the separation of rare-earth metals from them are considered in the following works [2-6].

In [7], the demagnetization of a neodymium magnet in the temperature range of 300-400 °C with different holding times in a muffle furnace is considered. The optimal time is 30 minutes at a temperature of 350 °C. The dissolution is carried out with organic acids, such as malic and citric. The best values of the parameters were observed at a temperature of 90 °C at a concentration of 1.0 M and a ratio of 1: 20 for both organic acids. The content of elements was determined by X-ray fluorescence analysis in the calcined and non-calcined form of magnetic powder, which is 66.69 % and 58.5 % iron, 25.19 % and 32.36 % neodymium, respectively.

In [8], rare-earth metals are deposited as oxalates. After thermal decomposition of oxalates, rare-earth metal oxides were obtained. Neodymium was separated by electrochemical method.

For the acid dissolution of the magnet, different acids and mixtures, such as nitric, hydrochloric, sulfuric, hydrogen fluoride, "Aqua regia" are used. In this work, concentrated nitric acid was applied. In concentrated HNO_3 (in small volumes), the magnet alloy was completely dissolved.

The main purpose of this work is to study and determine the optimal method for dissolving a neodymium magnet under various conditions and effectively removing iron — a macronutrient in the magnet. Acid dissolution is used to separate REE from the magnet and, also, it was conducted a comparative analysis with other works.

Experimental

Reagents

The following reagents were used for the experiment: nitric acid HNO_3 (67 %), oxalic acid (purity, 99.6 %), neodymium magnet Nd-Fe-B taken from a computer hard disk.

Apparatus

The following instruments were applied for sample preparation and analysis: ICP-MS inductively coupled plasma mass spectrometry (Agilent 7500a, USA), muffle furnace (SNOL 7,2/1300, Lithuania), analytical scales (Acculab, ALC-210.4, Germany), microwave sample preparation system (Speedwave four "Berghof", Germany), X-Ray Diffractometer (DRON -4-07, Russia).

Material preparation. Demagnetization

Neodymium magnet Nd-Fe-B from the computer hard disk is provided by the company "Taza Alemdik" LLP (Kazakhstan), which is engaged in the disposal of electronic waste. Several stages of sample preparation were carried out:

- 1) Removing the magnet from the hard disk drive (HDD);
- 2) Cleaning the nickel shell of the magnet;
- 3) Demagnetization of the sample in the muffle furnace;
- 4) Grinding the sample to a homogeneous mass.

After removing the nickel shell, the sample is ready for demagnetization. Demagnetization was carried out by heating at 750 °C in a muffle furnace (SNOL 7,2/1300, Lithuania) for 1 hour. The demagnetized sample is ground to a homogeneous mass.

Acid dissolution of a neodymium magnet in a closed system

The sample was decomposed in a closed system in an autoclave (Speedwave four "Berghof", Germany). Concentrated nitric acid (acid concentration of 15 M) is added to the sample. The decomposition process in HNO_3 must be carried out until the ending of the NO_2 release. Then the samples were placed in an autoclave at different temperatures and pressures (at 100 °C, $p = 3$ MPa, $\tau = 10$ min; 160 °C, $p = 2$ MPa, $\tau = 10$ min and cooled at 50 °C, $p = 2$ MPa, $\tau = 10$ min). After dissolution, the samples were cooled at room temperature and diluted with distilled water, and semi-quantitative analysis was performed using ICP-MS to determine the chemical composition of the sample. The total time for dissolving the magnet in the autoclave is 1 hour.

Acid dissolution of a neodymium magnet in an opened system

The 0.2 g magnet sample was dissolved in concentrated nitric acid at room temperature. When the magnet is dissolved, NO_2 is released, so the process must be carried out until the gas is released. After that, the magnet solution is diluted with distilled water (NO is released). Semi-quantitative analysis was performed using the ICP-MS method. The total time to dissolve the magnet is 30-40 minutes.

Precipitation of rare-earth metals and iron removal

In both methods, a saturated solution of oxalic acid was added to the resulting neodymium magnet solution. REE is deposited as oxalates. The precipitate was filtered through a paper filter "blue ribbon filter" and after 2 hours the filtrate was checked for the presence of Fe^{3+} , Fe^{2+} cations. Both forms of iron ions were present in the filtrate. The precipitate was then calcined in a platinum crucible at 650 °C for 40 minutes. The resulting precipitate was dissolved in concentrated nitric acid, and a pale lilac solution was obtained. The composition of the resulting solution was analyzed by inductively coupled plasma mass spectrometry. The operation parameters of the ICP-MS 7500 are as follows: the carrier gas flow rate is 0.82 L/min, the plasma gas flow rate is 0.17 L/min, the signal integration time is 0.1 s, and the high-frequency signal power is 1450 W. Figure 1 shows the scheme of dissolution in the open and closed systems and the removal of iron in a neodymium magnet sample.

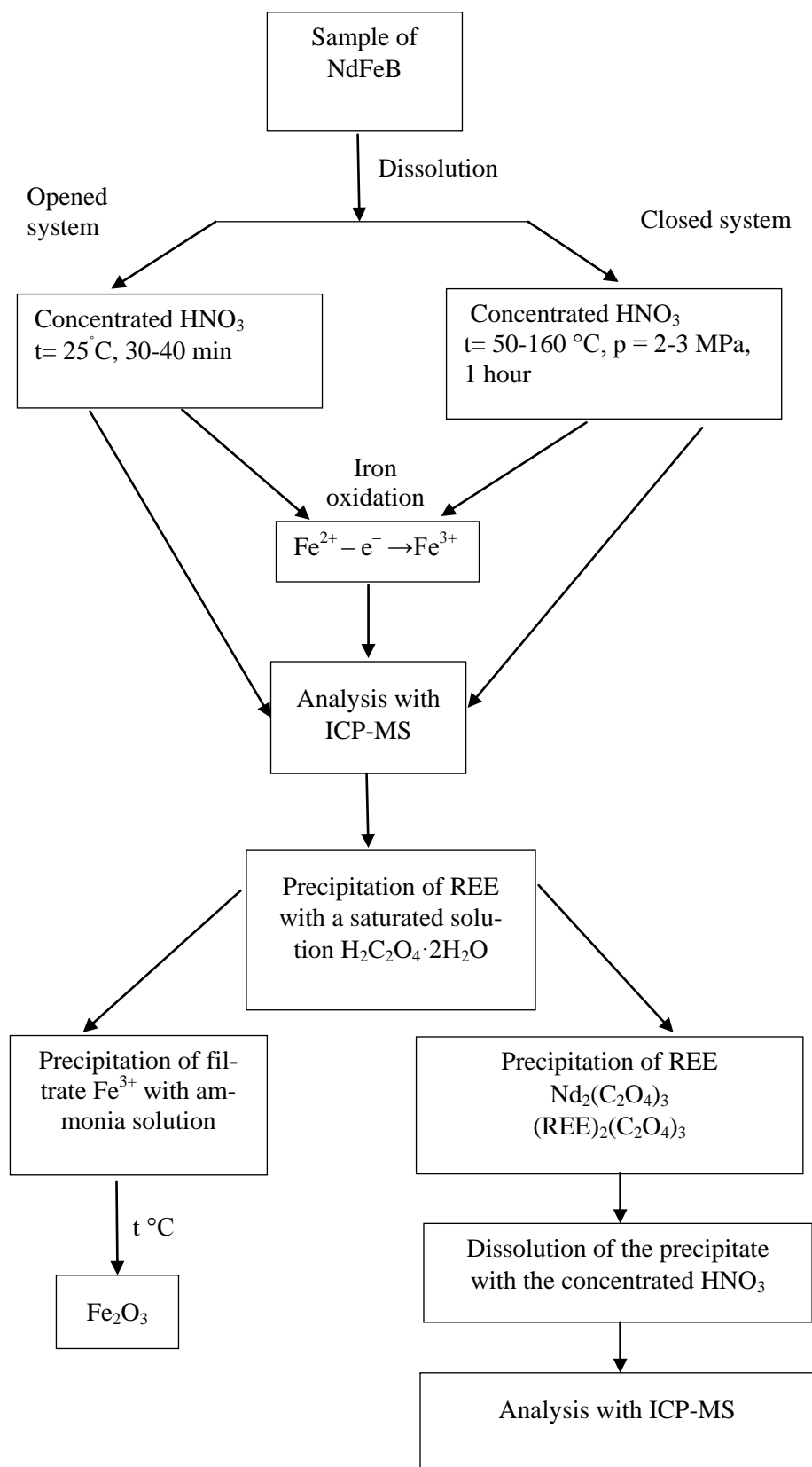


Figure 1. Scheme of acid dissolution and removal of iron in a neodymium magnet sample

Results and Discussion

In this paper, the dissolution of a neodymium magnet have been carried out in an open and closed system. The neodymium magnet was dissolved in nitric acid (Eq. (1)). Then a semi-quantitative analysis was performed using the ICP-MS method. The result showed that for further analysis is necessary to select elements with concentration values are significantly higher than those of other elements: iron, neodymium, praseodymium, dysprosium, and nickel. The concentration of boron is insignificant, but the neodymium magnet contains boron, and therefore, in the literature the formula of the neodymium magnet is written in the form of NdFeB.

Table 1

Advantages and disadvantages of open and closed dissolution systems

Open system of dissolution		Closed system of dissolution	
Advantages	Disadvantages	Advantages	Disadvantages
– simple; – safety; – not time-consuming; – non-energy-intensive; – cheap	– non-modern	– modern	– high temperature; – energy-intensive; – complex equipment; – explosive; – limited sample weight; – time-consuming; – restrictions on the choice of acid for dissolution

Table 1 describes the comparative characteristics of open and closed dissolution systems. It is illustrated that an open system is more efficient than a closed one, since they have many advantages. Therefore, an open system for dissolving a neodymium magnet was chosen for further research. A closed system has many disadvantages and limitations, such as sample weight limitations and restrictions on the use of different acids. In a closed system, an explosion can occur at high temperatures, even at low pressures. Therefore, this method is more complex than the open system.

Nevertheless, in a closed system, the neodymium magnet decomposes faster than in an open system, because in a closed system, the neodymium magnet solution is heated in an autoclave to 160 °C. This contributes to the rapid dissolution of the magnet.

In this paper, we considered a sample of a single neodymium magnet, with an average weight of 3.86 g, and 0.2 g of the sample was taken from this magnet for analysis. The magnet contains several rare-earth metals. However, the concentration of neodymium, praseodymium, and dysprosium is much higher than that of other rare-earth metals.

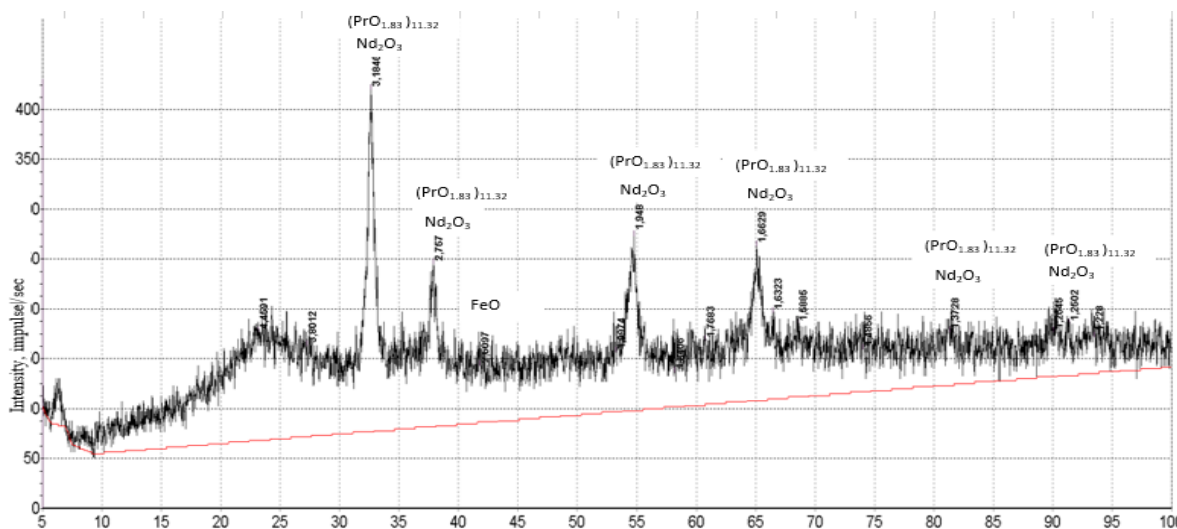


Figure 2. Composition of precipitate REE with X-Ray phase analysis

Table 2 demonstrates the comparative results of the analysis of the precipitate of REE after dissolution with nitric acid and the addition of oxalic acid (element concentrations in %). As can be seen from Table 2, the concentration of iron after acid dissolution was 2 times greater than that of neodymium. Therefore, it is necessary to remove the Fe in the sample. It is important to note the possibility of separating REE from iron ions by precipitation in the form of oxalates (Eq. (2)), and this helps to get rid of iron for further REE isolation. Iron (III) passes into solution, and Fe^{2+} in an acidic medium is oxidized to Fe^{3+} (Eq. (6)). Therefore, almost all of the iron passes into the filtrate. The composition of the precipitate is only 0.06 % Fe (Table 2). This proves that the iron was almost completely removed. Figure 2 indicates the content of REE sediment in X-Ray phase analysis. This shows the main composition of the precipitate of REE consists of neodymium oxide (praseodymium oxide together) and iron oxide in a small amount. Reflexes of neodymium and praseodymium oxides are the same.

Table 2

Results of the analysis of acid dissolution of neodymium magnet and REE precipitate

Element	Acid dissolution of magnet (opened and closed systems), HNO_3 , %	Precipitate of REE, HNO_3 , % (after removing macro- and microelements)
Nd	25.41	24.66
Pr	6.28	5.96
Dy	2.53	2.4
Fe	64.09	0.06
Ni	1.2	0
B	2.6×10^{-5}	2.6×10^{-5}
Other elements	0.5	-

It should be recalled that Table 2 illustrates the concentrations of elements after the decomposition of 0.2 g of the magnet. The analysis was conducted in an open and closed system 3 times, the table shows the average values of the concentrations of elements. The concentrations of neodymium, praseodymium, and dysprosium were almost the same in open and closed systems. After acid dissolution of the magnet, the concentration of iron was 2.5 times greater than that of neodymium. And after the addition of oxalic acid, the iron content was negligible, and nickel was also present in negligible amounts or absent. The boron content was low and the concentration was the same in both conditions. The result of the analysis with ICP-MS pointed out the concentration of REE in the precipitate which almost did not change after dissolution with nitric acid, as in the initial solution.

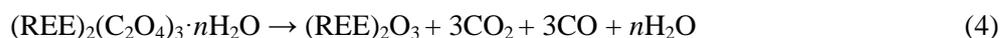
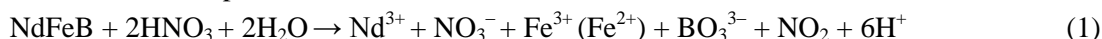
Table 3 shows the comparative composition of a neodymium magnet dissolved under different conditions in comparison with the works of other authors. According to the work [6], the content of the main elements (neodymium, iron, and boron) in the composition of magnet waste, three groups can be distinguished: waste with a low content of REE (REE < 20 %), waste with an average content of REE (REE about 20-30 %), and waste with a high content of REE (REE > 30 %). Table 3 designates the content of magnet waste with average concentrations of REE and it can be seen nitric acid and “aqua regia” are often used to dissolve the magnet.

Table 3

Comparative contents of main elements (%) of neodymium magnet NdFeB in this work and other data [6]

No	Condition of magnet dissolution	ω (Nd), %	ω (Fe), %	ω (B), %	References
1	A) Acid dissolution of neodymium magnet (in opened and closed systems) 67 % HNO_3	25.41	64.09	$\ll 1$	In this work
	B) 67 % HNO_3 , precipitation with $\text{H}_2\text{C}_2\text{O}_4 \cdot 2\text{H}_2\text{O}$	24.66	0.06	$\ll 1$	
2	Dissolution in “aqua regia” and 0.5M HNO_3	25.38	61.09	1.00	[9]
3	Dissolution in $\text{HCl}:\text{HNO}_3:\text{H}_2\text{O}$ (1:1:1) and precipitation with $\text{H}_2\text{C}_2\text{O}_4 \cdot 2\text{H}_2\text{O}/\text{Na}_2\text{S} \cdot 3\text{H}_2\text{O}$	26.1	63.5	0.73	[10]
4	Dissolution in 0.1M H_2SO_4 50 °C/“aqua regia”, and precipitation with $\text{H}_2\text{C}_2\text{O}_4 \cdot 2\text{H}_2\text{O}$	19.40	66.30	0.96	[11]
5	Dissolution in 65 % HNO_3 at 80 °C, 72 hour; and precipitated iron (II) with 35 % H_2O_2 at 40 °C	25.95	58.16	1.00	[12]

The chemical reactions of all processes are shown below:

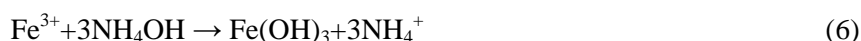


here, REE — rare-earth elements



Eq. (3) and (4) illustrate the decomposition of oxalates. The decomposition products were oxides of rare-earth metals and iron (II) oxide. In the initial solution of the magnet, iron Fe^{2+} is oxidized to Fe^{3+} (Eq. (5)). Most of the iron passes into the filtrate. The effective use of the filtrate can be described as follows.

For waste-free production, it is to use a filtrate separated from the REE precipitate. In the filtrate, iron ions Fe^{3+} are present in large quantities, so it is necessary to isolate iron in an effective way. For this purpose, an ion exchange reaction with an ammonia solution was carried out:



The resulting iron (III) hydroxide precipitate was subjected to thermal decomposition and iron (III) oxide was formed at 500 °C (Eq. (7)) (thermogravimetric analysis (TGA)).



The further task of this work is to effectively isolate rare-earth metals such as neodymium, dysprosium, and praseodymium from the matrix by extraction and sorption methods, and to consider the possibility of isolating other metals contained in significant amounts (iron, nickel, etc.).

Conclusions

The comparative acid dissolution of the NdFeB neodymium magnet alloy under open and closed conditions have been considered. To remove iron, REE was precipitated in the form of oxalates, in an acidic medium, iron (II) passed into iron (III). Therefore, iron in the composition of the REE precipitate is contained in a small amount, which contributes to the effective separation of REE from the magnet alloy. This method is simple and can be effectively used in production, in which a large amount of neodymium magnet can be dissolved, given the waste-free technology. The scheme of dissolving a neodymium magnet in an open system is very simple, not labor-intensive, and safer than in a closed system. It can be concluded that the open system of dissolution of neodymium magnet is effective in production for the separation of not only REE, but also other metals, such as iron, nickel, etc. Therefore, it is more effective to perform the dissolution in open conditions.

Acknowledgments

The authors express their gratitude to the recycling company “Taza Alemdik” LLP (Kazakhstan) for providing a neodymium magnet from electronic waste, as well as to Zlobina Elena Victorovna for ICP-MS analyses and “D.V. Sokolsky Institute of Fuel, Catalysis and Electrochemistry” JSC for X-Ray Diffractometer analyses.

References

- 1 Forti, V., Baldé, C.P., Kuehr, R., & Bel, G. (2020). The Global E-waste Monitor 2020: Quantities, Flows, and the Circular Economy Potential. *United Nations University (UNU)/United Nations Institute for Training and Research (UNITAR) — co-hosted SCYCLE Programme, International Telecommunication Union (ITU) & International Solid Waste Association (ISWA), Bonn/Geneva/Rotterdam*. 1–119. ISBN 9789280891140
- 2 Erust, C., Akcil, A., Tuncuk, A., Deveci, H., & Yazici, E.Y.A. (2021). Multi-stage Process for Recovery of Neodymium (Nd) and Dysprosium (Dy) from Spent Hard Disc Drives (HDDs). *Miner Process Extr Metall Rev.*, 42, 90–101. <http://dx.doi.org/10.1080/08827508.2019.1692010>
- 3 Abrahami, S.T., Xiao, Y., & Yang, Y. (2015). Rare-earth elements recovery from post-consumer hard-disc drives. *Trans Institutions Min Metall Sect C Miner Process Extr Metall*, 124, 106–115. <http://dx.doi.org/10.1179/1743285514Y.0000000084>
- 4 Yang, Y., Walton, A., Sheridan, R., Güth, K., Gauß, R., & Gutfleisch, O. et al. (2017). REE Recovery from End-of-Life NdFeB Permanent Magnet Scrap: A Critical Review. *J Sustain Metall*, 3, 122–149. <http://dx.doi.org/10.1007/s40831-016-0090-4>

- 5 Abbasalizadeh, A., Malfliet, A., Seetharaman, S., Sietsma, J., & Yang, Y. (2017). Electrochemical Recovery of Rare Earth Elements from Magnets: Conversion of Rare Earth Based Metals into Rare Earth Fluorides in Molten Salts. *J Sustain Metall*, 3, 627–637. <http://dx.doi.org/10.1007/s40831-017-0120-x>
- 6 Zhang, Y., Gu, F., Su, Z., Liu, S., Anderson, C., & Jiang, T. (2020). Hydrometallurgical recovery of rare earth elements from NdFeB permanent magnet scrap: A review. *Metals (Basel)*, 10, 1–34. <http://dx.doi.org/10.3390/met10060841>
- 7 Reisdörfer, G., Bertuol, D., & Hiromitsu, E. (2020). Recovery of neodymium from the magnets of hard disk drives using organic acids. *Miner Eng.*, 143, 105938. <http://dx.doi.org/10.1016/j.mineng.2019.105938>
- 8 Venkatesan, P., Vander Hoogerstraete, T., Binnemans, K., Sun, Z., Sietsma, J., & Yang, Y. (2018). Selective Extraction of Rare-Earth Elements from NdFeB Magnets by a Roomerature Electrolysis Pretreatment Step. *ACS Sustain Chem Eng.*, 6, 9375–9382. <http://dx.doi.org/10.1021/acssuschemeng.8b01707>
- 9 Gergoric, M., Ekberg, C., Foreman, S.J., Steenari, B.M., & Retegan, T. (2017). Characterization and Leaching of Neodymium Magnet Waste and Solvent Extraction of the Rare-Earth Elements Using TODGA. *J Sustain Metall*, 1, 3, 638–645. <http://dx.doi.org/10.1007/s40831-017-0122-8>
- 10 Mar, O., Aktan, E., Borra, C.R., Blanpain, B., Van Gerven, T., & Guo, M. (2017). Recycling of NdFeB magnets using nitration, calcination and water leaching for REE recovery. *Hydrometallurgy*, 167, 115–123. <http://dx.doi.org/10.1016/j.hydromet.2016.11.006>
- 11 Yamada, E., Murakami, H., Nishihama, S., & Yoshizuka, K. (2018). Separation process of dysprosium and neodymium from waste neodymium magnet. *Sep Purif Technol.*, 192, 62–68. <http://dx.doi.org/10.1016/j.seppur.2017.09.062>
- 12 Riano, S., & Binnemans, K. (2015). Extraction and separation of neodymium and dysprosium from used NdFeB magnets: an application of ionic liquids in solvent extraction towards the recycling of magnets. *Green Chem.* <http://dx.doi.org/10.1039/c5gc00230c>

А.Г. Исмаилова, Г.Ж. Аканова, Д.Х. Камысбаев

Әртүрлі жағдайда Nd-Fe-B неодимді магнитті қышқылдық еріту

Соңғы уақытта неодимді магниттен сирекжер элементтерін (СЖЭ) бөліп алу кеңінен зерттелуде. Қалдық магниттің құрамында 25,41 % неодим, 64,09 % темір және <<1 % бор бар. Сирекжер металдарын әрі қарай бөлу үшін магнитті ашық және жабық жүйеде қышқылдық еріту жүргізілді. Екі жағдайда да ерітуге концентрлі азот қышқылы қолданылды. Екі әдістің айырмашылығы магнитті еріту жағдайларында. Жабық жүйеде магнитті еріту микротолқынды үлгі дайындау жүйесінде әртүрлі температура мен қысымда жүргізілді. Ашық жүйеде магнитті қышқылдық еріту бөлме температурасында жасалды. Екі жағдайда да 0,2 г неодимді магнит үлгісі алынды және жабық жүйедегі еріту процесі 1 сағатқа, ал ашық жүйеде 30-40 минутқа созылды. Жабық жүйемен салыстырғанда ашық жүйе көп еңбекті қажет етпейтін, қарапайым және арзан әдіс болып табылады. Сондықтан, алдағы жұмыстарға ашық жүйеде үлгі дайындау қолданылады. Магниттің құрамындағы темірді жою үшін қымыздық қышқылы қолданылды және екі жағдайда да СЖЭ оксалат күйінде тұнбаға түсірілді. ICP-MS әдісінің нәтижесі бойынша, тұнбаның құрамындағы неодим мен темір сәйкесінше 24.66 % және 0,06 % болды. Бұл темірдің толықтай дерлік фильтратқа өткендігін көрсетеді.

Кілт сөздер: қышқылдық еріту, неодимді магнит, сирекжер металдары, неодим, празеодим, диспрозий, ашық жүйе, микротолқынды үлгі дайындау жүйесі, ICP-MS талдауы.

А.Г. Исмаилова, Г.Ж. Аканова, Д.Х. Камысбаев

Кислотное растворение неодимового магнита Nd-Fe-B в различных условиях

В последнее время выделение редкоземельных элементов (РЗЭ) из неодимового магнита широко исследуется. Авторами статьи показано, что отход магнита содержит 25,41 % неодима, 64,09 % железа и <<1 % бора. Для дальнейшего выделения редкоземельных металлов проведено кислотное растворение магнита в открытой и закрытой системах. В обоих способах растворения использована концентрированная азотная кислота. Разница между этими методами заключается в условиях проведения растворения магнита. В закрытой системе растворение магнита проводили в микроволновой системе пробоподготовки при разных температурах и давлениях, в открытой системе — при комнатной температуре. В обоих условиях были взяты 0,2 г образца неодимового магнита, и процесс растворения в закрытой системе длился 1 ч, а в открытой системе — 30-40 мин. По сравнению с закрытой системой, открытая система является нетрудоемким, простым и дешевым методом для растворения магнита. Поэтому для дальнейшей работы выбрана открытая система пробоподготовки. Для удаления железа в составе магнита применяли щавелевую кислоту и осаждали РЗЭ в виде оксалатов в обоих условиях. Результаты использования метода ICP-MS показали, что после осаждения содержание неодима и же-

леза составляет 24,66 и 0,06 % соответственно. Это указывает на то, что железо почти полностью перешло в фильтрат.

Ключевые слова: кислотное растворение, неодимовый магнит, редкоземельные металлы, неодим, празеодим, диспрозий, открытая система, микроволновая система пробоподготовки, ICP-MS анализ.

Information about authors

Ismailova Akmaral Gazizovna — Candidate of Chemical Sciences, Senior Lecturer, Al-Farabi Kazakh National University, Almaty, al-Farabi avenue 71, 050057, Kazakhstan, e-mail: akmaral.ismailova@kaznu.kz, <https://orcid.org/0000-0002-5555-2705>

Akanova Gulsara Zhakashovna (corresponding author) — PhD student, Department of Analytical, Colloidal Chemistry and Technology of Rare Elements, Al-Farabi Kazakh National University, Almaty, al-Farabi avenue 71, 050057, Kazakhstan, e-mail: gulsara_48@mail.ru, <https://orcid.org/0000-0003-3711-8793>

Kamysbayev Duisek Khaisagalievich — Doctor of Chemical Sciences, Professor, Al-Farabi Kazakh National University, Almaty, al-Farabi avenue 71, 050057, Kazakhstan, e-mail: d.kamysbayev@mail.ru, <https://orcid.org/0000-0002-3671-9303>

Zh.A. Baimuratova¹, M.S. Kalmakhanova^{1*}, B.K. Massalimova¹, A.A. Nurlibaeva¹,
A.S. Kulazhanova¹, J.L. Diaz de Tuesta², H.T. Gomes²

¹M.Kh. Dulati Taraz Regional University, Taraz Department of Chemistry and Chemical Engineering, Taraz, Kazakhstan;

²Centro de Investigação de Montanha (CIMO), Polytechnic Institute of Bragança, Bragança, Portugal

(*Corresponding author's e-mail: marjanseitovna@mail.ru)

Synthesis and characterization of a new magnetic composite MnFe₂O₄/clay based on a natural clay obtained from Turkestan deposit

The work is devoted to the development of a new method for the synthesis of magnetic composites based on manganese ferrite on a natural clay, coupling with their physico-chemical characterization. In the study, a natural clay of Kazakhstan obtained from the Turkestan deposit was used for the preparation of magnetic composites. The formation of materials with magnetic properties is an urgent task of our time, due to the needs of various applications of magnetically controlled materials for biomedical systems, electronic devices, catalytic and adsorption processes. The advantage of such materials is the ability to control them using a magnetic field for shaking, recovery, induction heating, among others. In this work, samples were prepared by co-precipitation of manganese and iron salts with 5 mol L⁻¹ NaOH over the Turkestan clay (TC). Materials were characterized by various analyses, such as Fourier-Transform infrared spectroscopy (FTIR), X-ray diffractometric analysis (XRD), and elemental analysis. According to the results of physical and chemical studies of the XRD and thermal analysis, kaolinite is the main mineral in the composition of TC. Magnetic adsorbents MnFe₂O₄/clay with perfect magnetic separation characteristics were successfully obtained by chemical co-precipitation.

Keywords: natural clays, magnetic material, manganese ferrite, adsorbent, modified composite, metal ions, chemical co-deposition, adsorption.

Introduction

Natural clays are inexpensive and readily available materials that work as excellent cation exchangers. The adsorption capacity of clays is due to the relatively high surface area and the net negative charge in their structure, which attracts and holds cations such as heavy metals [1–4]. Natural clays can also be modified to produce materials with enhanced properties, such as metallic pillared clays with improved textural characteristics [5]. Main applications include the action as catalytic materials (taking advantage of the catalytic properties of the incorporated metals) in advanced oxidation processes, such as catalytic wet peroxide oxidation, as well as for removing organic pollutants from contaminated waters [6–8]. The application of metallic particles with magnetic characteristics dispersed on the surface of clays is interesting for the development of magnetic materials that can be magnetically controlled for diverse applications, such as biomedical systems, electronic devices, catalytic and adsorption processes. Magnetic materials can be separated from the medium by a simple magnetic process in catalytic and adsorption processes. Therefore, there is a growing interest in low-cost materials with a high surface area, such as clays, due to their unique applications, including adsorption and catalysis [9].

There are several methods for the preparation such magnetic materials, as magnetite (Fe₃O₄) nanoparticles [10]. These are impregnation, sol-gel, solution combustion synthesis and co-precipitation. Among these methods, chemical co-precipitation is the most promising since it is simple and does not require special chemicals and procedures [11–13].

In this paper, we propose to study a sample of clay from the Turkestan fields. The clays were modified and the physical and chemical characteristics of the natural and modified clay were studied.

Experimental

Materials and reagents

The clays studied were obtained from the Turkestan deposit in Kazakhstan. Sodium hydroxide (NaOH, purity ≥0.97), iron(III) sulfate nonahydrate (Fe₂(SO₄)₃·9H₂O, purity ≥ 0.98), manganese chloride tetrahydrate (MnCl₂·4H₂O, purity ≥ 0.99), nickel sulfate heptahydrate (NiSO₄·7H₂O, purity ≥ 0.99) were used. Initial

solutions (50 mg L⁻¹) containing Ni(II) ions were obtained by dissolving pre-determined amounts of nickel sulfate heptahydrate in distilled water. It is worth noting that all the chemicals in this study were used without further purification.

Magnetic materials synthesis

Natural Turkestan clay (TC) was ground into powder in a mill and sorted through a sieve № 0.063, followed by storage in anti-wet bottles at room temperature. To prepare the magnetic composite MnFe₂O₄/TC, an aqueous solution containing manganese(II) chloride and iron (III) sulphate in a molar ratio of 1:2 was prepared. Then, 5 g of the sieved TC were added to the Mn(II)-Fe(III) solution, followed by mixing. Afterwards, the co-precipitation of Mn(II)-Fe(III) was conducted by the addition of NaOH solution (5 mol L⁻¹) until pH 10 was obtained. The resulting solution was stirred for 30 min on a magnetic stirrer at room temperature. Then, the suspension was heated to 95-100 °C. After cooling, the prepared magnetic composite was repeatedly washed with distilled water at 50 °C for 2 h. Using a simple magnetic procedure, the resulting materials were separated from the water and dried in an oven at 105 °C for 2 h, to be completely dehydrated and ready for use [14].

Characterization

To characterize the materials, various analyses were conducted. FTIR spectra of the natural and magnetic modified clay were obtained with a FTIR instrument (Infraspec, Model FSM 2202, Russia, St-Petersburg) with a resolution of 1 cm⁻¹ and a scan range of 5000 to 500 cm⁻¹ using a sample based on 1 % of clay with KBr. X-ray diffractometric analysis was carried out on an automated DRON-3 diffractometer with Cu_{Kα}-radiation, and a β-filter. Conditions for shooting diffractograms: U = 35 kV; I = 20 mA; shooting θ-2θ; detector 2 deg/min. The results of the elemental composition of natural clays were obtained by using EMP analysis.

Semi-quantitative X-ray diffractometric analysis was performed applying diffractograms of powder samples by the method of equal attachments and artificial mixtures. The quantitative ratios of the crystal phases have been determined. Interpretation of the diffractograms was carried out using data from the International Centre for Diffraction Data (ICDD) card file; these were the PDF2 Powder diffraction database (Powder Diffraction File) and diffractograms of minerals free of impurities. Shooting conditions: DRON diffractometer — 3.0; accelerating voltage — 35 kV; anode current — 20mA.

Results and Discussion

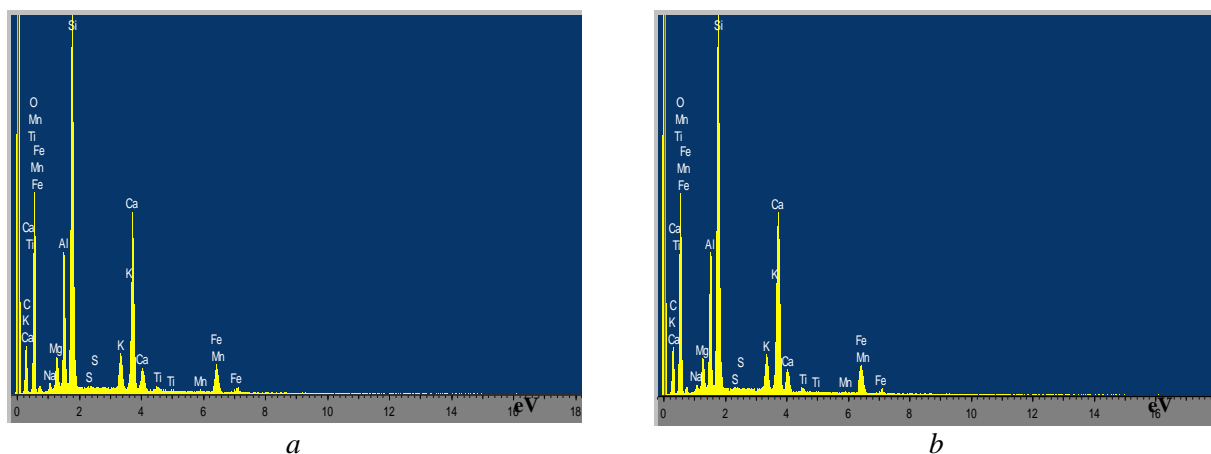
The results of the elemental composition of natural and modified clay were obtained using an electron microprobe (EMP) of the brand Superprobe 733 from JEOL coupled to a spectrometer Inca Energy from Oxford instruments (Figure 1). Table 1 shows the contents of elements in the natural and modified clay. As can be observed, the clay obtained in Turkestan has mainly aluminium (7.12 %), calcium (10.69 %), and silicium (18.97 %) metals (Table 1). Comparing this natural clay with others reported in the literature [15, 16], it is highlighted as positive features the high contents on iron, paramount for catalytic purposes, and on calcium, which allows the preparation of catalytic advanced materials such as pillared clays. The modified clay by co-precipitation also presents high concentration of those metals: aluminium (3.94 %), calcium (7.35 %), and silicium (10.40 %). However, the concentration of all of them decreased after the modification of TC by co-precipitation, whereas the content in iron and manganese strongly increased when compared to the concentration of TC, as expected. Specifically, the composition of the modified clay is rich in iron (22.37 %). In the natural TC, the quantity of Mn is 0.14 %, whereas in MnFe₂O₄/TC is 9.23 %. The results also show that the content of Fe increases in MnFe₂O₄/TC in comparison with the natural clay.

The magnetic characteristics of the developed material were confirmed using a magnet. Figure 2 is demonstrates an illustrative photo where the magnetic characteristics of MnFe₂O₄/TC are placed in evidence upon reaction to a magnetic field.

Table 1

Elemental composition

Materials	Weight of the element (%)										
	O	Na	Mg	Al	Si	S	K	Ca	Ti	Mn	Fe
TC	53.40	0.51	2.20	7.12	18.97	0.06	2.41	10.69	0.31	0.14	4.18
MnFe ₂ O ₄ /TC	43.55	0.32	1.24	3.94	10.40	0.17	1.26	7.35	0.19	9.23	22.37



a — natural TC; *b* — $\text{MnFe}_2\text{O}_4/\text{TC}$

Figure 1. Elemental analysis



Figure 2. The magnetic characteristics of $\text{MnFe}_2\text{O}_4/\text{TC}$ placed in evidence upon reaction to a magnetic field

To determine the quantitative ratio of the crystalline phases of the clay, the samples were submitted to X-ray diffractometric analysis. Possible impurities, the identification of which cannot be unambiguous due to the small contents and the presence of only 1-2 diffraction reflexes, the lack of chemical composition data, or poor crystallization, are indicated in Table 2.

Diffractograms of the sample of natural clay and $\text{MnFe}_2\text{O}_4/\text{TC}$ were carried out on an automated diffractometer DRON-3, β -filter. Terms and Conditions caring.com not responsible for diffractograms: $U = 35 \text{ kV}$; $I = 20 \text{ mA}$; shooting θ -2 θ ; detector 2 degree/minutes (Fig. 3).

The result of the analysis established that the sample of the studied Turkestan clay belongs to the group of layered silicates-kaolinite $\text{Al}_2(\text{Si}_2\text{O}_5)(\text{OH})_4$, with a low amount of chlorite $(\text{Mg}, \text{Fe})_5\text{Al}(\text{Si}_3\text{Al})\text{O}_{10}(\text{OH})_8$, admixtures of muscovite $\text{KAl}_2(\text{AlSi}_3\text{O}_{10})(\text{OH})_2$ and albite $\text{Na}(\text{AlSi}_3\text{O}_8)$.

In the modified $\text{MnFe}_2\text{O}_4/\text{TC}$ sample, the concentration of minerals increases, but the calcite concentration decreased from 29.9 to 21.4. It is worth noting that the modified vehicle does not contain the mineral kaolinite $\text{Al}_2(\text{Si}_2\text{O}_5)(\text{OH})_4$, however, the analysis showed the presence of the mineral dolomite $\text{CaMg}(\text{CO}_3)_2$ (Table 2). The characteristic peaks of MnFe_2O_4 were also identified, confirming the magnetic characteristics of the developed materials.

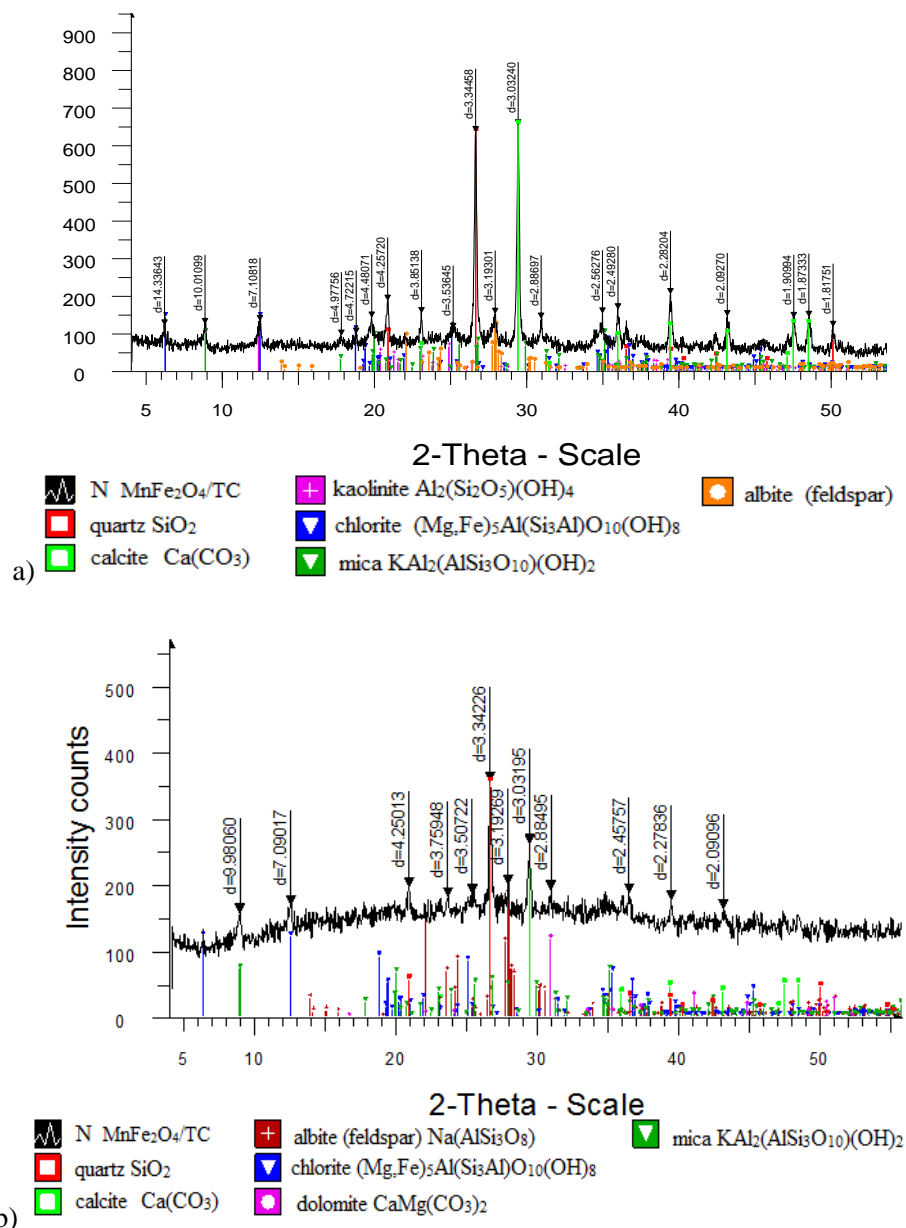


Figure 3. (a) Diffraction pattern of the TC and, (b) Diffraction pattern of MnFe₂O₄/TC

Table 2

Results of semi-quantitative X-ray diffractometric analysis of TC and MnFe₂O₄/TC

Mineral	Formula	Concentration, %	
		TC	MnFe ₂ O ₄ /TC
Calcite	Ca(CO ₃)	29.9	21.4
Quartz	SiO ₂	29.9	35.9
Kaolinite	Al ₂ (Si ₂ O ₅)(OH) ₄	23.7	
Dolomite	CaMg(CO ₃) ₂		9.5
Chlorite	(Mg, Fe) ₅ Al(Si ₃ Al)O ₁₀ (OH) ₈	8.2	12.3
Mica	KAl ₂ (AlSi ₃ O ₁₀)(OH) ₂	5.7	7.3
Feldspars (albite)	Na(AlSi ₃ O ₈)	3.4	13.6

The natural clay of the Turkestan deposit was studied by FTIR spectroscopy. Changes in the absorption bands on the spectra of these clays after modification of Mn(II) and Fe(III) were analyzed (Figure 4). The FTIR spectra of all compounds were recorded in solid form in KBr tablets.

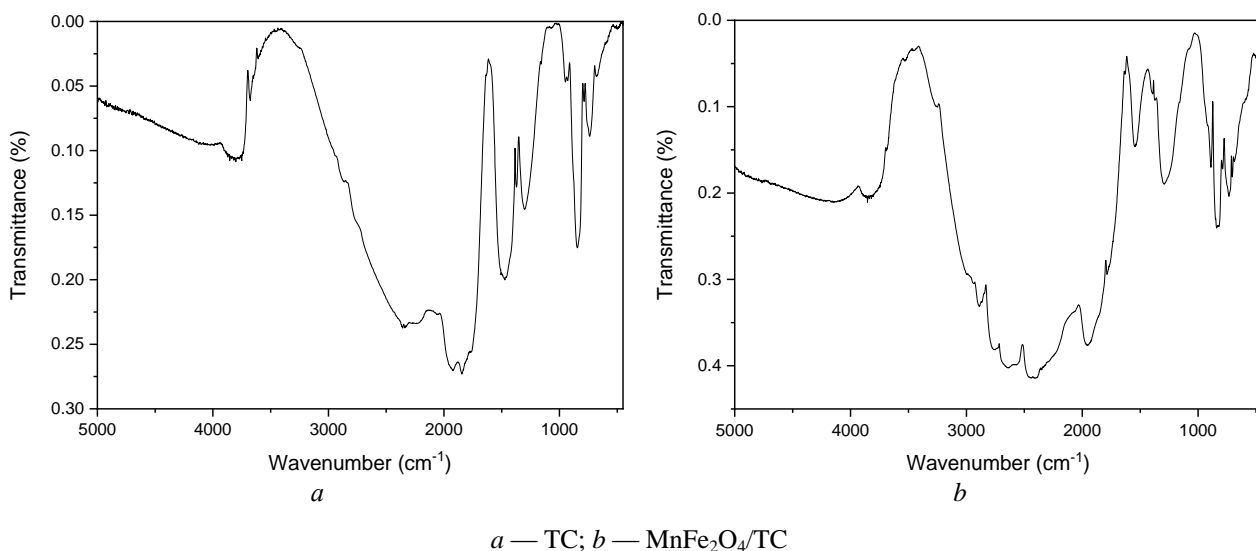


Figure 4. FTIR spectra

The analysis of the above FTIR spectrum illustrates that the main bands in natural clay relate to the valence bonds of silicon with oxygen and hydrogen with oxygen. The absorption band at *ca.* 1613 and 3637 cm^{-1} corresponding to the deformation vibrations of OH⁻ groups at the vertices of silicon-oxygen tetrahedra, is a distinctive feature of kaolinites (Fig. 4).

Having characterized the absorption bands on the FTIR spectrum of a sample of clay from the Turkestan deposit, it is possible to implement a similar assignment of the absorption bands on the spectrum of natural clay. The absorption bands at 1433, 2029, and 2517 cm^{-1} allow the identification of calcite (CaCO_3) in the clay, which is confirmed by X-ray diffractometric analysis. The FTIR spectrum of albite contains an intense band in the frequency range of 1757–1036 cm^{-1} with a maximum in the region of 1433 cm^{-1} (Fig. 4a).

Muscovite mica is an aqueous $\text{KAl}_2(\text{AlSi}_3\text{O}_{10})(\text{OH})_2$. The absorption bands of the SiOSi, SiOAl, Al(OH), and H(OH) groups are usually observed in their spectra. In the clay samples, absorption bands of 457, 794, 1035, and 3695 cm^{-1} are observed, which according to the database corresponds to the mineral muscovite (Fig. 4).

Oxygen atoms can be bound to two silicon atoms by Si–O–Si bridging bonds, or to one by Si–O non-bridging bonds. In particular, the bands 1022 and 1009 cm^{-1} are attributed to the valence vibrations of Si–O–Si(Al) bridging bonds in the crystal lattice. When silicon is partially replaced in the lattice, most of the valence bands of layered minerals (1000–900 cm^{-1}) move in the direction of low frequencies. The appearance of absorption bands in the region of 1000–900 cm^{-1} can be associated with valence vibrations of non-bridge Si–O bonds in various silicate and aluminosilicate groups, as well as in simple ortho- and diorthosilicate anions in the amorphous phase. Aluminum is found in aluminosilicates in either tetrahedral coordination or octahedral coordination. The very weak bands at 794 and 547 cm^{-1} in the samples can be explained by Si–O–Si (Al) bonds in distorted tetrahedral and octahedral layers. In particular, the band in the region of 547 cm^{-1} refers to the Si–O–Si strain vibrations involving bridged oxygen, and the band of 794 cm^{-1} refers to the Si–O–Si valence symmetric vibrations characteristic of silicon in the SiO_4 tetrahedron.

Figure 4b shows the FTIR spectrum of the modified MnFe_2O_4 /Turkestan sample. Two strong absorption peaks of 1442 cm^{-1} in the sample indicate the presence of ferrites. The stretching between 400 and 700 cm^{-1} is an oscillation (Fe–O) that indicates the formation of the spinel ferrite structure. In ferrites, metal ions occupy two different interstitial sites in the lattice. One is in a tetrahedral location, and the other is in an octahedral location. From the FTIR spectra, it was found that the high-frequency bands at 875 cm^{-1} are associated with the tetrahedral region, while the low-frequency bands at 629 cm^{-1} are associated with the octahedral region. The sharpness of these bands correlates with the high degree of crystallinity of MnFe_2O_4 structures. The wide band of vibrations at 3449 and 3421 cm^{-1} is associated with the stretching vibrations of O–H adsorbed water molecules, indicating a higher amount of surface OH [17].

The absorption bands in the modified clay at 547 and 457 cm^{-1} become more diffuse with a slight change in the position in the spectrum. The 457 cm^{-1} band indicates the presence of Fe–O oscillations, the absence of a band at 621 cm^{-1} (characteristic of the $\gamma\text{-Fe}_2\text{O}_3$ phase), and, at the same time, the appearance of a band at 520 cm^{-1} may indicate a phase transformation of $\gamma\text{-Fe}_2\text{O}_3 \rightarrow \alpha\text{-Fe}_2\text{O}_3$ [18].

Conclusions

A method for synthesizing clay composites based on a natural clay of Turkestan (TC) with manganese ferrite has been developed and physico-chemical properties determined. Magnetic adsorbents $\text{MnFe}_2\text{O}_4/\text{TC}$ with perfect magnetic separation characteristics were successfully obtained by chemical co-deposition. The clay of the Turkestan deposit in Southern Kazakhstan was studied by physico-chemical methods of analysis: the elemental composition of natural clay and the chemical composition of the modified $\text{MnFe}_2\text{O}_4/\text{TC}$ composite and the quantitative ratios of the crystal phases were determined. The study of the FTIR spectra of natural and modified clay deposits of Turkestan allowed us to establish their distinctive features, which consist in the imperfection of their crystal structures. It is expected that the resulting magnetic composite $\text{MnFe}_2\text{O}_4/\text{TC}$ can be used as potential catalysts and adsorbents for diverse applications.

References

- 1 Manjot, K.T. (2010). Enhancing adsorption capacity of Bentonite for dye removal: Physicochemical modification and Characterization. *M. Eng Thesis*, The University of Adelaide, 77–120.
- 2 Reimbaeva, S.M., Massalimova, B.K., & Kalmakhanova, M.S. (2020). New pillared clays prepared from different deposits of Kazakhstan. *Materials Today: Proceedings*, 31(3), 607–610. <https://doi.org/10.1016/j.matpr.2020.07.532>
- 3 Khenifi A., Bouberka, Z., Sekrane, F., Kameche, M., & Derriche, Z. (2007). Adsorption study of an industrial dye by an organic clay. *Adsorption*, 13(2), 149–158. <https://doi.org/10.1007/s10450-007-9016-6>
- 4 Oliveira, L., Rios, R., Fabris, J., Sapag, K., Krgarg, V., & Lago, R. (2003). Clay-iron oxide magnetic composites for the adsorption of contaminants in water. *Appl. Clay Sci.*, 22(4), 169–177. [https://doi.org/10.1016/S0169-1317\(02\)00156-4](https://doi.org/10.1016/S0169-1317(02)00156-4)
- 5 Kalmakhanova, M.S., Massalimova, B.K., Diaz de Tuesta, J.L., Kantarbaeva, S.M., & Kulbaeva, D.A. (2018). Catalytic wet peroxide oxidation of 4-nitrophenol with new pillared clays prepared from the natural material extracted in deposits of Kazakhstan, *Bulletin of Karaganda University. Chemistry series*, 4(92), 48–55.
- 6 Kalmakhanova M.S., Diaz de Tuesta J.L., Massalimova B.K., & Gomes H.T. (2020). Pillared clays from natural resources as catalysts for catalytic wet peroxide oxidation: Characterization and Kinetic Insights, *Environmental Engineering Research*, 25, 186–196.
- 7 Reimbaeva, S.M., Massalimova, B.K., & Kalmakhanova, M.S. (2020). New pillared clays prepared from different deposits of Kazakhstan, *Materials Today: Proceedings*, 31, 607–610.
- 8 Silva, A.S., Kalmakhanova, M.S., Massalimova, B.K., Diaz de Tuesta, J.L., & Gomes, H.T. (2019). Wet peroxide oxidation of paracetamol using acid activated and Fe/Co-pillared clay catalysts prepared from natural clays, *Catalysts*, 9(9), 705.
- 9 Wu R., & Qu, J. (2005). Removal of water-soluble azo dye by the magnetic material MnFe_2O_4 . *J. Chem. Technol. Biotechnol.*, 80, 20–27. <https://doi.org/10.1002/jctb.1142>
- 10 Korolkov, I.V., Ludzik, K., Lisovskaya, L.I., Zibert, A.V., Yeszhanov, A.B., & Zdorovets, M.V. (2021). Modification of magnetic Fe_3O_4 nanoparticles for targeted delivery of payloads. *Bulletin of the University of Karaganda — Chemistry*, 101(1), 99–108 <https://doi.org/10.31489/2021Ch1/99-108>
- 11 Wu, R. (2004). Removal of azo-dye acid red B (ARB) by adsorption and catalytic combustion using magnetic CuFe_2O_4 powder, *Appl. Catal. B: Environ*, 48(1), 49–56. <https://doi.org/10.1016/j.apcatb.2003.09.006>
- 12 Fu, W., Yang, H., Li, M., Li, Minghui, Yang, N., & Zou, G. (2005). Anatase TiO_2 nanolayer coating on cobalt ferrite nanoparticles for magnetic photo catalyst. *Mat. Lett.*, 59(27), 3530–3534. <https://doi.org/10.1016/j.matlet.2005.06.071>
- 13 Zhang, G., Qu, J., Liu, H., Cooper, A., & Wu, R. (2007). CuFe_2O_4 /activated carbon composite: A novel magnetic adsorbent for the removal of acid orange II and catalytic regeneration. *Chemosphere*, 68(6), 1058–1066. DOI: 10.1016/j.chemosphere.2007.01.081
- 14 Podder M., & Majumder C. (2019). Bacteria immobilization on neem leaves/ MnFe_2O_4 composite surface for removal of as (III) and as (V) from wastewater. *Arab J. Chem.*, 12(8), 3263–3288. <https://doi.org/10.1016/j.arabjc.2015.08.025>
- 15 Kalmakhanova, M.S., Massalimova, B.K., Diaz de Tuesta, J.L., Gomes, H.T., & Nurlibaeva, A. (2018). Novelty pillared clays for the removal of 4-nitrophenol by catalytic wet peroxide oxidation, *News of the National Academy of Sciences of the Republic of Kazakhstan, Series of Geology and Technical Sciences*, 3(429), 12–19.
- 16 Kalmakhanova, M.S., Diaz de Tuesta, J.L., Massalimova, B.K., Nurlibaeva, A.N., Darmenbaeva, A.S., & Kulbaeva, D.A. (2020). Catalytic wet peroxide oxidation process with new Fe/Cu/Zr-pillared clays developed from natural clay deposits of Kazakhstan, *News of the National Academy of sciences of the Republic of Kazakhstan. Series chemistry and technology*, 3, 441, 15–21.
- 17 Jacintha, A.M., Umopathy, V., Neeraja, P., & Rajkumar, S. (2017). Synthesis and comparative studies of MnFe_2O_4 nanoparticles with different natural polymers by sol-gel method: structural, morphological, optical, magnetic, catalytic and biological activities. *Journal of Nanostructure in Chem.*, 7, 375–387. <https://doi.org/10.1007/s40097-017-0248-z>
- 18 Chetverikova, A.G., Kanygina, O.N., Alpsybaeva, G. Zh., Yudin, A.A., & Sokabaeva, S.S. (2019). Infrared spectroscopy as the method for determining structural responses of natural clays to microwave exposure. *Kondensirovannye Sredy I Mezhfaznye Granitsy = Condensed Matter and Interphases*, 21(3), 446–454. <https://doi.org/10.17308/kcmf.2019.21/1155>

Ж.А. Баймуратова, М.С. Калмаханова, Б.К. Масалимова,
А.А. Нурлыбаева, А.С. Кулажанова, Х.Л. Диаз де Туеста, Х.Т. Гомес

Түркістан кен орнынан алынған табиғи сазбалшық негізінде жаңа $MnFe_2O_4$ /сазбалшық магниттік композиттің синтезі және сипаттамасы

Мақала магниттік композиттердің физика-химиялық сипаттамасымен байланысқан табиғи сазбалшықты марганец ферриті негізінде магниттік композиттерді синтездеудің жаңа әдісін жасауға арналған. Зерттеуде магниттік композиттер алу үшін Түркістан кен орнынан алынған Қазақстанның табиғи сазбалшығы пайдаланылды. Магниттік қасиеттері бар материалдарды қалыптастыру биомедициналық жүйелер, электронды құрылғылар, каталитикалық және адсорбциялық процестер үшін магнитті басқарылатын материалдарды әртүрлі қолдану қажеттіліктеріне байланысты біздің заманымыздың өзекті мәселесі. Мұндай материалдардың артықшылығы оларды араластыру, қалпына келтіру, индукциялық қыздыру және т.б. үшін магнит өрісінің көмегімен басқару мүмкіндігі болып табылады. Үлгілер 5 моль/л⁻¹ NaOH марганец пен темір тұздарын Түркістан сазбалшығының (ТС) негізінде тұндыру арқылы алынды. Материалдар Фурье-инфрақызыл спектроскопия (FTIR-спектроскопия), рентгендік дифрактометриялық талдау (XRD) және элементтік талдау сияқты әртүрлі талдау әдістерімен сипатталды. РДТ физика-химиялық зерттеулерінің және термиялық талдаудың нәтижелері бойынша ТС құрамындағы негізгі минерал каолинит болып табылады. Магниттік қасиеттері бар $MnFe_2O_4$ /Түркістан магниттік адсорбенттері химиялық тұндыру әдісі бойынша сәтті алынды.

Кілт сөздер: табиғи саздар, магниттік материал, марганец ферриті, адсорбент, модифицирленген композит, металл иондары, химиялық қосылыстар, адсорбция.

Ж.А. Баймуратова, М.С. Калмаханова, Б.К. Масалимова,
А.А. Нурлыбаева, А.С. Кулажанова, Х.Л. Диаз де Туеста, Х.Т. Гомес

Синтез и характеристика нового магнитного композита $MnFe_2O_4$ /глина на основе природных глин, полученных из Туркестанского месторождения

Статья посвящена разработке нового метода синтеза магнитных композитов на основе феррита марганца на природной глине с учетом их физико-химической характеристики. В исследовании для получения магнитных композитов использовалась природная глина Казахстана, полученная из Туркестанского месторождения. Формирование материалов с магнитными свойствами является актуальной задачей нашего времени, в связи с потребностями различных применений магнитоуправляемых материалов для биомедицинских систем, электронных устройств, каталитических и адсорбционных процессов. Преимуществом таких материалов является возможность управления ими с помощью магнитного поля для встряхивания, восстановления, индукционного нагрева и др. Образцы были получены авторами путем совместного осаждения солей марганца и железа с 5 моль/л⁻¹ NaOH с туркестанской глиной (ТГ). Материалы характеризовались различными методами анализа, такими как Фурье-инфракрасная спектроскопия, рентгеновский дифрактометрический анализ и элементный анализ. По результатам физико-химических исследований РДА и термического анализа основным минералом в составе ТГ является каолинит. Магнитные адсорбенты $MnFe_2O_4$ /Туркестан с совершенными характеристиками магнитной сепарации были успешно получены химическим соосаждением.

Ключевые слова: природные глины, магнитный материал, феррит марганца, адсорбент, модифицированный композит, ионы металлов, химическое соосаждение, адсорбция.

Information about authors

Baimuratova Zhaina Abilkhasimovna — 1st-year PhD student, Department “Chemistry and chemical technology”, Taraz Regional University named after M.Kh. Dulaty, Tole bi 61, Taraz, Kazakhstan. jaina.baimuratova@mail.ru, <https://orcid.org/0000-0003-2185-3697>

Kalmakhanova Marzhan Seitovna (*corresponding author*) — PhD, Taraz Regional University named after M.Kh. Dulaty, Tole bi 61, Taraz, Kazakhstan. marjanseitovna@mail.ru, <https://orcid.org/0000-0002-8635-463X>

Massalimova Bakytgul Kabykenovna — Candidate of chemical science, Head of “Chemistry and chemical technology” department of Taraz Regional University named after M.Kh. Dulaty, Tole bi 61, Taraz, Kazakhstan; massalimova15@mail.ru, <https://orcid.org/0000-0003-0135-9712>

Nurlybaeva Aisha Nurlybayevna — PhD, Taraz Regional University named after M.Kh. Dulaty, Tole bi 61, Taraz, Kazakhstan. rustem_ergali@mail.ru, <https://orcid.org/0000-0001-9904-9979>

Kulazhanova Aisulu Sadibayevna — Master of chemistry, Taraz Regional University named after M.Kh. Dulaty, Tole bi 61, Taraz, Kazakhstan. ausulu06@mail.ru, <https://orcid.org/0000-0002-8837-0529>

Jose Luis Díaz de Tuesta Triviño — PhD, Post-doctoral Researcher at Polytechnic Institute of Bragança, Bragança, Portugal. jl.diazdetuesta@ipb.pt, <https://orcid.org/0000-0003-2408-087X>

Hélder Teixeira Gomes — Adjunct professor at the Department of Chemical and Biological Technology, Polytechnic Institute of Bragança, Bragança, Portugal. htgomes@ipb.pt, <https://orcid.org/0000-0001-6898-2408>

CHEMICAL TECHNOLOGY

UDC 544.6.076.328.99

<https://doi.org/10.31489/2021Ch4/95-103>

S. Abdimomyn¹, D. Abduakhytova¹, A. Atchabarova^{1*}, G.L. Turdean²,
R. Tokpayev¹, K. Kishibayev¹, A. Kurbatov¹, M. Nauryzbayev¹

¹Center of Physical Chemical Methods of Research and Analysis, Al-Farabi Kazakh National University, Almaty, Kazakhstan;

²Babeş-Bolyai University, Faculty of Chemistry and Chemical Engineering, Cluj-Napoca, Romania

(*Corresponding author's e-mail: azhar.atchabarova@mail.ru)

Optimization of the preparation method of a mechanically strong carbon electrode

Nowadays, a strategy for the utilization of secondary resources to obtain valuable components is actual. It will lead to the most rational use of natural resources and environmental protection. Electrochemical methods are perfectly applicable to solve this problem. Electrochemical methods allow concentrating of the target components without preliminary preparation of the raw material. Carbon materials (CM) based on plant and carbon-mineral raw materials are an excellent option as a matrix for obtaining the electrodes, due to their availability, low cost, high specific surface area, and the presence of different functional groups. The lack of theoretical substantiation of the adsorption phenomena on carbon electrodes served as an incentive for the study and development of a method for obtaining a mechanically strong electrode based on modified carbon and polyethylene. The design and mechanical strength of carbon electrodes (CE) are of great importance for the efficiency of purification and extraction of valuable components. In this article, we obtained carbon material from walnut shells by hydrothermal carbonization with further steam-gas activation (the specific surface area is 754.0 m²/g). The structural, physicochemical characteristics of the carbon material, binder, and carrier material were studied by the following methods: scanning electron microscope (SEM), Brunauer–Emmett–Teller (BET), thermogravimetric analysis and differential scanning calorimetry (TGA-DSC). The method of hot-pressing is applied for obtaining the carbon electrodes. Using the method of full-factor experiment and steepest ascent, the values of pressure and temperature during pressing and the ratio of carbon material: binder was optimized: P = 226 atm; T = 90.8 °C; carbon material: binder ratio = 67.5:32.5 %, respectively.

Keywords: carbon electrode, full-factor experiment, adsorption, hydrothermal carbonization, carbon material, thermal carbonization, walnut shell, hot-pressing method.

Introduction

Today, there is a huge trend of environmental and natural resources pollution. Therefore, the transition to recycling strategy of secondary resources is substantial (desalination concentrates, microelectronic scrap, spent oil shale, and industrial wastewater). Rare earth metals such as Pt, V, W, Ge, Mo, Se, Sn, Hf, Nb, La, Ce, etc. are the first economic incentive for mastering separation and concentration methods [1]. The second incentive is the industrial wastewaters of the chemical, metallurgical, and pharmaceutical industries and as a consequence of this, the purification of water resources from the toxic metals (Cu, Zn, Cd, Co, Ni, Pb, Hg, As and Cr), surfactants, dyes, organic pollutants, etc. All of these are key economic and environmental problems not only in Kazakhstan but throughout the world.

Hydrometallurgy is a preferred technology for selective extraction and concentration of elements from both low-concentration and wastewater [2]. There are many hydrometallurgical methods that include different effective approaches for separation: selective precipitation, cementation, adsorption, ion flotation, resin-based sorption, liquid extraction, extraction chromatography, biosorption, and electrochemical methods [3–5]. Despite the variety of methods, there are many problems concerning the necessity of high separation and concentration, safety, low energy consumption, economy, negative environmental impact. All of these

reduce the probability of commercialization [6, 7]. In particular, the disadvantages for liquid extraction are non-regenerable acids, alkalis, organic solvents, etc; for ion exchange are interfering ligands and metal ions, expenses to the regeneration of ion exchange resins [8]; for biosorption are storage, control of the microorganisms living conditions [9]; for froth flotation are lower selectivity, high cost of flotation reagents and collectors, a large number of tailings [10], etc.

Recently, electrochemical methods have made progress and found wide application in industrial facilities, despite the high energy consumption, low conductivity, and mechanical strength of electrodes, occur side reactions on the electrodes surface, and membrane pollution. For example, electrochemical methods are used in the immobilization of target components on the surface of a solid electrode or in bulk, electrosorption, intercalation, electrodeposition [11]. In comparison with other hydrometallurgical methods, electrochemical methods have the following advantages [12]:

- 1) reversibility of the process by changing the polarity of the electrode, significantly reducing the consumption of reagents, water, and materials;
- 2) excluding the secondary waste formation with heavy metals or organic pollutants;
- 3) adsorption under the influence of current or voltage provides better adsorption capacity, selectivity, and kinetic control, expanding the ability to work in wide pH ranges using materials of simple composition;
- 4) simplicity and flexibility of using modular structures and combination with any methods of hydrometallurgy in order to increase selectivity and recovery efficiency;
- 5) simplicity of combination with renewable energy storage and conversion.

Electrochemical purification and separation methods are based on capacitive accumulation reactions and redox reactions on the surface of electrodes. Consequently, it is necessary to pay great attention to the development of new electrodes with a large specific surface area and a high capacity of the electric double layer (EDL), a fast reaction to ions oxidation — recovery, electrochemical and chemical inertness, obtaining simplicity, cheap and affordable raw materials to achieve mechanically resistant electrodes.

Carbon materials based on plant and carbon-mineral raw are great as initial material for obtaining electrodes because of the availability and cheapness of raw materials, high specific surface area and the presence of functional groups (-COOH, -COH, -OH, etc.). The functional groups contribute to the good hydrophilicity of the surface, the ease of modification in order to improve the electrocatalytic and electroadsorption properties [13]. There are a huge number of modified carbon materials: activated carbons, graphene, carbon nanotubes, nanofibers, carbide-carbon materials, carbon aerogels, etc. [14].

Currently, there is an increase in types, modifications, and methods of carbon electrodes obtaining [15, 16]. These electrodes with mechanical strength possess stability of the stationary potential, good adhesion to a solid substrate. Nevertheless, they have disadvantages: the use of liquid binders reduces the effective specific surface area of carbon electrodes; a percolation threshold decrease leads to blocking of carbon matrix particles and a decrease in electrical conductivity; the presence of an organic binder in the carbon electrode composition leads to an increase of a surface hydrophobicity; the introduction of liquid binder into the electrode composition leads to a mixed stationary potential, which makes impossible evaluating the carbon material contribution to the electrochemical reaction on the carbon electrode surface; an increase in the ohmic and kinetic characteristics of a carbon electrode, etc. [17].

The aim of this work is the optimization of the carbon electrode obtaining method by hot pressing, using the method of full-factor experiment and the steepest ascent.

Experimental

The study objects are carbon materials (CM) based on walnut shells obtained by the hydrothermal carbonization (HTC) at a temperature of 220–240 °C for 24 hours with further modification by the steam-gas activation (SGA) at $T = 800\text{--}850$ °C for 1 hour [18].

The specific surface area of the sorption materials was determined by the Sorbtometer-M analyzer using the Brunauer-Emmett-Teller (BET) single-point method (Table 1). In this work, the study of the CM by electron microscopy was carried out using a Quanta 3D 200i Dualsystem scanning electron microscope (FEI Company, USA) at the Al-Farabi KazNU “National nanotechnology laboratory of open type”.

The selected binder is ultra-fine polyethylene powder (UFPEP), GUR®, USA. The phase transformations analysis of the binder was carried out on an analyzer “NETZSCH STA 449F3”, Germany. Thermogravimetric (TG) and differential scanning calorimetry (DSC) curves were recorded in parallel with increasing temperature.

The mechanically strong carbon electrode was obtained by hot pressing. The optimal values of the pressure, pressing temperature and the CM/binder ratio were found. The following intervals of the main independent variables were selected to carry out a full-factor experiment (FFE). There are $T = 25\text{--}130\text{ }^{\circ}\text{C}$; $P = 150\text{--}250\text{ atm.}$; content of UFPEP = 15–30 %. In this research, a planning matrix for 2-level 3-factor experiment was used. It is described by 1st order polynomial. The mechanical bending strength of the carbon electrode (bending angle) was measured as a dependent variable. The path-of-steepest-ascent method along the response surface was applied to find the gradient direction of the parameters and reach the stationary region of the response surface. Statistical processing of the full-factor experiment matrix results was tested for reproducibility (3 parallels, Cochran's test), the significance of the regression coefficients (Student's t-test), and the adequacy of the regression equation to this planning matrix (Fisher's test) [19].

Results and Discussion

Two types of carbon materials were obtained. Sample #1 by HTC ($T = 240^{\circ}\text{C}$, $t = 24\text{h}$) and sample #2 by HTC ($T = 240^{\circ}\text{C}$, $t = 24\text{ h}$) with SGA ($T = 800\text{--}850\text{ }^{\circ}\text{C}$, $t = 1\text{h}$). The physicochemical properties of the obtained samples are summarized in Table 1.

It was found that carbon materials, based on walnut shells obtained by the HTC with further steam-gas activation, have the best indicators of the iodine number (82.2 %) and $S_{\text{specific}} = 754.0\text{ m}^2/\text{g}$. The results are represented in Table 1. The iodine adsorption number of the samples is one of the main parameters which characterized the pore surface area and, as a consequence, the sorption capacity of coal. Values of iodine adsorption number confirm the numerical values of the materials' specific pore surface area. The obtained SEM images (Fig. 1) indicate the texture of the samples based on plant raw materials is described by a large number of pores on the surface, especially in carbonizates after HTC with SGA.

Table 1

Physicochemical properties of carbon materials

Sample No.	Humidity, %	Ash content, %	pH of the aqueous extract	Iodine adsorption number, %	S_{sp} , m^2/g
1	2.05	1.05	7.9	17.6	464.9
2	1.07	4.38	8.3	82.2	754.0

According to the results, a walnut shell obtained by the HTC method ($T = 240\text{ }^{\circ}\text{C}$, $t = 24\text{ h}$) with further SGA ($T = 850\text{--}900\text{ }^{\circ}\text{C}$, $t = 1\text{h}$) was selected as the carbon material for obtaining the carbon electrode (CE).

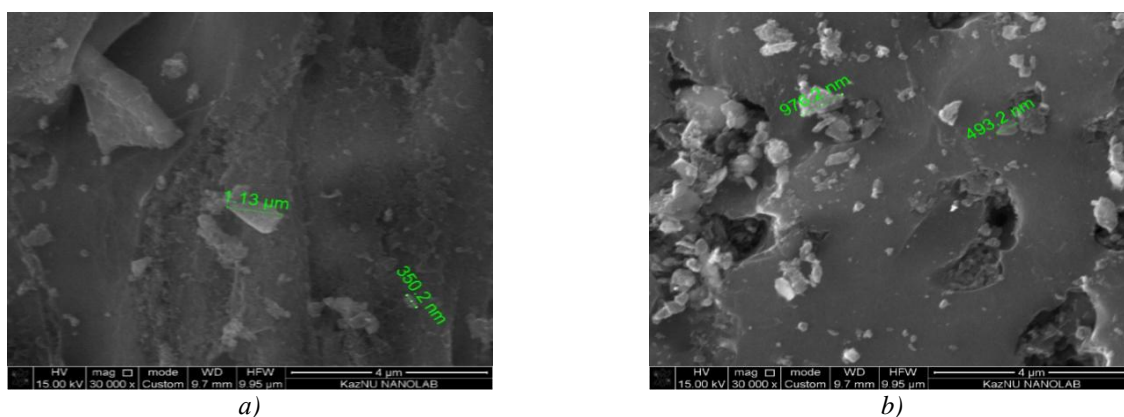


Figure 1. Scanning electron microscopy images of CM No. 1 (a) HTC and No. 2 (b) HTC + SGA. Magnification $\times 30000$

The phase transformations analysis of the binder by the TGA-DSC method are presented in Figure 2. It was found that ultra-fine polyethylene powder (UFPEP) is a homogeneous system with a destruction temperature of $419.6\text{ }^{\circ}\text{C}$ and a melting point of $125\text{--}135\text{ }^{\circ}\text{C}$ [20].

FFE was used with three independent variables to optimize the CE obtaining method. There are temperature, pressing pressure, and the CM/binder ratio. Based on preliminary experiments, the parameter values were selected for the FFE matrix (Table 2).

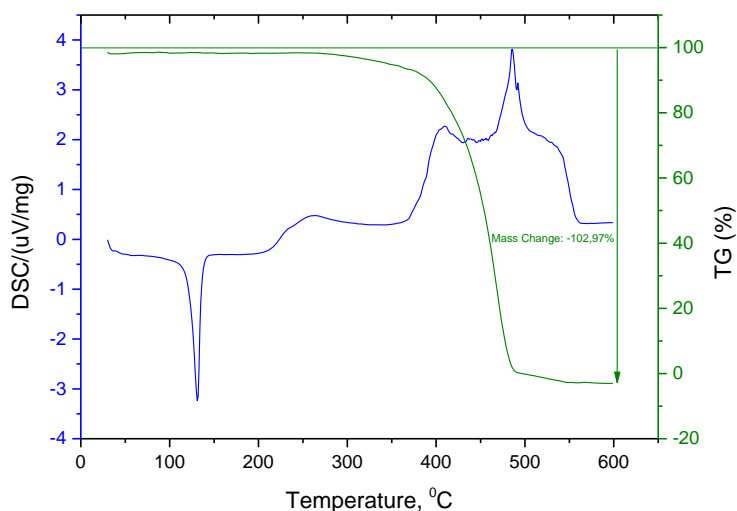


Figure 2. TG and DSC curves of the UFPEP sample

Table 2

Absolute values of the levels of the upper and lower factors

Factor characteristic	Value of factors		
	P, atm.	CM:UFPEP, %	T, °C
	X ₁	X ₂	X ₃
Upper level x _i = +1	250	70: 30	130
Lower level x _i = -1	150	85: 15	25

1st order regression equation was obtained using the matrix of a 2-level 3-factor experiment (Table 3):

$$y = 17.625 + 2x_1 + 5.125x_2 + 4.875x_3 + 1.125x_{23} \tag{1}$$

Table 3

Planning matrix and results of experiments in the study of the CE mechanical bending strength

Exper. number	X ₀	X ₁	X ₂	X ₃	X ₁ X ₂	X ₂ X ₃	X ₁ X ₃	X ₁ X ₂ X ₃	Y _{exp} (av)	σ ²	Y _{calc}
I	II	III	IV	V	VI	VII	VIII	IX	X	XI	XII
1	+	-	-	-	+	+	+	-	5	0.0	6.75
2	+	+	-	-	-	-	+	+	13	12.5	10.8
3	+	-	+	-	-	+	-	+	15	0.0	14.8
4	+	+	+	-	+	-	-	-	19	4.5	18.8
5	+	-	-	+	+	-	-	+	13	12.5	14.3
6	+	+	-	+	-	+	-	-	20	0.0	18.3
7	+	-	+	+	-	-	+	-	30	0.0	26.8
8	+	+	+	+	+	+	+	+	28	12.5	30.8

The reproducibility of the results and the adequacy of the simulation model to the experimental data on mechanical strength have been assessed by Cochran's, Student's, and Fisher's tests, respectively (Table 4) [19].

Table 4

Assessment of the experimental results reproducibility and the adequacy of the computational model

N ₀	Experimental value	Table value[19]
1	Cochran's test (G _t (β=0,1 at n=3 N=8) > G _{exp})	
	0.298	0.57
2	Fisher's test (F _{exp} < F _{table} (f ₁ = 4, f ₂ = 16))	
	1.590	3.80

The given above mathematical model showed that the second (CM:UFPEP, %) and third (pressing temperature) variables have the greatest influence on the electrode mechanical strength. The pressing pressure value is 2.5 times less. According to Fisher's test, the adequacy of the regression equation is established. It describes the response surface.

For the mathematical description of the extremum stationary region, the steepest ascent method was applied. The experimental and the corresponding calculated values of y_i are presented in Table 6. The interval of variation was determined by differentiating equation 1:

$$b_1 = 2.000;$$

$$b_2 = 5.125;$$

$$b_3 = 4.875.$$

Table 5

The value of variables in the study of the CE mechanical bending strength

Factor	P, atm.	CM:UFPEP, %	T, °C
Code designation	X_1	X_2	X_3
Main level $X_{i0} = 0$	200.0	77.5:22.5	77.5
Variation interval ΔX_i	13.0	5.0	6.65

Table 6

Plan and results of the experiment carried out by the steepest ascent method

Factors	X_1	X_2	X_3	Y_{calc}	Y_{exp}
Coefficient b_i	2	5.125	4.875		
Variation step	13	5.00	6.65		
Starting point	200	22.50	77.50	20.0	18.3
Realized experience I	213	27.50	84.15	22.2	24.7
Realized experience II	226	32.50	90.80	26.7	25.8
Realized experience III	239	37.50	97.45	31.3	22.3
Realized experience IV	252	42.40	104.10	35.9	20.4
Realized experience V	265	47.50	110.75	40.4	20.2

Based on the coefficients values the gradient equation for this system is derived:

$$\text{grad}Y = 2i + 5.125j + 4.875k \quad (2)$$

On the basis of this equation, the direction to the stationary region of the extremum is found by the steepest ascent method. The largest value of the coefficient — $b_2 = 5.125$ was taken as the basic factor X_2 . The step for which was set $\delta X_2 = 5$. Then the variation steps were calculated for the remaining factors (Table 5):

$$\delta X_1 = \frac{2 \cdot 50 \cdot 5}{5.125 \cdot 7.5} = 13;$$

$$\delta X_3 = \frac{4.875 \cdot 52.5 \cdot 5}{5.125 \cdot 7.5} = 6.65.$$

In order to assess the direction to the stationary extremum region, Student's t-test and Fisher's test were used for two independent samples (Table 7).

Table 7

Assessment of the adequacy approximated and experimental dependent variable

#	Experimental value	Table value [19]
1	Fisher's test ($F_{exp} < F_{table}(f_1 = 5, f_2 = 5)$)	
	4.54	5.05
2	Student's t-test ($t_{exp} < t_{table}(N=10, P = 0,95)$)	
	2.19	2.23

Based on the experiment results of the steepest ascent method, it was found that the third experiment did not illustrate an increase of CE mechanical strength in comparison with the second experiment. The experimental $Y_{\text{exp}} = 22.3$ and theoretical $Y_{\text{calc}} = 31.3$ values have a significant difference; therefore, further study in this direction does not make sense (Table 6).

Conclusion

In this paper, carbon materials based on walnut shells have been obtained by the hydrothermal carbonization method and modification by the steam-gas activation method. Their physicochemical and structural characteristics have been studied and optimized. The best value of S_{specific} is $754.0 \text{ m}^2/\text{g}$ and the iodine adsorption number is 82.2 %. The function of the extremum stationary region was achieved using a full-factor experiment and the steepest ascent method. The mathematical approach made possible to find the direction of the function gradient and to reach the region of the stationary extremum under the following experimental conditions:

$$P = 226 \text{ atm.}; T = 90.8 \text{ }^\circ\text{C}; \text{UFPEP:CM} = 32.5:67.5 \text{ \%}.$$

The steepest ascent method will allow optimizing the mechanical strength of the CE depending on 3 independent factors.

Acknowledgments

This research was funded by the Science Committee of the Ministry of Education and Science of the Republic of Kazakhstan (Grant No. AP08957598 “The use of electrochemical methods for studying adsorption to characterize new carbon materials”).

References

- 1 Perez J.P. Progress in hydrometallurgical technologies to recover critical raw materials and precious metals from low-concentrated streams / J.P. Perez, K.H. Folens, K. Leus, F. Vanhaecke, P. Van Der Voort, G. Du Laing // *Resources, Conservation and Recycling*. — 2019. — Vol. 142. — P. 177–188. DOI 10.1016/j.resconrec.2018.11.029
- 2 Sethurajan M. Recent advances on hydrometallurgical recovery of critical and precious elements from end of life electronic wastes — a review / M. Sethurajan, E.D. van Hullebusch, D. Fontana, A. Akcil, H. Deveci, B. Batinic, et al. // *Critical Reviews in Environmental Science and Technology*. — 2019. — Vol. 49, Is. 3. — P. 212–275. <https://doi.org/10.1080/10643389.2018.1540760>
- 3 Ramachandra Rao S. Resource Recovery and Recycling from Metallurgical Wastes / S. Ramachandra Rao. — Montreal: Elsevier, 2006. — 508 p.
- 4 Ahluwalia S.S. Microbial and plant derived biomass for removal of heavy metals from wastewater / S.S. Ahluwalia, D. Goyal // *Bioresource Technology*. — 2007. — Vol. 98. — P. 2243–2257. DOI: 10.1016/j.biortech.2005.12.006
- 5 Qi D. Hydrometallurgy of Rare Earths / D. Qi. — Amsterdam: Elsevier, 2018. — P. 631–669.
- 6 Wu T. Amidoxime-Functionalized Macroporous Carbon Self-Refreshed Electrode Materials for Rapid and High-Capacity Removal of Heavy Metal from Water / T. Wu, C. Liu, B. Kong, J. Sun, Y. Gong, K. Liu, et al. // *ACS Central Science*. — 2019. — Vol. 5. — P. 719–726. DOI: 10.1021/acscentsci.9b00130
- 7 Eskandari E. A review on polyaniline-based materials applications in heavy metals removal and catalytic processes / E. Eskandari, M. Kosari, M.H. Davood Abadi Farahani, N.D. Khiavi, M. Saeedikhani, R. Katal, et al. // *Separation and Purification Technology*. — 2020. — Vol. 231. — P. 1–27. DOI: 10.1016/j.colsurfa.2021.126274
- 8 Viel P. New concept to remove heavy metals from liquid waste based on electrochemical pH-switchable immobilized ligands / P. Viel, L. Dubois, J. Lyscawa, M. Salle, S. Palacin // *Applied Surface Science*. — 2007. — Vol. 253. — P. 3263–3269. DOI 10.1016/j.apsusc.2006.07.022
- 9 Bonificio W.D. Rare-Earth Separation Using Bacteria / W.D. Bonificio, D.R. Clarke // *Environmental Science and Technology Letters*. — 2016. — Vol. 3. — P. 180–184. DOI: 10.1021/acs.estlett.6b00064
- 10 Irannajad M. Surface dissolution-assisted mineral flotation: A review / M. Irannajad, O. Salmani Nuri, A. Mehdilo // *Journal of Environmental Chemical Engineering*. — 2019. — Vol. 7. — P. 103050. <https://doi.org/10.1016/j.jece.2019.103050>
- 11 Anjum N.A. Enhancing Cleanup of Environmental Pollutants / N.A. Anjum, S.S. Gill, N. Cham. Tuteja. — New York: Springer International Publishing, 2017. — P. 327.
- 12 Maarof H.I. Recent trends in removal and recovery of heavy metals from wastewater by electrochemical technologies / H.I. Maarof, W.M.A.W. Daud, M.Kh. Aroua // *Reviews in Chemical Engineering*. — 2017. — Vol. 33. — P. 359–386. DOI: <https://doi.org/10.1515/revce-2016-0021>
- 13 Abioye A.M. Advancement in the Production of Activated Carbon from Biomass Using Microwave Heating / A.M. Abioye, F. Nasir Ani, J. Bahru // *Jurnal Teknologi*. — 2017. — Vol. 79. — P. 2180–3722. DOI: <https://doi.org/10.11113/jt.v79.7249>
- 14 Liu C.F. Carbon materials for high-voltage supercapacitors / C.F. Liu, Y.C. Liu, T.Y. Yi, C.C. Hu // *Carbon*. — 2019. — Vol. 145. — P. 529–548. <https://doi.org/10.1016/j.carbon.2018.12.009>

15 Abioye A.M. Recent development in the production of activated carbon electrodes from agricultural waste biomass for supercapacitors: A review / A.M. Abioye, F.N. Ani // Renewable and Sustainable Energy Reviews. — 2015. — Vol. 52. — P. 1282–1293. <https://doi.org/10.1016/j.rser.2015.07.129>

16 Borenstein A. Carbon-based composite materials for supercapacitor electrodes: A review / A.Borenstein, O.Hanna, R. Attias, S.Luski, T.Brousse, D.Aurbach // Journal of Materials Chemistry A. — 2017. — Vol. 5. — P. 12653–12672. DOI: 10.1039/C7TA00863E

17 Тарасевич М.Р. Электрохимия углеродных материалов / М.Р. Тарасевич. — М.: Наука, 1984. — С. 218–223.

18 Atchabarova A.A. New electrodes prepared from mineral and plant raw materials of Kazakhstan / A.A. Atchabarova, R.R. Tokpayev, A.T. Kabulov, S.V. Nechipurenko, R.A. Nurmanova, S.A. Yefremov, et al. // Eurasian Chemico-Technological Journal. — 2016. — Vol. 18. — P. 141–147. DOI: 10.18321/ectj440

19 Берикашвили В.Ш. Статистическая обработка данных, планирование эксперимента и случайные процессы / В.Ш. Берикашвили, С.П. Оськин. — М.: Юрайт, 2019. — 162 с.

20 Ершова О.В. Использование метода дифференциальной сканирующей калориметрии и термогравиметрического анализа для определения состава и температуры деградации вторичных полимеров / О.В. Ершова, М.А. Мельниченко // Успехи современного естествознания. — 2015. — № 11. — С. 26–30.

С.К. Әбдімомын, Д.А. Абдухытова, А.А. Атчабарова, Г.Л. Турдеан,
Р.Р. Токпаев, К.К. Кишибаев, А.П. Курбатов, М.К. Наурызбаев

Механикалық берік көміртекті электродты дайындау әдісін оңтайландыру

Қазіргі әлемде табиғи ресурстарды ұтымды пайдалануға және қоршаған ортаны қорғауға әкелетін құнды компоненттерді алу мақсатында қайталама ресурстарды жою стратегиясы байқалып отыр. Мәселені шешу үшін шикізатты алдын-ала дайындамай-ақ мақсатты компоненттерді іріктеп шоғырландыруға мүмкіндік беретін электрохимиялық әдістер өте жақсы қолданылады. Өсімдік және минералды шикізатқа негізделген көміртекті материалдар (КМ) қол жетімділігіне, арзандығына, бетінің жоғары меншікті ауданына және әртүрлі функционалды топтардың болуына байланысты электродтарды өндіруге арналған матрица ретінде тамаша нұсқа болып табылады. Көмір электродтарындағы адсорбция құбылыстарын теориялық негіздеудің жетіспеушілігі модификацияланған көміртегі мен полиэтилен негізінде механикалық күшті электрод жасау әдісін зерттеуге және дамытуға түрткі болды. Көміртекті электродтардың (КМ) дизайны мен механикалық беріктігі тазартудың, құнды компоненттерді алудың тиімділігі үшін үлкен маңызға ие. Мақалада авторлар грек жаңғағының қабығынан гидротермальды карбонизация және бу газды белсендіреу әдісімен көміртекті материал алған, оның бетінің ауданы $754,0 \text{ м}^2/\text{г}$ құрады. Көміртек материалының, байланыстырушының және КМ субстратының материалының құрылымдық, физика-химиялық сипаттамалары келесі әдістермен зерттелді: СЭМ, БЭТ, ТГТ-ДСК. Көміртекті электродтарды жасау үшін ыстық пресеу әдісі қолданылды. Толық факторлы эксперимент және тік көтерілу әдісін қолдана отырып, қысым мен температураның мәндері және көміртекті материал: байланыстырушы қатынасы оңтайландырылды: $P = 226 \text{ атм.}$; $T = 90,8 \text{ }^\circ\text{C}$; көміртекті материал: байланыстырушы қатынасы $= 67,5:32,5 \%$.

Кілт сөздер: көміртекті электрод, толық факторлы эксперимент, адсорбция, гидротермальды карбонизация, көміртекті материал, термальды карбонизация, грек жаңғағы, ыстық пресеу әдісі.

С.К. Абдимомын, Д.А. Абдухытова, А.А. Атчабарова, Г.Л. Турдеан,
Р.Р. Токпаев, К.К. Кишибаев, А.П. Курбатов, М.К. Наурызбаев

Оптимизация метода изготовления механически прочного углеродного электрода

В современном мире наблюдается стратегия по утилизации вторичных ресурсов с целью получения из них ценных компонентов, которая приведет к наиболее рациональному использованию природных ресурсов и охране окружающей среды. Для решения проблемы отлично применимы электрохимические методы, которые позволяют селективно концентрировать целевые компоненты без предварительной подготовки сырья. Углеродные материалы (УМ) на основе растительного и минерального сырья являются отличным вариантом в качестве матрицы для изготовления электродов, вследствие доступности, дешевизны, высокой удельной площади поверхности и наличия разных функциональных групп. Недостаток теоретического обоснования явлений адсорбции на угольных электродах послужил стимулом для изучения и разработки способа изготовления механически прочного электрода на основе модифицированного углерода и полиэтилена. Конструкция и механическая прочность углеродных электродов (УЭ) имеют огромное значение для эффективности очистки,

извлечения ценных компонентов. В статье описано получение углеродного материала из скорлупы грецкого ореха методом гидротермальной карбонизации с дальнейшей парогазовой активацией, с удельной площадью поверхности $754,0 \text{ м}^2/\text{г}$. Структурные, физико-химические характеристики углеродного материала, связующего и материала подложки УЭ изучены следующими методами: СЭМ, БЭТ, ТГА-ДСК. Для изготовления углеродных электродов применен метод горячего прессования. С помощью метода полнофакторного эксперимента и круглого восхождения оптимизированы значения давления и температуры при прессовании и соотношении углеродный материал : связующее: $P = 226 \text{ атм.}$; $T = 90,8 \text{ }^\circ\text{C}$; соотношение УМ : связующее = $67,5:32,5 \%$ соответственно.

Ключевые слова: углеродный электрод, полнофакторный эксперимент, адсорбция, гидротермальная карбонизация, углеродный материал, термальная карбонизация, скорлупа грецкого ореха, метод горячего прессования.

References

- 1 Perez, J.P., Folens, K.H., Leus, K., Vanhaecke, F., Van Der Voort, P., & Du Laing, G. (2019). Progress in hydrometallurgical technologies to recover critical raw materials and precious metals from low-concentrated streams. *Resources, Conservation and Recycling*, 142, 177–188. DOI 10.1016/j.resconrec.2018.11.029
- 2 Sethurajan, M., van Hullebusch, E.D., Fontana, D., Akcil, A., Devenci, H., & Batinic, B., et al. (2019). Recent advances on hydrometallurgical recovery of critical and precious elements from end of life electronic wastes — a review. *Critical Reviews in Environmental Science and Technology*, 49, 212–275. <https://doi.org/10.1080/10643389.2018.1540760>
- 3 Ramachandra Rao, S. (2006). *Resource Recovery and Recycling from Metallurgical Wastes*. Montreal: Elsevier.
- 4 Ahluwalia, S.S., & Goyal, D. (2007). Microbial and plant derived biomass for removal of heavy metals from wastewater. *Bioresource Technology*, 98, 2243–2257. DOI: 10.1016/j.biortech.2005.12.006
- 5 Qi, D. (2018). *Hydrometallurgy of Rare Earths*. Amsterdam: Elsevier.
- 6 Wu, T., Liu, C., Kong, B., Sun, J., Gong, Y., & Liu, K., et al. (2019). Amidoxime-Functionalized Macroporous Carbon Self-Refreshed Electrode Materials for Rapid and High-Capacity Removal of Heavy Metal from Water. *ACS Central Science*, 5, 719–726. DOI: 10.1021/acscentsci.9b00130
- 7 Eskandari, E., Kosari, M., Davood Abadi Farahani, M.H., Khiavi, N.D., Saeedikhani, M., & Katal, R., et al. (2020). A review on polyaniline-based materials applications in heavy metals removal and catalytic processes. *Separation and Purification Technology*, 231, 1–27. DOI: 10.1016/j.colsurfa.2021.126274
- 8 Viel, P., Dubois, L., Lyscawa, J., Salle, M., & Palacin, S. (2007). New concept to remove heavy metals from liquid waste based on electrochemical pH-switchable immobilized ligands. *Applied Surface Science*, 253, 3263–3269. DOI 10.1016/j.apsusc.2006.07.022
- 9 Bonificio, W.D., & Clarke, D.R. (2016). Rare-Earth Separation Using Bacteria. *Environmental Science and Technology Letters*, 3, 180–184. DOI: 10.1021/acs.estlett.6b00064
- 10 Irannajad, M., Salmani Nuri, O., & Mehdilo, A. (2019). Surface dissolution-assisted mineral flotation: A review. *Journal of Environmental Chemical Engineering*, 7, 103050. <https://doi.org/10.1016/j.jece.2019.103050>
- 11 Anjum N.A., Gill S.S., & Tuteja N. Cham. (2017). *Enhancing Cleanup of Environmental Pollutants*. New York: Springer International Publishing.
- 12 Maarof, H.I., Daud, W.M.A.W., & Aroua, M.K.D. (2017). Recent trends in removal and recovery of heavy metals from wastewater by electrochemical technologies. *Reviews in Chemical Engineering*, 33, 359–386. DOI: <https://doi.org/10.1515/revce-2016-0021>
- 13 Abioye, A.M., Nasir Ani, F., & Bahru, J. (2017). Advancement in the Production of Activated Carbon from Biomass Using Microwave Heating. *Jurnal Teknologi*, 79, 2180–3722. DOI: <https://doi.org/10.11113/jt.v79.7249>
- 14 Liu, C.F., Liu, Y.C., Yi, T.Y., & Hu, C.C. (2019). Carbon materials for high-voltage supercapacitors. *Carbon*, 145, 529–548. <https://doi.org/10.1016/j.carbon.2018.12.009>
- 15 Abioye, A.M., & Ani, F.N. (2015). Recent development in the production of activated carbon electrodes from agricultural waste biomass for supercapacitors: A review. *Renewable and Sustainable Energy Reviews*, 52, 1282–1293. <https://doi.org/10.1016/j.rser.2015.07.129>
- 16 Borenstein, A., Hanna, O., Attias, R., Luski, S., Brousse, T., & Aurbach, D. (2017). Carbon-based composite materials for supercapacitor electrodes: A review. *Journal of Materials Chemistry A*, 5, 12653–12672. DOI: 10.1039/C7TA00863E
- 17 Tarasevich, M.R. (1984). *Elektrokhimiia uglerodnykh materialov [Electrochemistry of Carbon Materials]*. Moscow: Nauka [in Russian].
- 18 Atchabarova, A.A., Tokpayev, R.R., Kabulov, A.T., Nechipurenko, S.V., Nurmanova, R.A., & Yefremov, S.A., et al. (2016). New electrodes prepared from mineral and plant raw materials of Kazakhstan. *Eurasian Chemico-Technological Journal*, 18, 141–147. DOI: 10.18321/ectj440
- 19 Berikashvili, V.Sh., & Oskin, S.P. (2019). *Statisticheskaiia obrabotka dannykh, planirovanie eksperimenta i sluchainye protsessy [Statistical data processing, experiment planning and random processes]*. Moscow: Yurait [in Russian].

20 Ershova, O.V., & Melnichenko, M.A. (2015). Ispolzovanie metoda differentsialnoi skaniruyushchei kalorimetrii i termogravimetricheskogo analiza dlia opredeleniia sostava i temperatury destruktzii vtovichnykh polimerov [Using the method of differential scanning calorimetry and thermogravimetric analysis to determine the composition and temperature of degradation secondary polymers]. *Uspekhi sovremennogo estestvoznaniia — Advances in modern natural science*, 11, 26–30 [in Russian].

Information about authors

Abdimomyn Saken Kynabekuly — Master student, Junior Researcher of the Center of Physical Chemical Methods of Research and Analysis of Al-Farabi Kazakh National University, Tole bi str., 96A, 050000, Almaty, Kazakhstan; e-mail: abdimomyn03@gmail.com, <https://orcid.org/0000-0002-5985-9050>

Abduakhytova Dinara Aktaikyzy — PhD student, Researcher of the Center of Physical Chemical Methods of Research and Analysis of Al-Farabi Kazakh National University, Tole bi str., 96A, 050000, Almaty, Kazakhstan; e-mail: abduakhytova@mail.ru, <https://orcid.org/0000-0002-4316-0755>

Atchabarova Azhar Aidarovna (corresponding author) — PhD, Senior Researcher, Head of Laboratory of Hydroelectrometallurgical Processes, Center of Physical Chemical Methods of Research and Analysis of al-Farabi Kazakh National University, Tole bi str., 96A, 050000, Almaty, Kazakhstan; e-mail: azhar.atchabarova@mail.ru, <https://orcid.org/0000-0002-4600-2728>

Turdean Graziella Liana — Professor, Dr. habil. eng., Head of Department of Chemical Engineering, Babes-Bolyai University, Faculty of Chemistry and Chemical Engineering; 11, Arany Janos St., 400028 Cluj-Napoca, Romania; e-mail: graziella.turdean@ubbcluj.ro, <https://orcid.org/0000-0003-1273-6878>

Tokpayev Rustam Rishatovich — PhD, Leading Researcher, Head of Laboratory of Sorption and Catalytic Processes, Center of Physical Chemical Methods of Research and Analysis of al-Farabi Kazakh National University, Tole bi str., 96A, 050000, Almaty, Kazakhstan; e-mail: rustamtokpaev@mail.ru, <https://orcid.org/0000-0002-0117-4454>

Kishibayev Kanagat Kazhmukanovich — PhD, Senior Researcher of the Center of Physical Chemical Methods of Research and Analysis of Al-Farabi Kazakh National University, Tole bi str., 96A, 050000, Almaty, Kazakhstan; e-mail: kanagat_kishibaev@mail.ru, <https://orcid.org/0000-0003-1590-5243>

Kurbatov Andrey Petrovich — Professor, Doctor of chemical sciences, Chief Researcher, Head of Electrochemical Production Technologies Laboratory, Center of Physical Chemical Methods of Research and Analysis of al-Farabi Kazakh National University, Tole bi str., 96A, 050000, Almaty, Kazakhstan; e-mail: apkurbatov@gmail.com, <https://orcid.org/0000-0003-1883-310X>

Naurzybayev Mikhail Kassymovich — Professor, Doctor of technical sciences, Chief Researcher of the Center of Physical Chemical Methods of Research and Analysis of Al-Farabi Kazakh National University, Tole bi str., 96A, 050000, Almaty, Kazakhstan; e-mail: nauryzbaev@cfhma.kz, <https://orcid.org/0000-0002-6781-6464>

A.K. Abildina^{1,2}, K. Avchukir¹, R. Zh. Jumanova¹,
A.N. Beiseyeva¹, G.S. Rakhymbay¹, A.M. Argimbayeva^{1*}

¹Center of Physical Chemical Methods of Research and Analysis, Al-Farabi Kazakh National University, Almaty, Kazakhstan;

²Institute of Chemical and Biological Technologies, Satbayev University, Almaty, Kazakhstan

(*Corresponding author's e-mail: akmaral.argimbayeva@gmail.com)

Preparation and electrochemical characterization of TiO₂ as an anode material for magnesium-ion batteries

Anode on the basis of titanium dioxide powder was made. Its morphological characteristics were investigated using ellipsometry, scanning electron microscopy (SEM), energy-dispersive X-ray spectroscopy (EDS) and X-ray diffraction (XRD). Electrochemical properties were also investigated by cyclic voltammetry. Dispersing, mixing the initial reagents for obtaining homogenized paste and its coating to a substrate, drying and cutting the electrodes were main steps of anode production. The results of ellipsometry, SEM and EDS demonstrated a uniformly distributed layer of about 200 μm thickness with porous structure, particle diameter of 50–80 nm and titanium dioxide content (45.7 %). The XRD data confirmed the active anode matrix formation with a monoclinic crystal lattice corresponding to the modification of titanium dioxide (B) with small anatase inclusions. Electrochemical behavior of the electrode was examined in acetonitrile-based Mg(TFSI)₂ solution. Diffusion coefficient (DMg) and the charge transfer rate constant (kct) were determined from cyclic voltammograms 1.54·10⁻² cm²/s and 1.29·10⁻⁴ cm/s, respectively. A two-step electrochemical reaction was revealed by the ratio of the electricity amount consumed in the cathode and anode processes at varying the number of cycles. Small values of polarization resistance (Rp) calculated from cyclic voltammograms indicated rapid diffusion of magnesium ions during intercalation/deintercalation.

Keywords: magnesium ion batteries, anode, titanium dioxide, synthesis, analysis, intercalation, deintercalation, kinetics, polarization, diffusion.

Introduction

Because of the limited resource of lithium in the Earth's crust, it became an uneconomical option of chemical power source of current in portable electronics. That is why, nowadays, demand for alternative energy storage systems based on inexpensive materials increases. Magnesium-ion batteries (MIB) are the most attractive ones for researchers due to the magnesium abundance in nature, high capacity and the dendritic free Mg sediments. MIBs fully meet the requirements of environmentally friendly energy materials, since magnesium and its compounds are non-toxic. Thus, the lower price and theoretical volume capacity (3833 mAh/cm³) make MIBs to be promising candidates for next generation of electric storage systems. Despite these promising aspects, the development and practical application of MIBs require extensive and detailed research. In MIB one can find several problems of reversible reduction/dissolution and low diffusion rate of Mg²⁺ ions, which manifest in the absence of stable electrolytes and a strong polarization effect of Mg²⁺ ions with lattices of electrode material [1].

For eliminating these disadvantages, one can use alternative anode materials based on Mg²⁺ ions instead of a metal magnesium anode [2–4]. To realize this idea, the researchers tried to use magnesium-based alloys as an anode relying on their successful practical application in MIB anodes. Anodes from magnesium in MIB did not demonstrate good results due to the internal characteristics of magnesium ions. Therefore, several potential alloy-based anodes (for example, Bi, Sn, Pb, Sb, and In) were investigated; Bi and Sn are more attractive ones among them due to the formation of intermetallic compounds with magnesium with a higher theoretical capacity in comparison with Mg/Mg²⁺ [1, 5]. Several reports informed about the possibility of using bismuth and tin anodes in the development of MIB and also demonstrated good compatibility of the anode with a conventional electrolyte. However, during the study of these materials as an anode, certain disadvantages have been revealed that are manifested in productivity decrease and theoretical capacity decrease, which are caused by the slow diffusion of Mg²⁺ ions in the solid phase and a large change in electrode volume during alloying/dealloying reactions [1].

Other alternative anodes, such as 2D materials on the basis of transition metal disulfides, demonstrated good results by the theoretical capacitance at using as anode materials for sodium ion and lithium ion accu-

mulators. Their unique layered structure promotes the beneficial properties of these materials for enhancing practical value. The monolayers of 2D materials are good in adsorbing Mg²⁺ through increasing the conductivity of the anode material and illustrate relatively high capacity and good stability. However, applying these materials in MIBs is still at the theoretical stage and requires further experimental confirmation [5].

Titanium dioxide is considered to be a promising matrix for the reversible intercalation of Mg²⁺ ions among possible candidates for anode materials in MIB. There are several modifications of titanium dioxide: anatase, rutile, brookite, and bronze TiO₂ (B). It should be noted that the first three of them are widespread in nature; the fourth modification, TiO₂ (B), with a monoclinic structure is also found in nature, but rarely. Such main characteristics of crystalline modifications of TiO₂ as non-toxicity, availability, low deformation, stability in most organic electrolytes, and excellent cycling characteristics, as well as the ability to charge/discharge the material at a very high velocity were successfully demonstrated in lithium-ion and sodium-ion batteries [6–8]. However, at using titanium dioxide in MIB low electron and ion conductivity limit its practical capacity and productivity. Therefore, a plenty of studies are carried out to improve the electrochemical properties of TiO₂-based electrode materials. Methods for improving the ions kinetics and TiO₂ electrode conductivity, are often applied at producing anode materials, one of which is the production of nanostructured materials with various morphologies (nanotubes, nanosheets, nanomassives, nanoparticles, and hollow spheres) should be especially emphasized. For example, nanostructures of TiO₂ from 0D to 3D effectively reduce the diffusion length of lithium and sodium ions improving the electrochemical kinetics of ions. The TiO₂ electron conductivity, which is initially poor, influences the improvement of electrochemical properties [9]. Coating or mixing the matrix with conductive materials, creating oxygen vacancies, and alloying modifications, etc. are the methods for improving electronic conductivity. Rapid ions' transport is the cause of significant improvement in electronic conductivity at using these methods [10–12]. Therefore, the aim of this study is to obtain TiO₂ with the necessary morphology and diffusion characteristics for its use as an anode material in MIB. In this work, we report on the method for preparing an electrode based on TiO₂ powder and the kinetics of the magnesium ions diffusion into the synthesized anode material.

Experimental

Preparation of intercalation anode material. Preparation of the anode material was carried out in several steps represented in Figure 1. The main components of the anode mixture were active material (titanium dioxide), binder (PVDF (polyvinylidene fluoride), company “Alfa Aesar”, analytically pure), solvent (NMP (N-methyl-2-pyrrolidone), company “Alfa Aesar”, analytically pure), and electroconductive additive (carbon black, acetylene, 100 %, compressed, 99.9 %, company “Alfa Aesar”, analytically pure). Titanium dioxide was obtained in the “Photocatalysis and sustainable feedstock utilization” laboratory, Institute of Chemistry, Faculty of Mathematics and Natural Sciences, Carl von Ossietzky University Oldenburg, Germany using a hard template method described in the work [13].

The electrode paste was obtained by mixing active material, electroconductive additive, and binder with the required amount. The weight percent of the components were 75:15:10, respectively. The mixture of the active material and the electroconductive additive was pre-dispersed, followed by addition of the dissolved binder to the mixture. The active mass components were first mixed in the agate mortar, and then stirring was carried out using a magnetic stirrer for 24 hours and rate of 1000 rpm for forming the paste-like anode composite and its application onto copper substrate. After the homogenization process, the anode mass was applied onto the copper foil. Surface contaminants were removed from the substrate surface by abrasive paper and degreasing with ethyl alcohol to ensure good adhesion between the substrate and the anode layer. Application to the substrate was made by casting. In this process, the prepared anode mass was poured onto copper foil in front of the blade “Doctor Blade”, then the blade was manually moved forward, stretching the ink and forming the film with a given thickness. The coating thickness was about 50–100 μm after drying.

After coating the electrode was preliminary dried for 6 hours at a temperature of 60 °C to evaporate solvent residues from the surface. Then, it was dried in a vacuum oven for 24 hours at a temperature of 100 °C to remove moisture traces. After primary drying, electrodes were cut by diameter of 10 mm (area 0.785 cm²). The finished electrodes were placed into an inert atmosphere glove box for further storage and investigation.

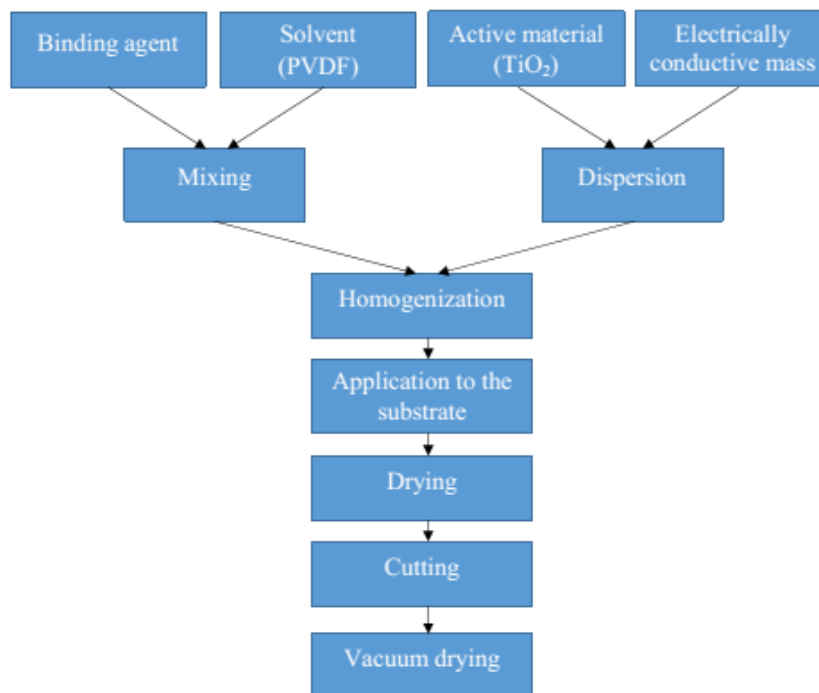


Figure 1. Diagram illustrating the main steps of the anode material making

Research methods and materials. Measurement of the electrode layer thickness from the center of the deepening (surface of the substrate) point to the upper edge of the anodic coating surface (1000 μm) of the synthesized material was carried out with the help of an ellipsometry in a Dektak 6M (Company Veeco, USA).

Micrographs of the synthesized electrode surface and its elemental composition were obtained by means of a scanning electron microscope Quanta 200i 3D (FEI Company, USA). The element distribution map was performed by scanning the electrode surface area from 1 μm to 100 μm in size. XRD patterns analysis of the anode material was performed by means of X-ray diffractometer Rigaku Miniflex 600ge (Japan). Samples were analyzed through CuK α radiation source of 0.1540 nm wave-length at scan rate of 0.05 min^{-1} starting at 10° angle and ending at 80° angle.

Cyclic voltammetry investigations were performed in the “Swagelok cell”. The synthesized electrode based on titanium dioxide powder was used as a working electrode, and metal magnesium (99.999 %) (diameter 10 mm, thickness 1.5 mm) was used as a reference and auxiliary electrode. The electrode surface was mechanically purified with an abrasive paper, and then degreased with acetone. Whatmann GF/D separator was applied as a membrane. Glass fiber separators of 10 mm diameter were placed between the working and auxiliary electrodes. Electrochemical measurements were carried out in 0.25 mol/l Mg(TFSI)₂ (Sigma Aldrich) solution on the basis of acetonitrile (AN, 99.9 %, company “Acros Organics”, analytically pure) with use of the potentiostat-galvanostat BioLogic SP-150 (France). Cycling was implemented at a scan rate from 0.05 mV/s to 1 mV/s and 5 cycles in the field of potentials (1.0 V \div -0.4 V). All the measurements were performed three times, followed by statistical analysis on blunder and averaging the obtained result.

Results and Discussion

Analysis of the intercalation anode material. The anode material have improved morphological and electrochemical characteristics such as high reversibility of intercalation/deintercalation processes, high diffusion capacity of metal ions into the matrix crystal lattice, etc. for practical use in magnesium ion batteries. The morphological properties of the anode material were tested by scanning electron microscopy, ellipsometry, and XRD methods. Figure 2 shows a gradual increase in the thickness of the electrode layer from the center of the deepening (surface of the substrate) point to the upper edge of the anodic coating surface (1000 μm). Using the ellipsometry gave opportunity to determine the thickness layer of the synthesized anode material, which was about 200 μm (Figure 2).

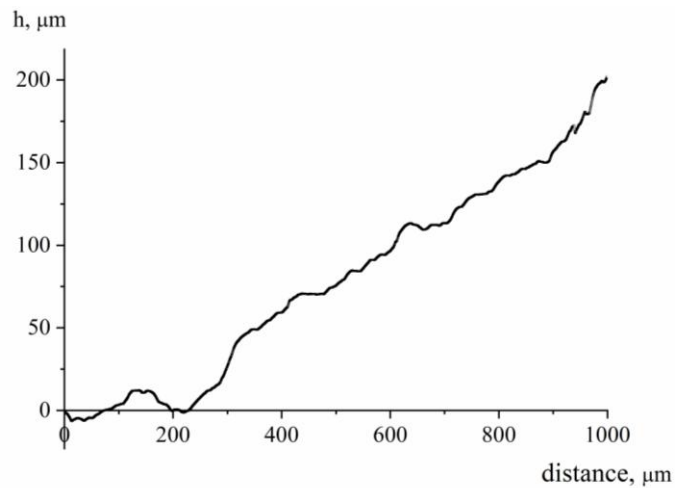


Figure 2. Thickness of titanium dioxide layer on the substrate

The morphologies of prepared anode material based on TiO₂ have been characterized by SEM and Figure 3 designates the results. It can be seen that the particles have a smooth surface and porous structure. A large amount of these particles are microspheres and, obviously, agglomeration. The size and shape of the particles are uniform. At the same time it points out that the diameter of the microsphere is approximately from 50 to 80 nm.

The surface radiograph of the anode material is presented at Figure 4.

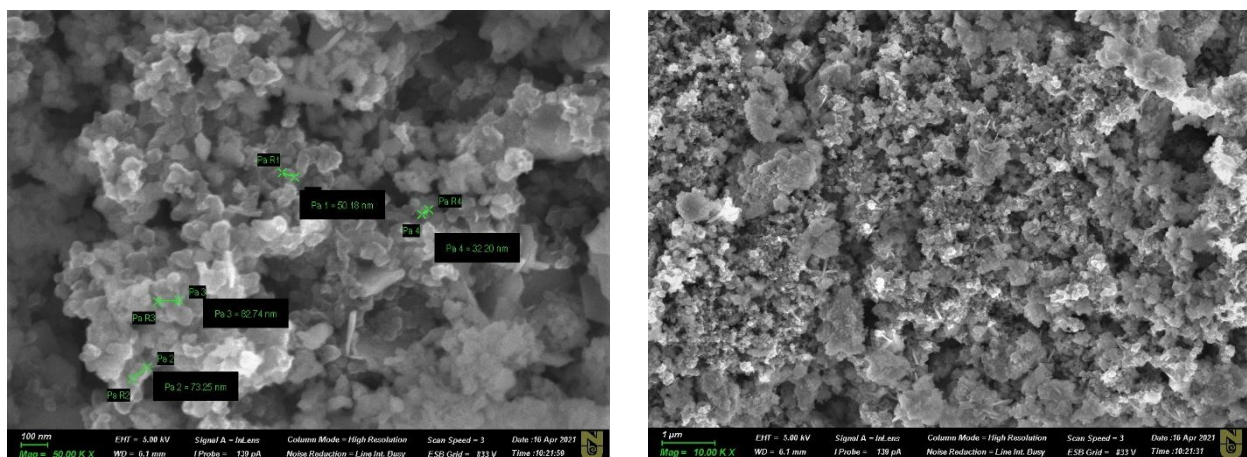


Figure 3. Micrographs of the surface of the obtained electrode material at different magnifications

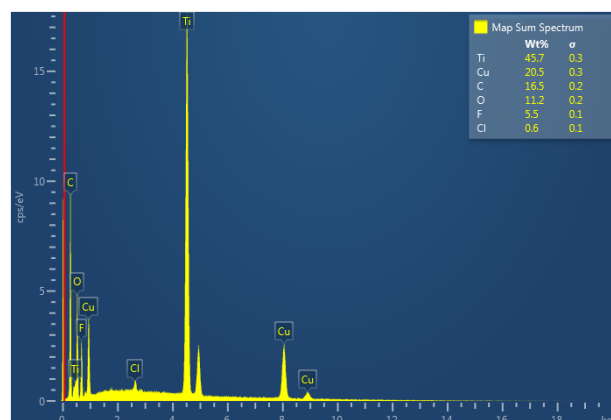


Figure 4. EDS spectral microanalysis of the obtained anode material

The EDS results of the synthesized electrode surface are presented in Table 1. It can be noticed that the main component of the electrode mass was titanium. The presence of copper in the composition can be explained by the substrate contribution.

Table 1

Elemental analysis of the synthesized electrode material

No.	Element	Wt, %
1	Ti	45.7
2	Cu	20.5
3	C	16.5
4	O	11.2
5	F	5.5
6	Cl	0.6

The map of elements distribution over the surface of anode material based on TiO_2 powder is presented in Figure 5 with high magnification. Elemental mapping results illustrated the distribution of such elements as Ti (red), C (purple), O (cyan) and F (yellow). Comparative analysis of the data showed that all the elements were evenly distributed on the surface of the synthesized electrode material.

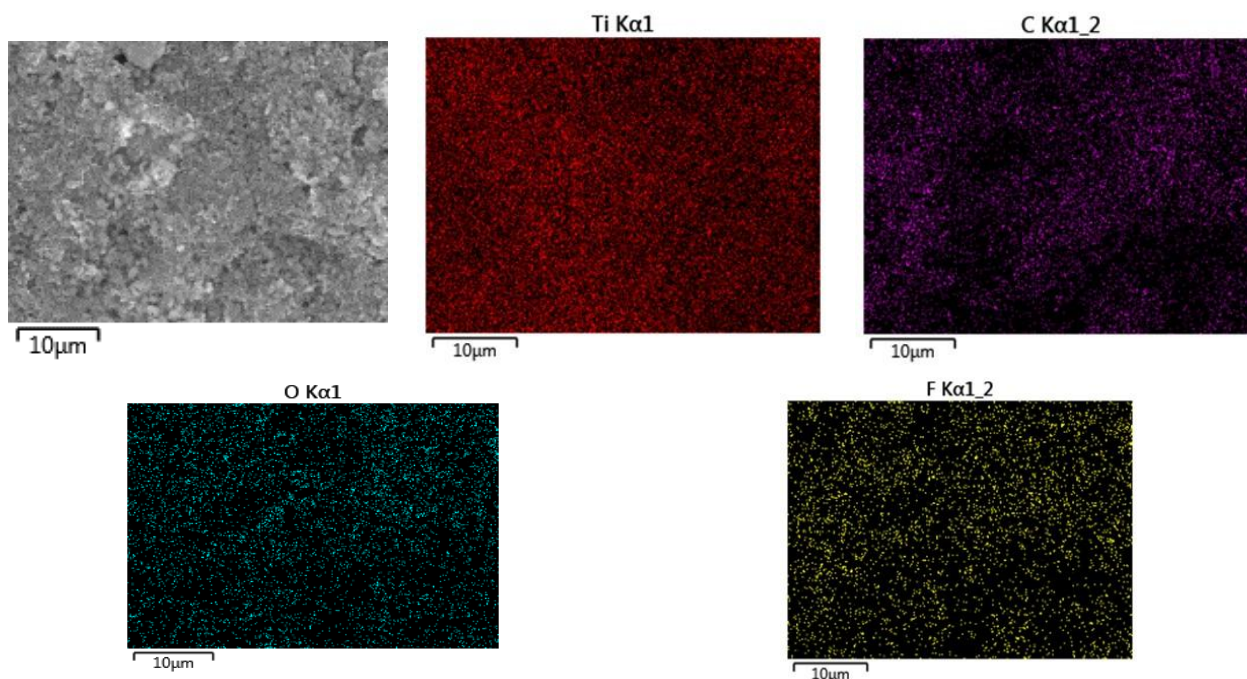


Figure 5. Map of elements distribution on the surface of the synthesized electrode material

XRD patterns (Fig. 6) represents that the synthesized anode material contained titanium dioxide and the crystalline salt of copper, Claringbullite, evidently formed due to the interaction of the metallic copper substrate and solvent, which corresponded to clearly visible spectra against the background of a significant content of the amorphous phase (Fig. 6), which was also confirmed by micrographs showing the formations of granular modification (Fig. 3).

According to the XRD data the crystal lattice parameters were determined (Table 2). Lattice has got monoclinic structure with volume of 0.1621 nm^3 and $C2/m$ structure (12). The synthesized material by monoclinic structure can be the modification of Bronze (B) [14]. In addition, according to XRD, this sample also has got titanium dioxide inclusions with anatase modification.

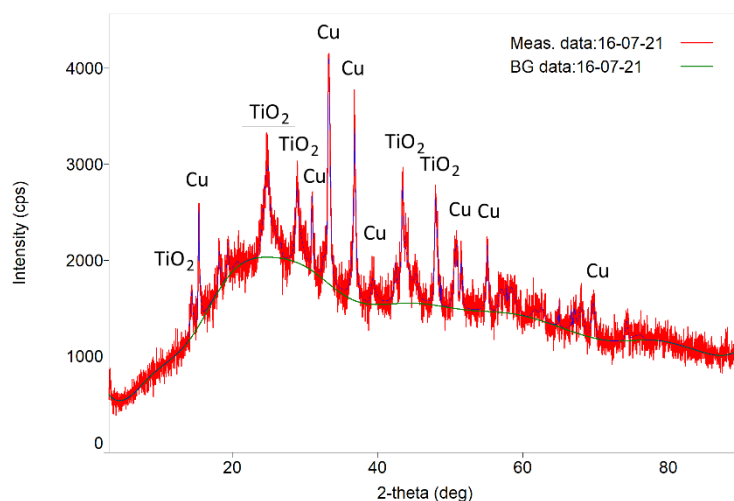


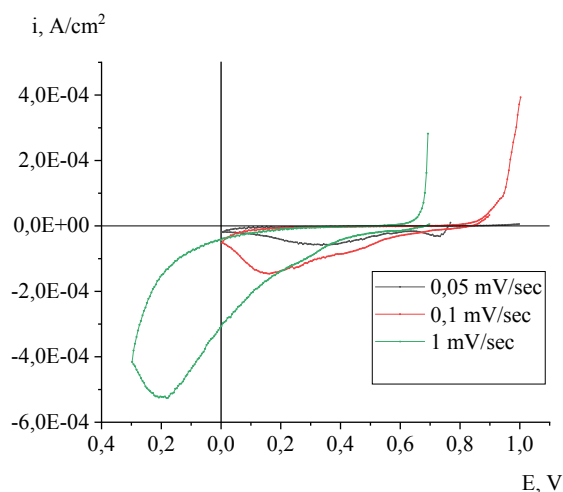
Figure 6. XRD patterns of anode mass based on titanium dioxide powder

Table 2

Parameters of crystal lattice of main components of anode mass

Name of the phase	a(nm)	b(nm)	c(nm)	α (deg)	β (deg)	γ (deg)	V(nm ³)
Titanium dioxide	1.2157	0.37347	0.65136	90.0000	107.0540	90.0000	0.2827
Claringbullite	0.6662	0.66627	0.91557	90.0000	90.0000	120.0000	0.3519

Electrochemical behavior of the synthesized anode. The cyclic voltammetry method was chosen for studying the kinetics of system electrochemical processes. The obtained cyclic voltammograms allowed evaluating the processes of intercalation and deintercalation of magnesium ions into the anode material.

Figure 7. Cyclic voltammograms of intercalation of magnesium ions into a synthesized anode based on titanium dioxide powder in the 0.25 mol/l solution of Mg(TFSI)₂/AN at different potential scanning rates, T = 25 °C

The voltammogram of the discharge-ionization cycle of magnesium ions on the surface of titanium dioxide at various potential scan rates was obtained in a solution of 0.25 mol/l Mg(TFSI)₂/AN. The dynamics of some peaks (Fig. 7) was allowed evaluating the redox properties of magnesium ions. The graph demonstrates that magnesium reduction at a scan rate of 0.05 mV/sec on the electrode surface began at a potential of 0.6 V. At polarization in the reverse direction, as seen in the curves, a peak of magnesium oxidation was observed at 1 V potential. In reversible processes, the values of the potentials of oxidation and reduction peaks characterizing the nature of the electroactive substance do not depend on the scan rate, and their difference ($E_{p(k)} - E_{p(a)}$) is a constant value. In our case, the difference of potentials between the peaks at the forward

and reverse scan cycles depends on the electron transition rate constant and the potential scan rate. According to the analysis of the presented cyclic polarization curves, it can be concluded that at high scan rates, the value of the peak potential difference becomes large, and the degree of irreversibility of electron transfer increases. Therefore, high values of difference of potentials of reduction and oxidation peaks are associated with limitations of electron transfer kinetics. Increase of scan rate of the potential from 0.05 mV/s to 1 mV/s causes the reduction peak of magnesium ions ($E_{p(k)}$) in the electrolyte to shift into the cathode region.

The relationship between peak current and potential scan rate for irreversible processes was described by P. Delachay's equation [15]. Analysis of the experimental results of cyclic voltammetry demonstrated linear dependence of the current density of the magnesium reduction peak (i_p) from the square root from the value of the potential scan rate (\sqrt{v}) (Fig. 8). This dependence shows that the line does not pass through the origin indicating the quasi-reversible nature of the investigated process. The diffusion coefficient of magnesium ions (D_{Mg}) was calculated from the dependence i_p from \sqrt{v} according to Randles-Ševčík equation for irreversible processes by the formula:

$$I_p = 0.4463n^{3/2} F^{3/2} C S R^{-1/2} T^{-1/2} D_{CV}^{1/2} v^{1/2}, \quad (1)$$

where, n is the number of electrons per molecule during the reaction; F is the Faraday constant; C is the molar concentration of Mg^{2+} ions; S is the surface area of the electrode; R is the gas constant; T is the absolute temperature; D_{CV} is the chemical diffusion coefficient (cm^2/s), and v is the scan rate (V/s). The diffusion coefficient D_{Mg} calculated by means of cyclic cyclic voltammograms was $1.54 \cdot 10^{-2} cm^2/s$.

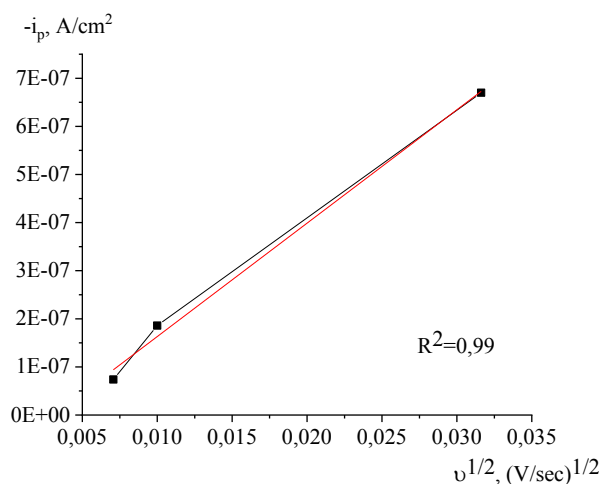


Figure 8. Dependence of current density of peak of magnesium ions intercalation (i_p) into the synthesized electrode on $v^{1/2}$ in 0.25 mol/l $Mg(TFSI)_2/AH$, $T = 25^\circ C$

The rate of charge transfer or mass transfer is the main characteristics of the rate of many electrochemical reactions. Determination of the process mode can be performed by comparing the order of the constants of the transport rate of the matter and the charge. According to cyclic voltammetry, the value of the constant of the charge transfer rate of magnesium ions at the interphase boundary of electrolyte-electrode was determined.

The limiting stage in irreversible processes is charge transfer; the charge velocity is determined by the rate constant (k^0) and the transfer coefficient (α). The boundary conditions of the Nernst equation for irreversible single-step and multi-electron reactions are expressed by the following equation [16; 234–236]:

$$\frac{i}{FA} = k_f(t) C_0(O, t), \quad (2)$$

where

$$k_f(t) = k^0 \exp\left\{-\alpha f [E(t) - E^0]\right\}. \quad (3)$$

If we recalculate $E(t)$ from equation (2) to equation (3), then we get equation (4):

$$k_f(t) C_0(O, t) = k_{fr} C_0(O, t) e^{bt}, \quad (4)$$

where $b = \alpha f v$,

$$k_{fi} = k^0 \exp[-\alpha f (E_i - E^0)]. \quad (5)$$

The current is calculated from the following equation:

$$i = FAC_0^* (\pi D_0 b)^{1/2} \chi^{(bt)}, \quad (6)$$

$$i = FAC_0^* D_0^{1/2} v^{1/2} \left(\frac{\alpha F}{RT} \right)^{1/2} \pi^{1/2} \chi^{(bt)}. \quad (7)$$

The function $\chi^{(bt)}$ passes through a maximum $\pi^{1/2} \chi^{(bt)} = 0.4958$. At recalculating this value, the equation (6) gives the following current peak equation:

$$i_p = (2.99 \cdot 10^5) \alpha^{1/2} AC_0^* D_0^{1/2} v^{1/2}. \quad (8)$$

The peak potential is described by the equation

$$E_p = E^0 - \frac{RT}{\alpha F} \left[0.780 + \ln \left(\frac{D_0^{1/2}}{k^0} \right) + \ln \left(\frac{\alpha F v}{RT} \right)^{1/2} \right]. \quad (9)$$

Next, equation (9) gives equation (10).

$$|E_p - E_{p/2}| = \frac{1.857 RT}{\alpha F} = \frac{47.7}{\alpha} \text{ mV at } 25 \text{ }^\circ\text{C}, \quad (10)$$

where $E_{p/2}$ is a potential, at which the current is half the peak value. For a fully irreversible wave E_p is a function of scan rate, shifting for reduction reaction, in negative direction by value $1.15 \frac{RT}{\alpha F}$ (or $30/\alpha$ mB at $25 \text{ }^\circ\text{C}$) for each ten-fold increase in velocity. Besides, E_p exceed the limit of E^0 (i.e. it is more negative for the reduction reaction) due to excessive activation potential associated with k^0 [17]. Alternative expression for peak current under conditions E_p can be obtained by combining equation (9) with (7):

$$i_p = 0.227 FAC_0^* k^0 \exp[-\alpha f (E_p - E^0)], \quad (11)$$

where E_p is the peak potential (V), E^0 is the formal electrode potential (V), i_p is the cathode current density of the peak (A), k^0 is the rate constant of the charge transfer stage (cm/s), α is the transfer coefficient, D_0 is the diffusion coefficient, (cm²/s), C_0^* is the concentration of ions in the volume of the solution (mol/cm³), C_0 is the concentration in the near-electrode region (mol/cm³), v is the potential scan rate (V/s).

Dependency diagram $\ln i_p$ from $E_p - E^0$ (at condition that E^0 can be obtained) determined at different scan rates must have a slope $-\alpha f$ and k^0 , ordinate of the point of intersection of the diagram with the y axis (Fig. 9).

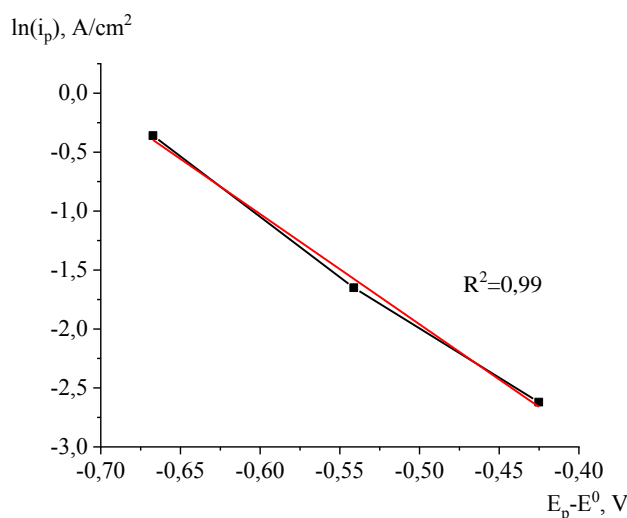


Figure 9. Dependence of logarithm of current density of magnesium intercalation peak in synthesized electrode $\ln(i_p)$ on $E_p - E^0$ in electrolyte 0.25 mol/l Mg(TFSI)₂/AN, T = 25 °C

A dependence of $\ln i_p$ on $E_p - E^0$ (Fig. 9) was obtained from cyclic voltammogram at different scan rates for synthesized electrodes. The charge transfer rate constant calculated from this relationship during magnesium intercalation to the synthesized titanium dioxide electrode in the electrolyte was 0.25 mol/l $\text{Mg}(\text{TFSI})_2/\text{AN}$ equal to $1.29 \cdot 10^{-4}$ cm/s.

Figure 10 points out cyclic voltammograms of intercalation and deintercalation of magnesium ions into a synthesized electrode in a solution of 0.25 mol/l $\text{Mg}(\text{TFSI})_2$ based on acetonitrile at different cycles.

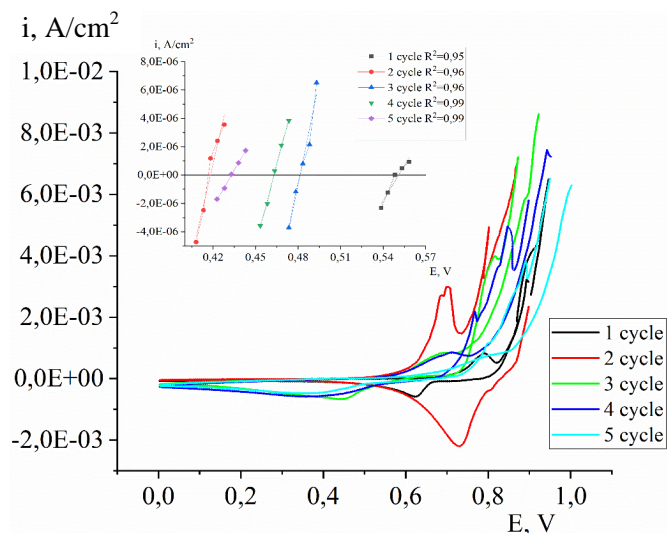


Figure 10. Cyclic voltammogram of intercalation and deintercalation of magnesium ions into a synthesized anode based on titanium dioxide of 0.25 mol/l $\text{Mg}(\text{TFSI})_2/\text{AN}$ at various cycles. Insert: linear site, area of low overvoltage of backward motion of CV, $T = 25^\circ\text{C}$

The amount of electricity (electric charge) is the product of the current strength at the time of current flow, and then the electric charge can be determined from cyclic voltammograms, calculating the ratio of the area of the cathode, and anode peaks. Table 3 presents the values of the amount of cathode, anode charges and the amount of electricity calculated from these data and also the polarization resistance. It can be seen that in the first cycle the amount of electricity is less than one. However, starting from the second cycle to the fifth cycle, the ratio of cathode charge to anode charge is approximately one, which indicates a two-charge electrochemical magnesium reduction reaction.

Table 3

Values of the amount of electricity of cathode and anode processes, as well as polarization resistance at different number of cycles

Cycle	Q_k, C	Q_a, C	Q_k/Q_a	$R_p, \Omega \cdot \text{cm}^2$
1	$9.80 \cdot 10^{-5}$	$1.76 \cdot 10^{-4}$	0.56	$1.29 \cdot 10^{-4}$
2	$3.22 \cdot 10^{-4}$	$2.91 \cdot 10^{-4}$	1.11	$3.40 \cdot 10^{-4}$
3	$1.78 \cdot 10^{-4}$	$2.12 \cdot 10^{-4}$	0.85	$3.82 \cdot 10^{-4}$
4	$1.93 \cdot 10^{-4}$	$1.80 \cdot 10^{-4}$	1.00	$2.95 \cdot 10^{-4}$
5	$1.53 \cdot 10^{-4}$	$1.73 \cdot 10^{-4}$	0.90	$1.35 \cdot 10^{-4}$

The polarization resistance is a measure of the increase in internal resistance of the chemical power source caused by polarization and depends on the passing current. The polarization value was calculated by processing the linear site of the region of small overvoltage of backward motion of cyclic voltammograms. (Fig. 10, insertion) [18]. According to the Table 3, depending on the number of cycles, a certain regularity in the change of the polarization resistance value is not observed: with an increase of the cycle, it first grows and then decreases, although the order is the same. Low polarization resistance values favorably affect the diffusion rate of magnesium ions during discharge and charge of chemical power sources.

Conclusions

In this work, the kinetics of electrochemical processes occurring on the anode in the acetonitrile solution Mg(TFSI)₂ was studied. The diffusion coefficient determined from the cyclic voltammograms was equal to $1.54 \cdot 10^{-2}$ cm²/s, the rate constant was equal to $1.29 \cdot 10^{-4}$ cm/s. The ratio of the electricity amount of the cathodic and anodic processes is approximately equal to one, which led to the reversible charging-discharging of magnesium occurrence.

The anode on the basis of powdered titanium dioxide, which has been prepared according to the scheme demonstrated in this work, illustrated high electrochemical active surface which has seen from the high value of the diffusion coefficient. Morphological and structural characteristics of the obtained anode material were studied by such methods as ellipsometry, Scanning electron microscopy, EDS, and X-ray diffraction. The thickness of the uniformly distributed anodic layer was on the order of 200 μm, and the particles had a diameter of 50 nm to 80 nm and a porous morphology. The XRD results confirmed the formation of an active mass with a monoclinic crystal lattice structure corresponding to the bronze modification with anatase inclusions.

The results obtained in our research is significant for the development of rechargeable magnesium batteries.

Acknowledgments

This work was financially supported by the Ministry of Education and Science of the Republic of Kazakhstan (AP09260383).

References

- 1 Arthur T.S. Electrodeposited Bi, Sb and Bi_{1-x}Sb_x alloys as anodes for Mg-ion batteries / T.S. Arthur, N Singh, M. Matsui // *Electrochemistry Communications*. — 2012. — Vol. 16, No. 1. — P. 103–106. <https://doi.org/10.1016/j.elecom.2011.12.010>
- 2 Truong D.Q. Ultrathin TiO₂ rutile nanowires enable reversible Mg-ion intercalation / Duc Q. Truong, T.S. Le, Thu H. Hoa // *Materials Letters*. — 2019. — Vol. 254. — P. 357–360. <https://doi.org/10.1016/j.matlet.2019.07.109>
- 3 Meng Y. Ultrathin TiO₂-B nanowires as an anode material for Mg-ion batteries based on a surface Mg storage mechanism / Y. Meng, D. Wang, Y. Zhao, R. Lian, Y. Wei, X. Bian, Yu Gao, Fei Du, B. Liu Gang Chen // *Nanoscale*. — 2017. — Vol. 35, No. 9. — P. 12934–12940. <https://doi.org/10.1039/C7NR03493H>
- 4 Le T.S. Shape-controlled F-doped TiO₂ nanocrystals for Mg-ion batteries / T.S. Le, Thu H. Hoa, Duc Q. Truong // *Journal of Electroanalytical Chemistry*. — 2019. — Vol. 848. — P. 113293. <https://doi.org/10.1016/j.jelechem.2019.113293>
- 5 Guo, Q. Recent developments on anode materials for magnesium-ion batteries: a review / Q. Guo, W. Zeng, Shi-Lin Liu, Yan-Qiong Li, Jun-Yao Xu, Jin-Xing Wang, Yu Wang // *Rare Met.* — 2021. — Vol. 40. — P. 290–308. <https://doi.org/10.1007/s12598-020-01493-3>
- 6 Dawson J.A. Improved calculation of Li and Na Intercalation properties in anatase, rutile and TiO₂(B) / J.A. Dawson, J. Robertson // *J. Phys. Chem.* — 2016. — Vol. 120, No. 40. — P. 22910–22917. <https://doi.org/10.1021/acs.jpcc.6b08842>
- 7 Hua X. The morphology of TiO₂ (B) Nanoparticles / X.Hua, Zh. Liu, P.G. Bruce, C.P. Grey // *J. Am. Chem. Soc.* — 2015. — Vol. 137, No. 42. — P. 13612–13623. <https://doi.org/10.1021/jacs.5b08434>
- 8 Arrouvel C. Lithium insertion and transport in the TiO₂-B anode material: a computational study / C. Arrouvel, S.C. Parker, M. S.Islam // *Chem. Mater.* — 2009. — Vol. 21. — P. 4778–4783. <https://doi.org/10.1021/cm900373u>
- 9 Songa T. TiO₂ as an Active or Supplemental Material for Lithium Batteries / T. Songa, U. Paik // *J. Mater. Chem. A*. — 2016. — Vol. 4. — P. 14–31. <https://doi.org/10.1039/C5TA06888F>
- 10 Liu S. A flexible TiO₂(B)-based battery electrode with superior power rate and ultralong cycle life / S. Liu, Z. Wang, C. Yu, H.B. Wu, G. Wang, Q. Dong, J. Qiu, A. Eychmüller, X.W. David Lou // *Adv. Mater.* — 2013. — Vol. 25. — P. 3462–3467. <https://doi.org/10.1002/adma.201300953>
- 11 Hu H. Hierarchical tubular structures constructed from ultrathin TiO₂(B) nanosheets for highly reversible lithium storage / H. Hu, L. Yu, X. Gao, Z. Lin, X.W. Lou // *Energ. Environ. Sci.* — 2015. — Vol. 8. — P. 1480–1483. <https://doi.org/10.1039/C5EE00101C>
- 12 Ren Y. Nanoparticulate TiO₂(B): An Anode for Lithium-Ion Batteries / Y. Ren, Z. Liu, F. Pourpoint, A.R. Armstrong, C.P. Grey, P.G. Bruce // *Angew. Chem. Int. Ed.* — 2012. — Vol. 51. — P. 2164–2167. <https://doi.org/10.1002/anie.201108300>
- 13 Ren Y. Lithium Intercalation into Mesoporous Anatase with an Ordered 3D Pore Structure / Y. Ren, J. Hardwick, P.G. Bruce // *Angew. Chem. Int. Ed.* — 2010. — Vol. 49. — P. 2570–2574. <https://doi.org/10.1002/anie.200907099>
- 14 Feist T.P. The soft chemical synthesis of TiO₂ (B) from layered titanates / T.P. Feist, P.K. Davies // *Journal of Solid State Chemistry*. — 1992. — Vol. 101. — P. 275–295. [https://doi.org/10.1016/0022-4596\(92\)90184-W](https://doi.org/10.1016/0022-4596(92)90184-W)

15 Delahay P. Theory of Irreversible Waves in Oscillographic Polarigraphy / P. Delahay // J. Am. Chem. Soc. — 1953. — Vol. 75. — P. 1190–1196.

16 Bard A. J.A. Electrochemical Methods: Fundamentals and Applications. 2nd Edition. / A.J. Bard, L.R. Faulkner. — JohnWiley and Sons, Inc, 2001. — 864 p. ISBN: 978-0-471-04372-0

17 Avchukir H. Kinetics of electrodeposition of indium on solid electrodes from chloride solutions / H. Avchukir, B.D. Burkitbayeva, A.M. Argimbayeva, G.S. Rakhymbay // Chemical Journal of Kazakhstan. — 2018. — Vol. 2. — P. 197–207.

18 Avchukir H. The kinetics of Indium Electroreduction from Chloride Solutions / H. Avchukir, B.D. Burkitbayeva, A.M. Argimbayeva, G.S. Rakhymbay, G.S. Beisenova, M.K. Nauryzbayev // Russian Journal of Electrochemistry. — 2018. — Vol. 54. — P. 1096–1103. <https://doi.org/10.1134/S1023193518120042>

А.К. Абильдина, Х. Авчукир, Р.Ж. Джуманова,
А.Н. Бейсеева, Г.С. Рахымбай, А.М. Аргимбаева

Магний-ионды батареялар үшін анодты материал ретінде TiO_2 дайындау және оның электрхимиялық сипаттамалары

Мақалада титан диоксиді ұнтағы негізіндегі анод дайындалды және оның морфологиялық сипаттамалары эллипсометрия, сканерлеуші электронды микроскопия (СЭМ), рентген-спектрлік (РСА) және рентген-фазалық анализ (РФА) көмегімен, сонымен қатар циклдік вольтамметрия әдісі арқылы электрхимиялық қасиеттері зерттелді. Электрод жасалынуының негізгі кезеңдері: бастапқы реагенттерді диспергерлеу және араластыру арқылы гомогенді паста алу, төсемеге жағу, кептіру және электродтарды кесу. Эллипсометрия, СЭМ және РСА нәтижелері түйіршіктерінің диаметрі 50–80 нм аралығында болатын, құрамы титан оксидінің бөлшектерінен тұратынын (45,7 %) құрылымы кеуекті, қалыңдығы 200 мкм біркелкі таралған қабат түзілгенін көрсетті. РФА мәліметтері құрамында анатаз бар титан диоксидінің (В) модификациясына сәйкес келетін моноклинді кристалл торына ие белсенді анод матрицасының пайда болатынын дәлелдейді. Дайындалған электродтың электрхимиялық қасиеттері ацетонитрил негізіндегі $Mg(TFSI)_2$ ерітіндісінде зерттелді. Циклдік вольтамперограммалардан диффузия коэффициенті (DMg) мен заряд тасымалдау жылдамдығының константасы (k) анықталды, $1,54 \cdot 10^{-2}$ см²/с және $1,29 \cdot 10^{-4}$ см/с сәйкесінше. Циклдер санын өзгерту арқылы катодтық және анодтық процестерде тұтынылатын электр мөлшерінің қатынасы бойынша екі сатылы электрхимиялық реакция жүретіні көрсетілді. Циклдік вольтамперограммалар бойынша есептелген поляризация кедергісінің төмен мәндері интеркаляция мен деинтеркаляция кезінде магний иондарының жылдам диффузиясын дәлелдейді.

Кілт сөздер: магний-ионды аккумуляторлар, анод, титан диоксиді, синтез, талдау, интеркаляция, деинтеркаляция, кинетика, поляризация, диффузия.

А.К. Абильдина, Х. Авчукир, Р.Ж. Джуманова,
А.Н. Бейсеева, Г.С. Рахымбай, А.М. Аргимбаева

Приготовление и электрохимические характеристики TiO_2 в качестве анодного материала для магний-ионных батарей

В статье описано изготовление анода на основе порошка диоксида титана и исследование его морфологических характеристик с использованием эллипсометрии, сканирующей электронной микроскопии (СЭМ) в купе с рентгено-спектральным (РСА) и рентгено-фазовым анализом (РФА), а также электрохимических свойств методом циклической вольтамперометрии. Основными стадиями изготовления анода выступили: диспергирование, смешивание исходных реагентов с получением гомогенизированной пасты, последующее нанесение ее на подложку, высушивание и нарезка электродов. Результаты эллипсометрии, СЭМ и РСА показали равномерно распределенный слой толщиной порядка 200 мкм с пористой структурой, диаметром частиц в интервале 50–80 нм и содержанием диоксида титана (45,7 %). Данные РФА подтверждают образование активной анодной матрицы с моноклинной кристаллической решеткой, соответствующей модификации диоксида титана (В) с небольшими включениями анатаза. Электрохимическое поведение полученного электрода исследовали в растворе $Mg(TFSI)_2$ на основе ацетонитрила. Из циклических вольтамперограмм были определены коэффициент диффузии (DMg) и константа скорости переноса заряда (k), которые составили $1,54 \cdot 10^{-2}$ см²/с и $1,29 \cdot 10^{-4}$ см/с соответственно. По соотношению количества электричества, расходуемого в катодном и анодном процессах при варьировании количества циклов, была установлена реализация двухступенчатой электрохимической реакции. Малые значения поляризационного сопротивления (Rp), рассчитанного из циклических вольтамперограмм, свидетельствуют о быстрой диффузии ионов магния при интеркаляции/деинтеркаляции.

Ключевые слова: магний-ионные батареи, анод, диоксид титана, синтез, анализ, интеркаляция, деинтеркаляция, кинетика, поляризация, диффузия.

References

- 1 Arthur, T.S., Singh, N., & Matsui, M. (2012). Electrodeposited Bi, Sb and Bi_{1-x}Sb_x alloys as anodes for Mg-ion batteries. *Electrochemistry Communications*, 16(1), 103–106. <https://doi.org/10.1016/j.elecom.2011.12.010>
- 2 Truong, D.Q., Le, T.S., & Hoa, T.H. (2019). Ultrathin TiO₂ rutile nanowires enable reversible Mg-ion intercalation. *Materials Letters*, 254, 357–360. <https://doi.org/10.1016/j.matlet.2019.07.109>
- 3 Meng, Y., Wang, D., Zhao, Y., Lian, R., Wei, Y., & Bian, X., et al. (2017). Ultrathin TiO₂-B nanowires as an anode material for Mg-ion batteries based on a surface Mg storage mechanism. *Nanoscale*, 35(9), 12934–12940. <https://doi.org/10.1039/C7NR03493H>
- 4 Le, T.S., Hoa, T.H., & Truong, D.Q. (2019). Shape-controlled F-doped TiO₂ nanocrystals for Mg-ion batteries. *Journal of Electroanalytical Chemistry*, 848, 113293. <https://doi.org/10.1016/j.jelechem.2019.113293>
- 5 Guo, Q., Zeng, W., Liu, Sh.L., Li, Y.Q., Xu, J.Y., Wang, J.X., & Wang, Y. (2021). Recent developments on anode materials for magnesium-ion batteries: a review. *Rare Metals*, 40, 290–308. <https://doi.org/10.1007/s12598-020-01493-3>
- 6 Dawson, J.A., & Robertson, J. (2016). Improved calculation of Li and Na Intercalation properties in anatase, rutile and TiO₂(B). *The Journal of Physical Chemistry*, 120(40), 22910–22917. <https://doi.org/10.1021/acs.jpcc.6b08842>
- 7 Hua, X., Liu, Zh., Bruce, P.G., & Grey, C.P. (2015). The morphology of TiO₂ (B) Nanoparticles. *Journal of the American Chemical Society*, 137(42), 13612–13623. <https://doi.org/10.1021/jacs.5b08434>
- 8 Arrouvel, C. Parker, S.C., & Islam, M.S. (2009). Lithium insertion and transport in the TiO₂-B anode material: a computational study. *Chemistry of Materials*, 21, 4778–4783. <https://doi.org/10.1021/cm900373u>
- 9 Song, T., & Paik, U. (2016). TiO₂ as an Active or Supplemental Material for Lithium Batteries. *Journal of Materials Chemistry*, 4(1), 14–31. <https://doi.org/10.1039/C5TA06888F>
- 10 Liu, S., Wang, Z., Yu, C., Wu, H.B., Wang, G., & Dong, Q., et al. (2013). A flexible TiO₂(B)-based battery electrode with superior power rate and ultralong cycle life. *Advanced materials*, 25, 3462–3467. <https://doi.org/10.1002/adma.201300953>
- 11 Hu, H., Yu, L., Gao, X., Lin, Z., & Lou, X.W. (2015). Hierarchical tubular structures constructed from ultrathin TiO₂(B) nanosheets for highly reversible lithium storage. *Energy & Environmental Science*, 8, 1480–1483. <https://doi.org/10.1039/C5EE00101C>
- 12 Ren, Y., Liu, Z., Pourpoint, F., Armstrong, A.R., Grey, C.P., & Bruce, P.G. (2012). Nanoparticulate TiO₂(B): An Anode for Lithium-Ion Batteries. *Angewandte Chemie International Edition*, 51, 2164–2167. <https://doi.org/10.1002/anie.201108300>
- 13 Ren, Y., Hardwick, J., & Bruce, P.G. (2010). Lithium Intercalation into Mesoporous Anatase with an Ordered 3D Pore Structure. *Angewandte Chemie International Edition*, 49, 2570–2574. <https://doi.org/10.1002/anie.200907099>
- 14 Feist, T.P., & Davies, P.K. (1992). The soft chemical synthesis of TiO₂ (B) from layered titanates. *Journal of Solid State Chemistry*, 101, 275–295. [https://doi.org/10.1016/0022-4596\(92\)90184-W](https://doi.org/10.1016/0022-4596(92)90184-W)
- 15 Delahay, P. (1953). Theory of Irreversible Waves in Oscillographic Polarigraphy. *Journal of the American Chemical Society*, 75, 1190–1196.
- 16 Bard, A.J., & Faulkner, L.R. (2001). *Electrochemical Methods: Fundamentals and Applications*. 2nd Edition. John Wiley and Sons, Inc. ISBN: 978-0-471-04372-0
- 17 Avchukir, H., Burkitbayeva, B.D., Argimbayeva, A.M., & Rakhymbay, G.S. (2018). Kinetics of electrodeposition of indium on solid electrodes from chloride solutions. *Chemical Journal of Kazakhstan*, 2, 197–207.
- 18 Avchukir, H., Burkitbayeva, B.D., Argimbayeva, A.M., Rakhymbay, G.S., Beisenova, G.S., & Nauryzbayev, M.K. (2018). The kinetics of Indium Electroreduction from Chloride Solutions. *Russian Journal of Electrochemistry*, 54, 1096–1103. <https://doi.org/10.1134/S1023193518120042>

Information about authors

Abildina Ainaz Kairatovna — PhD, assistant professor of Satbayev University, Senior Researcher of the laboratory “Protection of metals from corrosion” of the Center of Physical Chemical Methods of Research and Analysis, Al-Farabi Kazakh National University, Kazakhstan, Almaty, Tole bi str., 96A. e-mail: a.abildina@satbayev.university; <https://orcid.org/0000-0003-1761-7691>

Avchukir Khaiza — PhD, Senior Lecturer of the Department of Analytical, Colloid Chemistry and Technology of Rare Elements, Faculty of Chemistry and Chemical Technology, Senior Researcher of the laboratory “Protection of metals from corrosion” of the Center of Physical Chemical Methods of Research and Analysis, Al-Farabi Kazakh National University, Kazakhstan, Almaty, Tole bi str., 96A. e-mail: avchukir9@gmail.com; <https://orcid.org/0000-0001-6612-0775>

Jumanova Raigul — 3-rd year PhD student, Department of Analytical, Colloid Chemistry and Technology of Rare Elements, Faculty of Chemistry and Chemical Technology, Researcher of the laboratory “Protection of metals from corrosion” of the Center of Physical Chemical Methods of Research and Analysis, Al-Farabi Kazakh National University, Kazakhstan, Almaty, Tole bi str., 96A. e-mail: r.zh.shohaeva@mail.ru; <https://orcid.org/0000-0003-3826-3474>

Beiseyeva Assemay — 2-nd year Master’s student, Department of Analytical, Colloid Chemistry and Technology of Rare Elements, Faculty of Chemistry and Chemical Technology, Researcher of the laboratory “Protection of metals from corrosion” of the Center of Physical Chemical Methods of Research and Analysis, Al-Farabi Kazakh National University, Kazakhstan, Almaty, Tole bi str., 96A. e-mail: asbeis999@gmail.com; <https://orcid.org/0000-0001-8711-6150>

Rakhymbay Gulmira — PhD, Senior Lecturer of the Department of Analytical, Colloid Chemistry and Technology of Rare Elements, Faculty of Chemistry and Chemical Technology, Senior Researcher of the laboratory “Protection of metals from corrosion” of the Center of Physical Chemical Methods of Research and Analysis, Al-Farabi Kazakh National University, Kazakhstan, Almaty, Tole bi str., 96A. e-mail: gulmira.rakhymbay@kaznu.kz; <https://orcid.org/0000-0002-8814-9752>

Argimbayeva Akmaral — Candidate of Chemical Sciences, Associate Professor of the Department of Analytical, Colloid Chemistry and Technology of Rare Elements, Faculty of Chemistry and Chemical Technology, Main Researcher of the laboratory “Protection of metals from corrosion” of the Center of Physical Chemical Methods of Research and Analysis, Al-Farabi Kazakh National University, Kazakhstan, Almaty, Tole bi str., 96A. e-mail: akmaral.argimbayeva@gmail.com; <https://orcid.org/0000-0002-2467-8241>

Sh.K. Amerkhanova, A.S. Uali, R.M. Shlyapov*, D.S. Belgibayeva

L.N. Gumilyov Eurasian National University, Nur-Sultan, Kazakhstan
(*Corresponding author's e-mail: rustamshlyapov@gmail.com)

Alkali-activated metallurgical slag as a sustainable adsorbent

This paper is devoted to obtaining a zeolite-containing sorbent based on metallurgical waste — slag. The synthesis of zeolite adsorbent from ash and slag was carried out by hydrochemical and thermal treatment. The initial object and the obtained material were characterized using following methods: Fourier-transform infrared spectroscopy, scanning electron microscopy, energy dispersive analysis, X-ray phase analysis, titrimetry. The way of converting solid-phase waste into a beneficial product has been demonstrated. The study results showed that the surface of the obtained material is saturated with functional groups (hydroxy-, carboxy-, lactone), which predetermine the ability to bind metal ions during adsorption. The adsorption capacity of the product has been estimated for iodine and methylene blue. A thermodynamic analysis of the process of sorption of copper (II) ions from an aqueous solution has been conducted. It has identified that the sorbent can also be used for the adsorptive concentration of ions of rare-earth elements by the example of lanthanum and erbium. Laboratory testing of the possible use of the sorbent to purify industrial water was carried out using the example of wastewater from a chromium plating shop.

Keywords: metallurgical slag, recycling of slag, sorbents, sorption, absorption capacity, d-, f-metals ions, wastewaters purification, sorption isotherms, thermodynamics of adsorption.

Introduction

Zeolite materials are of great fundamental and industrial importance and widely used as commercial adsorbents and catalysts. All the unique properties of zeolites are specified with their structure based on porous aluminosilicates formed by a combination of tetrahedral $[\text{SiO}_4]_4^-$ and $[\text{AlO}_4]_5^-$. One way to obtain them is to converse metallurgical wastes into zeolites; however, the phase composition of the material obtained by the hydrochemical pathway is controlled by various factors such as temperature, type of modifying agent and its concentration, pH of the media, etc. [1–5].

The purification of natural and industrial water bodies from copper ions is a significant environmental issue due to its relatively high toxicity. The threshold limit value (TLV) for copper ions in drinking and sanitary waters for domestic and industrial use is 1 mg/L, then 0.001 mg/L is for reservoirs of fish economic purpose. Thus, practice shows the residual concentration of Cu in water purified at pH level from 8 to 9 is 0.1–0.2 mg/L generally, which conforms to theoretical calculations on the solubility of copper hydroxide in aqueous solutions [6, 7]. This issue may be solved by applying sorption methods of purification with inorganic sorbents. However, even though a considerable amount of research focused on an in-depth investigation of how to turn slag into a beneficial material (in this case, adsorbent), many open questions should be answered to clarify this mechanism [7–13].

This paper aims to demonstrate the behavior of the alkali-treated metallurgical slag in the water purification by testing it for both model metal-containing solutions and in industrial multi-component water system.

Experimental

The solid-phase waste of the metallurgy plant “ArcelorMittal Temirtau” was applied as a raw material. The technique that consists of two stages is used to design the adsorbent. Firstly, the initial material has been washed with distilled water for 48 h, then has been dried at room temperature. The ratio of S/L was one to ten (by weight). The intermediate was treated thermally in the muffle furnace at the temperature of 600 °C for 90 min. in the presence of sodium hydroxide solution (2 mol/L) used as a modifying agent. The ratio of S:L was the same. The final product has been tested for the adsorption properties.

The following methods have been applied to characterize the material synthesized: X-ray Powder Diffraction (XRD) analysis was conducted using the DRON-4-07 diffractometer. The scanning electron microscope Hitachi TM3030 with microanalysis system Bruker X Flash MINSVE (accelerating voltage of 15 kV) has been used to determine the elemental composition and structural features of the adsorbent. Finally, the IR-spectra of the samples have been taken by FTIR-spectrometer FSM-1201.

The concentration of functional groups concentrated on the adsorbent's surface has been determined by the Boehm method described in [14]. In addition, the material capacity in the adsorption toward iodine and methylene blue has been estimated by well-known procedures [15, 16]. Regarding the adsorption tests, samples of industrial multi-component waters have been taken to purify by the adsorption in a static mode at a temperature of 298 K. The duration of this treatment was 30 minutes. The analyte's volume of each portion was 20 ml, the mass of adsorbent for each test was 0.5 g. Both spectrophotometry and titration methods have been used to detect initial and residual concentrations of metal ions. The chemical composition of the water taken from industry has been detected by the XRF method (on the X-MET 8000 GEO portable X-ray fluorescence analyzer) before and after the adsorption tests.

The adsorption experiments with the wastewater taken from the industry were carried out at the following conditions: temperature was 293 K, mass of each portion of the sorbent was 0.5 g, the duration of the adsorbent/adsorbate contact was 19 h in the static mode. The stirring frequency with a magnetic router was 500 rpm. Three parallel series of purification experiments were performed.

Results and Discussion

It is known that the bulk of solid wastes like ashes and slags consists of both macroelements (Al, Fe, Ca, Si, Mg, S, C), which are significant constituents of mineral rocks, and microelements as minor components [17].

Experimentally (based on XRD analysis), the phase composition of the slag has included $\text{Ca}_5\text{Al}_2(\text{OH})_4\text{Si}_3\text{O}_{12}$, Fe_2O_3 , $\text{Mg}_3\text{Al}_4\text{TiO}_{25}$, MnS , and $\text{KOH}\cdot\text{H}_2\text{O}$ that are likely to be products of the coal agglomeration. However, after the thermal treatment experienced by the slag sample, which had dried before, there was a radical change in color that turns from greyish to light blue (Fig. 1), which can be caused by phase transformations.



Figure 1. The slag dispersed of the metallurgical enterprise “Arcelor Mittal Temirtau” (I); sorbent obtained after alkaline treatment (II)

The elemental composition of the material has been determined by the energy dispersive X-Ray analysis (EDXRA) (Fig. 2, 3); the ratio of Si/Al is 20.62 approximately, which is consistent with high-silica zeolites (Si/Al ratio for them is from 10 to ∞) [18].

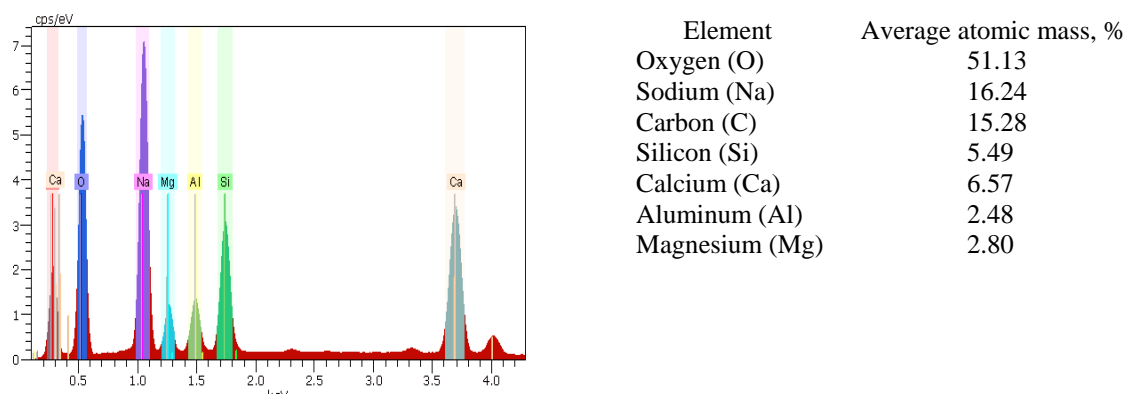


Figure 2. The EDXRA spectra and elemental composition of alkali-treated metallurgical slag

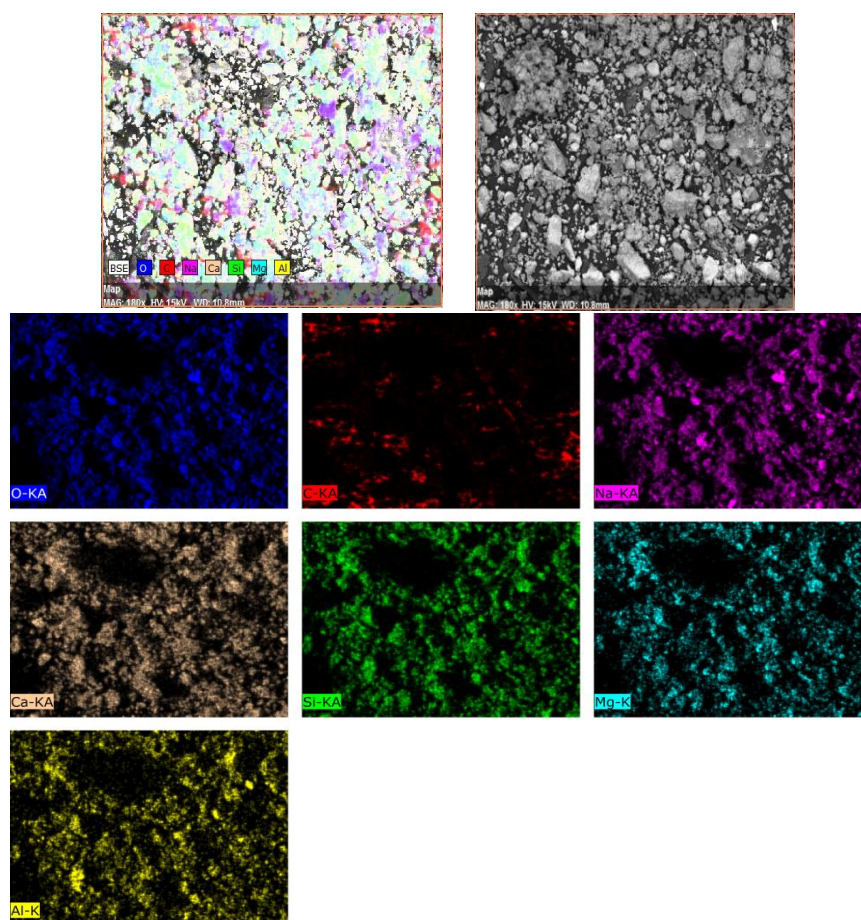


Figure 3. EDXRA pictures of alkali-treated metallurgical slag

The FTIR spectra of the studied samples can be conditionally divided into three frequency regions <470 – 1600 , 1600 – 2900 , and >2900 cm^{-1} (Fig. 4).

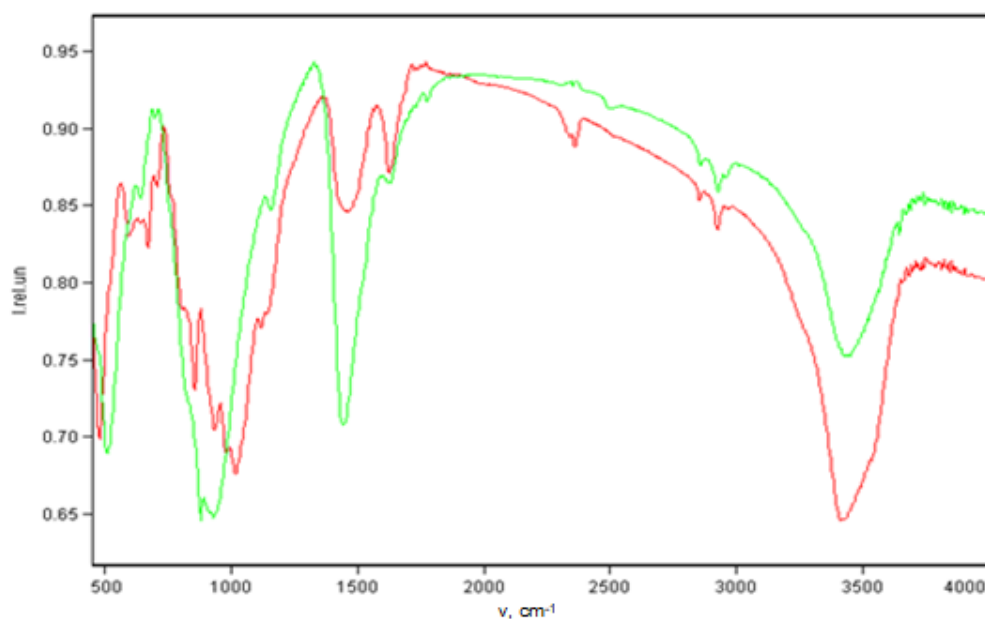


Figure 4. FT-IR spectra of the initial slag (green) and the alkali-treated sample (red)

The first region (<470 – 1600 cm^{-1}) includes vibration bands of Si-O (Si), SO_4^{2-} , Al-OH, Si-O groups. The prominent absorption bands present in all spectra are rather intense bands at 777 cm^{-1} . Since the Si-O

bond is common for all silicates and clay materials, it may be assumed that the absorption bands in the region of $777\text{--}1135\text{ cm}^{-1}$ are mainly due to the stretching vibrations of Si-O.

Because of alkaline treatment, changes occur on the material surface, which are observed in the FTIR spectrum in the form of a shift of absorption bands in one direction or another. For example, the absorption band at 509 cm^{-1} is shifted to the left by 19 cm^{-1} . The absorption band at 928 cm^{-1} has shifted to the right by 155 cm^{-1} . The intensity of the absorption band at 1442 cm^{-1} due to alkaline treatment decreases by a 0.15 relative unit (a.u.).

It can be seen from the above spectra that in the second region ($1600\text{--}2900\text{ cm}^{-1}$), the intensity of the absorption band at 2350 cm^{-1} as a result of alkaline treatment of the material increases by 0.05 a.u. The intensity of the absorption band at $2800\text{--}2900\text{ cm}^{-1}$ due to alkaline treatment increases by 0.02–0.03 relative units.

The third region $> 2900\text{ cm}^{-1}$ is mainly associated with the stretching vibrations of OH-groups its presence can be seen at absorption band 3435 cm^{-1} . Absorption in the region of $3440\text{--}3738\text{ cm}^{-1}$ is presented as bands associated with vibrations of free O-H groups. An absorption band at 3435 cm^{-1} increases by 0.07 a.u. in the intensity after the alkali treatment.

In addition, there is a growth in the intensity of the absorption band at $3647\text{--}3738\text{ cm}^{-1}$ by 0.04 a.u. after the treatment.

The results of the Boehm method based on acid-base titration have revealed that there are carboxyl, hydroxyl and lactone groups on the adsorbent surface (Table 1).

Table 1

Content of carboxyl-, hydroxyl and lactone functional groups in the sorbent sample

Functional group	Total	Hydroxyl groups	Carboxyl groups	Lactone groups
Concentration [mmole/g]	1.06	0.44	0.30	0.32

According to [14], the adsorbent samples were examined for the adsorption concentration of iodine and methylene blue (MB) (Table 2).

Table 2

Adsorption capacity of the sorbent synthesized toward iodine and MB

Adsorbate	Adsorption capacity	
	Carbon sorbent [17–18]	Synthesized sorbent
Iodine X, %	25.00	13.65
Methylene blue A, mg/g	40.00	55.00

It is found that sorbent has an adequate sorption capacity towards both substances. Nevertheless, compared to the carbon sorbent, the slag-based one works better for MB, while the former one is approximately twice efficient for iodine. Generally, it should be assumed zeolite-templated sorbent is applicable for the capture of organic and inorganic pollutants.

As for the capture of metal ions, copper was chosen for the adsorption tests. Figure 5 demonstrates the dependence of the adsorption capacity (a_e) on pH, and the highest a_e values have been achieved at pH 4,6–7.

However, these high indexes in the pH range 6–7 are likely to be related to the impact of hydrolysis that foster copper (II) hydroxide to form and precipitate. At pH 4, the deprotonation of hydroxyl groups increases the number of negatively charged centers on the sorbent surface. Since a negative charge raises the electrostatic gravitational force on the surface of sorbent and metal ions, the latter ones begin to concentrate on the sorbent surface quickly. Thus, further experimental tests were carried out at pH 4.

The adsorption isotherms for the pair consisting of alkali-treated slag as adsorbent and Cu^{2+} ions as adsorbate (at 318 K, under static conditions) are presented in Figure 6.

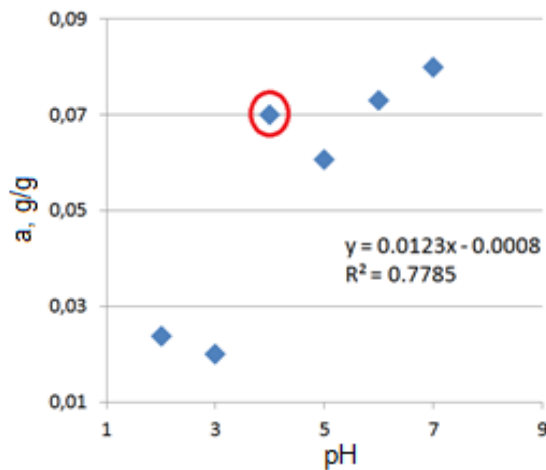


Figure 5. Effect of pH on the adsorption of copper (II) ions by the slag-based sorbent in aqueous solutions

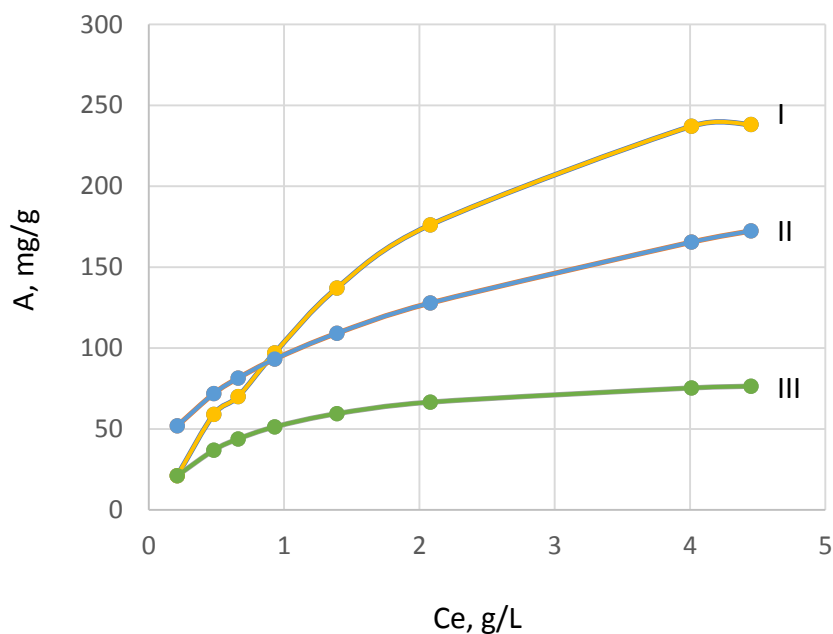


Figure 6. Adsorption isotherms Cu(II) onto sorbent at 318 K and pH 4: plotted from experimental data (I). Theoretical isotherms Freundlich (II) and Langmuir (III)

There is a level off at 4 g/L with the degree of purification of $\approx 88.72\%$ (Fig. 6(I)). In [19], authors have compared the adsorption capacities of copper (II) ions on various low-cost adsorbents: diatomite (27.55 mg/g) and modified diatomite (55.56 mg/g) [20], cassava waste (56.82 mg/g) [21], dehydrated wheat bran (51.51 mg/g) [22]; around low concentrations up to 1 g/L the sorbent investigated is likely to be the alternative to them. If the metal concentration is higher than 1 g/L, the adsorbent behaviors likely the materials based on citric acid modified soybean hulls (154.90 mg/g) [23], modified orange peel (289 mg/g) [24] or nanoporous metal-organic framework MOF-5 (290 mg/g) [24].

Next, the experimental adsorption isotherm was processed using the Langmuir and Freundlich equations. By comparing the approximation coefficients and the location of isotherms on the diagram can be concluded Freundlich's model is more suitable for this case. Finally, the thermodynamic parameters that describe Cu(II) adsorption onto the slag-based sorbent from aqueous solutions have been calculated (Table 3).

The adsorption constants for the Freundlich model and thermodynamic parameters of the adsorption of Cu(II) ions onto the sorbent

Value	298 K	318 K
1/n	0.41	0.39
$K \cdot 10^{-3}$	0.096	0.090
Correlation coefficient	0.97	0.99
$-\Delta H$, kJ/mole	2.29	
$-\Delta G$, kJ/mole	11.16	12.06
ΔS , J/mole·K	29.77	30.73

The values of the isobar-isothermal potential have a negative sign that indicates the spontaneous character of the adsorption. The higher temperature is, the higher are the Gibbs energy values. The chemisorption type of adsorption can be predicted on the basis of the change in enthalpy equal to -2.29 kJ/mole. The positive value of the change in entropy is likely to correspond to the feasibility of adsorption and the randomness that is raised at the sorbent/solution interface due to the adsorption of metal ions onto the slag-based material.

Besides that, the zeolite-templated sorbent is used to concentrate rare metals ions from aqueous solutions on the example of lanthanum (III) and erbium (III) (Table 4).

Table 4

Concentration of La^{3+} , Er^{3+} ions on the sorbent surface

Metal ions	r_{ion} , pm	a , mole/g	X , %
La^{3+}	101	$5 \cdot 10^{-4}$	99.80
Er^{3+}	226	$5 \cdot 10^{-5}$	99.90

Thus, the results demonstrated that the level of extraction is high for both La and Er. The literature review of the La(III) sorption capacities of different sorbents, illustrated that though the different experimental conditions, the reported materials has comparable sorption capacities: $\text{SnO}_2\text{-TiO}_2$ NCs nanocomposites [26] and polydopamine/nanofibrous mats [27], showing 0.473 and 0.429 mmole/g, respectively. That is close to the sorbent with 0.50 mmole/g in this work (Table 4), whilst grapefruit peel has an adsorption capacity of 1.233 mmole/g [28]. As for Er(III) ions, the sorbent based on rice husk demonstrates the monolayer capacity of $250 \text{ mg} \cdot \text{g}^{-1}$ for Er(III) [29] that is higher than the material developed has.

Regarding the purification of industrial waters, the investigated sorbent has been tested toward the wastewater that is oversaturated with metals ions from the chromium plating shop of the metallurgical plant "ArcelorMittal Temirtau". The following diagrams (Fig. 7–9) provides the results obtained by comparing the total content of metals before and after the purification (the conditions are presented in *Experimental*).

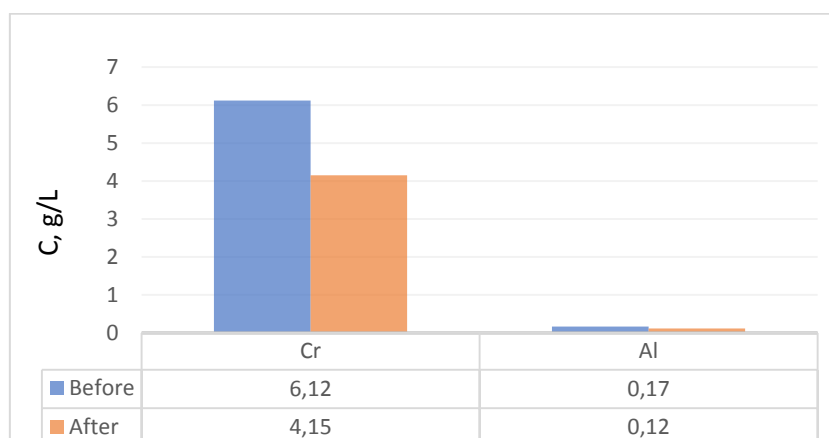


Figure 7. The change in the content of Cr and Al in the wastewater before purification and after

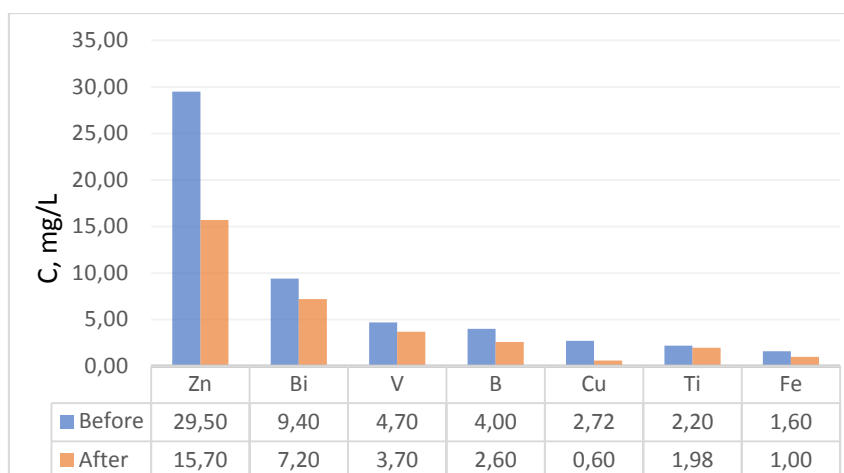


Figure 8. The change in the content of Zn, Bi, V, B, Cu, Ti, and Fe in the wastewater before and after purification

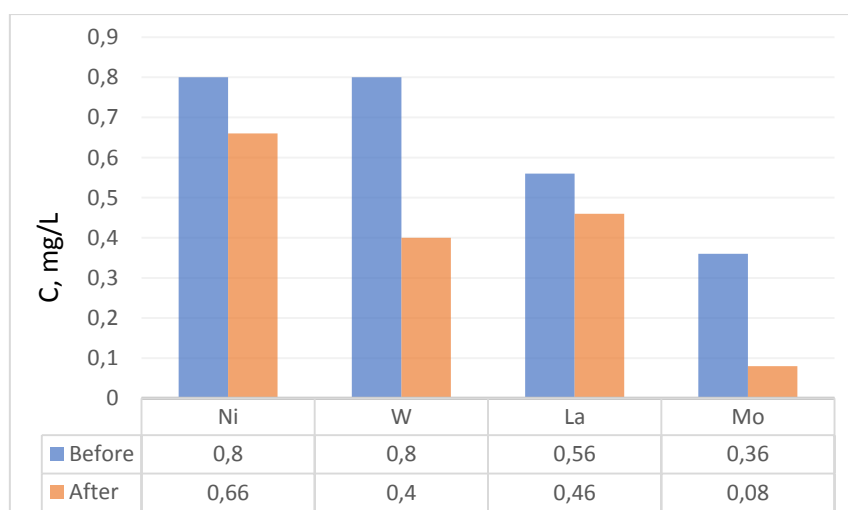


Figure 9. The change in the content of Ni, W, La, and Mo in the wastewater before and after purification

There is an overall trend of decreasing the concentrations for all metals tested. Turning to the details, the amounts of chromium and aluminum as main components have been down by 32.19 and 29.41 %, respectively. Likewise, the concentrations of zinc and wolfram have halved after the adsorption. As for copper and molybdenum, their amount in the wastewater has declined by four times approximately.

Conclusion

To sum up, it may be concluded that zeolite-templated adsorbent obtained by two-stage hydrochemical and thermochemical treatment from metallurgical slag has been influential in wastewater purification based on adsorption.

The possibility of using the sorbent obtained in water purification has been evaluated on the examples of model solutions that contains copper (II) ions and rare metal ions. Besides that, the adsorbent's capacity toward industrial wastewater from the metallurgical enterprise "ArcelorMittal Temirtau" has been estimated. Therefore, it can be assumed that obtained sorbent may be used in the sewage treatment.

References

- 1 Yong L. Synthesis and characterization of zeolite from coal fly ash / L. Yong, L. Qiong, W. Guodong, L. Xianlong, N. Ping // Journal Materials research express. — 2018. — Vol.5. — P. 1–5.
- 2 Худякова Л.И. Использование золошлаковых отходов тепловых электростанций / Л.И. Худякова, А.В. Залутский, П.Л. Палеев // XXI век. Техносферная безопасность. — 2019. — Т. 4, № 3. — С. 290–306.

- 3 Сигачев Н.П. Эффективность использования золошлаковых отходов Забайкальского края при производстве дорожно-цементных грунтов / Н.П. Сигачев, Н.А. Коновалова, В.И. Коннов, П.П. Панков, Н.С. Ефименко // *Экология и промышленность России*. — 2015. — Т. 19, № 1. — С. 24–27.
- 4 Казаков С.В. Принципы оценки радиоэкологического состояния водных объектов / С.В. Казаков // *Журн. радиационной биологии России*. — 2004. — Т. 44, № 6. — С. 694–700.
- 5 Pan M. Application of Nanosize Zeolite Molecular Sieves for Medical Oxygen Concentration/M. Pan, H.M. Omar, S. Rohani//*Nanomaterials (Basel)*. — 2017. — Vol. 7, № 8. — P. 195.
- 6 Tyagi B. Separation of oxygen and nitrogen from air by molecular sieve adsorbents/ B. Tyagi, C.D. Chudasama, R. Jasra//*Journal of the Indian Chemical Society*. — 2001. — Vol. 78. — P. 551–563.
- 7 Линников О.Д. Сорбция ионов меди фильтрующим материалом АС/ О.Д. Линников, И.В. Родина, А.П. Тютюнник, Д.А. Еселевич, Л.Л. Соколова // *Сорбционные и хроматографические процессы*. — 2017. — Т. 17, № 1. — С. 78–86.
- 8 Hutson N.D. Influence of residual water on the adsorption of atmospheric gases in Li-X zeolite: experiment and simulation / N.D. Hutson, S.C. Zajic, R.T. Yang // *Industrial & Engineering Chemistry Research*. — 2002. — Vol. 39, № 6. — P. 1775–1780.
- 9 Kim H. Characterization of Adsorption Enthalpy of Novel Water-Stable Zeolites and Metal-Organic Frameworks / H. Kim, H.J. Cho, Sh. Narayanan // *Scientific Report*. — 2016. — Vol. 6. — P. 19097.
- 10 Fomicheva T.I. Lignine Active Coals Used for Purification of Solutions from Inorganic Cations / T.I. Fomicheva, E.V. Koluzhnikova, J.S. Fomichev, N.G. Mihajlova // *13th International Congress Phitopharm: the book of abstracts (July, 29–31 2009)*. — Bonn, Germany, 2009. — P. 39.
- 11 Hamdi N. Removal of Phosphate Ions from Aqueous Solution Using Tunisian Clays Munerals and Synthetic Zeolite / N. Hamdi, E. Srasra // *Journal of Environmental Sciences*. — 2012. — Vol. 24, № 4. — P. 617–623.
- 12 Amerkhanova Sh.K. The active carbons modified by industrial wastes in process of sorption concentration of toxic organic compounds and heavy metals ions / Sh.K. Amerkhanova, R.M. Shlyapov, A.S. Uali // *Colloids and Surfaces A: Physicochemical and Engineering Aspects*. — 2017. — Vol. 532. — P. 36–40.
- 13 Nazarenko O. Application of Sakhaptinsk Zeolite for Improving the Quality of Ground Water / O. Nazarenko, R. Zarubina // *Energy and Environmental Engineering*. — 2013. — Vol. 1, № 2. — P. 68–73.
- 14 Boehm H.P. Chemical identification of surface groups. *Advances in catalysis and related subjects*. — 1966. — Vol. 16. — P. 197–274.
- 15 ГОСТ 6217–74. (1976). Уголь активный древесный дробленый. Технические условия. МКС 71.100.40, ОКП 21 6239.
- 16 ГОСТ 21283–93 (1983). Глина бетонитовая для тонкой строительной керамики. Методы определения показателя адсорбции емкости катионного обмена.
- 17 Blissett R.S. A review of the multi-component utilisation of coal fly ash / R.S. Blissett, N.A. Rowson // *Fuel*. — 2012. — Vol. 97. — P. 1–23.
- 18 Wang Ch. Quantitative arrangement of Si/Al ratio of natural zeolite using acid treatment / Ch. Wang, Sh. Leng, H. Guo, J. Yu, W. Li // *Applied Surface Science*. — 2019. — Vol. 498. — P. 143874.
- 19 Ojedokun At. (2015). An Overview of Low Cost Adsorbents for Copper (II) Ions Removal / At. Ojedokun, S.B. Olugbenga // *J Biotechnol Biomater*. — 2015. — Vol. 5(1). — P. 1000177.
- 20 Feng D. Removal of pollutants from acid mine wastewater using metallurgical by-product slags / D. Feng, JSJ. Van Deventer, Ch. Aldrich // *Sep. Purif. Technol*. — 2004. — Vol. 40(1). — P. 61–7.
- 21 Abia A.A. The use of chemically modified and unmodified cassava waste for the removal of Cd, Cu and Zn ions from aqueous solution / A.A. Abia, M.Jr. Horsfall, O. Didi // *Bioresour. Technol*. — 2003. — Vol. 90. — P. 345–348.
- 22 Ozer A. The adsorption of copper (II) ions on to dehydrated wheat bran (DWB): determination of the equilibrium and thermodynamic parameters / A. Ozer, D. Ozer, A. Ozer // *Process Biochem*. — 2004. — Vol. 39. — P. 2183–2191.
- 23 Marshall W.E. Enhanced metal adsorption by soybean hulls modified with citric acid / W.E. Marshall, L.H. Wartelle, D.E. Boler, M.M. Johns, and C.A. Toles // *Bioresour. Technol*. — 1999. — Vol. 69(3). — P. 263–268.
- 24 Feng N. Adsorption study of copper (II) by chemically modified orange peel / N. Feng, X. Guo, S. Liang // *J. Hazard. Mater*. — 2009. — Vol. 164(2–3). — P. 1286–1292.
- 25 Bakhtiari N. Adsorption of copper ion from aqueous solution by nanoporous MOF-5: A kinetic and equilibrium study / N. Bakhtiari, S. Azizian // *Journal of Molecular Liquids*. — 2015. — Vol. 206. — P. 114–118.
- 26 Rahman M.M. SnO₂-TiO₂ nanocomposites as new adsorbent for efficient removal of La (III) ions from aqueous solutions /M.M. Rahman, S.B. Khan, H.M. Marwani, A.M. Asiri // *J. Taiwan Inst. Chem. Eng*. — 2014. — Vol. 45. — P. 1964–1974.
- 27 Hong G. Nanofibrous polydopamine complex membranes for adsorption of lanthanum (III) ions / G. Hong, L. Shen, M. Wang, Y. Yang, X. Zhu, M. Wang, B.S. Hsiao // *Chem. Eng. J*. — 2014. — Vol. 244. — P. 307–316.
- 28 Torab-Mostaedi M. Biosorption of lanthanum and cerium from aqueous solutions by grapefruit peel: equilibrium, kinetic and thermodynamic studies / Torab-Mostaedi, M., Asadollahzadeh, M., Hemmati, A., Khosravi, A. // *Res. Chem. Intermed*. — 2013. — Vol.41. — P. 559–573.
- 29 Awwad N.S. Sorption of lanthanum and erbium from aqueous solution by activated carbon prepared from rice husk / N.S. Awwad, H.M.H. Gad, M.I. Ahmad, H.F. Aly // *Colloids and Surfaces B: Biointerfaces*. — 2010. — Vol. 81(2). — P. 593–599.

Ш.К. Амерханова, А.С. Уәли, Р.М. Шляпов, Д.С. Белгібаева

Сілтімен белсендендірілген металлургиялық қож тұрақты сорбент ретінде

Мақала металлургиялық қалдықтар — шлактар негізінде цеолит бар сорбент алуға арналған. Құл мен қождан цеолит адсорбентінің синтезі гидрохимиялық және термиялық өңдеу арқылы жүргізілген. Бастапқы объект және алынған материал келесі талдау әдістерін қолдану арқылы сипатталды: ИҚ-Фурье спектроскопия, сканерлейтін электронды микроскопия, энергия дисперсиялық анализ, рентгендік фазалық талдау, титриметрия. Қатты фазалық қалдықтарды пайдалы өнімге айналдыру тәсілі берілген. Зерттеу нәтижелері көрсеткендей, алынған материалдың беті адсорбция кезінде металл иондарын байланыстыру қабілетін алдын-ала анықтайтын функционалды топтармен (гидрокси-, карбокси-, лактон) қаныққан. Өнімнің адсорбциялық қабілеті йод пен метилен көгіне қатысты бағаланады. Мыс (II) иондарының сулы ерітіндіден сорбциялану процесіне термодинамикалық талдау жасалған. Сорбентті лантан мен эрбий мысалында сирек-жер элементтерінің иондарының адсорбтивті концентрациясы үшін де қолдануға болатындығы көрсетілген. Өндірістік суды тазарту үшін сорбентті қолдану мүмкіндігінің зертханалық сынағы хромдау цехының ағынды суларының мысалында жүргізілді.

Кілт сөздер: металлургиялық қож, қожды өңдеу, сорбенттер, сорбция, сорбция қабілеті, *d*-, *f*-металл иондары, ағынды суларды тазарту, сорбциялық изотермалар, адсорбцияның термодинамикасы.

Ш.К. Амерханова, А.С. Уали, Р.М. Шляпов, Д.С. Бельгибаева

Металлургический шлак, активированный щелочью, как устойчивый адсорбент

Статья посвящена получению цеолитсодержащего сорбента на основе отходов металлургического производства — шлака. Синтез цеолитного адсорбента из золошлака проводился посредством гидрохимической и термической обработки. Исходный объект и полученный материал охарактеризованы следующими методами анализа: ИК-Фурье спектроскопия, сканирующая электронная микроскопия, энергодисперсионный анализ, рентгенофазовый анализ, титриметрия. Продемонстрирован путь превращения твердофазных отходов в полезный продукт. Результаты исследования показали, что поверхность полученного материала насыщена функциональными группами (гидрокси-, карбокси-, лактоновые), предопределяющими способность связывать ионы металлов при адсорбции. Адсорбционная емкость продукта оценена по йоду и метиленовому голубому. Проведен термодинамический анализ процесса сорбции ионов меди (II) из водного раствора. Показано, что сорбент может быть использован и для адсорбционного концентрирования ионов редкоземельных элементов на примере лантана и эрбия. Кроме того, произведена лабораторная апробация возможного применения сорбента для очистки промышленных вод на примере сточной воды цеха хромирования.

Ключевые слова: металлургический шлак, переработка шлака, сорбенты, сорбция, сорбционная емкость, ионы *d*-, *f*-металлов, очистка сточных вод, изотермы сорбции, термодинамика адсорбции.

References

- 1 Yong, L., Qiong, L., Guodong, W., Xianlong, L. & Ping, N. (2018). Synthesis and characterization of zeolite from coal fly ash. *Journal Materials research express*, 5, 1–5. <https://doi.org/10.1088/2053-1591/aac3ae>.
- 2 Khudyakova, L.I., Zalutskiy, A.V. & Paleev, P.L. (2019). Ispolzovanie zoloshlakovykh otkhodov teplovykh elektrostantsii [Use of ash and slag waste of thermal power plants]. *XXI vek. Tekhnosferaia bezopastnot — XXI century. Technosphere Safety*, 4(3), 290–306 [in Russian]. <https://doi.org/10.21285/2500-1582-2019-3-375-391>.
- 3 Sigachev, N.P., Konovalova, N.A., Konnov, V.I., Pankov, P.P. & Yefimenko, N.S. (2015). Effektivnost ispolzovaniia zoloshlakovykh otkhodov Zabaikalskogo kraia pri proizvodstve dorozhnotsementnykh gruntov [The effectiveness of the use of the Zabaykalsky territory ash and slag waste in the production of road cement soils]. *Ekologiya i promyshlennost Rossii — Ecology and Industry of Russia*, 19(1), 24–27. <https://doi.org/10.18412/1816-0395-2015-11-24-27> [in Russian].
- 4 Kazakov, S.V. (2004). Printsipy otsenki radioekologicheskogo sostoiianiia vodnykh obektov [The principle of assessing the radioecological state of water bodies]. *Zhurnal of Radiatsionnoi biologii Rossii — Journal Radiation biology. Radioecology*, 44(6), 694–670. <https://pubmed.ncbi.nlm.nih.gov/15700812> PMID: 15700812 [in Russian].
- 5 Pan, M., Omar, H.M. & Rohani S. (2017). Application of Nanosize Zeolite Molecular Sieves for Medical Oxygen Concentration. *Nanomaterials (Basel)*, 7(8), 195. <https://doi.org/10.3390/nano7080195>.

- 6 Tyagi, B., Chudasama, C.D., Jasra, R. (2001). Separation of oxygen and nitrogen from air by molecular sieve adsorbents. *Journal of the Indian Chemical Society*, 78, 551–563. <https://www.semanticscholar.org/paper/Separation-of-oxygen-and-nitrogen-from-air-by-sieve-Tyagi-Chudasama/599ed12c049df8f036bd044c59fe56ca01aceb00>.
- 7 Linnikov, O.D., Rodina, I.V., Tiutiunnik, A.P., Eseevich, D.A., & Sokolova, L.L. (2017). Sorbtionnye i khromatograficheskie protsessy — Sorption and chromatographic processes, 17(1), 78–86. <http://www.sorpchrom.vsu.ru/articles/20170110.pdf> [in Russian].
- 8 Hutson, N.D., Zajic S.C. & Yang R.T. (2000). Influence of residual water on the adsorption of atmospheric gases in Li-X zeolite: experiment and simulation. *Industrial & Engineering Chemistry Research*, 39(6), 1775–1780. <https://doi.org/10.1021/ie990763z>.
- 9 Kim, H., Cho, H.J., & Narayanan, Sh., et al. (2016). Characterization of Adsorption Enthalpy of Novel Water-Stable Zeolites and Metal-Organic Frameworks. *Scientific Report*, 6, 19097. <https://doi.org/10.1038/srep19097>.
- 10 Fomicheva, T.I., Koluzhnikova, E.V., Fomichev, J.S., & Mihajlova, N.G. (2009). Lignine Active Coals Used for Purification of Solutions from Inorganic Cations. *13th International Congress Phytopharm*, 29-31 July 2009. (p. 39). Bonn, Germany. <http://harald-g-schweim.de/phytopharm2009/0-Abstratcs.pdf>.
- 11 Hamdi, N., & Srasra, E. (2012). Removal of Phosphate Ions from Aqueous Solution Using Tunisian Clays Munerals and Synthetic Zeolite. *Journal of Environmental Sciences*, 24(4), 617–623. [https://doi.org/10.1016/S1001-0742\(11\)60791-2](https://doi.org/10.1016/S1001-0742(11)60791-2).
- 12 Amerkhanova, Sh.K., Shlyapov, R.M., & Uali, A.S. (2017). The active carbons modified by industrial wastes in process of sorption concentration of toxic organic compounds and heavy metals ions. *Colloids and Surfaces A: Physicochemical and Engineering Aspects*, 532, 36-40. <https://doi.org/10.1016/j.colsurfa.2017.07.015>.
- 13 Nazarenko, O., Zarubina, R. (2013). Application of Sakhaptinsk Zeolite for Improving the Quality of Ground Water. *Energy and Environmental Engineering*, 1(2), 68–73. <https://doi.org/10.13189/eee.2013.010205>.
- 14 Boehm, H.P. (1966). Chemical identification of surface groups. *Advances in catalysis and related subjects*, 16, 197–274. https://jglobal.jst.go.jp/en/detail?JGLOBAL_ID=201602018030835593.
- 15 GOST 6217-74. (1976). Ugol aktivnyi drevesnyi droblenyi. Tekhnicheskije. usloviia [Wood crushed activated carbon. Specifications] MKS71.100.40, OKP 21 6239. Retrieved from: <https://docs.cntd.ru/document/1200017213> [in Russian].
- 16 GOST 21283-93 (1983). Glina betonitovaia dlia tonkoi stroitelnoi keramiki. Metody opredeleniia pokazatelia adsorbtsii emkosti kationnogo obmena [Bentonite clay for fine and building ceramics. Methods for determining the adsorption index and cation exchange capacity]. Retrieved from: <https://meganorm.ru/Data2/1/4294852/4294852851.pdf> [in Russian].
- 17 Blissett, R.S., & Rowson, N.A. (2012). A review of the multi-component utilisation of coal fly ash. *Fuel*, 97, 1–23. <https://doi.org/10.1016/j.fuel.2012.03.024>
- 18 Wang, Ch., Leng, Sh., Guo, H., Yu, J., & Li, W., et al. (2019). Quantitative arrangement of Si/Al ratio of natural zeolite using acid treatment. *Applied Surface Science*, 498, 143874. <https://doi.org/10.1016/j.apsusc.2019.143874>.
- 19 Ojedokun, At. & Olugbenga, S.B. (2015). An Overview of Low Cost Adsorbents for Copper (II) Ions Removal. *J Biotechnol Biomater*, 5(1), 1000177. <http://dx.doi.org/10.4172/2155-952X.1000177>.
- 20 Feng, D., Van Deventer, JSJ., & Aldrich, Ch. (2004). Aldrich C. Removal of pollutants from acid mine wastewater using metallurgical by-product slags. *Sep. Purif. Technol.*, 40(1), 61–7. <http://dx.doi.org/10.1016/j.seppur.2004.01.003>.
- 21 Abia, A.A., Horsfall, M.Jr., & Didi, O. (2003). The use of chemically modified and unmodified cassava waste for the removal of Cd, Cu and Zn ions from aqueous solution. *Bioresour. Technol.*, 90, 345–348. [https://doi.org/10.1016/S0960-8524\(03\)00145-7](https://doi.org/10.1016/S0960-8524(03)00145-7).
- 22 Ozer A., Ozer, D., & Ozer, A. (2004). The adsorption of copper (II) ions on to dehydrated wheat bran (DWB): determination of the equilibrium and thermodynamic parameters. *Process Biochem.*, 39, 2183–2191. <https://doi.org/10.1016/j.procbio.2003.11.008>.
- 23 Marshall, W.E., Wartelle, L.H., Boler, D.E., Johns, M.M. & Toles, C.A. (1999). Enhanced metal adsorption by soybean hulls modified with citric acid. *Bioresour. Technol.*, 69(3), 263–268. [https://doi.org/10.1016/S0960-8524\(98\)00185-0](https://doi.org/10.1016/S0960-8524(98)00185-0).
- 24 Feng, N., Guo, X., & Liang, S. (2009). Adsorption study of copper (II) by chemically modified orange peel. *J. Hazard. Mater.*, 164(2–3), 1286–1292. <https://doi.org/10.1016/j.jhazmat.2008.09.096>.
- 25 Bakhtiari, N., & Azizian, S. (2015). Adsorption of copper ion from aqueous solution by nanoporous MOF-5: A kinetic and equilibrium study. *Journal of Molecular Liquids*, 206, 114–118. <https://doi.org/10.1016/j.molliq.2015.02.009>.
- 26 Rahman, M.M., Khan, S.B., Marwani H.M., & Asiri, A.M. (2014). SnO₂-TiO₂ nanocomposites as new adsorbent for efficient removal of La (III) ions from aqueous solutions. *J. Taiwan Inst. Chem. Eng.*, 45, 1964–1974. <http://dx.doi.org/10.1016/j.jtice.2014.03.018>.
- 27 Hong, G., Shen, L., Wang, M., Yang, Y., Wang, X., Zhu, M., & Hsiao, B.S. (2014). Nanofibrous polydopamine complex membranes for adsorption of lanthanum (III) ions. *Chem. Eng. J.*, 244, 307–316. <https://doi.org/10.1016/j.cej.2014.01.073>.
- 28 Torab-Mostaedi, M., Asadollahzadeh, M., Hemmati, A., & Khosravi, A. (2013). Biosorption of lanthanum and cerium from aqueous solutions by grapefruit peel: equilibrium, kinetic and thermodynamic studies. *Res. Chem. Intermed.*, 41, 559–573. <http://dx.doi.org/10.1007/s11164-013-1210-4>.
- 29 Awwad, N.S., Gad, H.M.H., Ahmad, M.I., & Aly, H.F. (2010). Sorption of lanthanum and erbium from aqueous solution by activated carbon prepared from rice husk. *Colloids and Surfaces B: Biointerfaces.*, 81(2), 593–599. <https://doi.org/10.1016/j.colsurfb.2010.08.002>.

Information about authors

Amerkhanova Shamshiya Kenzhegazinovna — Doctor of chemical sciences, Professor, L.N. Gumilyov Eurasian National University, Kazhymukan street, 13, 010000, Nur-Sultan, Kazakhstan, e-mail: amerkhanovashk@gmail.com; <https://orcid.org/0000-0002-2492-4203>;

Uali Aitolkyn Sailaubekkyzy — Candidate of chemical sciences, Associate Professor, L.N. Gumilyov Eurasian National University, Kazhymukan street, 13, 010000, Nur-Sultan, Kazakhstan, e-mail: ualiaitolkyn@gmail.com; <https://orcid.org/0000-0002-5851-6566>;

Shlyapov Rustam Maratovich (*corresponding author*) — Candidate of chemical sciences, Associate Professor, L.N. Gumilyov Eurasian National University, Kazhymukan street, 13, 010000, Nur-Sultan, Kazakhstan, e-mail: rustamshlyapow@gmail.com; <https://orcid.org/0000-0003-0696-214X>;

Belgibayeva Dana Sapargaliyeva — Candidate of chemical sciences, L.N. Gumilyov Eurasian National University, Kazhymukan street, 13, 010000, Nur-Sultan, Kazakhstan, e-mail: dana0577.77@gmail.com; <https://orcid.org/0000-0002-4225-600X>

Ye.S. Mustafin¹, Kh.B. Omarov¹, A.S. Borsynbaev^{1*},
D. Havlichek², A.M. Pudov¹, N.V. Shuyev¹

¹Karagandy University of the name of academician E.A. Buketov, Karaganda, Kazakhstan;

²Charles University, Prague, Czech Republic

(*Corresponding author's e-mail: askhat.9@mail.ru)

Production of electrolytic copper from Zhezkazgan Processing Plant tailings leaching solutions using a hydro-impulse discharge

In this work, for the first time, studies of the mineralogical composition and chemical semi-quantitative spectral analysis (SQSA) of the Zhezkazgan processing plant tailings before and after leaching were carried out. It was found that copper is present in the tailings in the form of the chalcocite and bornite minerals. After leaching with the use of ammonium bifluoride and a hydro-pulse discharge, chalcocite and bornite are destroyed, and copper passes into a solution containing phosphoric acid. As a result of multiple placing of tailings into the solution, the copper content in it is brought to a concentration at which copper deposition on a stainless steel plate is possible. The identification of copper was implemented on a LAES-Matrix grain spectrometer. A visual comparative analysis of the changes in the structure of the treated ore waste was carried out using a TESCAN MIRA scanning electron microscope. Metallic copper was obtained from solution by electrochemical reactions in an experimental laboratory setup as a result. The technology was developed on an experimental laboratory setup for the extraction of metallic copper and brought the choice of the solution medium and electrochemical processes to the stage of obtaining the target metal with a purity of 99.99 %.

Keywords: hydro-impulse discharge, reactor, pulp, ammonium hydrofluoride, tailings samples, mineralogical composition, copper, electrolysis.

Introduction

The currently used beneficiation processes do not provide full extraction of useful components from minerals due to the constructive parameters of the working equipment and apparatuses, so they cannot be taken when developing off-balance sheet reserves of deposits [1].

Modernization of enrichment processes is carried out by involving hydrometallurgical and chemical processing operations, which increase the efficiency of enrichment through the use of a new type of energy, for example, reagent leaching technologies for metals.

One of the rapidly developing trends in the leaching of non-ferrous metals today can be considered the use of electro-hydro-impulse discharge (HID) technology. HID is characterized by a high coefficient of efficiency and universal capabilities of ultra-high pressures in combination with electromagnetic properties. The content of valuable components both in ores and concentrates extracted from dump tailings is usually low. That is why, the complete extraction of valuable metals from ore is impossible without the use of modern enrichment methods, such as the method of electro-hydro-impulse action [2, 3].

Currently, the use of ammonium salts is gaining new relevance due to their high productivity in the leaching of copper from hydrometallurgical production waste. They have the properties of breaking the intermolecular bonds of copper compounds and silicon compounds, thereby releasing the target product from the minerals. The study showed that when exposed to NH_4^+ ions at a concentration of 1.29 mol/l, as well as the impact of physical parameters such as partial pressure, time, mixing intensity, temperature, particle size, on the minerals chalcocite and siderite, the extractivity is 95 % of the ore mass. Then the kinetics of Cu leaching with a total content of 8.8 % of the ore mass indicates the feasibility of using ammonia derivatives for copper leaching [4]. The ability to form an unstable $\text{NH}_3 \cdot \text{Cu}^{+2}$ complex makes it possible to extract copper not only from the enriched ore, but also from their depleted products of the hydrometallurgical process, which together makes it possible to completely extract copper and other metals of the transition group of the periodic system of elements from ores without residues [5, 6]. For example, the authors [7] carried out work on the hydrofluoride opening of mines of scheelite, wolframite, ilmenite, sphene, baddeleyite, datolite, crystalline quartz and gold-containing technogenic waste. It is established that during fluorination, ammonium fluoro or oxofluorometallates are formed, which provide the solubility of the products and the possibility

of separating the mixtures by sublimation. It is shown that the opening of mineral raw materials with ammonium hydrodifluoride proceeds at low temperatures and allows for the extraction of all valuable components in the form of final oxides or intermediate simple and complex fluorides according to similar schemes.

The copper production industry in Kazakhstan has a huge potential for development with the introduction of new innovative and environmentally friendly methods of integrated ore processing, covering previously unused waste-tailings stored in the form of dumps. In this work, the “electro-hydro-impulse effect” was used, which allows achieving a high-quality yield of metals from the tailings of the Zhezkazgan processing plant (ZPP) at relatively low energy costs.

The aim of the study is to study the changes in the mineralogical composition of the tails of the Zhezkazgan processing plant after leaching by hydro-impulse discharge and deposition of copper on stainless steel by electrolysis from a fluid.

Experimental

A laboratory setup has been developed and installed for experimental work on the processing of studied samples of mining waste by electro-hydro-impulse (HID) exposure. This makes it possible to conduct experiments in a wide range of changes in the characteristics of the electric discharge.

Extraction of metals was carried out in a 1l cell, where 250 g of tailings of ZPP 1, ZPP 2, ZPP 3 were filled in, then 500 g of water was poured and 4 g of NH_4HF_2 were added [8].

Then it was treated with an electro-hydro-impulse discharge (HID) in the cell for 15 minutes, after that 15 ml of H_3PO_4 was added to pH 1–2, and GIR was treated in the cell for another 15 minutes.

Next, 100 ml of water was added, after filtration, the total solution was checked with a pH meter (pH meter / Etan ionomer) and brought to pH = 1–2 H_2SO_4 , then sedimentation on iron plates was carried out and the purity of the resulting copper was determined. The purity of copper deposition on the plate was implemented on a Laser atomic emission spectrometer “SPEKS LAES Matrix Continuum”.

The assembled installation is composed of the main blocks and nodes. The remote control for starting a high-voltage generator with current and voltage output sensors is made with a controlled transformer for 220 V. To obtain high-voltage electrical pulses, a pulse voltage generator was assembled. The generator unit consists of a high-voltage transformer, a high-voltage AC rectifier, a spark gap with a cell (reactor) and a circuit protection circuit for the generator housing, electricity metering devices (Fig. 1).

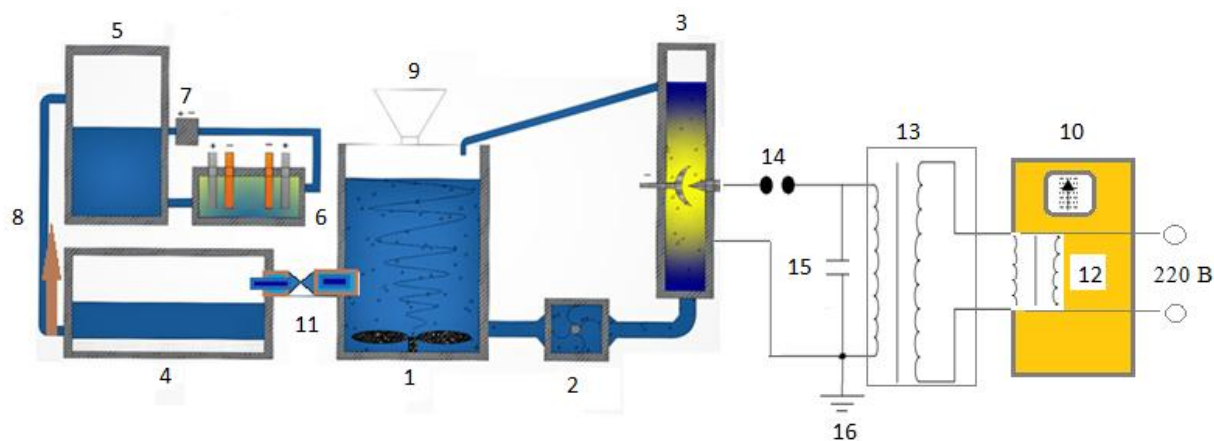


Figure 1. Diagram of a laboratory setup for extracting copper from the tailings of the ZPP 1, 2, 3

Description of a laboratory setup:

1. Stirring machine $v = 20$ l;
2. Pump feeding the pulp;
3. Pulp discharge reactor;
4. Decantator (sediment separation) with filtration;
5. Collector of the working fluid of the electrolyte $v = 10$ l;
6. Electrolyzer $v = 5$ l;
7. Circulation pump for electrolyte;
8. Post-decantation fluid supply pump with non-return valve;

9. Tailings loading hopper with water and reagents supply;
10. Hydraulic pulse control panel (HIR);
11. Switch valve for the solution supply to the reactor and decantator;
12. Low-voltage controlled transformer for 220 V;
13. High voltage transformer up to 60 kV/A;
14. Discharge switch;
15. 0.4 mF capacitor;
16. Grounding.

An I-160 MI laboratory ionomer was used to measure the pH of the medium. A microwave plasma atomic emission spectrometer (MP-AES) duplicated on an AA-140 atomic absorption spectrometer was applied for the quantitative determination of metals. The mineralogical composition of the tailings samples was determined using a Micromed POLAR 2 polarizing microscope. A visual comparative analysis of the changes in the structure of the treated ore waste was carried out using a TESCAN MIRA scanning electron microscope.

Results and Discussion

It is necessary to know the mineral composition of the samples, the size of mineral grains and the nature of their adhesion when choosing a method for processing ores [9]. This allows to determine the required fineness of grinding and facilitate the choice of methods for processing ore or waste. Table 1 shows the passport data of the imported samples of tailings ZPP-1, 2; ZPP-3.

Table 1

Passport data of “Kazakhmys” LLP tailings samples

Name of PP	Tailings	Cu	Fe	Zn	Pb	SiO	Al ₂ O ₃	S	CaO
ZPP 1, 2	Current	0.127	2.2	0.02	0.01	63.82	11.27	0.13	6.47
ZPP 1, 2	Stale	0.187	1.8	0.03	0.02	62.85	10.46	0.16	7.17
ZPP 3	Stale	0.176	2.3	0.04	0.02	64.68	11.88	0.16	4.76

The mineralogical composition of the obtained tailings samples was studied; the results before and after the HID treatment are represented in Tables 2–4.

Table 2

Copper content before and after HID treatment

Mineral	Sample name					
	Stale tailings ZPP № 1, 2		Current tailings ZPP № 1, 2		Stale tailings ZPP № 3	
	before leaching	after leach- ing	before leaching	after leaching	before leaching	after leaching
[Cu], total in %	0.213	0.024	0.13	0.012	0.176	0.014
Σ Cu oxidized phase, %	≤0.02	<0.01	≤0.02	<0.01	0.026	<0.01
Cu, free oxidized %	≤0.02	<0.01	≤0.02	<0.01	0.026	<0.01
Σ Cu of Malachite+ Azurite + atacamite % Cu ₂ CO ₃ (OH) ₂ + 2Cu[CO ₃] ×Cu[OH] ₂ +Cu ₂ Cl(OH) ₃	≤0.02	<0.01	≤0.02	<0.01	0.026	<0.01
Cu, chalcosine % (Cu ₂ S)	0.09	0.004	0.04	0.01	0.056	0.01
Cu, bornite % (Cu ₅ FeS ₄)	0.063	0.02	0.03	0.002	0.042	0.004

As can be seen from Table 2, copper is contained in the samples in the form of chalcosine and bornite minerals. The highest copper content is found in the sample “Stale ZPP No. 1, 2”. After the HID treatment, copper remains only in the form of the chalcosine and bornite minerals in small quantities, and from the remaining minerals it passes into solution.

Table 3

Lead content before and after HID treatment

Mineral	Sample names					
	Stale tailings ZPP № 1, 2		Current tailings ZPP № 1,2		Stale tailings ZPP № 3	
	before leaching	after leaching	before leaching	after leaching	before leaching	after leaching
[Pb], total in %	0.025	0.003	0.014	0.002	0.025	0.002
Galenite (PbS), %	0.011	0.001	0,008	0.001	0.012	0.001
Cerussite (PbCO ₃), %	0.005	0.0	<0.002	0.0	0.007	0.0
Lead (II) oxide (litharge, PbO), %	0.004	0.001	<0.002	0.001	0.004	0.001
Pyromorphite (Pb ₅ (PO ₄) ₃ Cl)	0.003	0.001	0.0	0.0	0.002	0.0

From Table 3 it can be noticed that lead is mainly contained in the samples in the form of the minerals of galena, cerussite and litharge. In the HID processing field, lead remains in the samples in the form of the minerals of galena and litharge in small quantities.

Table 4

Zinc content before and after HID treatment

Mineral	Sample names					
	Stale tailings ZPP № 1, 2		Current tailings ZPP № 1, 2		Stale tailings ZPP № 3	
	before leaching	after leaching	before leaching	after leaching	before leaching	after leaching
Zn total, %	0.018	0.0021	0.014	0.0027	0.019	0.0021
Carbonated Zn, %	0.003	0.0	0.001	0.0	0.004	0.0
Zn associated with iron and manganese oxides, %	0.007	0.001	0.002	0.001	0.007	0.001
Zn sphalerite (ZnS), %	0.008	0.0011	0.01	0.001	0.004	0.001
Zn related to aluminosilicates, %	0.003	0.0	0.001	0.0007	0.003	0.0001

As can be seen from Table 4, zinc is mainly contained in the mineral sphalerite in the samples of stale ZPP 1, 2 and ZPP 1, 2, 3 in minerals associated with iron and manganese oxides. After processing HID, zinc in small quantities remains in the samples of ZPP 1, 2, 3 mainly in the minerals sphalerite and minerals associated with iron and manganese oxides.

A semi-quantitative spectral analysis was performed applying a LAES-Matrix laser spectrometer to determine the valuable chemical elements in the tailings. The obtained data are illustrated in Table 5.

Table 5

Chemical semi-quantitative spectral analysis (SQSA) before and after treatment

№	Metals, %	Sample names					
		Stale tailings ZPP № 1, 2		Current tailings ZPP № 1, 2		Stale tailings ZPP № 3	
		before leaching	after leaching	before leaching	after leaching	before leaching	after leaching
1	Ag	0.0004	0.0001	0.0001	0.0001	0.0004	0.0001
2	Ba	0.092	0.066	0.081	0.071	0.074	0.053
3	Co	1.2	1.1	1.3	0.6	1.3	1.0
4	Cu	0.213	0.023	0.117	0.012	0.179	0.014
5	Ni	0.25	0.23	0.26	0.24	0.25	0.22
6	Pb	0.024	0.030	0.013	0.019	0.022	0.022
7	Sc	0.8	0.009	1.0	0.008	0.9	0.010
8	Fe	0.180	2.79	0.240	1.51	0.210	2.53
9	Zn	0.022	0.0021	0.013	0.0027	0.035	0.0021

It is clearly seen from Table 5 that there are other chemical elements besides copper. These are elements such as zinc, lead, silver and some others, and they are of interest for the development of technologies for their extraction. As can be seen from the data of quantitative analysis in Table 6, the metals in the working solution first go into solution, and then precipitate in the form of phosphates, and also partially form complexes with fluorides.

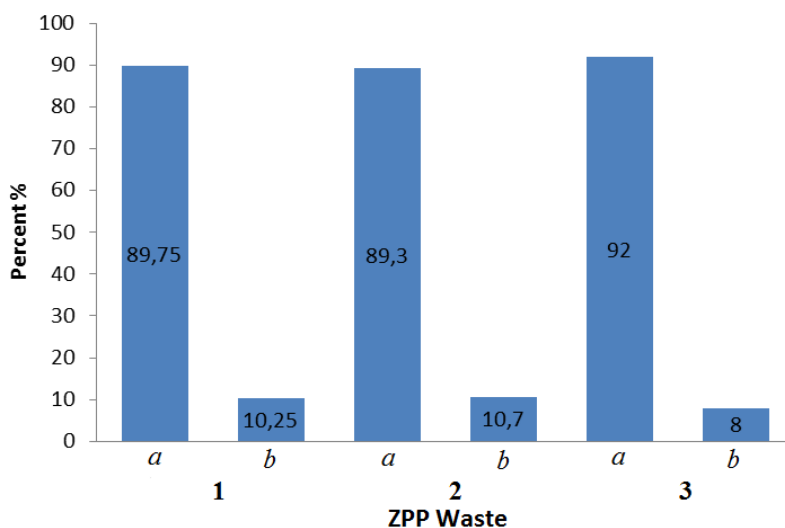
Table 6

Chemical analysis of sediment after decanting and deposition of other metals

№	Sample	Ag %	Ba %	Co %	Cu %	Ni %	Pb %	Sc %	Fe %	Zn %
1	ZPP 1, 2 Stale	0.0004	0.092	0.9	0.013	0.25	0.024	0.8	0.18	0.02
2	ZPP 1, 2 Current	0.0001	0.08	0.12	0.02	0.26	0.013	1.0	0.240	0.013
3	ZPP 3 Stale	0.0004	0.074	0.5	0.014	0.25	0.022	0.9	0.210	0.035

Table 6 shows that copper remained in solution.

Figure 2 demonstrates the percentage of copper in the fluid to its content in the tailings, after running the pulp through a laboratory unit with HID treatment for 30 minutes in the presence of phosphoric acid.



1 — ZPP 1, 2 Stale; 2 — ZPP 1, 2 Current; 3 — ZPP 3 Stale

Figure 2. Diagram of copper content in tailings before (a) and after (b) HID treatment

The average copper content for all fractions was calculated using the formula:

$$A = (x_1+x_2+\dots+x_n)/n = \sum x_i/n = 0.114+ 0.167 + 0.162 / 3 = 0.148.$$

Heap and underground leaching are widely used to extract copper from poor and off-balance ores or tailings. The main solvent for heap leaching is solutions of iron sulfuric oxide, which are obtained by irrigation of piles with water as a result of pyrite oxidation. Irrigation is carried out consistently with water and solution, followed by cementation of copper with iron scrap. In the case of using a leaching technology, the copper yield was 63.2 % (current ZPP 1,2), 63.6 % (stale ZPP 1,2), 64.2 % (stale ZPP 3).

During the use of a hydro-impulse discharge, the copper yield was 89.75 %; 89.3 %; 92.0 %, respectively.

The first 3 digits are reduced by 63, and the second by 89.3 for the convenience of calculations, then:

$$S_1^2 = 1/3[0.45^2 + 2,7^2 - (0.45 + 2.7)^2 / 3] = 1/3 [7.21 - 3.3] = 1.3;$$

$$S_2^2 = 1/5[0.2^2 + 0.6^2 + 1.2^2 - (0.2 + 0.6 + 1.2)^2 / 3] = 1/5[1.84 - 1.33] = 0.10;$$

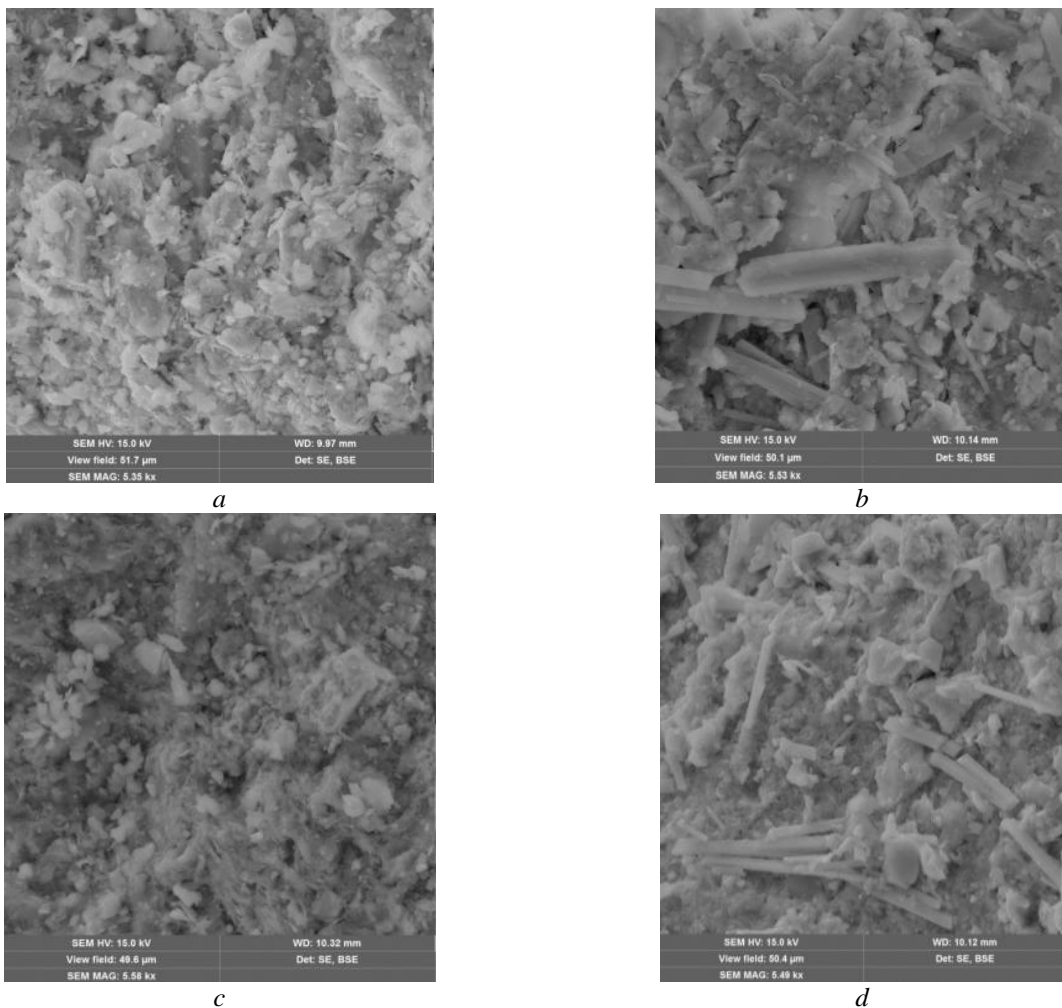
$$S_1^2 / S_2^2 = 13.$$

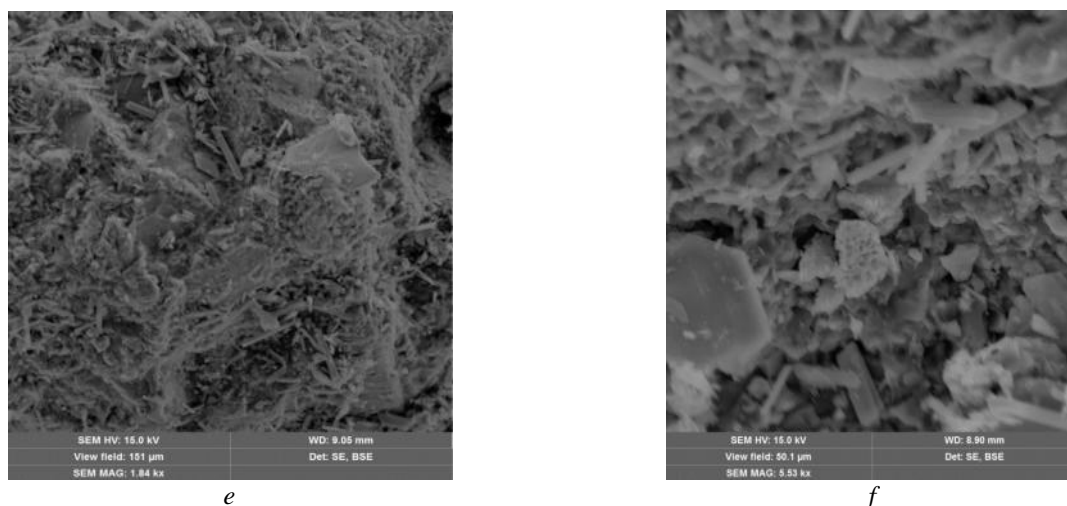
The number of freedom degrees were $f_1 = 5, f_2 = 3$. Improvement can only reduce the variance, so we apply a one-sided significance criterion. According to the table of quantiles of the Fisher distribution, we find $F_{0.95(5,3)} = 9.0$. We see that $S_1^2 / S_2^2 = 13$. Therefore, the observational data allow us to reject the null hypothesis and consider the improvement effective. Thus, the variance of dispersion is significant.

On the plates, after sedimentation and washing from the solution residues, the copper content was analyzed for its purity from contamination on a laser atomic emission spectrometer "SPEKS LAES Matrix Continuum". The above spectrum clearly shows the analytical lines of copper, which are characterized by high intensity and low content of impurities. The sedimentation of copper on iron plates and the analysis carried out on a laser spectrometer is illustrated in Figure 3, the laser operation zone in the form of burnt circles is clearly visible.



Figure 3. Copper sedimentation on iron plates and laser analysis





a — 1, 2 Current tails before HID treatment; *b* — ZPP 1, 2 tails after HID treatment;
c — ZPP 1, 2 stale tails before HID treatment; *d* — ZPP 1, 2 Stale tails after HID treatment;
e — ZPP 3 before HID treatment; *f* — ZPP 3 after HID treatment

Figure 4. Micrograph of ore waste samples (before and after processing)

To check the sediment remaining after the HID, images of the tailings samples were taken before and after processing (Fig. 4) on the TESCAN MIRA-scanning electron microscope (SEM).

The photos taken with a scanning microscope clearly show the difference between the tail samples before and after the HID treatment: 1) all small particles of clay crumble and dissolve; 2) transparent quartz crystals are clearly visible; 3) all mineral and fibrous formations disappear, there is no adhesion of particles to each other.

All this shows that as a result of treatment with HID and 4 grams of ammonium bifluoride NH_4HF_2 , mainly larger quartz crystals remain, and other types of minerals dissolve with them. After the deposition of other metals and their conversion to insoluble phosphates, the HID laboratory facility worked out the modes of extracting copper from the tailings and subsequent deposition on a stainless steel cathode with a high purity of 99.99 %.

Preliminary calculation of energy consumption

When processing 150 thousand tons of tailings per year, the costs will be:

The cost of equipment is 99,850,000 tenge.

Materials (provided that the working solution with ammonium bifluoride and sulfuric acid circulates during the daily operation of the installation until it is saturated with copper to approximately $35\text{--}38 \text{ kg/m}^3$).

$$150,000 * 34,248 \text{ tenge} = 5,137,200,000 \text{ tenge.}$$

When organizing the regeneration of ammonium bifluoride and sulfuric acid, i.e. the return to the leaching process of about 70 %, the annual cost of materials will be:

$$5,137,200,000 \text{ tenge} * 0.3 = 1,541,160,000 \text{ tenge.}$$

Resource costs:

– electricity: $150,000 \text{ t} * 10,260 \text{ tenge} / \text{t} = 1,539,000,000 \text{ tenge}$;

– water (if the unit is loaded three times for 10 tons of tailings, the loss of water at each discharge will be about 20 liters, that is, the daily additional volume of water will be 24 cubic meters):

$$365 \text{ days} * 24 \text{ cubic meters} * 150 = 1,314,000 \text{ tenge};$$

– salary: $3 \text{ people} * 180,000 \text{ tenge} * 12 = 6\,480\,000 \text{ tenge}$.

Conclusions

The following results were obtained for the first time: the mineralogical composition of the selected tailings samples, which are gray sand with clay inclusions, was determined. In these samples, copper residues are mainly found in the form of the minerals chalcocite and bornite. Then leaching was carried out using ammonium bifluoride hydro-pulse discharge.

A complete chemical analysis of the HID treated samples was carried out on the 4210 MP-AES atomic emission spectrometer, which showed that the metals had passed into solution. Next, the solution was treated

by acidification of the medium with phosphoric acid to pH = 1–2 to transfer other metals to the precipitate. In this solution, HID was repeatedly produced to increase its copper content to a concentration of 0.25 mol/l.

Electrochemical methods were used to obtain copper deposited on the matrix, where the anode is an oxidized ruthenium-titanium anode (ORTA) mesh, insoluble 3×5×15 cm, and the cathode of non-rusting steel plates is 3×5×15 cm. The purity of the obtained copper on the substrate was determined using an LAES-Matrix spectrometer. It was shown that the purity of the obtained copper is 99.99 %. An experimental laboratory setup was made, on which the modes of copper extraction on stainless steel plates were worked out.

Then, the images of the tailings samples before and after processing were taken with a TESCAN MIRA scanning electron microscope (SEM) to check the sediment remaining after the HID. It was shown, that all small particles of clay crumble and dissolve; transparent quartz crystals are clearly visible; all mineral and fibrous formations disappear, there is no adhesion of particles to each other.

References

- 1 Снуриков А.П. Комплексное использование сырья в цветной металлургии: учеб. пос. / А.П. Снуриков. — М.: Металлургия, 2006. — 16 с.
- 2 Goryachev A.A. A study of the Feasibility of Using Ammonium Sulfate in Copper–Nickel Ore Processing / E.V. Chernousenko, S.S. Potapov, N.S. Tsvetov, D.V. Makarov // Metals. — 2021. — Vol. 11. — P. 422. <https://doi.org/10.3390/met11030422>
- 3 Юткин Л.А. Электрогидравлический эффект и его применение в промышленности: учеб. пос. / Л.А. Юткин. — Л.: Машиностроение, 1986. — 253 с.
- 4 Baba A.A. Characterization and kinetic study on ammonia leaching of complex copper ore / A.A. Baba, M.K. Ghosh, S.R. Pradhan, D.S. Rao, A. Baral, F.A. Adekola // Transactions of Nonferrous Metals Society of China. — 2014. — Vol. 24. — P. 1587–1595. [https://doi.org/10.1016/S1003-6326\(14\)63229-5](https://doi.org/10.1016/S1003-6326(14)63229-5)
- 5 Sinclair L. In situ leaching of copper: Challenges and future prospects / L. Sinclair, J. Thompson // Hydrometallurgy. — 2015. — Vol. 157. — P. 306–324. <https://doi.org/10.1016/j.hydromet.2015.08.022>
- 6 Ochrowicz K., Jeziorek M., Wejman K. Copper (II) extraction from ammonia leach solution / K. Ochrowicz, M. Jeziorek, K. Wejman // Physicochem. Probl. Miner. Process. — 2014. — Vol. 50. — P. 327–335. <https://doi.org/10.5277/ppmp140127>
- 7 Медков М.А. Гидрофторидаммония — перспективный реагент для комплексной переработки минерального сырья / М.А. Медков, Г.Ф. Крысенко, Д.Г. Эпов // Вестн. ДВО РАН. — 2011. — № 5. — С. 60–65.
- 8 Раков Э.Г. Фториды аммония: учеб. пос. / Э.Г. Раков. — М.: ВИНТИ, 1988. — 154 с.
- 9 Минералы: справ. / под ред. Ф.В. Чухрова. — М.: Наука, 1974. — 514 с.

Е.С. Мустафин, Х.Б. Омаров, А.С. Борсынбаев,
Д. Хавличек, А.М. Пудов, Н.В. Шуев

Жезқазған байыту фабрикасы қалдықтарына гидроимпульсті разрядты қолдана отырып, ерітінділерінен электролиттік мысты алу

Мақалада алғаш рет Жезқазған байыту фабрикасының қалдықтарының, өндеуге дейінгі және өндеуден кейінгі минералогиялық құрамына және химиялық жартылай сандық спектрлік талдау (PSA) зерттеулері жүргізілген. Мыс қалдықтарында халькозин және борнит минералдары түрінде болатыны анықталды. Аммоний бифторидін және гидроимпульсті разрядты қолданғанда, бөлуден кейін халькозин және борнит ыдырайды, ал мыс құрамында фосфор қышқылы бар ерітіндіге өтеді. Қалдықтарды ерітіндіге қайта-қайта енгізу нәтижесінде оның құрамындағы мыс мөлшері тот баспайтын болаттан жасалған мысқа шөгу мүмкін болатын концентрацияға жеткізілді. Авторлар мысты талдауды LAES-Matrix лазерлік спектрометрінде зерттеулерды, сонымен қатар, өңделген кен қалдықтарының құрылымындағы өзгерістерге визуалды салыстырмалы талдауды TESCAN MIRA сканерлейтін электронды микроскопта жүргізген. Нәтижесінде тәжірибелік зертханалық қондырғыда, электрохимиялық реакциялар арқылы ерітіндіден мысты металл түрінде алу, металл мысын алуға арналған қондырғыда технологиясы зерттелді және ерітінді ортасын таңдау арқылы электрохимиялық процестер кезінде 99,99 % тазалықпен металды алу сатына дейін зерттеулер жасалды.

Кілт сөздер: гидроимпульсті разряд, реактор, кенді су, аммоний гидрофториді, қалдық үлгілері, минералогиялық құрамы, мыс, электролиз.

Е.С. Мустафин, Х.Б. Омаров, А.С. Борсынбаев,
Д. Хавличек, А.М. Пудов, Н.В. Шуев

Получение электролитической меди из растворов выщелачивания хвостов Жезказганской обогатительной фабрики с применением гидроимпульсного разряда

В статье впервые проведены исследования минералогического состава и химический полуколичественный спектральный анализ (ПСА) хвостов Жезказганской обогатительной фабрики до и после выщелачивания. Установлено, что медь присутствует в хвостах в виде минералов халькозина и борнита. После выщелачивания с применением бифторида аммония и гидроимпульсного разряда халькозин и борнит разрушаются, а медь переходит в раствор, содержащий фосфорную кислоту. В результате многократного введения хвостов в раствор содержание меди в нем доведено до концентрации, при которой возможно осаждение меди на пластинке из нержавеющей стали. Авторами проведена идентификация меди на лазерном спектрометре LAES-Matrix, визуальный сравнительный анализ изменения структуры обработанных рудных отходов на сканирующем электронном микроскопе TESCAN MIRA. Результатами стали получение металлической меди из раствора путем электрохимических реакций, отработка технологии на опытной лабораторной установке по извлечению металлической меди и доведение подбором среды раствора и электрохимических процессов до стадии получения целевого металла с чистотой 99,99 %.

Ключевые слова: гидроимпульсный разряд, реактор, пульпа, гидрофторид аммония, образцы хвостов, минералогический состав, электролиз, медь.

References

- 1 Snurnikov, A.P. (2006). *Kompleksnoe ispolzovanie syria v tsvetnoi metallurgii* [Complex use of raw materials in non-ferrous metallurgy]. Moscow: Metallurgiya [in Russian].
- 2 Goryachev, A.A., Chernousenko, E.V., Potapov, S.S., Tsvetov, N.S., & Makarov, D.V. (2021). A Study of the Feasibility of Using Ammonium Sulfate in Copper–Nickel Ore Processing, *Metals*, 11, 422. <https://doi.org/10.3390/met11030422>
- 3 Yutkin, L.A. (1986). Elektrogidravlicheskiy effekt i ego primeneniye v promyshlennosti [Electrohydraulic effect and its application in industry]. Leningrad: Mashinostroeniye [in Russian].
- 4 Baba, A.A., Ghosh, M.K., Pradhan, S.R., Rao, D.S., Baral, A., & Adekola, F.A. (2014). Characterization and kinetic study on ammonia leaching of complex copper ore. *Transactions of Nonferrous Metals Society of China*, 24, 1587–1595. [https://doi.org/10.1016/S1003-6326\(14\)63229-5](https://doi.org/10.1016/S1003-6326(14)63229-5)
- 5 Sinclair, L. & Thompson, J. (2015). In situ leaching of copper: Challenges and future prospects. *Hydrometallurgy*, 157, 306–324. <https://doi.org/10.1016/j.hydromet.2015.08.022>
- 6 Ochrowicz, K., Jeziorek, M., & Wejman, K. (2014). Copper (II) extraction from ammonia leach solution. *Physicochem. Probl. Miner. Process*, 50, 327–335. <https://doi.org/10.5277/ppmp140127>
- 7 Medkov, M.A., Krysenko, G.F., & Epov, D.G. (2011). Gidroftorid ammoniia — perspektivnyi reagent dlia kompleksnoi pererabotki mineralnogo syria [Ammonium hydro difluoride — a promising reagent for complex processing of mineral raw materials]. *Vestnik DVO RAN — Bulletin of the Far Eastern Branch of the Russian Academy of Sciences*, 5, 60–65 [in Russian].
- 8 Rakov, E.G. (1988). *Ftoridy ammoniia* [Ammonium fluorides]. Moscow: VINITI [in Russian].
- 9 Chukhrov, F.V. (1974). *Mineraly* [Minerals]. Moscow: Nauka [in Russian].

Information about authors

Mustafin Yedige Suindikovich — Full Professor, Doctor of Chemical Sciences, Director of Research Center “Applied Chemistry”, Karagandy University of the name of academician E.A. Buketov, Universitetskaya street, 28, 100028, Karaganda, Kazakhstan; e-mail: edigemus@mail.ru; <https://orcid.org/0000-0001-9450-9227>

Omarov Khylysh Beysenovich — Full Professor, Doctor of technical sciences, Professor, Senior staff scientist of Research Center “Applied Chemistry” Karagandy University of the name of academician E.A. Buketov, Universitetskaya street, 28, 100028, Karaganda, Kazakhstan; e-mail: homarov1963@mail.ru; <https://orcid.org/0000-0003-2931-652X>

David Khavlichek — Doc. RnDr. associate prof., dept. of Inorg. Chem. Faculty of science Charles University, Albertov 6, 128 43 Prague 2 Czech Republic; e-mail: havlicek@natur.cuni.cz; <https://orcid.org/0000-0002-8854-6213>

Borsynbayev Askhat Sakenovich (corresponding author) — 3rd year PhD student, Karagandy University of the name of academician E.A. Buketov, Universitetskaya street, 28, 100028, Karaganda, Kazakhstan; e-mail: askhat.9@mail.ru; <https://orcid.org/0000-0001-7709-5552>

Pudov Aleksandr Mikhaylovich — Candidate of chemical sciences, Senior research of Research Center “Applied Chemistry”, Karagandy University of the name of academician E.A. Buketov, Universitetskaya street, 28, 100028, Karaganda, Kazakhstan; e-mail: pudovam@list.ru; <https://orcid.org/0000-0002-0566-6890>

Shuyev Nikita Viktorovich — Master student, Karagandy University of the name of academician E.A. Buketov, Universitetskaya street, 28, 100028, Karaganda, Kazakhstan; e-mail: nick.shuev@gmail.com

A.M. Kozhanova^{1*}, B.S. Temirgazyev¹, A. Zhanarbek¹,
B.I. Tuleuov¹, T.M. Seilkhanov², S.M. Adekenov¹

¹JSC “International Research and Production Holding “Phytochemistry”, Karaganda, Kazakhstan;

²Sh.Ualikhhanov Kokshetau University, Kokshetau, Kazakhstan

(*Corresponding author’s e-mail: alhs@mail.ru)

Synthesis of a hydrophilic derivative of ecdysterone and development of its water-soluble form

The article presents materials on the isolation of ecdysterone substance from medicinal plant raw materials *Silene wolgensis* (Hornem.) Bess. ex. Spreng (Volga smolyovka). For the first time, the optimization of the method for ecdysterone substance obtaining from the aboveground part of the superconcentrator of phytoecdysteroids of the *Silene wolgensis* was carried out and based on it a pilot industrial regulation for the isolation of ecdysterone and an encapsulated water-soluble form were developed. It was found, that the interaction of the substrate molecule and the clathrate forms a substance that can dissolve in water and other more polar solvents, thereby solving the problem of bioavailability of the main hydrophobic drug. The method developed for producing the substance ecdysterone and its water-soluble encapsulated with β -cyclodextrin form was implemented into production at the Karaganda pharmaceutical plant. NMR studies of changes in the chemical shifts of protons of substrates and receptors illustrated that ecdysterone interacts with β -cyclodextrin to form supramolecular inclusion complexes with stoichiometric composition of 1:1.

Keywords: ecdysterone, optimization of isolation, *Silene wolgensis*, β -cyclodextrin, encapsulation, water solubility, NMR, supramolecular complexes.

Introduction

Ecdysteroids (ecdysones or polyoxysteroids) regulate the molting processes of insects and crustaceans [1]. Additionally, they are also isolated from plant sources [2, 3]. To date, more than 500 ecdysteroids are known, among which ecdysterone (20-hydroxyecdysone or 20E) is found in plants in large quantities.

In modern conditions, the problem of developing new drugs and biologically active food supplements containing minor components of phytoecdysteroids is becoming paramount to correct the body's adaptive reactions under stress, exposure to unfavorable technogenic and environmental factors, and high physical and emotional stress. Ecdysteroids have a wide spectrum of biological activity, are non-toxic and do not possess androgenic properties.

Ecdysteroids are found in plants, as a rule, in trace and minor amounts — 0.001–0.1 %, but there are also superproducer species containing up to 3.0 % [4]. Phytochemical methods for the isolation of phytoecdysteroids and ecdysteroid preparations are usually traditional. For their production, such basic methods are used as grinding of raw materials, extraction, separation of solid and liquid phases, evaporation of the extract, isolation and purification of the target product [5].

The main problem in the development and creation of phytopreparations based on secondary plant metabolites is their water solubility and bioavailability. The rate and degree of bioavailability of a pharmaceutically active substrate directly depends on its water solubility and, therefore, on the ability of the drug to penetrate through obstacles to the intended target organ. However, it should be noted that along with the high and diverse biological activity and low toxicity of many natural compounds, the issues of water solubility of phytopreparations based on them, in most cases remain open. The water solubility of the substance and drugs can be increased by grinding them to nanoparticles, microemulsions, solid dispersions, or by extrusion. An alternative method to increase the solubility of phytopreparations is to obtain water-soluble cyclodextrin inclusion complexes (CIC) with many lipophilic poorly soluble compounds [6]. The main distinguishing feature of cyclodextrins (CD) is their ability to hydrophobic binding of the “guest” molecule in its cavity (encapsulation) in an aqueous medium.

A promising source of raw materials for producing the substance of ecdysterone is a plant of the genus *Silene* L. of the *Caryophyllaceae* family. This genus includes about 500 species, 62 of which grows in Kazakhstan (12 endemic species) in almost all floristic regions [7–9]. Currently, *Silene wolgensis* (Hornem.)

Bess. ex. Spreng (*Caryophyllaceae* Juss. family), widespread in Central Kazakhstan, attracts special attention as another type of super-concentrator (1.76 %), as well as an alternative and promising industrially significant source of biologically active substances, primarily 20E [10].

The aim of this work is to obtain a water-soluble bioactive supramolecular complex based on 20-hydroxyecdysone and its commercially available clathrate with β -cyclodextrin in a stoichiometric ratio of 1:1, followed by the subsequent development of a technology for the production of a substance for pharmaceutical purposes. One of the important tasks in the production of medicinal substances is standardization, thus, using the physicochemical parameters of the study, a number of works were conducted on which criteria for the inclusion complex of 20E with β -CD were set, on the basis of which emphasis will be placed in the production of a water-soluble adaptogen in industrial scales.

The physicochemical properties and structural features of the obtained water-soluble complex of ecdysterone with β -CD were studied applying modern physicochemical methods, namely HPLC, UV-, IR-, ^1H and ^{13}C NMR spectroscopy, on the basis of which data on complex formation are presented.

Experimental

β -Cyclodextrin (99 %) produced by Fluka was used in this work.

^1H and ^{13}C NMR spectra were recorded by the spectrometer Jeol JNM-ECA 400 (399.78 and 100.53 MHz on nuclei ^1H and ^{13}C , respectively) in solutions of DMSO- d_6 CDCl $_3$ and D $_2$ O at room temperature. Chemical shifts were measured relative to the residual signals of the protons or carbon atoms of the solvent.

The melting points of the isolated and obtained samples were determined on a Boetus instrument. IR spectra were recorded on an Avatar 360 ESP spectrometer in KBr pellets. UV absorption spectra were recorded on an Agilent Technologies "CARY 60 UV-Vis" spectrometer.

The purity of the isolated compound was controlled by thin layer chromatography (TLC) on Sorbfil plates using a chloroform-ethanol 60:40 system, as well as by HPLC (purity 97.85 % and higher).

Quantitative analysis of studied samples was carried out by high-pressure reversed-phase HPLC on a Hewlett Packard Agilent 1100 Series instrument in isocratic mode under the following conditions:

- analytical column filled with Zorbax SB-C $_{18}$ sorbent, 4.6*150 mm, with a particle size of 5 microns;
- mobile phase composition: 10 % isopropyl alcohol;
- detection at a wavelength of 254 nm;
- column temperature — room temperature;
- the speed of the mobile phase — 0.75 ml / min;
- the volume of the injected sample — 20 μl .

The processing data was carried out using the ChemStation software.

The aerial part of *Silene wolgensis* raw material was collected in the Bukhar-Zhyrau region, in vicinity of village of Kyzyl-Kaiyn, Karaganda region in the flowering phase.

Extraction of the aerial part (leaves, buds, stems) of the crushed air-dry raw material of *Silene wolgensis* with a mass of 1.0 kg was carried out four times with 10 liters of 96 % ethanol by heating on ERSND-1 extractor at the boiling point of the solvent for 1–1.5 hours. The extract was cooled, decanted, and evaporated on a rotary evaporator at a temperature not exceeding 50 °C. After that 0.2 l of ethanol was added to the resulting thick brown syrupy mass. Next, the resulting ethanol extract was treated with a mixture of petroleum ether and ethyl acetate in a ratio of 2:1 (0.4:0.2 l) in order to remove non-polar components, the remaining water-soluble part was extracted with isobutanol (0.6 l), resulting in a thick extract. Isobutanol extracts were combined, then distilled off to dryness under vacuum. Sum of ecdysteroids (86.5 g) with related substances in the form of a thick green syrupy mass was obtained. The presence of ecdysterone was established by TLC and qualitative analysis. By repeated column chromatography on Al $_2$ O $_3$ (Ith degree of activity according to Brockmann, sorbent weight 1.6 kg) and elution of the column with a mixture of chloroform-ethanol (60:40), a fraction (1.0 g) was isolated on the basis of TLC ("Sorbfil"), physicochemical constants and spectral data. It was characterized as a chromatographically individual substance — ecdysterone.

The inclusion complexes of ecdysterone with β -cyclodextrin were obtained by the interaction of equimolar amounts of 20E and CD solutions. 113 mg CD (0.1 mmol) dissolved in 4 ml of distilled water was added to 50 mg (0.1 mmol) of 20E dissolved in 3 ml of absolute ethanol. The solution was stirred using a magnetic stirrer at 50 °C for 8 hours. The formed precipitate was filtered off, washed with ethanol and dried at 40 °C. The 20E- β -CD inclusion complexes were obtained in the form of white powders. In a similar way,

inclusion complexes 1:2 were obtained. 226 mg β -CD (0.2 mmol) were dissolved in 4 ml of distilled water and added to 0.05 g (0.1 mmol) of 20E dissolved in 3 ml of absolute ethanol.

Results and Discussion

In this regard, the optimization of the technology for producing ecdysterone was carried out in order to increase the yield. In particular, reextraction of a thick total alcoholic extract (the sum of substances extracted with 96 % ethanol by maceration with solvent boiling followed by distillation of the extractant in vacuum to obtain a thick essence) using petroleum ether (extraction gasoline) was used to remove lipophilic components.

On the basis of the described optimized technology, a pilot industrial regulation for the isolation of ecdysterone was developed, the technological scheme for production of which includes the stage of preparation of materials (preparation of the extractant and processing of raw materials), 7 main stages (Fig. 1): preparation of raw materials, extractant; obtaining of thick extract of *Silene wolgensis* after extraction with ethanol; treatment of thick extract of *Silene wolgensis*; chromatographic separation on aluminum oxide; recrystallization of native ecdysterone; obtaining a water-soluble form of ecdysterone; packaging and labeling of the water-soluble form of ecdysterone.

The superconcentrator plant *Silene wolgensis*, characterized by a high yield of ecdysterone (1.76 %), exceeding its content in *Serratula coronata* L. (1.5 %), the plant basis of the domestic adaptogenic preparation "Ecdiphyt", is a promising and alternative species [10, 11].

Therefore, the aim of this work is to optimize the extraction of 20E isolation from this plant, collected in the Karaganda region, for its further use as an industrially available and alternative plant source. The influence of a number of technological factors (concentration of the selective extractant, temperature and time) on the quantitative extraction of 20E from the aerial parts and roots of the plant under study was also investigated in order to develop optimal conditions and carry out effective extraction of *silene wolgensis*.

A herb, crushed to 8 mm and a GMP-compliant extractant were applied to determine the optimal degree of extraction of ecdysterone from plant raw materials. The ecdysterone content was determined within 3, 24 and 48 hours, at extraction temperatures of 20° and 78 °C. The obtained results are presented in Table 1.

Table 1

Results of the study of the dynamics of the extraction of *silene wolgensis* raw materials depending on technological factors

Extraction	part of a plant	grinding degree of raw materials, mm	Extraction temperature, °C	Extraction time, hour	The quantitative content of ecdysterone, %
Water-ethanol (70 %)	aerial part	before 8	20	24	0.3
Water-ethanol (50 %)	aerial part	before 8	20	24	0.26
Ethanol (96.2 %)	aerial part	before 8	20	24	1.7
Ethanol (96.2 %)	aerial part	before 8	78	3	5.24
Ethanol (96.2 %) in percolator	aerial part	before 8	20	48	1.0
Water-ethanol (70 %)	root	before 8	80	3	5.24

It was experimentally established that ethyl alcohol is the main selective extractant providing the quantitative extraction of 20E from *silene wolgensis*.

During extraction under different temperature and times conditions with other identical parameters, it was identified that an increase in temperature as one of the main factors (extractions 3 and 4 at 20 °C and 78 °C) does not significantly affect the yield of 20E.

Further search for optimal conditions for the extraction of *silene wolgensis* led to the conclusion that the increase in the yield of 20E is mainly influenced by the change in the concentration of the extractant.

It should be also noted that the complex processing of plant raw materials as a renewable material is one of the priority approaches in the rational use and chemical study of plants in terms of obtaining practically valuable substances.

Table 1 illustrates that when the aerial parts are extracted using 96.2 % ethanol, and the roots with 70 % ethyl alcohol, the yield of 20E from this plant is 5.24 % and 5.24 %, respectively.

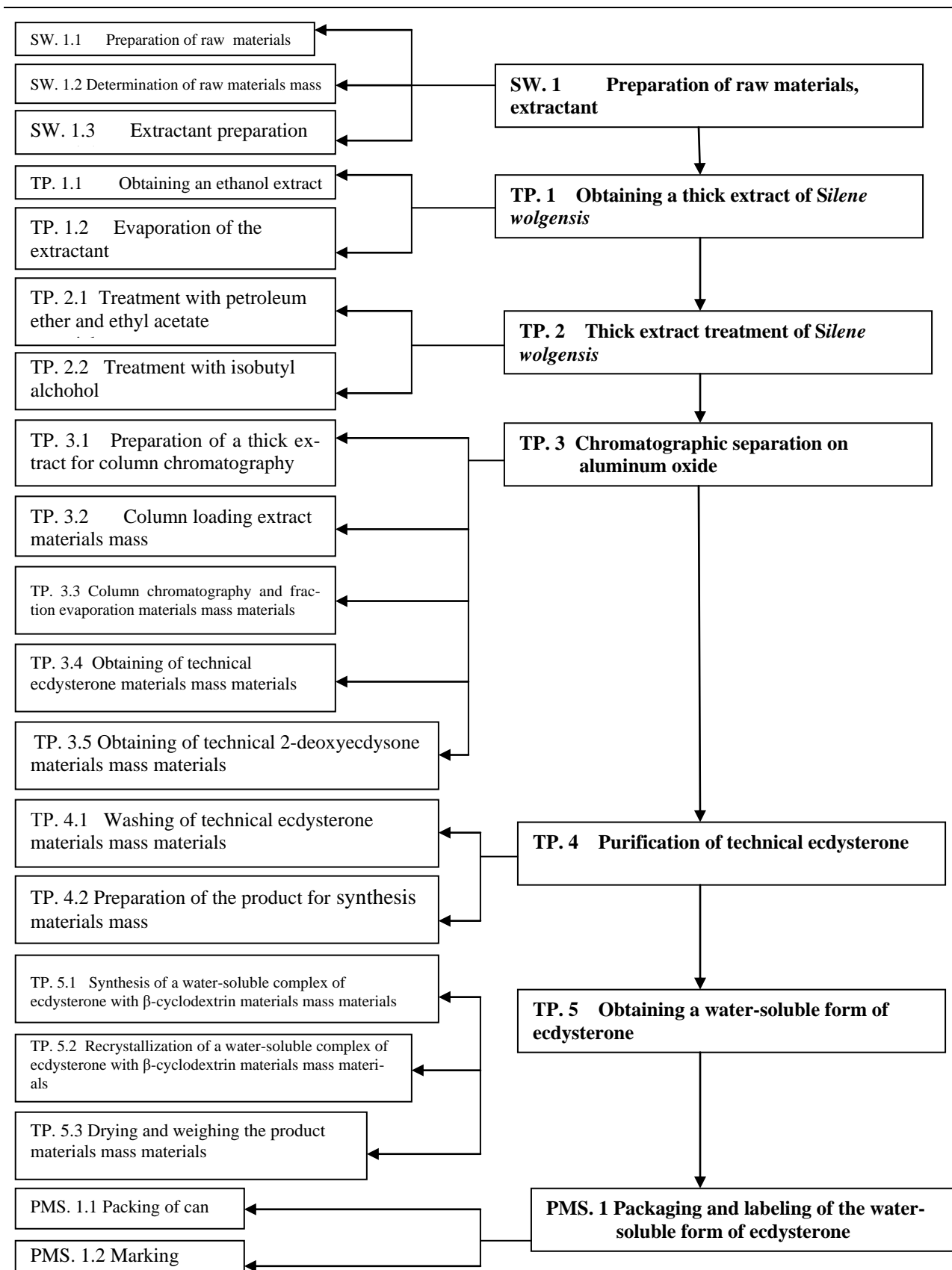


Figure 1. Technological scheme for the production of a water-soluble form of ecdysterone

As a result of the research, effective, express, and economical in terms of hardware execution conditions for the release of 20E were developed, using an extractant that meets GMP standards from industrially significant raw materials *Silene wolgensis*.

On the basis of the results of one-factor experiments, the above factors and intervals of variation (concentration of the extractant, duration of the process, extraction temperature, degree of grinding of raw materials) were selected. The result of the application is the first developed experimental industrial regulations for the isolation of ecdysterone and the production of a water-soluble form on its basis [12–16].

As result of the work conducted to optimize the extraction of bioactive steroid compounds and column chromatography of the ethanol extract *Silene wolgensis*, the main phytosteroid ecdysterone $2\beta,3\beta,14\alpha,20R,22R,25$ -hexahydroxy- $5\beta(H)$ -cholest-7-en-6-one) $C_{27}H_{44}O_7$ was obtained as a white odorless powder with a purity of 98 % according to HPLC. In order to establish the basic data on the physicochemical constants characteristic of ecdysterone, the following results were obtained: M.p. 236–238 °C (ethyl acetate-methanol); $[\alpha]_D^{20} + 66.0^\circ$ (1.0, methanol); IR (KBr) ν_{max} , cm^{-1} : 3450, 2950, 1652, 1450, 1390, 1060, 880; UV spectrum (EtOH), λ_{max} , nm: 243 (log ϵ 4.10). The substance is soluble in ethanol, dioxane, insoluble in water, ethyl acetate and chloroform. According to the data of primary analyzes, all available results completely coincide with the target compound ecdysterone, which is confirmed by the literature data [17].

The finished product is also a substance of a water-soluble form of ecdysterone; it is a supramolecular inclusion complex with β -cyclodextrin, obtained according to the scheme in Figure 2 and representing an odorless white powder with a basic substance content of at least 98 %.

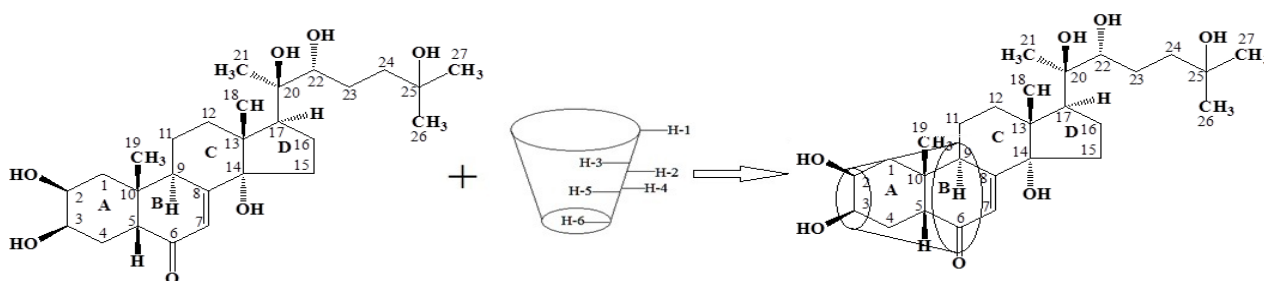


Figure 2. Scheme of the ecdysterone molecule entry into the β -cyclodextrin cavity

The possibility of creating nanocapsulated complexes of a biologically active component helps not only to increase the solubility and physicochemical stability of the substrate, but also to improve its bioavailability and local tolerance.

Thus, to establish the type of the formed inclusion complex of ecdysterone with β -cyclodextrin, the values of chemical shifts of 1H of the substrate and receptors in the free state and in the composition of the supramolecule were studied (Table 2). Ecdysterone is poorly soluble in water, and its spectra are difficult to record in deuterated water. Upon complexation of 20E with β -CD, supramolecular complexes are formed, which have a relatively high solubility in water compared to the initial 20E. Therefore, to confirm the water solubility of the complexes, NMR spectra were obtained in water. In Table 2, the first two columns demonstrate the 20E NMR spectra in deuterated chloroform and DMSO. 20E dissolves in these solvents, and can be identified by NMR spectra. The 20E NMR data in chloroform and DMSO presented in columns 1 and 2 of the table were applied to correctly identify the 20E spectra in the supramolecular complex. The 20E NMR signals slightly decrease in the supramolecular complex. Comparative data on changes in the chemical shifts of protons in the inner sphere are presented for free β -CD-n and its complex with 20E, obtained in deuterated water.

The chemical shifts of β -CD in water are well-known and were not presented by us in Table 2.

The main results on the structure of complexes of 20E with β -CD were obtained from ROESY spectra recorded in deuterated water. Based on the tabulated data, it can be noted that the protons of the inner sphere of cyclodextrin, H-3 and H-5, experience the greatest shift.

One of our goals is to characterize and disclose more detailed information on the molecular geometry of complexes of 20E with β -CD. First, we tried to fully decipher the signals and reveal the intermolecular interactions between 20E and CD using 2D ROESY NMR experiments.

Full assignment of 1H and ^{13}C NMR signals was made for pure 20E in DMSO d_6 (15.5 mg of pure 20E in 0.5 ml of water), excluding OH protons, which have two broad signals at 4.09 and 4.56 ppm, three broad superimposed signal at about 4.36 ppm, and a sharp signal at 4.63 ppm, which was designated as OH on carbon C14 due to the strong correlation of HMBC with carbon C13, and two weak correlations with carbon atoms C14 and C15.

Table 2

**^1H and ^{13}C NMR chemical shifts in the free state (δ_0 , DMSO- d_6)
and in the composition of the complexes (δ , D_2O), ppm**

No	20E in CDCl_3	20E in DMSO- d_6	20E- β -CD in D_2O
1	2	3	4
20E Signals			
C1 H1 α H1 β	37.96	36.610 1.263, dd, 13.3, 12.0 1.598, dd, 13.3, 4.3	35.499 1.299, dd, 13.5, 12.5 1.788, dd, 13.5, 4.4
C2 H2	68.03	66.754 3.604, ddd, 11.9, 4.3, 3.1	67.367 3.880
C3 H3	68.12	66.570 3.764, ~q, 2.9	67.128 3.968, ~q, 2.9
C4 H4 α H4 β	32.41	31.526 1.473, ~dt, 13.7, 3.8 1.593, td, 13.4, 2.5	31.154 1.705, br d 1.627
C5 H5	51.37	50.072 2.200, dd, 13.1, 4.2	50.358 2.270, dd, 12.6, 5.0
C6	203.43	202.620	208.101
C7 H7	121.64	120.432 5.626, d, 2.6	121.017 5.891, d, 2.6
C8	166.03	165.187	168.242
C9 H9	34.43	33.144 3.007, ddd, 11.6, 7.1, 2.7	33.831 3.025, ddd 11.5, 7.2, 2.6
C10	38.64	37.601	38.161
C1 H1 α H1 β	37.96	36.610 1.263, dd, 13.3, 12.0 1.598, dd, 13.3, 4.3	35.499 1.299, dd, 13.5, 12.5 1.788, dd, 13.5, 4.4
C2 H2	68.03	66.754 3.604, ddd, 11.9, 4.3, 3.1	67.367 3.880
C3 H3	68.12	66.570 3.764, ~q, 2.9	67.128 3.968, ~q, 2.9
C4 H4 α H4 β	32.41	31.526 1.473, ~dt, 13.7, 3.8 1.593, td, 13.4, 2.5	31.154 1.705, br d 1.627
C5 H5	51.37	50.072 2.200, dd, 13.1, 4.2	50.358 2.270, dd, 12.6, 5.0
C6	203.43	202.620	208.101
C7 H7	121.64	120.432 5.626, d, 2.6	121.017 5.891, d, 2.6
C8	166.03	165.187	168.242
C9 H9	34.43	33.144 3.007, ddd, 11.6, 7.1, 2.7	33.831 3.025, ddd 11.5, 7.2, 2.6
C10	38.64	37.601	38.161
C15 H15a H15P	31.98	30.303 1.781, ~td, 11.6, 5.5 1.507, ~q, 9.6	30.454 1.979, ~td 10.4, 6.2 1.631, ~dt
C16 H16a H16P	21.47	20.251 1.871 1.556	20.493 1.859, ~q, 11.1 1.759, ~dt, 14.1, 3.4

Continuation of Table 2

1	2	3	4
C17 H17	50.08	48.676 2.259, ~t, 9.0	49.216 2.250, dd, 10.0, 8.8
C18 H18	17.87	17.114 0.763, s	17.268 0.796, s
C19 H19	24.46	23.841 0.836, s	23.352 0.925, s
C20	76.82	75.682	77.599
C21 H21	21.68	20.959 1.062, s	20.095 1.175
C22 H22	77.52	76.182 3.115, dd, 10.5, 1.7	77.010 3.341, dd, 10.6, 1.9
C23 H23	27.45	26.073 1.475, ~td, 12.4, 3.9, 18. 1.111, dddd, 13.6, 11.6, 10.6, 4.5	26.018 1.535 1.237
C24 H24	42.62	41.377 1.645, ~td, 12.8, 5.0 1.253, ddd, 13.1, 11.6, 4.3	40.818 1.651, ddd 13.2, 10.6, 5.3 1.417, ddd, 13.2, 11.1, 4.3
C25	69.52	68.673	71.265
C26 H26	29.99	29.972 1.077, s	28.052 1.138, s
C27 H27	30.09	28.990 1.052, s	27.949 1.135, s
β -cyclodextrin signals			
C1 H1	-	-	102.238 4.991, d, 3.8
C2 H2	-	-	72.161 3.575, dd, 9.9, 3.7
C3 H3	-	-	73.248 3.885, dd, 9.9, 9.0
C4 H4	-	-	81.466 3.512, ~t, 9.3
C5 H5	-	-	71.929 3.781
C6 H6(2H)	-	-	60.282 ~3.79

The formation of an internal complex with ecdysterone is assumed. The study of the integral intensities of the signals of the guest and host molecules allows us to conclude that the stoichiometric ratio is 1:1. To identify the fragment of the 20E molecule located in the inner sphere of the CD, the changes in the values of the chemical shift were studied. The overlapping of ^1H signals of the substrate significantly complicates the analysis of NMR data; however, one can assume the formation of a supramolecular ensemble according to Figure 2.

Wide signal of residual water at 3.30 ppm has an intensity of 0.17 H. Other signals and most of their characteristics are shown in Table 2. JHH values, cross-peak intensities in HMBC and ROESY were used to establish the geometry of the 20E steroid part (aliphatic part from C23 rotates freely).

The signal of the ^1H β -CD proton was chosen as an internal reference, since this proton is located outside the β -CD cavity and therefore should be least affected by complexation. The changes ($\delta 27^\circ\text{C} - \delta 1^\circ\text{C}$) on the signals H1, H2, H3, H4, and H5 of the CD part were 0, +4, -12, -7, and -8 ppb, respectively, i.e. a large change was observed on the internal H3 β -CD. Similar changes were observed on H1 α (-2), H2 (+38), H3 (+18), H5 (-13), H7 (-8), H9 (+4), H17 (+3), H18 (-9), H19 (-19), H21 (-6), H22 (-3), H23 (-8), H24' (0), H26 (-2), H27 (-4) signals of 20E part; other signals were not observed due to overlap.

In general, an unambiguous conclusion about the geometry of the complex can be made by interpreting the intermolecular interactions in the ROESY spectra.

As expected, final ROEs between 20E and H1, H2, or H4 signals (outer hydrogen atoms) β -CD were not observed in all samples. This suggests that 20E forms a complex inside the β -CD cavity or that the concentration of other complexes was not detected under the studied conditions. This indicates that all the observed intermolecular ROEs are associated with the fact that 20E is located more or less inside the β -CD cavity. Despite a number of signal overlaps, it was possible to establish whether the aliphatic or steroid portion of 20E is in the β -CD at O6 (ROE to H5 / H6) or O3 (ROE to H3), based on the unambiguous presence/absence of ROE on the recognizable signals. H5 and both H6 β -CD signals overlap; however, since they are within the β -CD molecule, this is not a serious problem. The H3 β -CD signal overlaps with the H2 20E signals, thus only ROE cross-peaks that are not observed in pure 20E can be attributed to H3 β -CD.

These signals were separated at 1 °C, allowing for a more unambiguous interpretation.

We identified a strong ROE H5 / H6 β -CD for the 20E H23, H23', H24', H26/H27 signals, as well as the ROE H3 β -CD for the 20E H17, H18, H19, and H22 signals. This suggests that the 20E aliphatic portion is inserted deep into the β -CD through the O3 rim. Surprisingly, there are also weak ROE H5 / H6 β -CD for 20E H18, H21 and H22 signals and H3 β -CD on 20E H26 and H27 signals. This can be explained by simultaneous complexation through the O6 rim or complex formation through the O3 rim, however, with β -CD has at least one inverted sugar unit. ROE H3 β -CD for 20E signals H1 β , H4 α , H4 β , H5 and H19 suggests ring A complexation, but no ROE for H1 α . This can be understood as hindering H1 α from constant ROE by the nearby H19 methyl and OH group (s).

Pure 20E has a strong ROE between H9 and H2, and no ROE between H9 and H3, which is consistent with the molecular model where the H9-H2 distance is 0.18 nm and the H9-H3 distance is 0.38 nm. The change in the conformation of ring A can also be supported by the largest changes in chemical shifts on this ring with changes in temperature. Unfortunately, we were unable to identify significant changes in HMBC to reveal more details about the geometry changes.

Based on the obtained NMR spectroscopy data, which accurately describes the formation of a hydrophilic complex of ecdysterone entry into the cavity of the β -cyclodextrin molecule, thereby relying on the obtained result, we can confidently formulate the final data, which undoubtedly represent the characteristics of the supramolecular inclusion complex. Thus, the study of the target complex in D₂O yielded a result in which the main proton signal of H-7 was revealed, that is precise characteristic for compounds of the cholestanic structure, indicating that this substance is already capable of dissolving in water, and thereby makes it possible to conduct experiments on the study of hydrophilicity.

Conclusions

This work proposes the most optimal method for obtaining the inclusion complex of 20-hydroxyecdysone, isolated from the industrially significant plant *Silene wolgensis* with β -CD in a 1:1 ratio (substrate-clathrate). Based on the results obtained on preparative chromatography of the target product and the development of its chemically modified form, an optimal technological scheme has been proposed, in which the main stages of the production of a water-soluble substance are established. On the basis of the primary data on physicochemical constants, the criteria for standardization of the finished medicinal substance were established. The fine structure of the 20E inclusion complex with β -CD was fully confirmed by the data of two-dimensional correlation of the ¹H and ¹³C NMR spectra, thus, studying the main structural features of the supramolecular-clathrate inclusion complex. For the first time, on the basis of ecdysterone, a water-soluble drug substance of ecdysterone with β -cyclodextrin was obtained and its fine structure was confirmed. For the first time, a pilot industrial regulation for the isolation of ecdysterone from the *Silene wolgensis* and the production of a water-soluble form on its basis was developed. The developed method for obtaining a water-soluble form of ecdysterone is of great interest for the pharmaceutical industry as the basis for many actoprotective phytopreparations.

Acknowledgments

This work was financially supported by the Science Committee, a grant from the Ministry of Education and Science of the Republic of Kazakhstan (Project No. AP09260549).

References

- 1 Butenandt A. Crystallization of insectmoulting hormone / A. Butenandt, P. Karlson // *Naturforsch.* — 1954. — Vol. 9. — P. 389–391.
- 2 Nakanishi K. Insect hormones. The structure of ponasterone A, an insectmoulding hormone from the leaves of *Podocarpus nakaii* Hay / K. Nakanishi, A. Butenandt, M. Koreeda, S. Sasaki // *J. Chem. Soc. Chem. Commun.* — 1996. — Vol. 24. — P. 915–917.
- 3 Ахрем А.А. Экдистероиды: Химия и биологическая активность / А.А. Ахрем, Н.В. Ковганко. — Минск: Наука и техника, 1989. — 327 с.
- 4 Тулеуов Б.И. Стероидные соединения растений и лекарственные препараты на их основе. Поиск, химическая модификация и практические аспекты применения / Б.И. Тулеуов. — Караганда: Гласир, 2009. — 208 с.
- 5 Рамазонов Н.Ш. Химия, биология и технология получения фитоэкдистероидов / Н.Ш. Рамазонов, И.Д. Бобаев, В.Н. Сыров, Ш.Ш. Сагдуллаев, А.У. Маматханов. — Ташкент: Fan va texnologiya, 2016. — 260 с.
- 6 Сейлханов Т.М. ЯМР-спектроскопия циклодекстриновых комплексов включения / Т.М. Сейлханов. — Кокшетау: КГУ им. Ш. Уалиханова, 2015. — 155 с.
- 7 Бобров Е.Г. Флора СССР / Е.Г. Бобров, С.К. Черепанов. — М.: АН СССР, 1963. — С. 308.
- 8 Бондаренко О.Н. Род *Silene* L. — Смолевка // *Определитель растений Средней Азии* / О.Н. Бондаренко. — Ташкент: Фан, 1971. — С. 253–277.
- 9 Павлов Н.В. Флора Казахстана / Н.В. Павлов. — Алма-Ата: Наука КазССР, 1966. — 366 с.
- 10 Тулеуов Б.И. Технология фитостероидных препаратов / Б.И. Тулеуов. — Караганда: Гласир, 2017. — 112 с.
- 11 Лабораторный регламент на выделение полиоксистероидов из сырья *Silene wolgensis* (Hornem.) Bess. и получение водорастворимых форм на их основе // ЛР-№ 40761819–06–20., 2020 г.
- 12 Temirgazyev B.S. Bioavailability and structural study of 20-hydroxyecdysone complexes with cyclodextrins / B.S. Temirgazyev, K. Kucakova, Ye.A. Baizhigit, M. Jurasek et al. // *Steroids.* — 2019. — Vol. 147. — P. 37–41. <https://doi.org/10.1016/j.steroids.2018.11.007>
- 13 Кожанова А.М. Синтез, ЯМР-спектроскопическое исследование α -, β - и γ -циклодекстриновых комплексов включения 2-дезоксизекдизона и их противовоспалительная активность / А.М. Кожанова, Б.И. Тулеуов, П.К. Кудабаяева, Б.С. Темиргазиев, Т.М. Сейлханов, Р.Б. Сейдахметова, Л.К. Салькеева, С.М. Адекенов // *Макрогетероциклы.* — 2020. — № 3. — С. 292–297. DOI: 10.6060/mhc200602t
- 14 Tuleuov B.I. Supramolecular Complexes of 20-hydroxyecdysone-3-acetate with β -Cyclodextrin and Its Biological Activity / B.I. Tuleuov, B.S. Temirgazyev, A.M. Kozhanova, R.B. Seidakhmetova, K.M. Turdybekov, T.M. Seilkhanov, O.T. Seilkhanov, P. Drasar, S.M. Adekenov // *Russian Journal of General Chemistry.* — 2020. — Vol. 90. — P. 2258–2263. DOI: 10.1134/S1070363220120075
- 15 Kozhanova A.M. Technology of Obtaining a new water-soluble form of ecdysterone-substance from *Silene wolgensis* / A.M. Kozhanova, B.S. Temirgazyev, Ye.V. Minayeva, B.I. Tuleuov, A.A. Rakhatayeva, P. Drasar, S.M. Adekenov // XIII International Symposium on the Chemistry of Natural Compounds (ISCNC 2019). October 16–19, 2019. — Shanghai. — P. 125.
- 16 Kozhanova A.M. Synthesis, Structure and Bioactivity of a new water-soluble 20-Hydroxyecdysone Derivative / A.M. Kozhanova, B.S. Temirgazyev, Ye.V. Minayeva, T.M. Seilkhanov, R.B. Seidakhmetova, B.I. Tuleuov, S.M. Adekenov // XIII International Symposium on the Chemistry of Natural Compounds (ISCNC 2019). October 16–19, 2019. — Shanghai. — P. 126.
- 17 Государственная фармакопея Республики Казахстан. — Алматы: Изд. дом “Жибек жолы”, 2014. — 872 с.

А.М. Қожанова, Б.С. Темірғазиев, Ә. Жанарбек,
Б.И. Төлеуов, Т.М. Сейлханов, С.М. Әдекенов

Экдистеронның гидрофильді туындысының синтезі және оның негізінде суда еритін түрін алу

Мақалада *Silene wolgensis* (Hornem.) Bess. ex. Spreng (волга сылдыршөбі) дәрілік өсімдік шикізатынан экдистерон субстанциясын бөліп алу бойынша мәліметтер келтірілген. Алғаш рет фитоэкдистероидтардың асқын концентраттары волга сылдыршөбінің жерүсті бөлігінен экдистерон алу әдісінің оңтайландырылуы жүргізілді және экдистерон мен оның негізіндегі инкапсуленген суда еритін түрін алудың тәжірибелік-өнеркәсіптік регламенті жасалынды. Субстрат молекуласы мен клатраттың өзара әрекеттесуінен суда және басқа полярлы еріткіштерде ери алатын зат түзілетіні, сол арқылы негізгі гидрофобты препараттың биожетімділігі мәселесі шешілетіні анықталды. Экдистерон субстанциясы және оның β -циклодекстринмен инкапсуленген суда еритін түрін алу әдісі Қарағанды фармацевтикалық зауытында өндіріске ендірілді. Субстраттар мен рецепторлар протондарының химиялық жылжуларының өзгерістерін ЯМР-зерттеулер кезінде, экдистеронның β -циклодекстринмен 1:1 стехиометриялық құрамдағы молекулаүстілік ену кешендерін түзе отырып әрекеттесетіні

табылды. Экдистеронның β-циклодекстринмен инкапсулденген кешенінің, фитоэкдистеронның өзіне караганда суда ерігіштігінің 100 есе артатыны анықталды.

Кілт сөздер: экдистерон, бөліп алуды оңтайландыру, *Silene wolgensis*, β-циклодекстрин, инкапсулдеу, суда ерігішті.

А.М. Кожанова, Б.С. Темиргазиев, А. Жанарбек,
Б.И. Тулеуов, Т.М. Сейлханов, С.М. Адекенев

Синтез гидрофильного производного экдистерона и разработка водорастворимой формы на его основе

В статье представлены материалы по выделению экдистерона субстанции из лекарственного растительного сырья *Silene wolgensis* (Hornem.) Bess. ex. Spreng (смолевка волжская). Впервые проведена оптимизация способа получения экдистерона из надземной части сверхконцентратора фитоэкдистероидов смолевки волжской и разработан опытно-промышленный регламент выделения экдистерона и инкапсулированной водорастворимой формы на его основе. Найдено, что при взаимодействии молекулы субстрата и клатрата образуется вещество, способное растворяться в воде и других более полярных растворителях, тем самым решая проблему биодоступности основного гидрофобного лекарственного соединения. Разработанный способ получения экдистерона субстанции и его инкапсулированной с β-циклодекстрином водорастворимой формы внедрен в производство на Карагандинском фармацевтическом заводе. При ЯМР-изучении изменений химических сдвигов протонов субстратов и рецепторов найдено, что экдистерон взаимодействует с β-циклодекстрином с образованием надмолекулярных комплексов включения стехиометрического состава 1:1.

Ключевые слова: экдистерон, оптимизация выделения, *Silene wolgensis*, β-циклодекстрин, инкапсулирование, водорастворимость, ЯМР-спектроскопия, супрамолекулярные комплексы.

References

- 1 Butenandt, A. (1954). Crystallization of insectmoulting hormone. *Naturforsch*, 9, 389–391.
- 2 Nakanishi, K., Koreeda, M., Sasaki, S., Chang, M.L., & Hsu, H.Y. (1996). Insect hormones. The structure of ponasterone A, an insectmoulding hormone from the leaves of *Podocarpus nakaii* Hay. *J. Chem. Soc. Chem. Commun.*, 24, 915–917.
- 3 Akhrem, A.A. & Kovganko, N.V. (1989). *Ekdisteroidy: khimiia i biologicheskaiia aktivnost* [Ecdysteroids: chemistry and biological activity], Minsk: Nauka i tekhnika [in Russian].
- 4 Tuleuov, B.I. (2009). *Steroidnye soedineniia rastenii i lekarstvennye preparaty na ikh osnove. Poisk, khimicheskaiia modifikatsiia i prakticheskie aspekty primeneniia* [Steroid compounds of plants and drugs based on them. Search, chemical modification and practical aspects of application]. Karaganda: Glasir [in Russian].
- 5 Ramazonov, N.Sh., Bobayev, I.D., Syrov, V.N., Sagdullayev, Sh.Sh., Mamatkhanov, A.U. (2016). *Khimiia, biologiia i tekhnologiia polucheniia fitoekdisteroidov* [Chemistry, biology and technology of phytoecdysteroid production]. Tashkent: Fan va texnologiya [in Russian].
- 6 Seylkanov, T.M. (2015). *YAMR-spektroskopiia tsiklodekstrinovykh kompleksov vklyucheniya* [NMR spectroscopy of cyclodextrin inclusion complexes]. Kokshetau: KGU imeni Sh. Ualikhanova [in Russian].
- 7 Bobrov, E.G., Cherepanov, S.K. (1963). *Flora SSSR* [Flora of the USSR]. Moscow: Akademiia nauk SSSR [in Russian].
- 8 Bondarenko, O.N. (1971). *Rod Silene L. — Smolevka* [Genus *Silene L. — Smolevka*]. *Opredelitel rastenii Srednei Azii — Keys to plants of Central Asia*. Tashkent: Fan [in Russian].
- 9 Pavlov, N.V (1966). *Flora Kazakhstana* [Flora of Kazakhstan]. Alma-Ata: Nauka KazSSR [in Russian].
- 10 Tuleuov, B.I. (2017). *Tekhnologiia fitosteroidnykh preparatov* [Phytosteroid drug technology]. Karaganda: Glasir [in Russian].
- 11 Laboratory regulations for the isolation of polyoxysteroids from raw materials *Silene wolgensis* (Hornem.) Bess. and obtaining water-soluble forms on their basis. LR-№ 40761819–06–20. — 2020.
- 12 Temirgaziyeu, B.S., Kucakova, K., Baizhigit, Ye.A., Jurasek, M., Dzubak, P., & Hajduch, M., et al. (2019). Bioavailability and structural study of 20-hydroxyecdysone complexes with cyclodextrins. *Steroids*, 147, 37–41. <https://doi.org/10.1016/j.steroids.2018.11.007>
- 13 Kozhanova, A.M., Tuleuov, B.I., Kudabaeva, P.K., Temirgaziyeu, B.S., Seikhanov, T.M., & Seidakhmetova, R.B. et al. (2020). Sintez, IaMR-spektroskopicheskoe issledovanie α-, β- i γ-tsiklodekstrinovykh kompleksov vklucheniia 2-dezoksiekdizona i ikh protivovospalitelnaia aktivnost [Synthesis, NMR Spectroscopic Study of α-, β- and γ-Cyclodextrin Inclusion Complexes of 2-Deoxyecdysone and Their Anti-inflammatory Activity]. *Makroheterotsikly — Macroheterocycles*, 13, 292–297. DOI: 10.6060/mhc200602t

- 14 Tuleuov, B.I., Temirgazyev, B.S., Kozhanova, A.M., Seidakhmetova, R.B., Turdybekov, K.M., & Seilkhanov, T.M. (2020). Supramolecular Complexes of 20-hydroxyecdysone-3-acetate with β -Cyclodextrin and Its Biological Activity. *Russian Journal of General Chemistry*, 90, 12, 2258–2263. DOI: [10.1134/S1070363220120075](https://doi.org/10.1134/S1070363220120075)
- 15 Kozhanova, A.M., Temirgazyev, B.S., Minayeva, Ye.V., Tuleuov, B.I., Rakhatayeva, A.A., Drasar, P., & Adekenov, S.M. (2019). Technology of obtaining a new water-soluble form of ecdysterone-substance from *Silene wolgensis*. Proceedings from XIII International Symposium on the Chemistry of Natural Compounds (16–19 October 2019 year). (p. 125). Shanghai: ISCNC 2019.
- 16 Kozhanova, A.M., Temirgazyev, B.S., Minayeva, Ye.V., Seilkhanov, T.M., Seidakhmetova, R.B., Tuleuov, B.I., & Adekenov, S.M. (2019). Synthesis, Structure and Bioactivity of a new water-soluble 20-Hydroxyecdysone Derivative. Proceedings from XIII International Symposium on the Chemistry of Natural Compounds (16–19 October 2019 year). (p. 126). Shanghai: ISCNC 2019.
- 17 *Gosudarstvennaia farmakopeia Respubliki Kazakhstan* (3th ed.) (2014). Almaty: Izdatelskii dom “Zhibek zholy” [in Russian].

Information about authors

Kozhanova Aizhan Mukhametkaliyeva — Master's degree of Technical Sciences; Junior Researcher of the Laboratory of Chemistry of Steroid Compounds of JSC “International Research and Production Holding “Phytochemistry”, Gazaliev street 4, 100009, Karaganda, Kazakhstan; e-mail: alhss@mail.ru; <https://orcid.org/0000-0002-1048-9749>

Temirgazyev Bakhtiyar Serikovich — Master's degree of Technical Sciences; Researcher of the Laboratory of Chemistry of Steroid Compounds of JSC “International Research and Production Holding “Phytochemistry”, Gazaliev street 4, 100009, Karaganda, Kazakhstan; e-mail: alhss@mail.ru; e-mail: b_a_h_a1990@mail.ru; <https://orcid.org/0000-0001-6994-3478>

Zhanarbek Alima Zhanarbekkyzy — Engineer of the Laboratory of chemistry of steroid compounds of JSC “International Research and Production Holding “Phytochemistry”, Gazaliev street 4, 100009, Karaganda, Kazakhstan; e-mail: zhalima17@mail.ru; <https://orcid.org/0000-0003-3955-0213>

Tuleuov Borash Iglikovich — Doctor of Chemical Sciences, Professor, Academician of the National Academy of Sciences of the Republic of Kazakhstan; Head of the Laboratory of Chemistry of steroid Compounds of JSC “International Research and Production Holding “Phytochemistry” Gazaliev street 4, 100009, Karaganda, Kazakhstan; e-mail: tulbor@mail.ru; <https://orcid.org/0000-0002-7592-9768>

Seilkhanov Tulegen Muratovich — Candidate of Chemical Sciences, Professor, Head of the Laboratory of engineering profile of NMR Spectroscopy of the Sh. Ualikhanov Kokshetau University, Abay street 76, 020000, Kokshetau, Kazakhstan; e-mail: tseilkhanov@mail.ru; <https://orcid.org/0000-0003-0079-475>

Adekenov Sergazy Mynzhasarovich — Doctor of Chemical Sciences, Professor, Academician of the National Academy of Sciences of the Republic of Kazakhstan; General Director of JSC “International Research and Production Holding “Phytochemistry”, Gazaliev street 4, 100009, Karaganda, Kazakhstan; e-mail: arglabin@phyto.kz; <https://orcid.org/0000-0001-7588-6174>

Y.B. Raiymbekov^{1*}, U. Besterekov¹, P.A. Abdurazova¹,
U.B. Nazarbek¹, I.A. Pochitalkina²

¹*M.Auezov South Kazakhstan University, Shymkent, Kazakhstan;*

²*Mendeleev University of Chemical Technology of Russia, Moscow, Russia*

(*Corresponding author's e-mail: epusr@bk.ru)

Recovery of used acetic acid via sulfuric acid

Kazakhstan has a huge phosphate raw material base, where the basis is made up of micro-grained phosphate ores of the Karatau basin. The depletion of reserves of high-quality commercial ores leads to the search for new methods of using the enrichment and sorting of low-grade technogenic ores, one of which is phosphate-siliceous slates. The presented study was carried out in two stages: at the first stage, phosphate-siliceous shales were enriched by the acetic acid method, regime technological parameters, kinetic and thermodynamic regularities of the process were determined. At the second stage of the research a method for recycling used acetic acid during the enrichment of low-grade phosphate-siliceous slates is proposed. In this case, sulfuric acid was chosen as the regenerating agent of acetic acid. The reliability of the performed studies was proved by the use of modern complex research methods: scanning electron microscopy, Energy Dispersive X-Ray and X-Ray diffraction analyses. To determine the course of a particular reaction, a thermodynamic analysis was performed using modern HSC 6.0 software. The kinetic data are determined by calculation. The obtained experimental data were subjected to statistical analysis (Chaddock scale, standard deviation, coefficient of determination). The mechanism of interaction of an acetate solution with sulfuric acid is illustratively described. In conclusion, the sulfuric acid method is suitable for the regeneration of applied acetic acid. In this case, a by-product is formed in the form of calcium sulfate. This product can be used as a building binder (confirmed by the protocol of the "National Center of Expertise" of the Republic of Kazakhstan).

Keywords: acid recovery, acetic acid, low-grade phosphorites, beneficiation, sulfuric acid, phosphate-siliceous slates, Chaddock scale, calcium sulfate.

Introduction

The globalization process of the economy and ensuring the sustainable development of all sectors of the national economy requires timely and effective solutions to the problems accumulated by mankind. The steadily increasing consumption of mineral raw materials ensures the dynamic development of the economy and society of many countries of the world, including Kazakhstan.

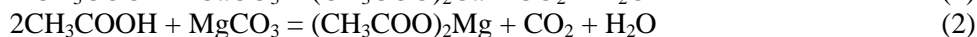
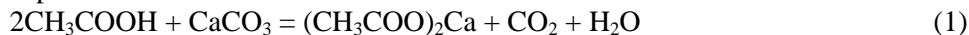
The Republic of Kazakhstan is one of the countries in the world that has large deposits of phosphorite in the Karatau phosphorite-bearing basin. When extracting phosphorites, an open method is usually used and it is always accompanied by the formation of various wastes. The main by-products of open-pit mining of phosphorites in the Karatau basin are phosphate-siliceous shales. The approximate volume of accumulated waste is about 40 million tons. This indicator is growing every year, while high-grade (23–27 % P₂O₅) and medium-grade (20–23 % P₂O₅) deposits of phosphorites are being depleted [1, 2]. Scientists attribute this type of waste to the technogenic resources of the Karatau basin [3].

According to the lithological composition, this type of waste belongs to a variety of clay-siliceous shales with an interlayer of carbonate-siliceous and pelitomorphous carbonate-siliceous phosphorites with phosphate-clay-siliceous shales [3-4]. Its composition is dominated by clay compounds (SiO₂) and one-and-a-half oxides (Fe₂O₃, Al₂O₃), which complicate the enrichment process [5].

With an increase in the consumption of phosphorus-containing products [6], the reserves of rich and ordinary phosphorites are being depleted, and in a few years industrialists may face the problem of an acute shortage of high-quality raw materials. In this regard, the strategy for the development of the mineral resource base should be based on the rational use of the identified resources and their timely reproduction.

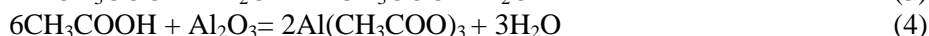
The world reserves of phosphorites are dominated by hard-to-enrich ores of carbonate, siliceous-carbonate and carbonate-siliceous composition [7, 8]. There are various methods for enriching low-grade phosphorites: flotation, calcination, magnetic separation [9, 10]. One of the promising methods is the use of dilute organic acids, the so-called chemical enrichment. Organic acids with slow heating have the ability to dissolve dolomites and calcites in the composition of phosphorite, while not affecting the phosphate part of

the raw material [11]. The use of organic acids is relevant for countries where the production of phosphorus-containing products is one of the main sectors of the economy. So, scientists from China [11, 12], Egypt [13], Uzbekistan [14], Pakistan [15, 16], and Russia [17, 18] conducted similar studies. In their works, organic acids of various types were used. However, in many studies [11–18], the use of acetic acid as the main reagent that dissolves carbonate minerals well is particularly noted. The chemistry of the reaction of acetic acid with carbonates can be represented as follows:



As can be seen from the reaction equation, acetic acid reacts with carbonates to form salts of calcium and magnesium acetates. The dissolved carbonates in the form of an acetate salt remain in the solution, and, accordingly, the content of total P_2O_5 increases in the insoluble part.

In addition, we have determined that potassium and aluminum-containing compounds in the composition of phosphorite also actively interact with acetic acid:



Although these studies indicate that the process of enriching low-grade phosphorites has been successfully carried out, there is also a problem of disposing of the acetate solution. This issue is relevant, since a large amount of dilute acetic acid is spent during enrichment (liquid/solid ratio = 8:1, 5:1, 3:1). Consequently, a considerable volume of the solution is formed. The authors propose various methods of disposal: the use of the ion exchange method, regeneration with hydrochloric acid and hydrofluoric acid [19]. Also, in the future, the sulfuric acid can be applied to obtain calcium sulfate [20].

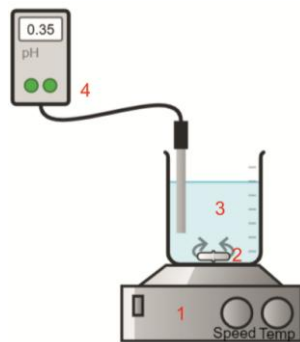
All of the above studies are only at the theoretical level. Until now, no experimental studies have been conducted on the recovery of acetic acid, so there is an acute lack of comprehensive data on this problem.

Thus, the aim of the research is to study the process of acetic acid recovery with the use of sulfuric acid and the production of calcium sulfate. The given experimental data are new and can serve for further development of research in the field of enrichment of low-grade phosphorites with organic acids.

The studies were conducted in two stages. At the first stage, the process of enrichment of phosphate-siliceous shales of the Zhanatas deposit (Karatau basin) with acetic acid was carried out. The optimal operating parameters are established: the highest yield of P_2O_5 is 21 % at 30 °C, 15 min and liquid/solid ratio = 1:3 [21]. Kinetic regularities are determined, a thermodynamic analysis of the acetic acid enrichment process is carried out. During the enrichment process, an acetate solution was obtained, which must be disposed of or returned to the process. Considering this issue, the second stage of the study provides the results.

Experimental

The recovery process of acetic acid was studied in the laboratory using experimental lab equipment (Fig. 1): an acetate solution and sulfuric acid were mixed at temperatures of 333, 348, and 363 K on a magnetic stirrer, to which a pH meter I-160MI was attached to observe changes during the process. The mixing time varied from 15 min to 45 min. The suspension was filtered on a Buchner funnel with a constant dilution of 0.06 MPa. The sediment on the filter was dried at 110 °C to a constant weight.



1 — magnetic stirrer; 2 — magnetic stir bar; 3 — solution of acetates and sulfuric acid; 4 — pH-meter

Figure 1. Experimental lab equipment

The study of the element-weight composition and structural features of the source material and the resulting product was implemented on a scanning electron microscope JSM-64901 V [22].

The X-ray diffraction (XRD) analysis of the feedstock and the resulting product was performed on the D8 Advance (Bruker), α -Cu apparatus. The processing of the obtained diffractogram data and the calculation of interplane distances were carried out applying EVA software. The samples were decoded and the phases were searched using the Search / match program and the PDF-2 powder diffractometric data base.

The multifunctional software package HSC 6.0 was used to conduct a thermodynamic analysis of the acetic acid recovery process, taking into account the phase changes of the initial components and final products, with the calculation of changes in the enthalpy, entropy, Gibbs energy, and the logarithm of the equilibrium constant.

The calculation of the reaction rate of the acetic acid recovery process was performed according to the formula:

$$\partial = \frac{\Delta n}{V \Delta \tau},$$

where: Δn — change in the amount of moles of starting substances, mol; V — volume of the mixture, l; $\Delta \tau$ — time, min.

The study's results of the kinetic regularities of the acetic acid recovery are processed using the Pavlyuchenko equation [23]:

$$1 - (1 - \alpha)^{1/3} = \kappa \cdot \sqrt{\tau}. \quad (2)$$

This equation is typical for the processes that begin on the entire surface but the progress of the reaction into the depth of the particle depends on the thickness of the layer formed by the reaction products through which the reagent diffuses. This equation describes the processes, the limiting stage of which is diffusion.

The calculation of the apparent activation energy of the process (E_{app}) is graphically determined from the dependence $\ln \kappa = f\left(\frac{1}{T}\right)$, when the value of the reaction rate constant is known at certain process temperatures.

E_{app} determined by the formula:

$$E_{app} = 8.314 \cdot \text{tg}_{\phi} \text{ (J/mol)}.$$

Kinetic data were subjected to statistical processing (standard deviation and correlation analysis) [24, 25].

Results and Discussion

Characteristics of the acetate solution

The acetate solution obtained during the enrichment of low-grade phosphate-siliceous shales was subjected to evaporation to study its element-weight composition. The evaporated acetate solution is presented in the form of a white crystalline substance that is highly soluble in water. It has a faint smell of vinegar. The results are shown in Figure 1 and in Table 1.

Table 1

Element-weight composition of the acetate solution

Element	Weight, %	In terms of oxides, %
C	26.77	-
O	45.88	-
Mg	0.59	0.97
Al	0.21	0.39
Si	0.62	1.32
S	0.68	1.7
Ca	24.15	33.78
Mn	0.32	0.41
Fe	0.79	1.12

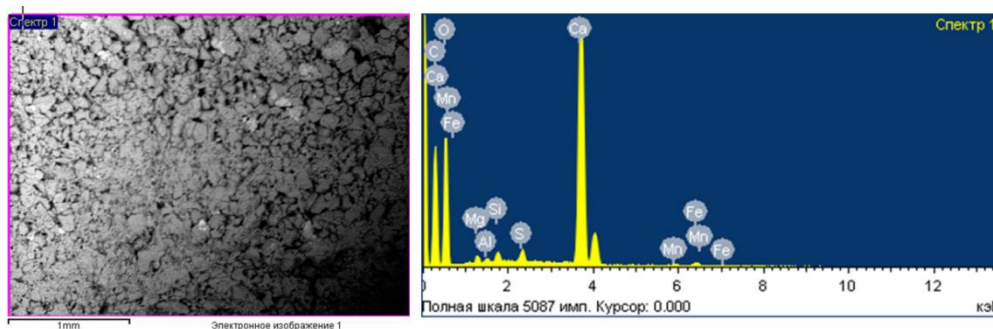


Figure 2. SEM image and EDX analysis of evaporated acetate solution

The data of the element-weight composition illustrate the predominant presence of calcium compounds. There are also impurity elements in the form of magnesium, sulfur, silicon, iron, and manganese, which were transferred during the acetic acid leaching of low-grade phosphate-siliceous shales by reactions 1–4.

For a more detailed study of the composition of the acetate solution, the method of XRD analysis was used. The results are represented in Figure 3 and in Table 2.

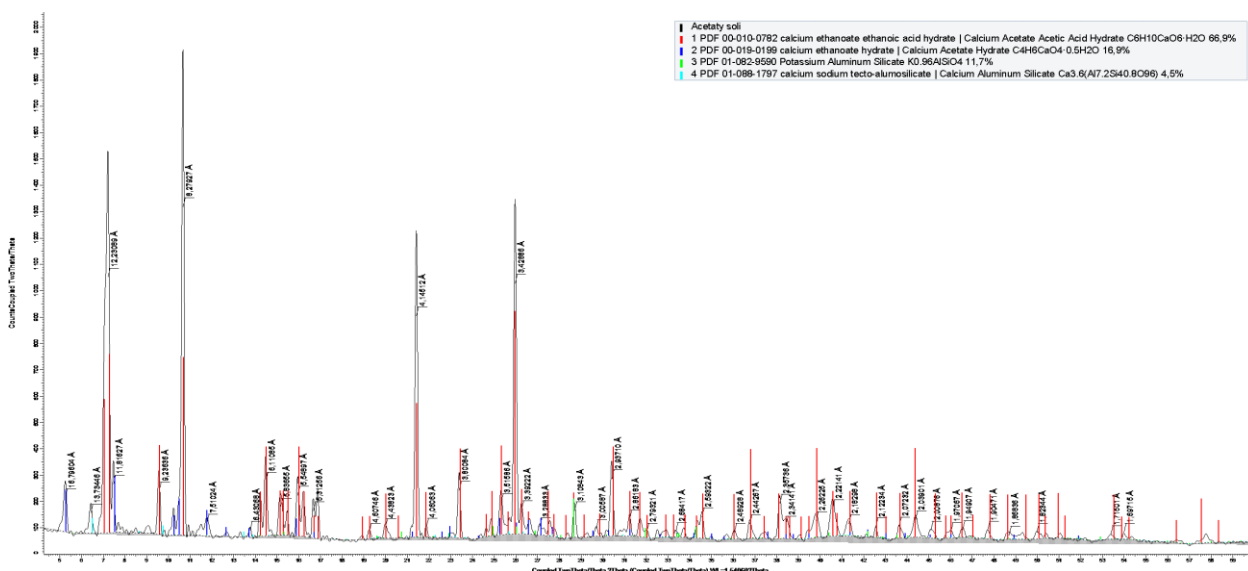


Figure 3. XRD image of evaporated acetate solution

Table 2

XRD decryption of evaporated acetate solution

Pattern #	Compound Name	Formula	S-Q
PDF 00-010-0782	Calcium ethanoate ethanoic acid hydrate Calcium Acetate Acetic Acid Hydrate	$C_6H_{10}CaO_6 \cdot H_2O$	66.9 %
PDF 00-019-0199	Calcium ethanoate hydrate Calcium Acetate Hydrate	$C_4H_6CaO_4 \cdot 0.5H_2O$	16.9 %
PDF 01-082-9590	Potassium Aluminum Silicate	$K_{0.96}AlSiO_4$	11.7 %
PDF 01-088-1797	Calcium sodium tecto-alumosilicate Calcium Aluminum Silicate	$Ca_{3.6}(Al_{7.2}Si_{40.8}O_{96})$	4.5 %

The data of the XRD analysis clearly demonstrate the presence of the main compounds in the composition of the evaporated acetate solution. The main compound is calcium acetate hydrate in the amount of 83.8 %. There is also the presence of impurity compounds of potassium-aluminosilicates and calcium-aluminosilicates.

Reaction mechanism and thermodynamic analysis

The chemistry of used acetic acid recovery process with sulfuric acid can be represented as follows:

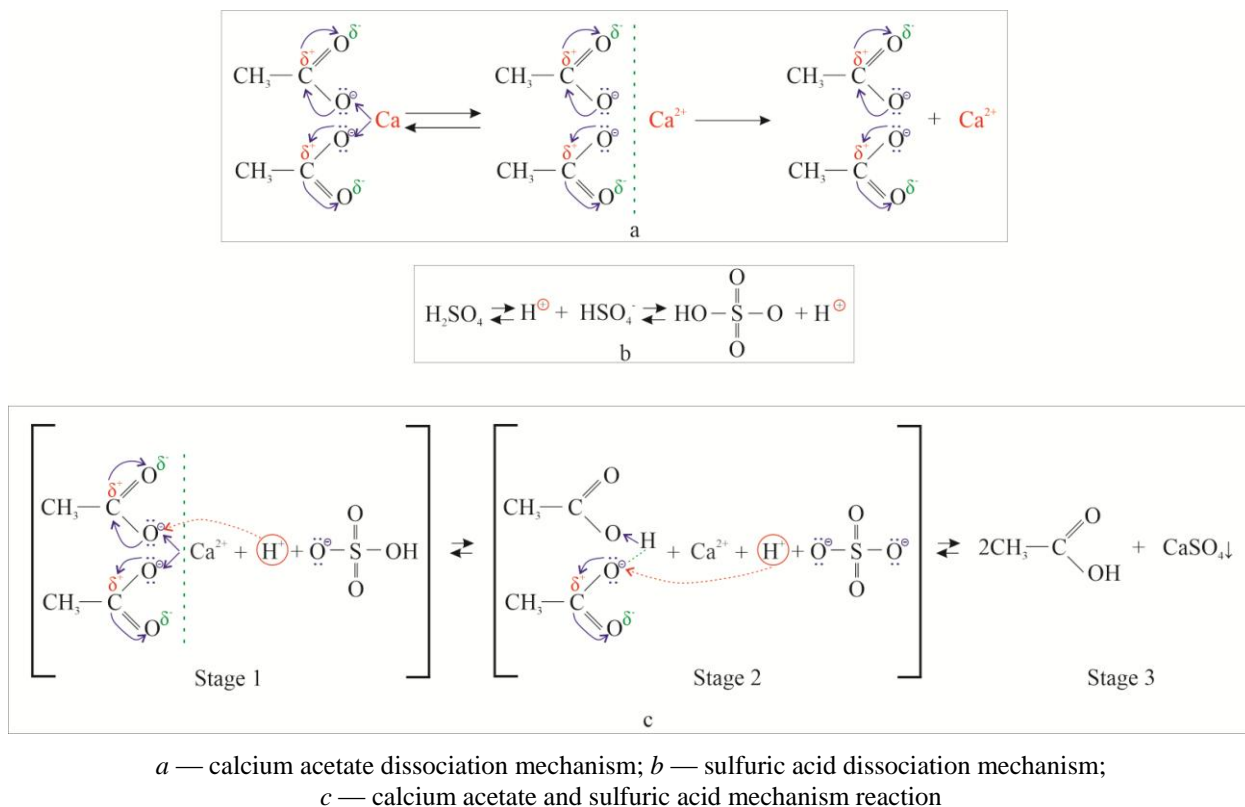
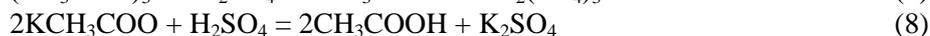
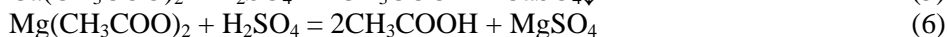
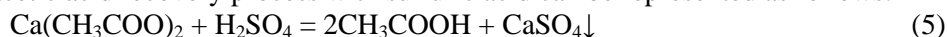


Figure 4. Reaction mechanism

Interacting molecule (substrate) — the carboxylic acid salt dissociates as follows (Fig. 4a): the stability (hence the acidic properties) of the carboxylate anion is explained by the delocalization of the negative charge in 2 oxygen atoms due to ρ, π -pairing (fusion). Concentrated H_2SO_4 is a very strong oxidizing agent [26], especially when heated (Fig. 4b). The concentration of sulfuric acid determines the rate and direction of the sulfating process, as well as the mass of the sulfate reagent necessary for its implementation, since the reaction occurs and the acid concentration decreases (as a result of diluting it with reaction water). This leads to an increase in the possibility of acid dissociation of H_2SO_4 and a decrease in the concentration of sulfonated particles.

At Stage 1 (Fig. 4c), the electrophilic center (S_E) is a carbon atom of the carboxyl group, in the presence of which carboxylic acids and their functional derivatives enter into nucleophilic substitution reactions. At Stage 2, the main center-an oxotope with one pair of electrons is protonated at the catalysis stage in nucleophilic substitution reactions. At Stage 3, the oxotope forms a salt after protonation, displacing the calcium cation and the formation of weak acetic acid. All stages of the reaction are reversible. A detailed illustration of the process of interaction of an acetate solution and sulfuric acid is shown in Figure 5.

During the reaction 5–8, calcium sulfate precipitates, and the remaining formed compounds, such as magnesium, aluminum, and potassium sulfate, are soluble and thus will be present in the solution.

To determine the ability of a particular reaction to proceed, a thermodynamic analysis was carried out taking into account the phase changes of the initial components and final products, with the calculation of changes in the enthalpy, entropy, Gibbs energy, and the logarithm of the equilibrium constant. The thermodynamic characteristics of the processes were determined in the temperature range of 333, 348, and 363 K. The results of calculating the thermodynamic characteristics as a function of the temperature in the proposed reaction are represented in Table 3.

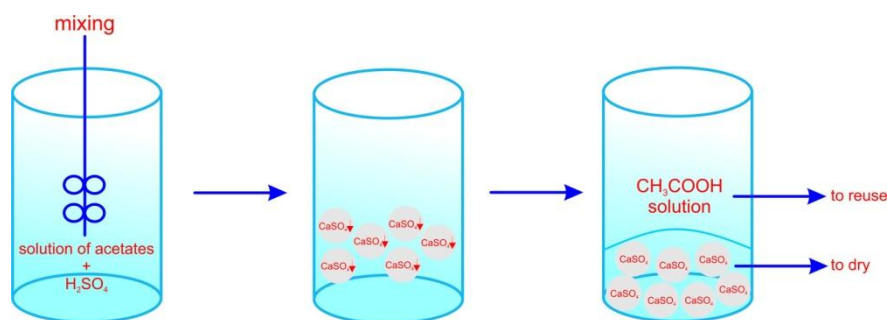


Figure 5. Schematic illustration of the process

Table 3

Thermodynamic parameters of the reactions (5–8)

T, K	ΔH^0 , kJ/mol	ΔS^0 , J/(mol·K)	ΔG^0 , kJ/mol	K	log(K)
$\text{Ca}(\text{CH}_3\text{COO})_2 + \text{H}_2\text{SO}_4 = 2\text{CH}_3\text{COOH} + \text{CaSO}_4\downarrow$					
333	-69.207	221.692	-141.031	2.740E+022	22.438
348	-64.295	236.120	-146.465	9.686E+021	21.986
363	-59.308	250.149	-150.112	4.004E+021	21.603
$\text{Mg}(\text{CH}_3\text{COO})_2 + \text{H}_2\text{SO}_4 = 2\text{CH}_3\text{COOH} + \text{MgSO}_4$					
333	30.789	285.047	-64.131	1.150E+010	10.061
348	35.627	299.255	-68.514	1.927E+010	10.285
363	40.532	313.055	-73.107	3.317E+010	10.521
$2\text{Al}(\text{CH}_3\text{COO})_3 + 3\text{H}_2\text{SO}_4 = 6\text{CH}_3\text{COOH} + \text{Al}_2(\text{SO}_4)_3$					
333	222.513	1210.239	-180.496	2.066E+028	28.315
348	212.167	1179.832	-198.415	6.087E+029	29.784
363	203.133	1154.406	-215.916	1.181E+031	31.072
$2\text{KCH}_3\text{COO} + \text{H}_2\text{SO}_4 = 2\text{CH}_3\text{COOH} + \text{K}_2\text{SO}_4$					
333	-132.494	-33.184	-121.444	1.126E+019	19.051
348	-133.098	-34.961	-120.931	1.423E+018	18.153
363	-133.432	-35.905	-120.399	2.121E+017	17.327

The values of ΔG^0 in the studied temperature range are in the negative region, and this indicates the thermodynamic probability of reactions 5-8. From the comparison of the values of ΔG^0 reactions, it follows that from a thermodynamic point of view, the probability of reactions occurring at these temperatures changes in the following sequence: $\text{Al}(\text{CH}_3\text{COO})_3 > \text{Ca}(\text{CH}_3\text{COO})_2 > \text{KCH}_3\text{COO} > \text{Mg}(\text{CH}_3\text{COO})_2$. In this case, reactions 5 and 8 are exothermic, which follows from the negative values of ΔH^0 .

Kinetic regularities

Based on the above reactions, temperatures in the range of 333, 348, and 363 K were selected for effective recovery of acetic acid. The process time is 15, 30, and 45 minutes. The reaction rate was calculated according to the formula (1). The results of the experiments are illustrated in Table 4.

The data in Table 4 designate the reaction rate slows down with increasing temperature and time. An increase in temperature negatively affects the value of α -the degree of expenditure of sulfuric acid, since this value decreases. This means the remaining part of the sulfuric acid did not have time to react with the acetates in the solution.

Statistical processing of experimental data showed that at 333 K, the relationship between the studied features is direct, the closeness (strength) of the connection on the Chaddock scale is high, the average approximation error (characterizes the adequacy of the regression model) is 5.0 %. Data at 348 and 363 K, the dependence between the studied features is direct, the closeness (strength) of the connection on the Chaddock scale is functional, the average approximation error is 1.8 % and 2.1 %, respectively.

Table 4

The obtained experimental data

Time, min	pH	C, mol/l	The degree of expenditure, α	v , mol/l·min	Standard deviation	Coefficient of determination
333 K						
15 min	0.117	0.76383	42.23	0.07436	3.02	0.975
30 min	0.129	0.74190	76.30	0.06718	3.18	
45 min	0.150	0.70794	95.46	0.05603	2.66	
348 K						
15 min	0.169	0.67622	25.92	0.04564	1.52	0.998
30 min	0.172	0.67236	50.40	0.04437	2.32	
45 min	0.177	0.66484	71.40	0.04191	2.15	
363 K						
15 min	0.190	0.64534	20.17	0.03551	0.83	0.997
30 min	0.197	0.63530	36.60	0.03222	1.91	
45 min	0.203	0.62661	49.99	0.02934	1.89	

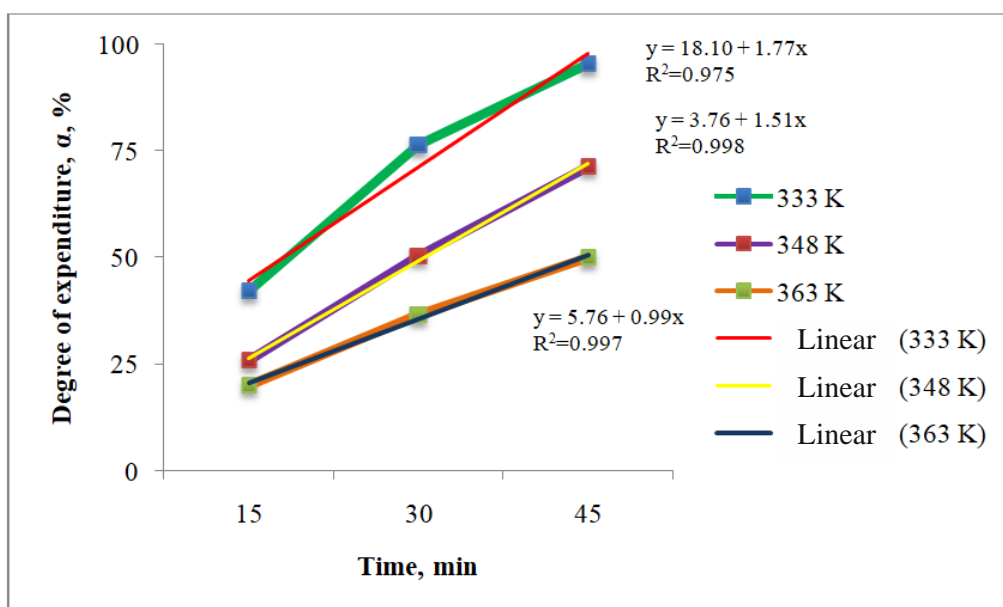
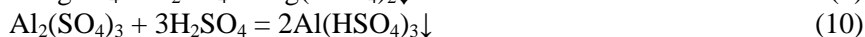


Figure 6. Dependence of sulfuric acid expenditure degree on time

The highest degree of expenditure of sulfuric acid, as presented in Table 4 and Figure 6, is 333 K and 45 min. This means that not all the sulfuric acid has been reacted and an excess of acid remains in the solution. The unreacted free sulfuric acid will interact with the formed soluble sulfates of magnesium, aluminum, and potassium:



According to the reaction 9–10, insoluble compounds of magnesium, aluminum, and potassium hydrosulfate are formed, which precipitate without passing into solution.

The experimentally found kinetic parameters are processed by the Pavlyuchenko method applying the equation (2).

The effect of temperature and time on the degree of expenditure (α) during the recovery of acetic acid and the results of processing experimental data in relation to the Pavlyuchenko equation are shown in Table 5.

Results of experimental data processing

α (shares of 1)	$1-\alpha$	$\sqrt[3]{1-\alpha}$	$1-\sqrt[3]{1-\alpha}$	τ , min	$\sqrt{\tau}$
T=333K					
0.4223	0.5777	0.832851	0.167149	15	3.87298
0.7630	0.2370	0.618846	0.381154	30	5.47722
0.9546	0.0454	0.356740	0.643260	45	6.70820
T=348K					
0.2592	0.7408	0.904830	0.095170	15	3.87298
0.5040	0.4960	0.791578	0.208422	30	5.47722
0.7140	0.2860	0.658853	0.341147	45	6.70820
T=363K					
0.2017	0.7983	0.927660	0.072340	15	3.87298
0.3660	0.6340	0.859072	0.140928	30	5.47722
0.4999	0.5001	0.793753	0.206247	45	6.70820

Based on the data in Table 5, a dependency graph $1-(1-\alpha)^{1/3} = f(\sqrt{\tau})$ is constructed:

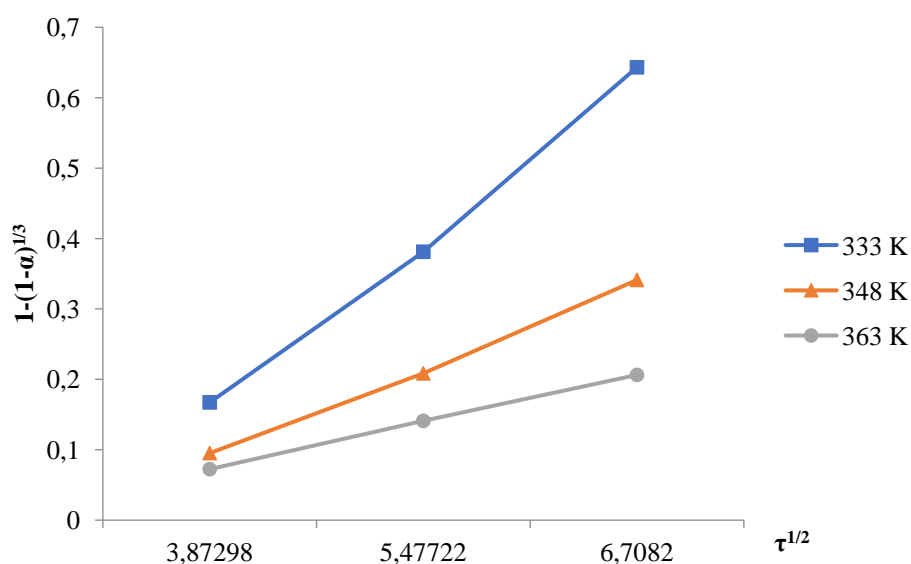


Figure 7. Dependency graph $1-(1-\alpha)^{1/3} = f(\sqrt{\tau})$

The reaction rate constants are found by the tangent of the angle of the straight lines to the abscissa axis shown in Figure 7:

- at 333K, $\text{tg}_{\varphi_1}=k_1=0.1175827$;
- at 348K, $\text{tg}_{\varphi_2}=k_2=0.0315797$;
- at 363K, $\text{tg}_{\varphi_3}=k_3=0.0096065$.

The “apparent” activation energy of the recovery process is found by the graphical method. For these purposes, a dependency graph $\ln k = f\left(\frac{1}{T}\right)$ is constructed (Fig. 8).

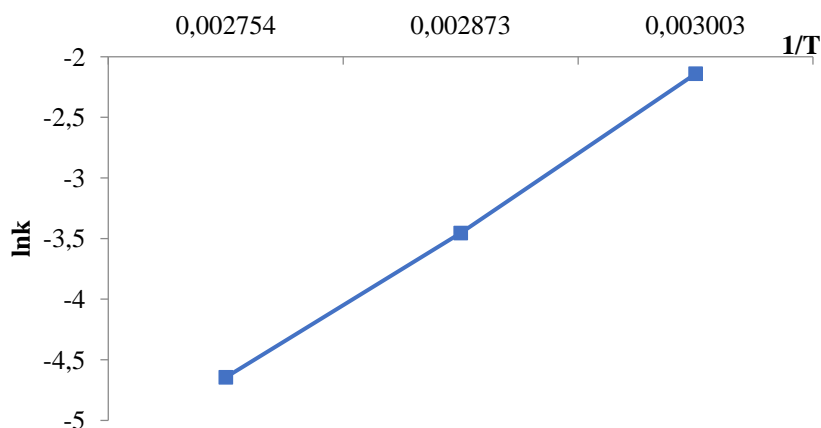


Figure 8. Dependency graph $\ln k = f\left(\frac{1}{T}\right)$

Based on Figure 8 and using the formula (3), the “pparent” activation energy of the process was calculated. For the studied process, the E_{app} was 59.65 kJ/mol. The found value of the apparent activation energy allows concluding that the studied process takes place in the intra-diffusion region [23].

Characteristics of the resulting product

During the mixing of the acetate solution and sulfuric acid, a white crunocrystalline precipitate and a solution of acetic acid were formed. The precipitate was pure calcium sulfate (gypsum). For the analysis, the resulting calcium sulfate was dried isothermally at a temperature of 110 C to a constant weight. Dried calcium sulfate was subjected to SEM and XRD analysis (Table 6, Fig. 9).

Table 6

Element-weight composition of the formed sediment

Element	Weight, %	In terms of oxides, %
O	48.03	-
Mg	0.29	0.48
Al	0.58	1.09
Si	0.54	1.15
S	22.33	55.82
K	0.32	0.38
Ca	27.91	39.04

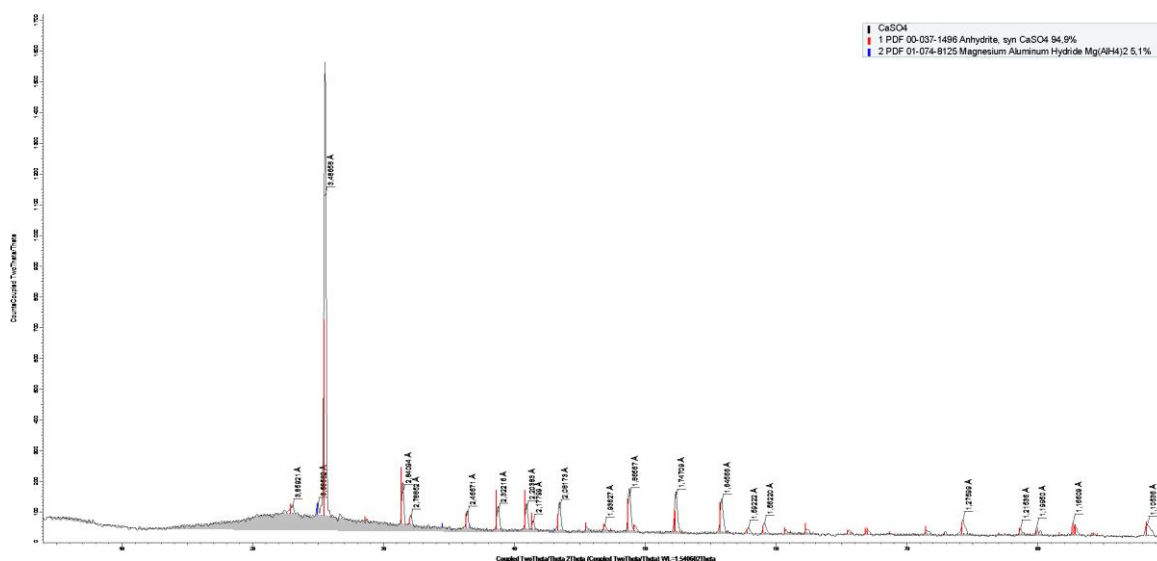


Figure 9. XRD analysis of sediment

As mentioned above, in addition to calcium sulfate, there were compounds in the form of magnesium, aluminum, and potassium hydrosulfate in the sediment. The data of element-weight and XRD analysis proved the presence of these compounds in the composition of the sediment. From the XRD analysis, it was found out the main structural compound in the sediment was calcium sulfate — 94.9 %. The remaining 5.1 % was probably occupied by the magnesium aluminum hydride compound. The white crystalline product was acidic with a pH = 0.159, since it contained a small amount of free sulfuric acid.

The resulting by-product in the form of calcium sulfate can be used as a building material (gypsum) [27]. To determine the suitability and use, a radiological analysis was carried out in the “National Center of Expertise”. The samples were examined in accordance with the requirements of regulatory documents, in particular “GOST 30108-94. Building materials and elements. Determination of specific activity of natural radioactive nuclei” at the Progres BG gamma-spectrometric equipment. The results are shown in Table 7.

Table 7

Results of measurements of specific radioactivity

Sample name	Specific effective activity, Bk/kg	Permissible level of specific effective activity, Bq/kg	Construction material class	Terms of use of building materials
Calcium Sulfate	10±2	370	1	Use in residential and public buildings under construction and reconstruction

As the measurement results show, the specific effective activity is within the permissible level and corresponds to the conditions of use in residential and public buildings under construction and being reconstructed. The results of the study were confirmed by Protocol No. 18-pl/s / RO-21-0-1170 from 03.06.2021 “National Center of Expertise”.

Conclusions

The obtained research results demonstrate the suitability of the sulfuric acid method of recovery of an acetate solution for reuse in the enrichment of low-grade phosphorites. The obtained and statistically processed experimental data illustrate the operating technological parameters that are the temperature at 60 °C and the time of 45 min. It was at these indicators that the highest degree of consumption of sulfuric acid was achieved for the complete precipitation of calcium sulfate. Thermodynamic analysis revealed the regularity of the reaction. The calculated “apparent” activation energy of the heterogeneous process was 59.65 kJ/mol. This means the process takes place in the intradiffusion region. The resulting by-product in the form of calcium sulfate can be used as a building material (gypsum). The presented results are complementary to the information about the acid enrichment of low-grade phosphorites.

References

- 1 Елкондиева Г.Б. Каратауский бассейн — крупнейшая фосфатная сырьевая база Евразии / Елкондиева Г.Б. // Фосфатное сырье: производство и переработка: материалы Междунар. науч.-практ. конф. (17 мая 2012 г.). — М., 2012. — С. 21–30.
- 2 Перфильева Н.Н. Фосфорный путь / Н.Н. Перфильева. — Тараз: ТОО Казфосфат, 2018. — [Электронный ресурс]. Режим доступа: http://www.kpp.kz/upload/kf_video_files/Fosfor_way.pdf.
- 3 Киперман Ю.А. Фосфаты в XXI веке: моногр. / Ю.А. Киперман. — Тараз: ТОО Казфосфат, 2006. — [Электронный ресурс]. Режим доступа: http://www.kpp.kz/upload/kf_video_files/fosfati_XXI.pdf.
- 4 Glenn C.R., Phosphorites // Sedimentology. Encyclopedia of Earth Science. — Berlin: Springer, Heidelberg, 1978. — 255 p. <https://doi.org/10.1007/3-540-31079-7>
- 5 СТ РК 2213-2012. Сырье измельченное фосфатное Каратау. Технические условия, Комитет технического регулирования и метрологии Министерства промышленности и новых технологий Республики Казахстан. — Астана, 2012.
- 6 Schroder J.J. Sustainable Use of Phosphorus / J.J. Schroder, D. Cordell, A.L. Smit, A. Rosemarin. — Wageningen: Plant Research International, 2010. — 140 p.
- 7 Van Kauwenbergh S.J. World Phosphate Rock Reserves and Resources / S.J. Van Kauwenbergh. — IFDC: Muscle Shoals, Alabama, 2010. — 60 p.

- 8 Garside M. Global phosphate rock reserves by country 2020. — [Electronic resource]. Access mode: <https://www.statista.com/statistics/681747/phosphate-rock-reserves-by-country/>.
- 9 Komar Kawatra S. Beneficiation of Phosphate Ore. Society for Mining, Metallurgy, and Exploration / S. Komar Kawatra, J.T. Carlson. — Englewood, 2013. — 168 p.
- 10 Ptacek P. Mining and Beneficiation of Phosphate Ore, Apatites and their Synthetic Analogues — Synthesis, Structure, Properties and Applications / P. Ptacek. — London: IntechOpen, 2016. — 514 p. <https://doi.org/10.5772/62215>
- 11 Fei X. Research on Enrichment of P₂O₅ from Low-Grade Carbonaceous Phosphate Ore via Organic Acid Solution / X.Fei, Zh.Jie, Ch.Jiyan, W.Jianrui, W.Lin // J. Anal. Methods Chem. — 2019. — P. 7. <https://doi.org/10.1155/2019/9859580>
- 12 Patent 104445112A. People's Republic of China. Method for recycling phosphate ores by using acid leaching method / W. Zhang, J. Wang, Y. Zhang. — Guizhou University. Publ. 25.03.2015.
- 13 Bakry A.R. Upgrading of Abu-Tartur calcareous phosphate via selective leaching by organic acids / A.R. Bakry, N.A. Abdelfattah, A.B. Farag // Int. J. Eng. Res. — 2015. — No. 6. — P. 57–64. <https://www.ijser.org/researchpaper/Upgrading-of-Abu-Tartur-calcareous-phosphate-via-selective-leaching-by-organic-acids.pdf>
- 14 Seitnazarov A. Beneficiation of High-Calcareous Phosphorites of Central Kyzylkum with Organic Acid Solutions / A.Seitnazarov, S.Namazov, B.Beglov // J. Chem. Technol. Metall. — 2014. — No. 49. — P. 383–390. https://dl.uctm.edu/journal/node/j2014-4/JCTM_2014_4_Beneficiation%20of%20high-calcareous%20phosphorites%20of%20central%20kyzylkum%20with%20organic%20acid%20s.pdf
- 15 Zafar I.Z. Beneficiation of low grade carbonate-rich phosphate rocks using dilute acetic acid solution // Fertilizer Research. — 1993. — No. 34. — P. 173–180. <https://doi.org/10.1007/BF00750112>
- 16 Zafar I.Z. Selective leaching of calcareous phosphate rock in formic acid: Optimisation of operating conditions / I.Z. Zafar, M.M. Anwar, P.W. Pritchard // Min. Eng. — 2006. — No. 19. — P. 1459–1461. <https://doi.org/10.1016/j.mineng.2006.03.006>
- 17 Патент 2097139C1. Российская Федерация. Способ обогащения карбонатсодержащего фосфатного сырья / Йелстаун Корпорейшн Н.В. (NL). Оpubл. 27.11.1997.
- 18 Патент 469664A1. Советский Союз. Способ обогащения фосфоритов / Г.О. Григорян. Оpubл. 05.05.1975.
- 19 Zafar I.Z. A New Route for the Beneficiation of Low Grade Calcareous Phosphate Rocks / I.Z. Zafar, M.M. Anwar, P.W. Pritchard // J. Fert. Res. — 1996. — No. 44. — P. 133–142. <https://doi.org/10.1007/bf00750803>
- 20 Ashraf M. Reaction kinetics and mass transfer studies in selective leaching of low-grade calcareous phosphate rock: PhD thesis: Chemistry / M. Ashraf. — Multan, Pakistan, 2010. — 194 p.
- 21 Raiymbekov Y. Beneficiation of phosphate-siliceous slates via acetic acid / Y. Raiymbekov, U. Besterekov, P. Abdurazova, U. Nazarbek, I. Petropavlovskiy // International Journal of Chemical Reaction Engineering. — 2021. — Vol. 19, Iss. 11. — P. 1187–1195. <https://doi.org/10.1515/ijcre-2021-0071>
- 22 Reed S.J.B. Electron Microprobe Analysis and Scanning Electron Microscopy in Geology. — University of Cambridge, Cambridge, 2005. — 189 p. <https://doi.org/10.1017/CBO9780511610561>
- 23 Вольдман Г.М. Теория гидрометаллургических процессов / Г.М. Вольдман, А.Н. Зеликман // — М.: Интернет Инжиниринг, 2003. — 464 с.
- 24 Hatcher L. Advanced Statistics in Research: Reading, Understanding, and Writing Up Data Analysis Results / L. Hatcher. — Shadow Finch Media LLC, Michigan, 2013. — 644 p.
- 25 Martin W.E. Quantitative and Statistical Research Methods: From Hypothesis to Results 1st Edition / W.E. Martin, K.D. Bridgmon. — Jossey-Bass, 2012. — 496 p.
- 26 Davenport W.G. Sulfuric Acid Manufacture. Analysis, Control and Optimization / W.G. Davenport, M.J. King // Elsevier Science, 2006. — 413 p.
- 27 Guerra-Cossío M.A. Calcium sulfate: an alternative for environmentally friendly construction / M.A. Guerra-Cossío, J.R.G. Lopez, A.A. Zaldivar-Cadena // 2nd International Conference on Bio-based Building Materials & 1st Conference on Ecological valorisation of GRANular and FIBrous materials, Clermont-Ferrand, France, 2017. — P. 1–6. <https://doi.org/10.26168/icbbm2017.37>

Е.Б. Райымбеков, У. Бестереков, П.А. Абдуразава, У.Б. Назарбек, И.А. Почиталкина

Қолданылған сірке қышқылын күкірт қышқылымен регенерациялау

Қазақстанда Қаратау бассейнінің шағын түйіршікті фосфат кендерінің негізін құрайтын орасан зор фосфат шикізат базасы бар. Жоғары сапалы тауарлық кен қорларының сарқылуы төмен сұрыпты техногендік кендерді байыту мен сұрыптаудың жаңа әдістерін іздеуге әкеледі, олардың бірі фосфат-кремнийлі қатпар тастар болып табылады. Зерттеу екі кезеңде жүргізілді: бірінші кезеңде фосфат-кремнийлі қатпар тастар сірке қышқылы әдісі арқылы байытылды, режимдік технологиялық параметрлер, үрдістің кинетикалық және термодинамикалық заңдылықтары анықталды. Осы мақалада зерттеудің екінші кезеңі қарастырылған: онда төмен сұрыпты фосфат-кремнийлі қатпар тастарды байыту кезінде пайдаланылған сірке қышқылын кәдеге жарату әдісі ұсынылған. Бұл жағдайда күкірт қышқылы сірке қышқылының қалпына келтіретін агенті ретінде таңдалды. Жүргізілген зерттеулердің

шынайылығы қазіргі заманғы кешенді зерттеу әдістерін қолданумен негізделеді: растрлық электронды микроскопия, EDX және XRD талдау. Нақты реакцияның жүру мүмкіндігін анықтау үшін қазіргі заманғы HSC 6.0 бағдарламалық жасақтамасын қолдана отырып, термодинамикалық талдау жүргізілді. Кинетикалық деректер есептеу жолымен анықталды. Алынған эксперименттік мәліметтер статистикалық талдаудан өтті (Чеддок шкаласы, стандартты ауытқу, анықтау коэффициенті). Ацетат ерітіндісінің күкірт қышқылымен әрекеттесу механизмі суреттелген. Зерттеу нәтижелері пайдаланылған сірке қышқылын қалпына келтіруге күкірт қышқылы әдісінің жарамдылығы туралы қорытынды жасауға мүмкіндік береді. Бұл жағдайда кальций сульфаты түрінде жанама өнім пайда болады. Бұл өнімді құрылыс материалы ретінде пайдалануға болады (ҚР «Ұлттық сараптама орталығы» хаттамасымен расталған).

Кілт сөздер: қышқылды алу, сірке қышқылы, төмен сұрыпты фосфориттер, байыту, күкірт қышқылы, фосфат-кремнийлі қатпар тастар, Чеддок шкаласы, кальций сульфаты.

Е.Б. Райымбеков, У. Бестереков, П.А. Абдуразова, У.Б. Назарбек, И.А. Почиталкина

Регенерация использованной уксусной кислоты серной кислотой

Казахстан располагает огромной фосфатной сырьевой базой, где основу составляют микрозернистые фосфатные руды Каратауского бассейна. Истощение запасов качественных товарных руд приводит к поискам новых методов использования обогащения и сортировки низкосортных техногенных руд, одним из которых являются фосфатно-кремнистые сланцы. Представленное исследование было выполнено в два этапа: на первой стадии фосфатно-кремнистые сланцы обогащались посредством уксусно-кислотного метода, были определены режимные технологические параметры, кинетические и термодинамические закономерности процесса. В статье рассмотрен второй этап исследования, где предложен метод утилизации использованной уксусной кислоты при обогащении низкосортных фосфатно-кремнистых сланцев. В этом случае серная кислота была выбрана в качестве регенерирующего агента уксусной кислоты. Достоверность выполненных исследований обоснована применением современных комплексных методов исследований: растровой электронной микроскопии, EDX- и XRD-анализа. Для определения протекания конкретной реакции был проведен термодинамический анализ с помощью современного программного обеспечения HSC 6.0. Кинетические данные получены расчетным путем. Экспериментальные данные были подвергнуты статистическому анализу (шкала Чеддока, стандартное отклонение, коэффициент детерминации). Иллюстративно описан механизм взаимодействия ацетатного раствора с серной кислотой. Результаты исследований позволяют сделать вывод о пригодности сернокислотного метода для регенерации использованной уксусной кислоты. При этом образуется побочный продукт в виде сульфата кальция, который можно применять в качестве строительного вяжущего материала (подтвержден Протоколом Национального центра экспертизы Республики Казахстан).

Ключевые слова: извлечение кислоты, уксусная кислота, низкосортные фосфориты, обогащение, серная кислота, фосфатно-кремнистые сланцы, шкала Чеддока, сульфат кальция.

References

- 1 Elkindieva, G.B. (2012). Karatauskii bassein — krupneishiaia fosfatnaia syrevaia baza Evrazii [The Karatau basin is the largest phosphate resource base in Eurasia]. Proceedings from Phosphate raw materials: production and processing: *Mezhdunarodnaia nauchno-prakticheskaiia konferentsiia — International scientific and practical conference* (17, May, 2012). (pp. 21–30). Moscow [in Russian].
- 2 Perfileva, N.N. (2018). *Fosfornyi put [Phosphorus pathway]*. Taraz: Kazphosphate LLC. Retrieved from http://www.kpp.kz/upload/kf_video_files/Fosfor_way.pdf [in Russian].
- 3 Kiperman, Yu.A. (2006). *Fosfaty v XXI veke [Phosphates in the XXI century]*. Taraz: Kazphosphate LLC. Retrieved from http://www.kpp.kz/upload/kf_video_files/fosfati_XXI.pdf [in Russian].
- 4 Glenn, C.R. (1978). Phosphorites. *Sedimentology. Encyclopedia of Earth Science*. Berlin: Springer. <https://doi.org/10.1007/3-540-31079-7>
- 5 *Standart Respubliki Kazahstan 2213–2012. Syre izmelchennoe fosfatnoe Karatau. Tehnicheskie usloviia [Standard Republic of Kazakhstan 2213–2012. Raw materials are crushed phosphate Karatau. Technical conditions]*. (2012). Astana: Committee of Technical Regulation and Metrology of the Ministry of Industry and New Technologies of the Republic of Kazakhstan [in Russian].
- 6 Schroder, J.J., Cordell, D., Smit, A.L. & Rosemarin, A. (2010). *Sustainable Use of Phosphorus*. Wageningen, Netherlands: Plant Research International.
- 7 Van Kauwenbergh, S.J. (2010). *World Phosphate Rock Reserves and Resources*. Muscle Shoals, Alabama, USA: IFDC.
- 8 Garside, M. (2021). *Global phosphate rock reserves by country 2020*. Retrieved from: <https://www.statista.com/statistics/681747/phosphate-rock-reserves-by-country/>.

- 9 Komar Kawatra, S., & Carlson, J.T. (2013). *Beneficiation of Phosphate Ore*. Society for Mining, Metallurgy, and Exploration. USA: Englewood.
- 10 Ptacek, P. (2016). *Mining and Beneficiation of Phosphate Ore, Apatites and their Synthetic Analogues — Synthesis, Structure, Properties and Applications*. London: IntechOpen. <https://doi.org/10.5772/62215>
- 11 Fei, X., Jie, Zh., Jiyang, Ch., Jianrui, W. & Lin, W. (2019). Research on Enrichment of P₂O₅ from Low-Grade Carbonaceous Phosphate Ore via Organic Acid Solution. *J. Anal. Methods Chem.*, 7. <https://doi.org/10.1155/2019/9859580>
- 12 Zhang, W., Wang, J. & Zhang, Y. (2015). *People's Republic of China Patent No. 104445112A*. Guizhou: Guizhou University.
- 13 Bakry, A.R., Abdelfattah, N.A., & Farag, A.B. (2015). Upgrading of Abu-Tartur calcareous phosphate via selective leaching by organic acids. *Int. J. Eng. Res.*, 6, 57–64. <https://www.ijser.org/researchpaper/Upgrading-of-Abu-Tartur-calcareous-phosphate-via-selective-leaching-by-organic-acids.pdf>
- 14 Seitnazarov, A., Namazov, S., & Beglov, B. (2014). Beneficiation of High-Calcareous Phosphorites of Central Kyzylkum with Organic Acid Solutions, *J. Chem. Technol. Metall.* 49, 383–390. Retrieved from: https://dl.uctm.edu/journal/node/j2014-4/JCTM_2014_4_Beneficiation%20of%20high-calcareous%20phosphorites%20of%20central%20kyzylkum%20with%20organic%20acid%20s.pdf
- 15 Zafar, I.Z. (1993). Beneficiation of low grade carbonate-rich phosphate rocks using dilute acetic acid solution. *Fertilizer Research*, 34, 173–180. <https://doi.org/10.1007/BF00750112>
- 16 Zafar, I.Z., Anwar, M.M., & Pritchard, P.W. (2006). Selective leaching of calcareous phosphate rock in formic acid: Optimization of operating conditions. *Min. Eng.*, 19, 1459–1461. <https://doi.org/10.1016/j.mineng.2006.03.006>
- 17 Potashnik, B.A., Avakjan, Z.A., & Karavajko, G.I. (1997). Sposob obogashcheniia karbonatsoderzhashchego fosfatnogo syrja [Method for enrichment of carbonate-containing phosphate raw materials]. *Patent No. 2097139C1. Rossiiskaia Federatsiia — Russian Federation Patent No. 2097139C1*. Moscow: Russia, Russian Agency for Patents and Trademarks [in Russian].
- 18 Grigoryan, G.O. (1975). Sposob obogashcheniia fosforitov [Phosphate enrichment method]. *Patent No. 469664A1. Sovetskii Soiuz — Soviet Union Patent No. 469664A1*. Moscow: Soviet Union, State Committee of the Council of Ministers of the USSR for Inventions and Discoveries [in Russian].
- 19 Zafar, I.Z., Anwar, M.M., & Pritchard, P.W. (1996). A New Route for the Beneficiation of Low Grade Calcareous Phosphate Rocks. *J. Fert. Res.* 44, 133–142. <https://doi.org/10.1007/bf00750803>
- 20 Ashraf, M. (2010). Reaction kinetics and mass transfer studies in selective leaching of low-grade calcareous phosphate rock. *Doctor's thesis*. Multan, Pakistan.
- 21 Raiymbekov, Y., Besterekov, U., Abdurazova, P., Nazarbek, U. & Petropavlovskiy, I. (2021). Beneficiation of phosphate-siliceous slates via acetic acid. *International Journal of Chemical Reaction Engineering*, 19(11), 1187–1195. <https://doi.org/10.1515/ijcre-2021-0071>
- 22 Reed, S.J.B. (2008). *Electron Microprobe Analysis and Scanning Electron Microscopy in Geology*. Cambridge: University of Cambridge. <https://doi.org/10.1017/CBO9780511610561>
- 23 Voldman, G.M., & Zelikman, A.N. (2003). *Teoriia gidrometallurgicheskikh protsessov [Theory of hydrometallurgical processes]*. Moscow: Intermet Engineering [in Russian].
- 24 Hatcher, L. (2013). *Advanced Statistics in Research: Reading, Understanding, and Writing Up Data Analysis Results*. Michigan: Shadow Finch Media LLC.
- 25 Martin, W.E. & Bridgmon, K.D. (2012). *Quantitative and Statistical Research Methods: From Hypothesis to Results 1st Edition*. San Francisco: Jossey-Bass.
- 26 Davenport, W.G. & King, M.J. (2006). *Sulfuric Acid Manufacture. Analysis, Control and Optimization*. Netherlands: Elsevier Science.
- 27 Guerra-Cossío, M.A., Lopez, J. R. G. & Zaldivar-Cadena, A.A. (2017). Calcium sulfate: an alternative for environmentally friendly construction. *2nd International Conference on Bio-based Building Materials & 1st Conference on ECOlogical valorisation of GRAnular and FIBrous materials* (pp. 1–6). Clermont-Ferrand, France. <https://doi.org/10.26168/icbbm2017.37>

Information about authors

Raiymbekov Yerkebulan (*corresponding author*) — PhD-student, M.Auezov South Kazakhstan University, Department of Chemical Technology of Inorganic Substances, Tauke Khan Avenue, 5, 160000, Shymkent, Kazakhstan; e-mail: eplusr@bk.ru; <https://orcid.org/0000-0002-2119-2406>;

Besterekov Uilesbek — Doctor of Technical sciences, Professor, M.Auezov South Kazakhstan University, Department of Chemical Technology of Inorganic Substances, Tauke Khan Avenue, 5, 160000, Shymkent, Kazakhstan; e-mail: besterek80@mail.ru;

Abdurazova Perizat — PhD, Ass. Professor, M.Auezov South Kazakhstan University, Department of Chemical Technology of Inorganic Substances, Tauke Khan Avenue, 5, 160000, Shymkent, Kazakhstan; e-mail: abdurazova-p@mail.ru, <https://orcid.org/0000-0002-5244-7678>;

Nazarbek Ulzhalgas — PhD, Ass.Professor, M.Auezov South Kazakhstan University, Department of Chemical Technology of Inorganic Substances, Tauke Khan Avenue, 5, 160000, Shymkent, Kazakhstan; e-mail: unazarbek@mail.ru, <https://orcid.org/0000-0001-8890-8926>;

Pochitalkina Irina — Doctor of Technical sciences, Professor, Department of Technology of Inorganic Substances and Electrochemical Processes, Miuskaya Square, 9, 125047, Moscow, Russia; e-mail: ipochitalkina@muctr.ru.

**Index of articles published in
«Bulletin of the Karaganda University. Chemistry Series»
in 2021**

№ p.

ORGANIC CHEMISTRY

<i>Ayazbayeva A.Ye., Shakhvorostov A.V., Seilkhanov T.M., Aseyev V.O., Kudaibergenov S.E.</i> Synthesis and characterization of novel thermo- and salt-sensitive amphoteric terpolymers based on acrylamide derivatives.....	4	9
<i>Bhole R.P., Jadhav S., Chikhale R., Shinde Y., Bonde C.G.</i> Synthesis and evaluation of vitamin-drug conjugate for its anticancer activity.....	3	21
<i>Bhole R.P., Yogita Shinde, Bonde C.G., Wavhale R.D.</i> Vitamin Drug conjugate: a systematic review of pharmacological potential.....	1	27
<i>Iskineyeva A., Mustafaeva A., Zamaratskaya G., Fazylov S., Pustolaikina I.A., Nurkenov O.A., Sarsenbekova A., Seilkhanov T., Bakirova R.</i> Preparation of encapsulated α -tocopherol acetate and study of its physico-chemical and biological properties	3	27
<i>Ivasenko S.A., Shakarimova K.K., Bokayeva A.B., Marchenko A.B., Lavrinenko A.V., Kolesnichenko S.I.</i> Study of the phenolic compounds of the dry extract of <i>Thymus crebrifolius</i> using a combined HPLC–UV and HPLC-ESI-MS/MS method	2	18
<i>Klivenko A.N., Mussabayeva B.Kh., Gaisina B.S., Sabitova A.N.</i> Biocompatible cryogels: preparation and application	3	4
<i>Kudaibergenov N.Zh., Shalmagambetov K.M., Vavasori A., Zhaksylykova G.Zh., Kanapiyeva F.M., Almatkyzy P., Mamyrkhan D.B., Bulybayev M.</i> The use of Lewis acid $AlCl_3$ as a promoter in the Pd-complex catalytic system of the cyclohexene hydroethoxycarbonylation reaction.....	2	8
<i>Minakova A.A., Chikina M.V., Il'yasov S.G.</i> Study of uric acid oxidation reaction products in medium of ammonia or primary amines	4	30
<i>Nurkenov O.A., Fazylov S.D., Seilkhanov T.M., Nurmaganbetov Zh., Gazaliev A.M., Karipova G.Zh.</i> Synthesis and structure of thiourea derivatives of functionally substituted pyridines	1	4
<i>Nurmaganbetov Zh.S., Mukusheva G.K., Ye.V.Minayeva, Turdybekov D.M., Turdybekov K.M., Makhmutova A.S., Zhasymbekova A.R., Nurkenov O.A.</i> Synthesis, quantum-chemical calculations and virtual screening of the alkaloid cytosine derivatives	4	21
<i>Salkeeva L.K., Muratbekova A.A., Minayeva E.V., Voitichek P., Tayshibekova E.K., Dostanova A.R., Tateeva A.B., Salkeeva A.K.</i> Phosphorylation of glycoluryl derivatives with phosphorus pentachloride	1	12
<i>Sinitsyna A.A., Il'yasov S.G.</i> Synthesis of alkyl derivatives of 3,7,10-trioxo-2,4,6,8,9,11-hexaaza[3.3.3]-propellane and evaluation of their biological activity.....	1	19

PHYSICAL AND ANALYTICAL CHEMISTRY

<i>Bakibaev A.A., Panshina S.Yu., Ponomarenko O.V., Malkov V.S., Kotelnikov O.A., Tashenov A.K.</i> 1D and 2D NMR spectroscopy for identification of carbamide-containing biologically active compounds	1	71
<i>Bhujbal S.S., Kale M., Chawale B.</i> Molecular docking identification of plant-derived inhibitors of the COVID-19 main protease	3	37
<i>Burkeyev M.Zh., Tuleuov U.B., Bolatbay A.N., Khavlichek D., Davrenbekov S.Zh., Tazhbayev Ye.M., Zhakupbekova E.Zh.</i> Investigation of the destruction of copolymers of poly(ethylene glycol)-fumarate with methacrylic acid using differential equations	3	47
<i>Fomin V.N., Aynabaev A.A., Kaykenov D.A., Sadyrbekov D.T., Aldabergenova S.K., Turovets M.A., Kelesbek N.K.</i> Optimization of coal tar gas chromatography conditions using probabilistic-deterministic design of experiment.....	4	39
<i>Jumadilov T.K., Malimbayeva Z.B., Khimersen Kh., Saparbekova I.S., Imangazy A.M., Suberlyak O.V.</i> Specific features of praseodymium extraction by intergel system based on polyacrylic acid and poly-4-vinylpyridine hydrogels	3	53
<i>Jumadilov T.K., Utesheva A.A., Khimersen Kh., Kondauronov R.G., Grazulevicius J.V.</i> Abnormal activity of functional groups during uranyl ions sorption by polymethacrylic acid-poly-4-vinylpyridine intergel system	4	47

<i>Kamani V.G., Sujatha M., Daddala G.B.</i> Development and validation of a novel stability indicating HPLC method for the separation and determination of darolutamide and its impurities in pharmaceutical formulations	4	57
<i>Malyshev V.P., Makasheva A.M., Bekbayeva L.A.</i> Invariants of ratio of crystal-mobile, liquid-mobile, and vaporized chaotized particles in solid, liquid, and gas states of substance	4	69
<i>Mammadova S.R.</i> Pd(II) extraction from acid solutions by bis-(2-hydroxyl-5-alkylbenzyl)amine	2	24
<i>Shipunov B.P., Zakharova M.V.</i> Change in the volume of water crystallization as a result of exposure to a high-frequency electromagnetic field	1	53
<i>Tazhbayev Ye.M., Galiyeva A.R., Zhumagaliyeva T.S., Burkeyev M.Zh., Kazhmuratova A.T., Zhakupbekova E.Zh., Zhaparova L.Zh., Bakibayev A.A.</i> Synthesis and characterization of isoniazid immobilized polylactide-co-glycolide nanoparticles	1	61

INORGANIC CHEMISTRY

<i>Asadov S.M.</i> Modeling of nonlinear processes of nucleation and growth of GaS _x Se _{1-x} (0 ≤ x ≤ 1) solid solutions.....	2	31
<i>Baimuratova Zh.A., Kalmakhanova M.S., Massalimova B.K., Nurlibaeva A.A., Kulazhanova A.S., Diaz de Tuesta J.L., Gomes H.T.</i> Synthesis and characterization of a new magnetic composite MnFe ₂ O ₄ /clay based on a natural clay obtained from Turkestan deposit	4	87
<i>Imamaliyeva S.Z., Mekhdiyeva I.F., Jafarov Y.I., Babanly M.B.</i> Thermodynamic study of the thallium-thulium tellurides by EMF method	2	43
<i>Ismailova A.G., Akanova G.Zh., Kamysbayev D.Kh.</i> Acid dissolution of neodymium magnet Nd-Fe-B in different conditions.....	4	79
<i>Kasenova Sh.B., Sagintaeva Zh.I., Kasenov B.K., Turtubaeva M.O., Nukhuly A., Kuanyshbekov Ye.Ye., Isabaeva M.A.</i> New nanostructured manganites of LaMe ^{II} CuZnMnO ₆ (MeII — Mg, Ca, Sr, Ba)	3	60
<i>Toibek A.A., Rustembekov K.T., Kaikenov D.A., Stoev M.</i> Synthesis and properties of double gadolinium tellurites	3	67

CHEMICAL TECHNOLOGY

<i>Abdimomyn S., Abduakhytova D., Atchabarova A., Turdean G.L., Tokpayev R., Kishibayev K., Kurbatov A., Naurzybayev M.</i> Optimization of the preparation method of a mechanically strong carbon electrode.....	4	95
<i>Abildina A.K., Avchukir K., Jumanova R.Zh., Beiseyeva A.N., Rakhymbay G.S., Argimbayeva A.M.</i> Preparation and electrochemical characterization of TiO ₂ as an anode material for magnesium-ion batteries.....	4	104
<i>Aitbekova D.E., Makenov D.K., Andreikov E.I., Tsaurov A.G., Feng Yung Ma, Baikenova G.G., Tusipkhan A., Muratbekova A.A., Baikenov M.I.</i> Hydrogen distribution in primary coke oven tar and its fractions	1	82
<i>Amerkhanova Sh.K., Uali A.S., Shlyapov R.M., Belgibayeva D.S.</i> Alkali-activated metallurgical slag as a sustainable adsorbent	4	117
<i>Baikenov M.I., Aitbekova D.E., Balpanova N.Zh., Tusipkhan A., Baikenova G.G., Aubakirov Y.A., Brodskiy A.R., Fengyun Ma, Makenov D.K.</i> Hydrogenation of polyaromatic compounds over NiCo/chrysotile catalyst.....	3	74
<i>Balpanova N.Zh., Baikenov M.I., Gyulmaliev A.M., Absat Z.B., Batkhan Zh., Ma F., Su K., Kim S.V., Baikenova G.G., Aitbekova D.E., Tusipkhan A.</i> Thermokinetic parameters of the primary coal tars destruction in the presence of catalysts and polymeric materials	2	86
<i>Glukhikh V.V., Shkuro A.E., Krivonogov P.S.</i> The effect of chemical composition on the biodegradation rate and physical and mechanical properties of polymer composites with lignocellulose fillers.....	3	83
<i>Guseinova E.A., Adzhomov K.Yu., Yusubova S.E.</i> Catalytic conversion of isopropyl alcohol on the heteropolic acid – titanium oxide system.....	2	53
<i>Korolkov I.V., Ludzik K., Lisovskaya L.I., Zibert A.V., Yeszhanov A.B., Zdorovets M.V.</i> Modification of magnetic Fe ₃ O ₄ nanoparticles for targeted delivery of payloads	1	99
<i>Kozhanova A.M., Temirgazyev B.S., Zhanarbek A., Tuleuov B.I., Seilkhanov T.M., Adekenov S.M.</i> Synthesis of a hydrophilic derivative of ecdysterone and development of its water-soluble form	4	138
<i>Melikova I.G., Efendi A.J., Babayev E.M., Faradjev G.M., Musazade K.Sh., Salahli A.M., Maqer-ramova L.G.</i> Catalytic oxidation of CO in gases emitted by industrial processes and vehicle exhaust.	2	69

<i>Mustafin Ye.S., Omarov Kh.B., Borsynbaev A.S., Havlichek D., Pudov A.M., Shuyev N.V.</i> Production of electrolytic copper from Zhezkazgan Processing Plant tailings leaching solutions using a hydro-impulse discharge	4	128
<i>Nikulin S., Verezhnikov V., Bulatetskaya T., Nikulina N.</i> Investigation of the process of latex coagulation by cationic surfactants	2	63
<i>Pirniyazov K.K., Tikhonov V.E., Rashidova S.Sh.</i> Synthesis and properties of oligochitosan ascorbate from <i>Bombyx mori</i>	1	91
<i>Plotnikova M.D., Shein A.B., Shcherban' M.G., Solovyev A.D.</i> The study of thiadiazole derivatives as potential corrosion inhibitors of low-carbon steel in hydrochloric acid	3	93
<i>Raiymbekov Y.B., Besterekov U., Abdurazova P.A., Nazarbek U.B., Pochitalkina I.A.</i> Recovery of used acetic acid via sulfuric acid.....	4	149
<i>Seitmagzimova G.M., Assylkhankyzy A., Petropavlovsky I.A., Dzhanmuldaeva Zh.K.</i> Research of the process of obtaining potassium fertilizers from carnallite ore	2	77

METHODS OF TEACHING CHEMISTRY

<i>Nurdillayeva R.N., Zhuman G.O.</i> Application of the CLIL method in the classes of Inorganic Chemistry ...	2	96
<i>Sadykov T., Ctrnactova H., Kokibasova G.T.</i> Students' opinions toward interactive apps used for teaching chemistry	3	103
<i>Yaroshenko O.G.</i> Chemistry textbooks as a means of supporting cognitive activity of general secondary education students.....	2	105

MEMORABLE DATES

<i>Nikolskiy S.N., Pustolaikina I.A.</i> Masalimov A.S. as the founder and leader of a new direction in ESR spectroscopy and quantum chemistry of free radicals	4	5
<i>Tazhbayev Ye.M., Burkeyev M.Zh.</i> Congratulations on the anniversary of Professor S.E. Kudaibergenov....	2	4